2002

Laser Induced Plasma Spectroscopy and Applications

Technical Digest

September 25–28, 2002

Caribe Royale Resort Suites and Villas
Orlando, Florida

OSA®
Optical Society of America

Sponsored by
Optical Society of America

REPORT DOCUMENTATION PAGE

1. AGENCY USE ONLY (Leave Blank)	2. REPORT DATE 02/28/03	3. REPORT TYPE AND DATES COVERED FINAL 01-01-2002 - 12-31-2002
4. TITLE AND SUBTITLE ~~Organization of the 2002 Photonic Science Topical Meetings~~		5. FUNDING NUMBERS F49620-02-1-0065
6. AUTHOR(S) Optical Society of America		
7. PERFORMING ORGANIZATION NAME(S) AND ADDRESS(ES) Optical Society of America 2010 Massachusetts Ave., NW Washington, DC 20036		8. PERFORMING ORGANIZATION REPORT NUMBER
9. SPONSORING / MONITORING AGENCY NAME(S) AND ADDRESS(ES) U. S. Air Force Office of Scientific Research 4015 Wilson Blvd. Rm. 713 Arlington, VA 22203		10. SPONSORING / MONITORING AGENCY REPORT NUMBER

11. SUPPLEMENTARY NOTES

The views, opinions and/or findings contained in this report are those of the author(s) and should not be construed as an official US AFOSR position, policy or decision, unless so designated by other documentation.

12 a. DISTRIBUTION / AVAILABILITY STATEMENT	12 b. DISTRIBUTION CODE
Approved for public release; distribution unlimited.	

13. ABSTRACT (Maximum 200 words)

The OSA topical meetings that received support under this grant provided a forum for researchers in various specialty areas to meet and share ideas and technology in their fields. Following are the meetings that were supported by this grant:

- Advanced Solid State Lasers – This meeting provided a forum for leading edge results in the fields of solid state lasers, laser materials, nonlinear optical materials and high power diode lasers.
- Laser Applications to Chemical and Environmental Analysis – This meeting presented and discussed advances in the use of lasers for chemical analysis and environmental monitoring.
- Biomedical Optics – This meeting was composed of three meetings that offered a unique venue to present and discuss recent research activities and developments in the field of lasers and optics in biomedicine.
- Ultrafast Phenomena - This meeting brought together a multidisciplinary group sharing a common interest in the generation of ultrashort pulses in the picosecond, femtosecond, and attosecond regimes and their application to studies of ultrafast phenomena in physics, chemistry, biology, material sciences and electronics.
- Nonlinear Optics – This meeting provided and international forum for discussion of all aspects of nonlinear optics, including new phenomena, novel devices, advanced materials and applications.
- Nonlinear Guided Waves and their Applications – This meeting emphasized on development of new ideas and novel techniques in the areas of materials, fabrication, devices , applications and nonlinear theory.
- Laser Induced Plasma Spectroscopy and Applications – This Meetings focused on major advances in LIBS fundamentals, instrumentation and applications and featured new commercial laboratory LIBS systems and advanced components, as well as field portable systems.

14. SUBJECT TERMS			15. NUMBER OF PAGES 16. PRICE CODE
17. SECURITY CLASSIFICATION OR REPORT **UNCLASSIFIED**	18. SECURITY CLASSIFICATION ON THIS PAGE **UNCLASSIFIED**	19. SECURITY CLASSIFICATION OF ABSTRACT **UNCLASSIFIED**	20. LIMITATION OF ABSTRACT **UL**

Laser Induced Plasma Spectroscopy and Applications

Postdeadline Papers

September 25–28, 2002

Caribe Royale Resort Suites and Villas
Orlando, Florida

Sponsored by
Optical Society of America
2010 Massachusetts Avenue, NW
Washington, DC 20036-1023

LIBS
September 25, 2002
Caribe Royale Resort and Villas
Postdeadline Papers

Poster Presentations

PD1 **Applications of LIBS to laser assisted processing and reactive nanopowers,** Tyler T. Kerr, *South Dakota School of Mines and Tech., USA;* Jan A. Puszynski, *South Dakota School of Mines and Tech., USA.* Resent research is focused on nondestructive in-situ measurement of spatial compositions in metallic parts built by laser-assisted technique, as well as characterization of Metastable Intermolecular Composites (MIC) and metallic nanopowders.

PD2 **Trace metal analysis in bulk aqueous solution using nanosecond dual pulse laser induced breakdown spectroscopy,** William F. Pearman, *Univ. of South Carolina, USA;* Jonathan Scaffidi, *Univ. of South Carolina, USA*; S. Michael Angel, *Univ. of South Carolina, USA.* An orthogonal beam orientation of dual pulse laser induced breakdown spectroscopy for trace metal analysis in a bulk aqueous solution is studied. Optimization methodology and limits of detection for Ca and Cr are reported.

PD3 **A combined remote LIBS and Raman instrument for spectroscopic analysis,** S. Michael Angel, *Univ. of South Carolina, USA;* Manash Ghosh, *Indian Assoc. for the Cultivation of Science, India.* We present a combined Raman and laser-induced breakdown spectroscopy (LIBS) system based on a portable remote Raman spectroscopic system. This system measures the elemental composition and provides mineralogical information at a distance of 10 meters.

PD4 **Analysis of Bronze age vitreous materials. Experience with a new LIBS instrument,** K. Melessanaki, *Inst. Of Electronic Structure and Laser, Greece;* M. Panagiotaki, *Greece;* S. Chlouveraki, *Inst. Of Aegean Prehistory – Study Center of Eastern Crete, Greece;* P.P. Betancourt, *Temple Univ., USA;* D. Anglos, *Inst. Of Electronic Structure and Laser, Greece.* A broad variety of Bronze Age vitreous material objects from Crete (faience, Egyptian blue, glass) were examined using a new LIBS instrument constructed at FORTH-IESL. Analytical results and instruments operation and performance are presented.

Application of LIBS to Laser Assisted Processing and Reactive Nanopowders

Tyler T. Kerr and Jan A. Puszynski
South Dakota School of Mines and Technology
Department of Chemistry and Chemical Engineering
501 St. Joseph Street
Rapid City, South Dakota 57701
Tel: (605) 394-1230, e-mail: Jan.Puszynski@sdsmt.edu **,**
ttkerr@hotmail.com

Advanced Materials Processing Center

The South Dakota School of Mines and Technology (SDSM&T) in Rapid City, SD, has recently established the Advanced Materials Processing (AMP) Center, which is focused on the research, development, and application of two emerging and strategic technologies: a) *Friction Stir Processing (FSP)* and *b) Intelligent Laser Processing (ILP).* The ILP equipment, shown in fig. 1, will allow direct deposition of various metal alloys, metal-ceramic composites, graded alloys, as well as solid freeform fabrication. Detailed analysis of pure metals, alloys and ceramics will be conducted in order to develop a comprehensive database. A significant research effort will be on 2D mapping of the interfacial regions and deposited bulk material.

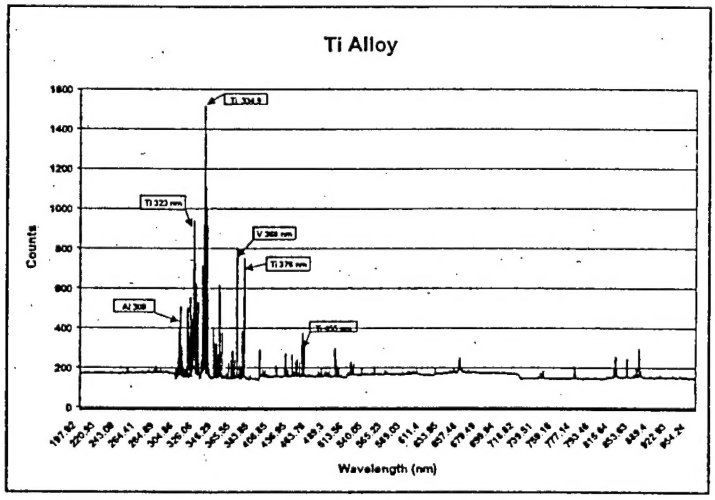

Figure 1: LIBS Spectrum of Ti alloy parts.

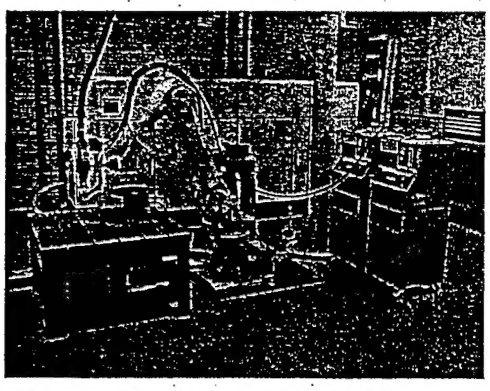

Figure 1: ILP equipment as seen in AMP Center.

LIBS Analyses of Intermetallics

NiAl and Ni_3Al

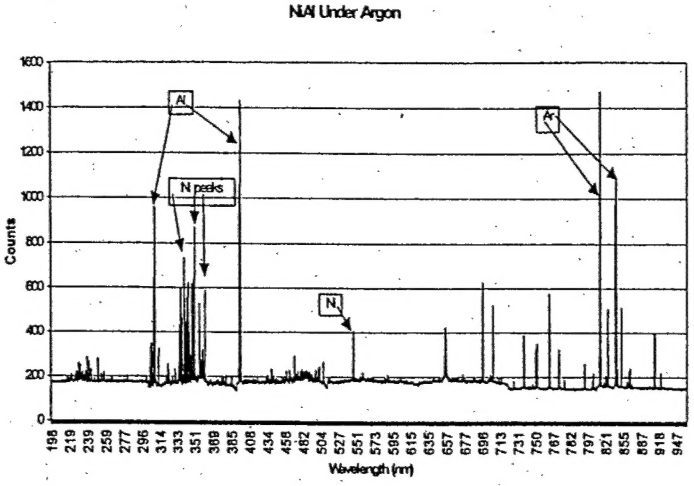

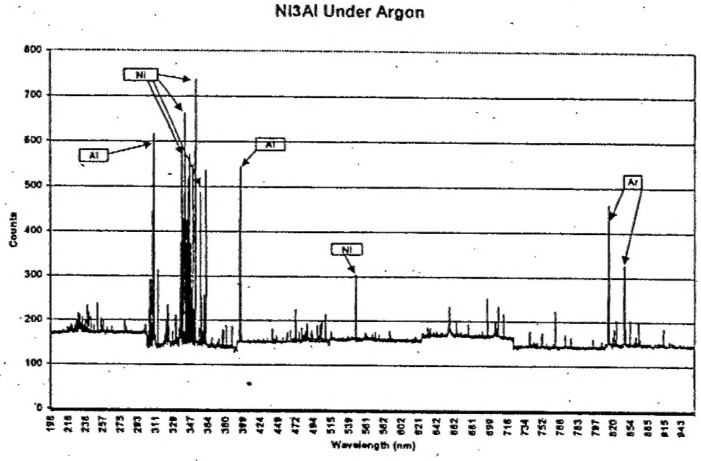

LIBS Analyses of Ceramic Micron- and Nano-sized Powders

Alumina powders

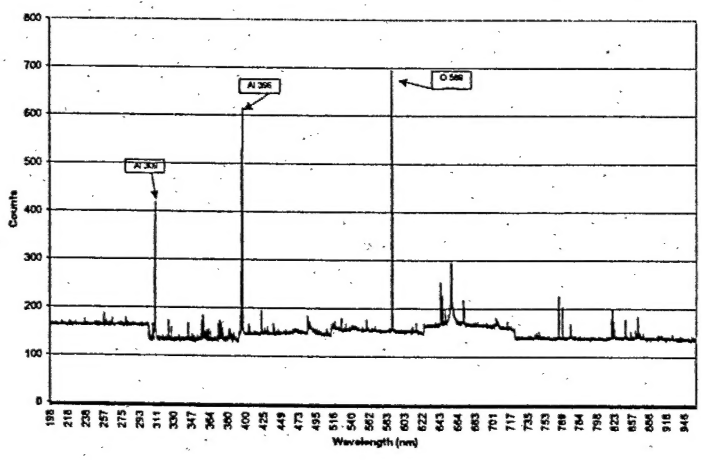

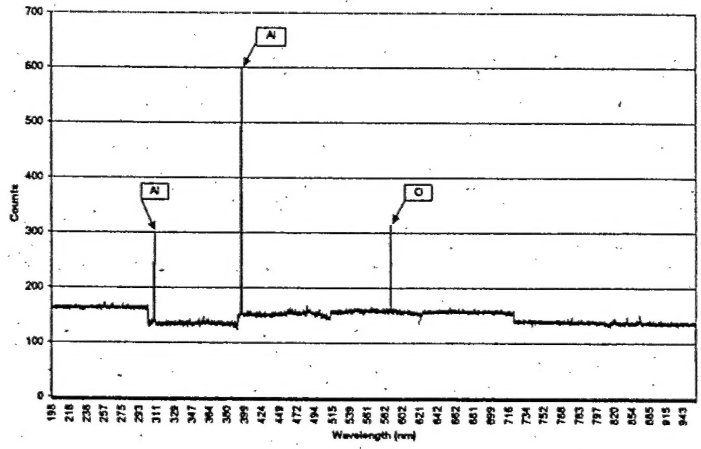

LIBS Analysis of AlN ceramics

Aluminum Nitride ceramic articles were pressureless sintered with 4% wt. Y_2O_3 as a sintering additive.

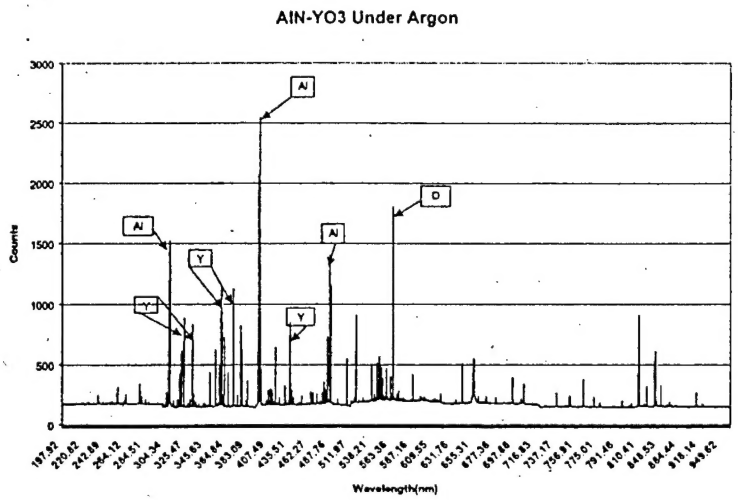

Future Research

- Application of LIBS technique for in-situ monitoring of spatial concentrations.
- Analysis of nanopowders and coatings.
- In-situ characterization of reaction products (MIC systems)

Acknowledgements

The authors of this presentation would like to give special thanks to Dr. Andrzej Miziolek and Dr. Frank DeLucia, from The Army Research Laboratory, for their technical input and support.

Also, the authors acknowledge Mr. Walter Roy and The Army Research Laboratory for their financial support. Research was sponsored by the Army Research Laboratory and was accomplished under Cooperative Agreement Number DAAD19-02-2-0011. The views and conclusions contained in this document are those of the authors and should not be interpreted as representing the official policies, either expressed or implied, of the Army Research Laboratory or the U.S. Government. The U.S. Government is authorized to reproduce and distribute reprints for Government purposes notwithstanding any copyright notation hereon.

Trace metal analysis in bulk aqueous solution using nanosecond dual pulse laser induced breakdown spectroscopy

William F. Pearman, Jonathan Scaffidi
Dept. of Chemistry and Biochemistry, University of South Carolina. , 631 Sumter Street, Columbia, SC 29208

S. Michael Angel
Dept. of Corresponding Author, Chemistry and Biochemistry, University of South Carolina. , 631 Sumter Street, Columbia, SC 2920
Telephone: 803-777-2779; Fax: 803-777-9521; email: angel@mail.chem.sc.edu

Summary:

A systematic optimization study was conducted in order to isolate the experimental parameters that produced the best results. Once identified, experiments were completed to determine detection limits for Ca and Cr. Limits of detection were comparable to or better than those currently reported in the literature.

Optimization

A preliminary study using the timing scheme utilized by Pichahchy *et al.* in the sampling of solids in an aqueous solution yielded promising results during the detection of Na in bulk utilizing the set up shown in figure 1 solution [1].

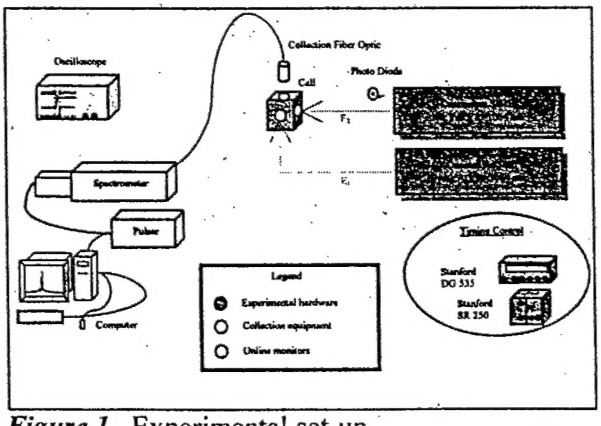

Figure 1. Experimental set-up

Figure 2 shows the comparison between single pulse and orthogonal dual pulse for this test utilizing a saturated Na solution.

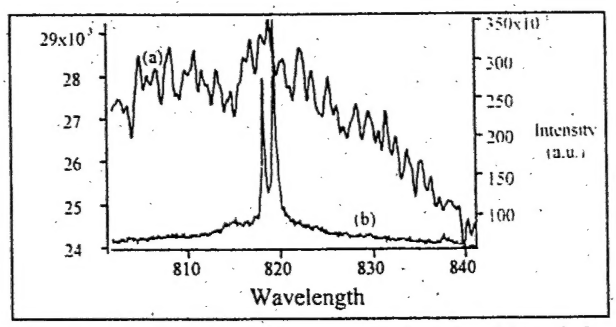

Figure 2. Comparison between single pulse (a) on left axis and dual pulse (b) on left axis for a 95mJ pulse (a) and a 95 mJ / 175mJ dual pulse crossing orthogonal.

Based upon these results, the experimental parameters of laser spark intersection, gate width, gate delay, and inter pulse timing were optimized using the oxygen line at 777 nm. At the conclusion of the optimization process, a 314 fold enhancement of the emission intensity was obtained as shown in figure 3. These results are higher than the 50 fold

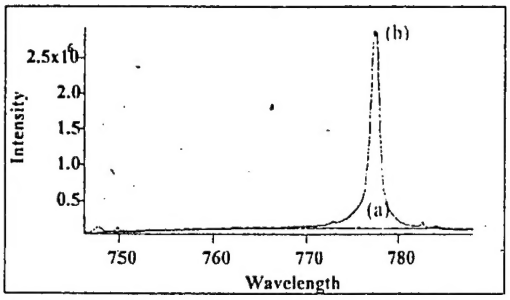

Figure 3. Comparison of single pulse (a) and orthogonal dual pulse (b) for oxygen at 777nm.

Enhancements reported earlier in the literature [2]. Additionally, the time between pulses (ΔT) at which the maximum emission intensity for oxygen was observed was constant in a range from 70μs to 330μs which was also different than the 18μs in the literature [2]. Using a 400 ppm Ca test solution, all experimental parameters were verified and the signal to noise ratio was optimized for future limits of detection studies.

Detection Limit for Ca and Cr

The limit of detection for both Ca and Cr was determined using equation 1 where the LOD (C_L) is defined as three times the signal of the background (σ) divided by the slope (S) of the calibration curve at low concentrations.

Equation 1: $C_L = 3\sigma/S$ [4]

The calibration curve for Ca and Cr is shown in figures 4 and 5 respectively. A spectrum for 50 ppm concentrations for Ca and Cr are also shown in figures 6 and 7 respectively.

The LODs for Ca and Cr were determined to be 0.04 ppm and 1.04 ppm respectively. The LOD for Ca are lower than currently tabulated in the literature[4,5,6]. The LOD for Cr is also comparable to or lower than those found in the literature[6,7,8].

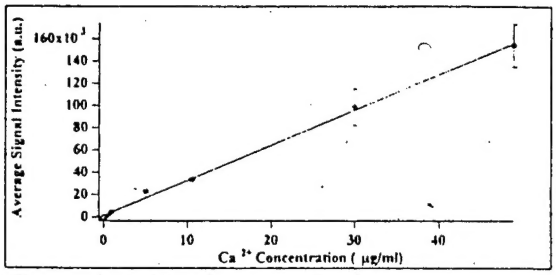

Figure 4. Calibration curve for the determination of the detection limit for Ca.

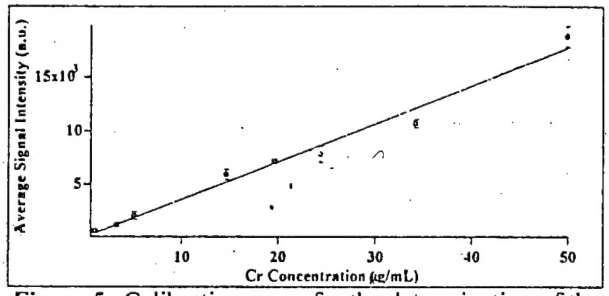

Figure 5. Calibration curve for the determination of the detection limit for Cr.

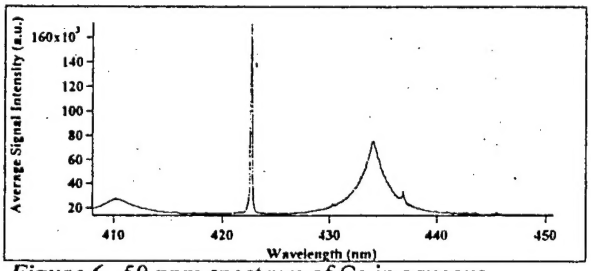

Figure 6. 50 ppm spectrum of Ca in aqueous solution

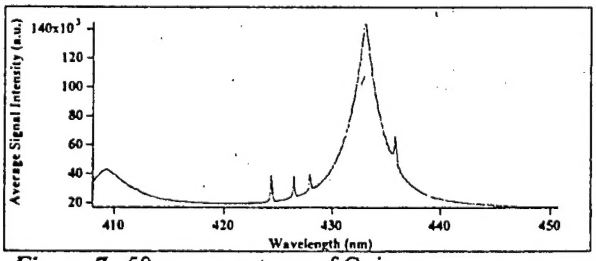

Figure 7. 50 ppm spectrum of Cr in aqueous solution

References:

[1] Pichahchy, A.E.; Cremers, D.A.; Ferris, M.J., "Elemental analysis of metals under water using laser-induced breakdown spectroscopy," Spectrochim. Acta B, **52**, 25-39 (1997).

[2] Cremers, D.A.; Radziemski, L.J.; Loree, T.R."Spectrochemical analysis of liquids using the laser spark," Appl. Spectrosc., **38 (5)**, 721-729 (1984).

[3] Kennedy, P.K.; Hammer, D.X.; Rockwell, B.A., "Laser-induced breakdown ion aqueous media." Prog. Quant. Electr., **21 (3)**, 155-248 (1997).

[4] Bundschuh, T.; Yun, J-I.; Knopp, R "Determination of size, concentration and elemental composition of colloids with laser-induced breakdown detection/spectroscopy.(LIBD/S)," Fresenius J. Anal. Chem., **371 (8)**, 1063-1069 (2001).

[5] Knopp, R.; Scherbaum, F.J.; Kim, J.I."Laser induced breakdown spectroscopy (LIBS) as an analytical tool for the detection of metal ions in aqueous solutions," Fresenius J. Anal. Chem., **355**, 16-20 (1996).

[6] Samek, O.; *et al.*"Application of laser-induced breakdown spectroscopy to *in situ* analysis of liquid samples," Opt. Eng. **39 (8)**, 2248-2262 (2000).

[7] Fichet, P.; Toussaint, A.; Wagner, J.-F.Laser-induced breakdown spectrosopy: A tool for analysis of different types of liquids," Appl. Phys. A, **69[Suppl.]** S591-S592 (1999).

[8] Arca, G.; *et al.* "Trace element analysis in water by laser-induced breakdown spectroscopy technique," Appl. Spectrosc., **51 (8)**, 1102-1105 (1997).

[9] Stratis, D.N.; Eland, K.L.; Angel, S.M. "Dual-pulse LIBS: Why are two lasers better than one?," SPIE, **3853**, 61-68 (1999).

A Combined Remote LIBS and Raman Instrument for Spectroscopic Analysis of Minerals on Planetary Surfaces

Shiv K. Sharma, Paul G. Lucey, Hugh W. Hubble and Keith A. Horton

University of Hawaii, Hawaii Institute of Geophysics and Planetology, 2525 Correa Rd., Honolulu, HI 96822. USA

Tel.: +1-808-956-8476; fax: +1-808-956-3188; Email: sksharma@soest.hawaii.edu (S. K. Sharma)

S. Michael Angel

Department of Chemistry and Biochemistry, University of South Carolina, Columbia, SC 29208. USA

Manash Ghosh

Department of Spectroscopy, Indian Association for the Cultivation of Science, Jadavpur, Calcutta 700 032. India

Summary

Advancements in lasers, spectrographs and holographic optical components have made laser based techniques such as Raman spectroscopy and laser-induced breakdown spectroscopy (LIBS) effective tools for analyzing natural and synthetic materials. Advanced Raman spectroscopic techniques have been employed to investigate the mineralogy of meteorites [1-3], and have been proposed for *in situ* mineral characterization on planetary surfaces [4,5]. Both micro-Raman [6,7] and remote Raman systems [8-10] are being considered for future exploration on planetary surfaces. The feasibility of using the remote LIBS technique for the rapid, on-line determination of the major and minor constituents of mineral drill core samples as well as for space applications has been demonstrated [11,12].

We have explored the use of LIBS combined with pulsed-laser Raman spectroscopy for mineral analysis at a distance of 10 m. We modified our remote pulsed Raman system to collect LIBS data, thus obtaining quantitative values for cation composition in our samples. By analyzing the cation information collected in the LIBS experiment alongside the anion information provided by Raman scattering, a more complete image of the mineral's structure and composition can be obtained.

Figure 1 shows a schematic representation of the experimental setup for the remote LIBS and Raman experiment. A Q-switched Nd:YAG laser (Quanta-Ray Model DCR-2, 1064 nm, 20 Hz), operating at ~200 mJ/pulse, was focused on the sample approximately 10 m away creating a plasma spark. The telescope is placed beside the laser in order to get as close to the 180-degree back scattering geometry as possible. The LIBS data is collected and analyzed by our Raman receiver using a thermoelectrically cooled, gated and intensified CCD (I-Max-1024-E) and a 0.25 m spectrograph (Spex Model 270M with 1800 grooves/mm grating, blazed at 500 nm). The holographic notch filter (Figure 1) is removed during LIBS measurements and the 532 nm laser is turned off. The LIBS spectra were collected with slit width of 50 μm.

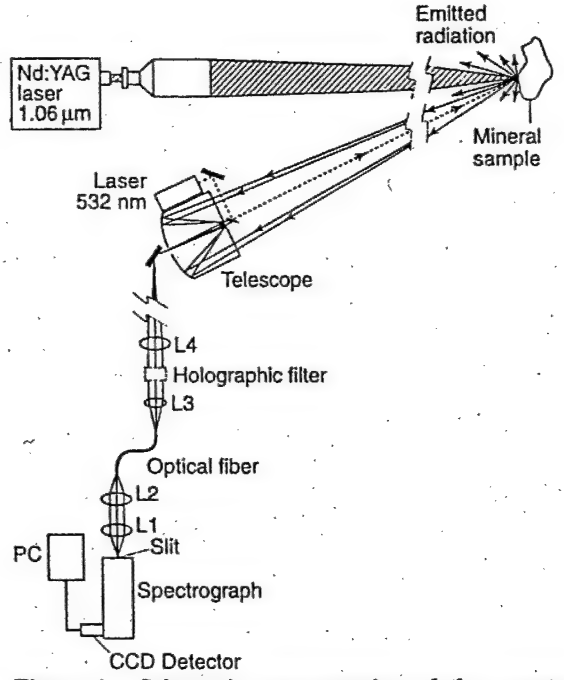

Figure 1. Schematic representation of the remote LIBS and Raman system.

The averaged number of accumulations for each spectrum was 100. Excellent quality LIBS spectra of biogenic and abiogenic carbonates, and of olivine samples with varying iron contents were recorded with this system [13]. A radiometrically calibrated broadband light source, a Labsphere® integrating sphere, is used to determine the response function of the system. By placing the integrating sphere at the sample location and collecting a spectrum with the identical gain and integration settings used during LIBS measurements, we can calibrate the observed signal over the entire optical path to units of radiance. By dividing the sample spectrum by the measured response function, the system response effects are removed and the sample spectrum is calibrated directly in spectral radiance units ($Wm^{-2}sr^{-1}\mu m^{-1}$). For Raman measurements the 1064 nm laser was turned off, the 532 nm holographic notch filter was inserted in the beam path. The minerals and rocks were excited with 532 nm pulsed laser (Big Sky Model Ultra CFR, 20 Hz) and the Raman scattering spectrum was obtained. This system thus allows the measurement of the Raman and LIBS spectra at the same location at the mineral surface at a distance of 10 m. It should be noted, however, that the sampling diameter for LIBS is much smaller (> 1 mm in diameter) than the sampling diameter in Raman experiment (a few cm in diameter) at 10 meter distance.

Selected LIBS spectra collected in the region around 530 nm (Figure 2) show a strong calcium line at 534.94 nm (Figure 2, calcite). Three strong peaks of calcium are visible in the 526-528 nm region of the spectrum. Five lines are expected in this region, but these lines were not resolved. Also, there is a calcium line at 518.9 nm. Three magnesium lines appear at 516.73 nm, 517.26 nm, and 518.36 nm (Figure 2, magnesite). We chose to evaluate the magnesium data at 517.26 nm, as this line is well resolved. The dolomite spectrum (Figure 2, dolomite) is used to adjust for the strength of the individual lines, as the ratio of calcium to magnesium in dolomite is 1:1. In this way, we can determine that the Ca:Mg in our pink coral sample (Figure 2, pink coral) is 89.3:10.7 mol%. This value of Ca:Mg for pink coral is within $\pm$0.5% to the value of 90.1:9.9 mol% measured by electron microprobe [14]. We did the same experiment using gypsum and white coral, as well as an analysis of the Fe content in magnesium-rich olivine (Fo90, Fo92). The Fe content of these minerals determined with remote LIBS is in agreement (within +0.5%) with the electron microprobe analysis of the respective samples [13].

In the Raman spectra of all four carbonate samples, measured at the same location as that used in the LIBS experiments, Raman bands at ~ 1085 cm^{-1} are observed (Figure 3). This band is very strong in the Raman spectra of calcite, magnesite and dolomite and is very weak in the spectrum of pink coral. The presence of a 1085 cm^{-1} band in the spectra of these samples indicates that these minerals contain CO_3^{2-} ions [15]. The strong Raman band at 1130 cm^{-1} in the spectrum of pink coral is characteristic of resonance Raman spectra of the carotene pigment [14], and implies biogenic origin of this sample. The low frequency lattice modes of calcite, magnesite and dolomite, respectively, appear at 281, 329 and 299 cm^{-1} (Figure 3), and can be used to

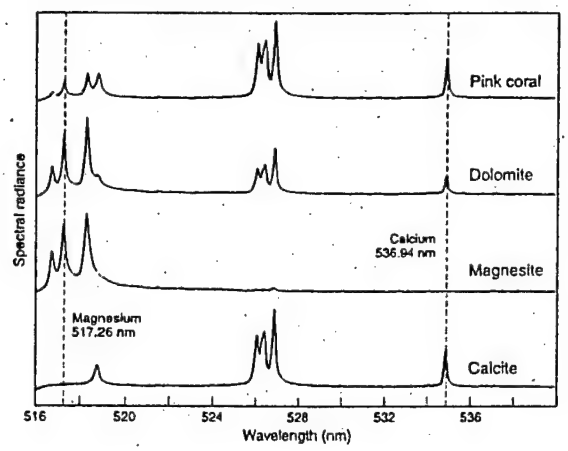

Figure 2. Portions of the LIBS spectra of biogenic (pink coral) and a-biogenic carbonates recorded with a combined LIBS/Raman system at a stand-off distance of 10 m.

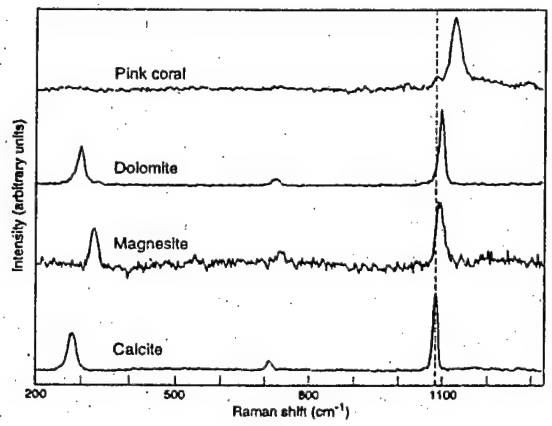

Figure 3. Portions of the Raman spectra of biogenic (pink coral) and a-biogenic carbonates recorded with the combined LIBS/Raman spectroscopic system at a stand-off distance of 10 m.

identify the types of carbonate minerals. The lattice modes are very weak and broad in the spectrum of pink coral because of disorder and the nano-crystalline nature of the biogenic carbonate [14]. The quantitative information about cations from the LIBS data, when combined with the unique Raman signature of the anion groups, will allow us to remotely identify and characterize the composition and the mineralogy of crystals and rocks on planetary surfaces. The remote LIBS and Raman data on selected minerals clearly demonstrates that development of a combined LIBS and Raman instrument will be very useful for planetary applications.

We have also measured good quality Raman spectra of various silicates, and hydrous silicates and sulfate minerals and ices at stand-off distances [10]. We have measured the relatively weak Raman spectra of silicate glasses, organic vapors and atmospheric gases at a distance of 10 m using a HoloSpec spectrometer (f/2.2, Kaiser Optical Systems, Inc.), and can easily use our system for atmospheric LIDAR (light detection and ranging) measurements. These results indicate that this versatile system can be used to analyze both a-biogenic and biogenic minerals, various types of ices, and atmospheric constituents on planetary surfaces. Efforts are underway for combining the remote Raman and LIBS techniques in a single, compact instrument for a remote *in situ* mineralogical and elemental analysis of planetary surfaces.

[1] A. Wang, B.L. Jolliff, and L.A. Haskin *J. Geophys. Res.*, **104** (1999) 8509.

[2] T.F. Cooney, E.R.D. Scott, A.N. Krot, S.K. Sharma, and A. Yamaguchi, *Amer. Min.*, **84** (1999) 1569.

[3] T.J. Fagan, E.R.D. Scott, K. Keil, T.F. Cooney, S.K. Sharma, *Meteorit. Planet. Sci.*, **35** (2000) 319.

[4] E.J. Israel, R.E. Arvidson, A. Wang, J.D. Pasteris, and B.L. Jolliff, *J. Geophys. Res.*, **102** (1997) 28705.

[5] B.L. Jolliff, A. Wang, K. Kuebler, L.A. Haskin, and G. Klingelhöfer, *Lunar Planet. Sci.*, **30** (1999) 1529.

[6] L.A. Haskin, A. Wang. K.M. Rockow, B.L. Jolliff, R.L. Korotev, and K.M. Viskupic, *J. Geophys. Res.*, **102** (1997) 19293.

[7] A. Wang, L.A. Haskin, and E. Cortez, *Appl. Spectr.*, **52** (1998) 477.

[8] P.G. Lucey, T.F. Cooney, S.K. Sharma, *Lunar Planet. Sci.*, **29** (1998) 1354.

[9] K.A. Horton, N. Domergue-Schmidt, S.K. Sharma, P. Deb, and P.G. Lucey, *Lunar Planet. Sci.*, **31** (2000) 1514.

[10] S.K. Sharma, S.M. Angel, M. Ghosh, H.W. Hubble and P.G. Lucey, *Appl. Spectrosc.*, **56** (2002) 699.

[11] J.A. Bolger, *Appl. Spectrosc.*, **54** (2000) 181.

[12] D.A. Cramers and M.J. Ferris. *Appl. Spectrosc.*, **54** (2000) 331.

[13] H.W. Hubble, M. Ghosh, S.K. Sharma, K.A. Horton, P.G. Lucey, S.M. Angel and R.C. Wiens, *Lunar Planet. Sci.*, **33** (2002) 1935.

[14] T.M.K. Nedungadi, *Proc. Indian Acad. Sci. A*, **11**, 86 (1940).

[15] W.B. White, 1974: The carbonate minerals. In Farmer V.C. (ed) Infrared Spectra of Minerals, Mineralogical Society, London, Chapter 12, p. 227.

Analysis of Bronge age vitreous materials. Experience with a new LIBS instrument

K. Melessanaki
Foundation for Research and Technology-Hellas (FO.R.T.H.), Institute of Electronic Structure and Laser, P.O.Box 1527, GR 71110 Heraklion, Crete, Greece
Tel. +30 810 391134, Fax +30 810 391318, e-mail: alina@iesl.forth.gr

M. Panagiotaki
25 D. Solomou St., GR 71306 Heraklion, Crete, Greece

S. Chlouveraki
Institute of Aegean Prehistory – Study Center of Eastern Crete, Pahia Ammos, Crete, Greece

P. P. Betancourt
Department of Art History, Temple University, Philadelphia, PA 19122, USA

D. Anglos
Foundation for Research and Technology-Hellas (FO.R.T.H.), Institute of Electronic Structure and Laser, P.O.Box 1527, GR 71110 Heraklion, Crete, Greece
Tel. +30 810 391154, Fax +30 810 391318, e-mail: anglos@iesl.forth.gr

Abstract: A broad variety of Bronze Age vitreous material objects from Crete (faience, Egyptian blue, glass) were examined using a new LIBS instrument constructed at FORTH-IESL. Analytical results and instrument operation and performance are presented.

OCIS codes: (140.3440) Laser induced breakdown; (300.6210) Atomic spectroscopy

Key to Authors

Anglos, D. • PD4
Angel, S. Michael • PD2, PD3
Betancourt, P.P • PD4
Chlouveraki, S. • PD4
Ghosh, Manash • PD3
Kerr, Tyler T. • PD1
Melessanaki, K. • PD4
Panagiotaki, M. • PD4
Pearman, William F. • PD2
Puszynski, Jan A. • PD1
Scaffidi, Jonathan • PD2

Laser Induced Plasma Spectroscopy and Applications

Technical Digest

September 25–28, 2002

Caribe Royale Resort Suites and Villas
Orlando, Florida

Sponsored by
Optical Society of America
2010 Massachusetts Avenue, NW
Washington, DC 20036-1023

Articles in this publication may be cited in other publications. To facilitate access to the original publication source, the following form for the citation is suggested:

Name of Author(s), "Title of Paper," in OSA *Trends in Optics and Photonics (TOPS) Vol. 81, Laser Induced Plasma Spectroscopy and Applications*, OSA Technical Digest, Postconference Edition (Optical Society of America, Washington DC, 2002), pp. xx-xx.

Technical Digest (meeting edition)

ISBN 1-55752-717-2
LCCN 2002101865

TOPS Vol. 81: LIBS Technical Digest–Postconference Ed.

ISBN 1-55752-725-3
LCCN 2002106617

Printed in the U.S.A.

Contents

Technical Program Committee

Committee Chairs
Andrzej Miziolek, *ARL, USA, Program Chair*
Vincenzo Palleschi, *IFAM, Italy, General Chair*

Committee Members
Dennis Alexander, *Univ. of Nebraska-Lincoln, USA*
S. Michael Angel, *Univ. of South Carolina, USA*
Demetrios Anglos, *FORTH, Greece*
Simon Bechard, *PharmaLaser, Canada*
Bruce L. Chadwick, *CRC, Australia*
David Cremers, *Los Alamos Natl. Labs., USA*
Yoshihiro Deguchi, *Mitsubishi Heavy Industries, Japan*
Mohamed Abdel Harith, *NILES Inst., Egypt*
Russell S. Harmon, *ARO/ARL, USA*
Amy Hunter, *P.S. Inc., USA*
Javier Laserna, *Univ. of Malaga, Spain*
Patrick Mauchien, *CEA, France*
Kevin McNesby, *ARL, USA*
Nicolò Omenetto, *Univ. of Florida, USA*
Ulrich Panne, *TUM, Germany*
Leon Radziemski, *Washington State Univ., USA*
Mohamed Sabsabi, *NRC, Canada*
Israel Schechter, *Technion, Israel*
Andrew Whitehouse, *Applied Photonics Ltd., UK*
Ben Smith, *Univ. of Florida, USA*

Agenda of Sessions

All technical sessions are held in the Royal Palm III

Tuesday, September 24, 2002		
4:00pm–7:00pm		Registration
7:00pm–8:30pm		Conference Welcome Reception
Wednesday, September 25, 2002		
8:10am–8:30am		Opening Remarks
8:30am–10:10am	WA	Exotic LIBS
10:10am–10:40am		Coffee Break
10:40am–12:20pm	WB	Hyphenated Techniques
12:30pm–2:00pm		Lunch Break
2:00pm–3:40pm	WC	New LIBS Methodologies and Instrumentation: I
3:40pm–4:10pm		Coffee Break
4:10pm–5:30pm	WD	New LIBS Methodologies and Instrumentation: II
5:30pm–8:00pm		Dinner Break
8:00pm–10:00pm		Panel Discussion — LIBS & Homeland Defense
Thursday, September 26, 2002		
8:30am–10:10am	ThA	LIBS for the Environment and Art
10:10am–10:40am		Coffee Break
10:40am–12:20pm	ThB	LIBS in Life Sciences and Materials
12:30pm–2:00pm		Lunch Break
2:00pm–3:40pm	ThC	Fundamentals of LIBS: I
3:40pm–4:10pm		Coffee Break
4:10pm–5:30pm	ThD	Fundamentals of LIBS: II
5:30pm–8:00pm		Dinner Break
8:00pm–10:00pm	ThE	Poster Session
Friday, September 27, 2002		
8:30am–9:50am	FA	Femtosecond LIBS
9:50am–10:20am		Coffee Break
10:20am–12:20pm	FB	LIBS for Materials Analysis
12:20pm–2:00pm		Lunch Break
2:00pm–3:00pm	FC	LIBS Analysis of Particulate Matter
3:00pm–4:00pm	FD	Laser Ablation and Desorption
4:00pm–4:30pm		Coffee Break
4:30pm–5:30pm	FE	Imaging, Surface Mapping and Stratigraphy by LIBS
6:00pm–10:00pm		Conference Social Event
Saturday, September 28, 2002		
9:00am–10:30am		Panel Discussion — Future of LIBS Sensor Technology and Applications I
10:30am–11:00am		Coffee Break
11:00am–12:30pm		Panel Discussion — Future of LIBS Sensor Technology and Applications II
12:30pm–12:40pm		Closing Remarks

Abstracts

■ Wednesday
■ September 25, 2002

Room: Royal Palm III

8:10am–8:30am
Opening Remarks
Andrzej Miziolek, ARL, USA

8:30am–10:10am
WA ■ Exotic LIBS
Vincenzo Palleschi, Inst. of Atomic and Molecular Physics, Italy, Presider Presider

WA1 8:30am Invited
Extreme LIBS, *A.I. Whitehouse, J. Young, C.P. Evans, Applied Photonics Ltd., UK.*
A summary of selected applications of Laser-Induced Breakdown Spectroscopy (LIBS) conducted for the nuclear power generation and spent-fuel reprocessing industries within the United Kingdom are presented. Various types of fibre-optic probe and telescope LIBS instrument, together with a description of the methods adopted for their deployment, are discussed.

WA2 9:10am
Capabilities of LIBS for analysis of geological samples at stand-off distances in a Mars atmosphere, *David A. Cremers, Roger C. Wiens, Monty J. Ferris, Los Alamos Natl. Lab., USA; René Brennetot, CEA Saclay, France; Sylvestre Maurice, Midi Pyrenees Observatory, France.*
The use of LIBS for stand-off elemental analysis of geological and other samples in a simulated Mars atmosphere is being evaluated. Analytical capabilities, matrix effects, and other factors affecting analysis are being determined.

WA3 9:30am
Open-path laser induced plasma spectrometry for the stand-off detection and fast screening of solid samples, *D. Romero, P.L. García, S. Palanco, J.M. Vadillo, J.J. Laserna, Univ. of Málaga, Spain; J.M. Baena, Acerinox S.A., Spain.*
LIPS has been applied for remote analysis (20-100 meters) of solid samples using an open path optical configuration. Several applications including hot stainless steel analysis, geochemistry or analysis of hostile environments is currently in progress.

WA4 9:50am
Application of Doehlert experimental design for the optimization of LIBS analysis in Martian conditions, *René Brennetot, Jean Luc Lacour, Evelyne Vors, Pascal Fichet, Dominique Vailhen, Annie Rivoallan, CEA Saclay, France; Sylvestre Maurice, Midi Pyrennees Observatory, France.*
A project called MALIS (Mars elemental Analysis by Laser Induced breakdown Spectroscopy) is under investigation to perform in situ analysis of Mars soils and rocks. An experimental design based on a Doehlert matrix has been used for the first time to study the influence of major parameters on LIBS signal.

10:10am–10:40am
Coffee Break

Room: Royal Palm III

10:40am–12:20pm
WB ■ Hyphenated Techniques
Mohamad Sabsabi, Natl. Res. Council Canada, Canada, Presider Presider

WB1 10:40am Invited
LIBS using dual-laser pulses, *S. Michael Angel, Bill Pearman, Jonathan Scaffidi, Scott R. Goode, Univ. of South Carolina, USA.*
An orthogonal, dual-beam geometry provides enhanced emission and material ablation for solid samples and has recently been extended to aqueous solutions. We are also investigating subpicosecond dual-pulse excitation.

WB2 11:20am
Resonance-enhanced LIBS, *K.M. Lo, S.L. Lui, X.Y. Pu, N.H. Cheung, Hong Kong Baptist Univ., China.*
Resonant photoexcitation of major species in the vapor plume generated plasmas with lower continuum background and stronger analyte emissions than non-resonant LIBS plasmas. When applied to solid and aqueous samples, orders of magnitude improvement in sensitivity was demonstrated.

WB3 11:40am
Spectroscopic characterization of plasmas produced by dual-laser ablation, *V.S. Burakov, A.F. Bokhonov, M.I. Nedel'ko, N.A. Savastenko, N.V. Tarasenko, Natl. Acad. of Sciences of Belarus, Belarus.*
Based on the results of spectroscopic diagnostics a role of laser-surface and laser-plasma interactions in enhancement of line emission from plasma produced by the sequence of two laser pulses at different wavelengths is discussed.

WB4 12:00pm
Resonance-enhanced laser-induced plasma spectroscopy: Time-resolved studies and ambient gas effects, *Siu-lung Lui, Nai-ho Cheung, Hong Kong Baptist Univ., China.*
The dynamics of resonance-enhanced LIBS plasmas was investigated by time-resolved studies. In resonance case, a larger plume volume was heated. With right ambient gas, the plasma temperature could be sustained to enhance the analyte signal.

12:30pm–2:00pm
Lunch Break

Room: Royal Palm III

2:00pm–3:40pm
WC ■ New LIBS Methodologies and Instrumentation: I
Kevin L. McNesby, ARL, USA, Presider Presider

WC1 2:00pm Invited
Long term assessment of LIBS instrumentation in an industrial environment, *Doug Body, Bruce L. Chadwick, CRC Clean Power and Laser Analysis Tech., Australia.*
Testing of daily coal samples at commercial power stations using LIBS instrumentation and standard acid-extraction, AAS analysis has revealed excellent correlation ($R > 0.9$) between the two methods over 18 months of operation.

WC2 2:40pm
Geiger photodiode spectrometer for compact, lightweight LIBS instrumentation, *R.A. Myers, A.M. Karger, Radiation Monitoring Devices, Inc., USA; D.W. Hahn, Univ. of Florida, USA.*
We will discuss a unique spectrometer based on an array of Geiger photodiodes resulting in enhanced performance of laser induced breakdown spectroscopy instrumentation. These compact, silicon-based detectors eliminate the need for post amplification electronics and allow detection of single photons at room temperature.

WC3 3:00pm
Fiber optic modular spectroscopy and its application to LIBS, *Roy A. Walters, Jeremy B. Rose, Ocean Optics, Inc., USA.*
The application of miniature fiber optic modular spectroscopy to LIBS allows for great flexibility in data retrieval. A spectrometer with 200 nm to 980 nm range and 0.1 nm resolution observing only one laser event has been commercialized.

WC4 3:20pm
Optimization of laser-induced breakdown spectroscopy for liquid samples at millijoule pulse energies, *Mike Taschuk, Ying Tsui, Robert Fedosejevs, Univ. of Alberta, Canada.*
LIBS of Na in water samples results in detection limits of 2 to 200 ppm for pulse energies of 100 to 3 mJ respectively. The optimum conditions are consistent with the expansion of blast waves in air.

3:40pm–4:10pm
Coffee Break

Room: Royal Palm III

4:10pm–5:30pm
WD ■ New LIBS Methodologies and Instrumentation: II
Russell S. Harmon, US Army Research Office, USA, Presider Presider

WD1 4:10pm
Quantitative elemental analysis of metal alloys by laser induced breakdown spectroscopy using multivariate calibration, *Scott R. Goode, Richard Hoskins, Stephen L. Morgan, Univ. of South Carolina, USA.*
Laser induced breakdown spectroscopy has enjoyed acceptance as an analytical tool in many areas despite its spectral interferences. We demonstrate here the application of multivariate calibration for quantitative elemental analysis of metal alloys.

WD2 4:30pm
Shooting slurries: Sampling is the name of the game, *Daniel Michaud, Eric Proulx, Jean-Guy Chartrand, Louis Barrette, COREM, Canada.*
While analysing iron ore slurries in industrial and laboratory environments, many physical and geometric parameters were found to affect the stability and reproducibility of the LIBS response. A thorough re-examination of the sampling strategy lead to a revised sampling layout which ensures true representative sampling of the slurry and significantly improves sensitivity and repeatability.

WD3 4:50pm
Optimal boiler control through real-time monitoring of unburned carbon in fly ash using laser induced breakdown spectroscopy, *Miki Kurihara, Koji Ikeda, Yoshinori Izawa, Yoshihiro Deguchi, Mitsubishi Heavy Industries, Ltd., Japan; Hitoshi Tarui, Tohoku Electric Power Co. Inc., Japan.*
A LIBS technique has been applied to detect the unburned carbon in fly ash in a 1000MW pulverized coal fired power plant with the objective of achieving optimal and stable boiler control.

WD4 5:10pm
On-line analysis of liquid samples by laser induced plasma spectroscopy (LIPS), *M. Sabsabi, R. Héon, L. St-Onge, V. Detalle, A. Hamel, Industrial Materials Inst., Canada; J. Lucas, Noranda Tech. Ctr., Canada.*
A LIPS monitor for real-time analysis of aqueous and other liquids has been developed. This system enables the laser to sample a fresh surface while preventing problems associated with the laser liquid interaction. We outline its successful laboratory and on-line industrial operation.

5:30pm–8:00pm
Dinner Break

Room: Royal Palm III

8:00pm–10:00pm
Panel Discussion — LIBS & Homeland Defense
A. Miziolek, ARL, USA, Presider

Presider

■ Thursday
■ September 26, 2002

Room: Royal Palm III

8:30am–10:10am
ThA ■ LIBS for the Environment and Art
Mohamed Abdel Harith, Cairo Univ., Egypt, Presider

Presider

ThA1 8:30am Invited
Environmental application of laser induced breakdown spectroscopy, *Jagdish P. Singh, Virendra N. Rai, Mississippi State Univ., USA.*
Laser induced breakdown spectroscopy (LIBS) has the capability to perform rapid, online and real time analysis of materials in difficult and harsh environmental conditions. The application of LIBS, as a multi metal continuous emission monitor for off gases, in the analysis of soil and nuclear waste, is presented.

ThA2 9:10am
Environmental monitoring of total carbon and nitrogen in soils using laser-induced breakdown spectroscopy, *Madhavi Martin, Stan Wullschleger, Charles Garten Jr., Anthony Palumbo, Oak Ridge Natl. Lab., USA.*
We have successfully demonstrated the technique of laser-induced breakdown spectroscopy (LIBS) in the determination of the total concentration of carbon and nitrogen in soils. We have obtained a linear calibration curve for carbon in 15 soil samples directly correlated to the soil combustion technique.

ThA3 9:30am
Ambient measurements of inorganic species in an urban environment using LIBS, *Gregg A. Lithgow, Steven G. Buckley, Univ. of Maryland, USA; Allen L. Robinson, Carnegie Mellon Univ., USA.*
Inorganic species measurements of ambient aerosol in an urban environment are made using LIBS. Challenges of this type of sampling, including sampling configuration and spectrometer choice are discussed along with temporal measurement results.

ThA4 9:50am
LIBS: A new tool in archaeometry? *K. Melessanaki, S. Kotoulas, A. Petrakis, A. Hatziapostolou, D. Anglos, FORTH-IESL, Greece; S. Ferrence, P.P. Betancourt, Temple Univ., USA.*
Our experience with the development and use of a transportable, user-friendly LIBS instrument designed for use in the museum, the conservation laboratory or even at the excavation site is described and the potential of LIBS in archaeometry is discussed.

10:10am–10:40am
Coffee Break

Room: Royal Palm III

10:40am–12:20pm
ThB ■ LIBS in Life Sciences and Materials
Amy Hunter, Physical Sciences Inc., USA, Presider

Presider

ThB1 10:40am Invited
Biomedical applications of laser-induced breakdown spectroscopy, *Helmut Telle, Univ. of Wales Swansea, UK.*
Applications of laser-induced breakdown spectroscopy to the analysis of biological and medical samples are surveyed, and possible spatial resolution information (lateral and/or depth) will be discussed. Samples include calcified tissue, soft tissue and bio-fluid materials.

ThB2 11:20am
Fast identification of urinary tract stones via laser induced breakdown spectroscopy, *Mohamad A. Azooz, H. Imam, M.A. Harith, NILES, Cairo Univ., Egypt.*
Laser-induced breakdown spectroscopy has been used to identify five types of the most commonly known urinary stones. Specific combinations of spectral lines were selected as the finger print lines for each stone type.

ThB3 11:40am
Investigation of the analysis of pellet samples by laser-induced breakdown spectroscopy: Application to steel making slags, *C. Aragón, J.A. Aguilera, Univ. Pública de Navarra, Spain; F. Peñalba, Fundación INASMET, Spain.*
Experimental factors affecting laser-induced breakdown spectroscopy applied to steel making slags are investigated. Laser plasmas generated with pellet samples prepared from oxides (CaO, Fe_2O_3, SiO_2, Al_2O_3) and metallic Fe are characterized by emission spectroscopy.

ThB4 12:00pm
On-line detection of heavy metals and brominated flame retardants in technical polymers with laser-induced breakdown spectrometry, *M. Stepputat, R. Noll, Fraunhofer Inst. of Laser Tech., Germany.*
A LIBS analyzer with an autofocusing unit for the detection of heavy metals and brominated flame retardants in moving EOL-WEEE pieces is presented. Detection limits and classification results are discussed.

12:30pm–2:00pm
Lunch Break

Room: Royal Palm III

2:00pm–3:40pm

ThC ▪ Fundamentals of LIBS: I

Nicolo Omenetto, Univ. of Florida, USA, Presider

Presider

ThC1 2:00pm Invited

The potential of LIBS in spectrochemical analysis, *Kay Niemax, ISAS, Germany.*

The potential and limitations of LIBS for element analysis of solid samples are discussed. Particular attention will be paid to possible systematic errors in LIBS-analysis and how to reduce them.

ThC2 2:40pm

Experimental and theoretical investigation of the early stage of laser induced plasma produced by the interaction between a KrF excimer laser and a metallic titanium target, *A. De Giacomo, Dipartimento di Chimica, Italy; G. Colonna, IMIP-CNR, Italy; A. Casavola, Dipartimento di Chimica, Italy; O. De Pascale, IMIP-CNR, Italy.*

Time and space resolved Optical Emission Spectroscopy has been employed to investigate the evolution of the plasma produced by the interaction of UV laser beam with a metallic target of titanium at 10-5 Torr, until 3 mm from the target. By time of flight measurements and Boltzmann plots both the dynamic and the kinetic aspects have been discussed. A self-consistent model coupling collisional/radiative kinetics and fluid dynamic equations of the plume expansion has been successfully used for the interpretation of the experiments. The quasi-equilibrium state of the laser-induced plasma has been established as a result of the loss of Saha balance. The effect of three bodies recombination on atomic titanium temporal distribution has been explained.

ThC3 3:00pm

Laser-induced breakdown: Pressure and temperature dynamics, *C.G. Parigger, Univ. of Tennessee Space Inst., USA; I.G. Dors, Univ. of New Hampshire, USA.*

Fluid Physics phenomena following laser-induced breakdown are computed and compared with experimental records. Comparison of computational and experimental results give insight into the dynamics of the temperature and pressure profiles during the decay process.

ThC4 3:20pm

Semiempirical model of an optically thick laser induced plasma, *I.B. Gornushkin, C.L. Stevenson, B.W. Smith, N. Omenetto, J.D. Winefordner, Univ. of Florida, USA.*

A model of an optically thick inhomogeneous laser induced plasma is used to describe the time evolution of the plasma continuum and specific atomic emission after the laser pulse has terminated and interaction with a target material has ended.

3:40pm–4:10pm

Coffee Break

Room: Royal Palm III

4:10pm–5:30pm

ThD ▪ Fundamentals of LIBS: II

Stanley Michael Angel, Univ. of South Carolina, USA, Presider

Presider

ThD1 4:10pm

Spatial characterization of laser-induced plasmas by deconvolution of spatially resolved spectra, *J.A. Aguilera, C. Aragón, J. Bengoechea, Univ. Pública de Navarra, Spain.*

A numerical procedure has been developed to deconvolute the lateral integrated spectra of a laser-induced plasma. Three-dimensional distributions of emissivity, temperature, electron density and relative atom density have been obtained for an iron plasma.

ThD2 4:30pm

Temporal and spatial evolution of a laser induced plasma from a steel target, *M. Corsi, G. Cristoforetti, M. Hidalgo, D. Iriarte, S. Legnaioli, V. Palleschi, A. Salvetti, E. Tognoni, Inst. per i Processi Chimico, Italy.*

Temporally and spatially resolved measures of emission lines by a photomultiplier and shadow images by a frame camera were used to study the dynamical evolution of different elements in a steel plume in air produced by a Q-switched Nd:Yag laser.

ThD3 4:50pm

Study of the influence of Er:YAG and Nd:YAG wavelengths upon LIBS measurements under air or helium atmosphere, *V. Detalle, M. Sabsabi, L. St-Onge, A. Hamel, R. Héon, Natl. Res. Council Canada, Canada.*

Nd:YAG and Er:YAG lasers, with 1.06 and 2.94 μm wavelengths, have been used for LIBS analysis of solids. Using air or He buffer gases, the influence of the wavelength on the laser-produced plasma is studied.

ThD4 5:10pm

Plasma morphology and matrix effects interrelation in LIBS analysis, *Israel Schechter, Valery Bulatov, Rivie Krasniker, Israel Inst. of Tech., Israel.*

The interrelation between plasma morphology and the matrix effects may release LIBS analysis from the necessity of obtaining independent information on the matrix. This information can also be utilized for performing sophisticated LIBS analysis, such as distinguishing the organic carbon from the total carbon.

5:30pm–8:00pm

Dinner Break

Room: Royal Palm III

8:00pm–10:00pm
ThE ▪ Poster Session

ThE1
Laser-induced breakdown spectroscopy for quantitative analysis of aluminum alloy, *Awadhesh K. Rai, G.B. Pant Univ. of Agriculture and Tech., India; Fang Yu Yueh, Jagdish P. Singh, Mississippi State Univ., USA.*
LIBS spectra of molten Al alloys were recorded inside the melt and used to obtain the calibration curves for the minor elements. The methods to improve the measurement precision of LIBS application were studied and presented.

ThE2
Analysis of alluvial soils for environment survey by micro LIBS (μLIBS), *Denis Menut, Jean Luc Lacour, Pascal Fichet, Annie Rivoallan, CEA Saclay, France; Philippe Le Coustumer, Bordeaux 1 Univ., France.*
The LIBS technique has been mainly applied for bulk analysis of solids, liquids or gases but more sparsely for elemental micro analysis of solid surfaces. A μLIBS device devoted to element distribution analysis is described. Finally, the μLIBS technique appeared as a powerful analytical method for geological samples.

ThE3
A LIBS spectral database obtained in Martian conditions with an echelle spectrometer for in situ analysis of Mars soils and rocks, *Cécile Fabre, Jean Dubessy, Marie-Christine Boiron, CREGU UMR, France; René Brennetot, Pascal Fichet, Evelyne Vors, Jean Luc Lacour, Annie Rivoallan, CEA Saclay, France; Sylvestre Maurice, Midi Pyrenees Observatory, France; David Cremers, Roger Wiens, Los Alamos Natl. Lab., USA.*
MALIS (Mars elemental Analysis by Laser Induced breakdown Spectroscopy) is a project under study to perform in-situ geochemical analysis of Mars surface. Using specific standards, a spectral LIBS database is developed to observe actual sensitive emission lines of each element and to ensure their reliable recognition in Mars atmospheric conditions.

ThE4
Laser-induced plasma spectroscopy in near vacuum ultraviolet using ordinary spectrograph and ICCD, *Saara Kaski, Heikki Häkkänen, Jouko Korppi-Tommola, Univ. of Jyväskylä, Finland.*
An experimental setup to measure laser-induced plasma emission spectra with an ordinary Czerny-Turner spectrograph and intensified charge-coupled device in the near vacuum ultraviolet down to 130 nm is described. Spectra of bromine, chlorine and iodine were recorded to demonstrate the performance of the setup.

ThE5
Laser-induced breakdown spectroscopy: Analysis of OH spectra, *C.G. Parigger, J.O. Hornkohl, Univ. of Tennessee Space Inst., USA; G. Guan, Polytechnic Univ., Brooklyn, USA.*
Measured laser induced emission spectra of the OH radical subsequent to laser-induced optical breakdown in air are analyzed to infer spectroscopic temperature by use of Monte Carlo simulations.

ThE6
Laser-induced breakdown spectroscopy: Molecular spectra with BESP and NEQAIR, *C.G. Parigger, J.O. Hornkohl, Univ. of Tennessee Space Inst., USA; Anna M. Keszler, László Nemes, Chemical Res. Ctr., Hungary.*
Diatomic molecular spectra are modeled and compared with measured spectra to infer temperature and species density by use of the programs BESP (Boltzmann Equilibrium Spectrum Program) and NEQAIR (Non Equilibrium Air Radiation).

ThE7
Laser-induced breakdown spectroscopy used to detect palladium metal dispersed in cellulose membranes, *Madhavi Martin, Barbara Evans, Hugh O'Neill, Jonathan Woodward, Oak Ridge Natl. Lab., USA.*
Laser-induced breakdown spectroscopy (LIBS) was used to detect palladium in cellulose membranes. Different concentrations of palladium solution were used in the uptake of palladium into cellulose films. We have correlated the palladium concentration in various cellulose membranes to the technique of atomic absorption spectroscopy (AAS).

ThE8
Supersensitive detection of Na in water using dual-pulse laser-induced breakdown spectroscopy, *Akira Kuwako, Yutaka Uchida, Katsuji Maeda, Toshiba Corp., Japan.*
Supersensitive Na detection in water has been performed by using the LIBS technique, in which double pulsed and crossed beam Nd:YAG lasers are used. The detection limit was achieved in the range of 0.1ppb.

ThE9
Laser-induced breakdown spectroscopy: Balmer series H-beta measurements, *C.G. Parigger, Univ. of Tennessee Space Inst., USA; D.H. Plemmons, Plemmons Consulting, USA.*
Balmer series hydrogen-beta emission profiles are measured in a pulsed laser-induced breakdown micro-plasma. The line widths are used to infer electron number densities during the plasma decay.

ThE10
Quantum degeneracy and line emission in LIBS plasmas, *V.G. Molinari, D. Mostacci, F. Rocchi, M. Sumini, Univ. of Bologna, Italy.*
The effect of quantum degeneracy on collisional excitation is investigated, and its effect on line emission evaluated for application to quantitative spectroscopy in LIBS. Response matrix techniques are used to evaluate sensitivity to quantum degeneracy.

ThE11

Combination of nanosecond and femtosecond pulses in dual-pulse LIBS of solids and aqueous solutions, *Jonathan Scaffidi, Jack Pender, Univ. of South Carolina, USA; Bill Colston, Lawrence Livermore Natl. Lab., USA; S.R. Goode, S.M. Angel, Univ. of South Carolina, USA.*

Signal enhancement, limits of detection, and relevance to environmental concentrations for metals and metal ions in aqueous solution using combined 1064 nm nanosecond and 800 nm femtosecond pulses in dual-pulse LIBS will be presented.

ThE12

Spatio-temporal study of laser induced plasma on water surface of ionic solutions, *J. Ben Ahmed, G. Taieb, CNRS, Univ. de Paris XI, France; Z. Ben Lakhdar, Univ. El Manar, Tunisia.*

Spatio-temporal study of laser induced plasma on the surface of Ca^{++}, Mg^{++} water solutions is reported. Initial electronic temperature of 28000K and electronic density of 1.25 10^{18} cm^{-3} at t= 500 ns in the plasma center are measured.

ThE13

LIBS analysis of lichens as bioindicators of environmental pollution, *A. Tozzi, R. Barale, Univ. degli Studi di Pisa, Italy; G. Cristoforetti, M. Corsi, M. Hidalgo, D. Iriarte, S. Legnaioli, V. Palleschi, A. Salvetti, E. Tognoni, Inst. per i Processi Chimico, Italy.*

The concentration of pollutants in the epiphytic lichen Xanthoria parietina was measured with Laser-Induced Breakdown Spectroscopy technique. The analysis shown a very good agreement between the pollutant distribution and the location of the sampling sites.

ThE14

Single element recognition and quantitative analysis using a minimalist laser-induced breakdown spectroscopy system, *H.H. Telle, G.W. Morris, Univ. of Wales Swansea, UK; O. Samek, M. Liška, Brno Univ. of Tech., Czech Republic.*

We report on a simple set-up for laser-induced breakdown spectroscopy including an avalanche photodiode detector (gating by delayed bias voltage or frustrated total internal reflection modulator) and a narrow bandwidth interference filter for wavelength selection.

ThE15

The application of frustrated total internal reflection devices to analytical laser spectroscopy, *D.C.S. Beddows, H.H. Telle, Univ. of Wales Swansea, UK; O. Samek, Brno Univ. of Tech., Czech Republic.*

Novel implementations of single-fiber set-ups for laser-induced breakdown spectroscopy (LIBS) and laser-induced fluorescence spectroscopy (LIFS) systems in remote analysis applications are described, based on gated light switches exploiting Frustrated Total Internal Reflection (FTIR).

ThE16

Comparison between intensified CCD and non-intensified gated CCD detectors for LIPS analysis of solid samples, *M. Sabsabi, R. Héon, V. Detalle, L. St-Onge, A. Hamel, Industrial Materials Inst., Canada.*

An evaluation of the performance of spectrometer/ICCD and spectrometer/non-intensified gated CCD systems is carried out in terms of the spectrochemical analysis of metallic alloy samples by LIPS.

ThE17

A specific case of correction for laser-target coupling effect, *Louis Barrette, Daniel Michaud, Jean-Guy Chartrand, COREM, Canada; Marc L. Dufour, CNRC, Canada; François Lippens, EPSIMAGE, Canada.*

For material with a high transmittance coefficient at 1064 nm such as NaCl, minor contaminants like Ca and Mg heavily affect laser-target coupling. This results in a negative correlation between NaCl concentration and the net Na signal detected. This paper explores and discusses two methods of correction for this effect. The first one implies sample preparation where the coupling is standardized by the addition of an internal reference. The second may be used on-line and consists in measuring the amount of ablated material to correct the detected signal.

ThE18

Use of LIBS to determine carbon in soil for terrestrial carbon sequestration programs, *David A. Cremers, Mike Ebinger, Monty J. Ferris, David Breshears, Pat J. Unkefer, Los Alamos Natl. Lab., USA.*

LIBS in being developed as a field-deployable method to determine carbon in soil. Such a method is important to verify the efficiency of terrestrial carbon sequestration programs aimed at reducing global warming.

ThE19

2-D and 3-D chemical mapping of heterogeneous samples using microline-imaging laser-induced plasma spectrometry, *M.P. Mateo, L.M. Cabalín, J.J. Laserna, Univ. of Málaga, Spain.*

The performance and application of plasma spectrometry induced with a line-focused laser beam in generating fast 2 and 3-Dimensional compositional maps of different manufactured materials as well as of inclusionary material in stainless steel will be discussed.

ThE20

Characterization and identification of ammunition by laser induced breakdown spectroscopy, *Scott R. Goode, Andrea Thomas, Alexander A. Nieuwland, Stephen L. Morgan, Univ. of South Carolina, USA.*

Laser induced breakdown spectroscopy was used to characterize bullets, jackets, and cartridge cases from a small number of different manufacturers. LIBS spectra of these samples showed significant differences and could be accurately classified by source.

ThE21

Spectral analysis of the acoustic emission of laser-produced plasmas, *S. Palanco, J.J. Laserna, Univ. of Málaga, Spain.*

The acoustic analysis of shock wave emission from laser produced plasmas is presented. Characteristic frequency domain spectra from a number of elements and alloys are discussed.

ThE22

Development and testing of a prototype LIBS instrument for a NASA Mars rover, *David A. Cremers, Roger C. Wiens, Monty J. Ferris, James D. Blacic, Los Alamos Natl. Lab., USA.*

A compact LIBS instrument was built for NASA's Mars Instrument Development Program. The instrument was tested in the laboratory and on the NASA AMES K-9 rover and figures-of-merit obtained for analysis of geological samples.

ThE23

LIBS for real-time equivalence ratio measurements in a spark-ignited engine, *Francesco Ferioli, Steven G. Buckley, Univ. of Maryland, USA; Paulius V. Puzinauskas, U.S. Naval Acad., USA.*

LIBS is used to measure C, H, O, and N in real time to determine equivalence ratio of individual cylinder charges in a spark-ignited engine.

ThE24

Enhancement in the sensitivity of LIBS using magnetic field and sequensial double laser pulse, *V.N. Rai, A. Kumar, F.Y. Yueh, J.P. Singh, Mississippi State Univ., USA.*

The study of emission from laser-produced plasma from liquid jet is reported. Laser–induced plasma expanding in the magnetic field provides a 1.5-2 times enhancement in the plasma emission where as sequential double laser pulse excitation enhances the emission by more than four times.

ThE25

Assessment of metal and chlorine emissions from molten salt oxidation using laser-induced breakdown spectroscopy, *Jaya Kumar P. Patil, Steven G. Buckley, Univ. of Maryland, USA; Jerry S. Salan, Indian Head Naval Surface Warfare Ctr., USA.*

Molten salt oxidation is a promising waste destruction technique with potential for trapping halides and heavy metals. LIBS is used to measure Cl and metals in the effluent, and efficiency is investigated as a function of operational parameters.

ThE26

Influence of spark size and temperature on LIBS gating for optimal detection limits for toxic metals, *Steven G. Buckley, Gregg Lithgow, Francesco Ferioli, Elizabeth Smallwood, Univ. of Maryland, USA.*

This work experimentally examines the influence of initial spark size and temperature upon the optimum gating and ultimate detection limits of selected RCRA toxic metals. The results are compared with simple theoretical analysis to facilitate extension to additional elements.

ThE27

Reduction of spatial effects on emission line intensity observed from single aerosol particles via diffuse reflectance from an integrating sphere, *Emily Gibb, Erica Corbett, Igor Gornushkin, Ben Smith, David Hahn, Jim Winefordner, Univ. of Florida, USA.*

Collection of emission via diffuse reflectance from an integrating sphere reduces the influence of spatial effects observed when viewing LIBS plasma emission from the backscatter collection mode.

ThE28

Two photon excited fluorescence of donor-acceptor conjugated materials in crystalline form, *Ekaterina V. Sevostiyanova, David M. Sammeth, Mikhial Yu. Antipin, New Mexico Highlands Univ., USA.*

The crystal structures and fluorescence properties of organic materials that possess high efficiency two-photon excited fluorescence in crystalline form and do not display considerable molecular two-photon absorption resonance were investigated. The structural features responsible for the properties were determined.

ThE29

LIBS analyses of Martian soils under controlled atmosphere, *F. Colao, R. Fantoni, V. Lazic, A. Paolini, ENEA, FIS-LAS, Italy.*

LIBS measurements were performed under controlled atmosphere on the samples with the composition similar to the Martian crust. The experiment demonstrated that quantitative LIBS analyses are feasible in Mars-similar conditions.

■ Friday
■ September 27, 2002

Room: Royal Palm III

8:30am–9:50am
FA ■ Femtosecond LIBS
Yoshihiro Deguchi, Mitsubushi Heavy Ind. Ltd., Japan, Presider Presider

FA1 8:30am Invited
Exotic LIBS- Femtosecond Domain, *Dennis Alexander, Univ. of Nebraska, USA.*
Femtosecond lasers with pulse lengths down to 5 fs are available for performing femtosecond laser induced breakdown spectroscopy (FLIBS). The linear and nonlinear effects of these short pulses interacting with materials produce complicated ionization processes and plasmas. Experimental FLIBS has been carried out and the results will be presented on several materials.

FA2 9:10am
Investigation of femtosecond laser produced plasma expansion by laser-induced fluorescence imaging, *V. Margetic, F. Leis, K. Niemax, R. Hergenröder, Inst. of Spectrochemistry and Applied Spectroscopy, Germany; T. Ban, Inst. of Physics, Croatia; O. Samek, V. Malina, Inst. of Physical Engineering, Brno Univ. of Tech., Czech Republic.*
In order to investigate temporally and spatially resolved expansion dynamics of the femtosecond laser-induced plasma we measured fluorescence light emission. To obtain the radial distribution of emitting atoms the Abel inversion was employed.

FA3 9:30am
In-depth profiling of multi-layer samples with femtosecond laser, *V. Margetić, K. Niemax, R. Hergenröder, Inst. of Spectrochemistry and Applied Spectroscopy, Germany.*
Femtosecond laser induced plasma spectroscopy (LIBS) and femtosecond laser ablation time of flight mass spectrometry (LA-TOF-MS) were used for analysis of multi-layered samples with sub-micrometer thickness. Feasibility of the fs-LA in-depth profiling is discussed.

9:50am–10:20am
Coffee Break

Room: Royal Palm III

10:20am–12:20pm
FB ■ LIBS for Materials Analysis
Dennis R. Alexander, Univ. of Nebraska, USA, Presider Presider

FB1 10:20am
In situ LIBS analysis of steel pipes at high temperature, *G. Cristoforetti, M. Corsi, M. Hidalgo, D. Iriarte, S. Legnaioli, V. Palleschi, A. Salvetti, E. Tognoni, Inst. per i Processi Chimico, Italy; S. Green, Progressive Energy Tech. Ltd., UK; D. Bates, DRB Materials Tech., UK; A. Steiger, J. Fonseca, J. Martins, UNINOVA, Portugal; J. McKay, ENICHEM, UK; B. Tozer, D. Wells, R. Wells, LASERMET, UK.*
The results of a measurement campaign for analysis of steel pipes in a styrene plant are reported. The measurements were performed during the normal operation of the plant.

FB2 10:40am
Detecting gunshot residue by laser induced breakdown spectroscopy, *Scott R. Goode, Christopher R. Dockery, Michael F. Bachmeyer, Alexander A. Nieuwland, Stephen L. Morgan, Univ. of South Carolina, USA.*
Laser induced breakdown spectroscopy was used to detect gunshot residue (GSR) on a shooter's hand. Double sided tape pressed to the skin of the shooter was directly analyzed. Characteristic emission lines indentified GSR presence.

FB3 11:00am
LIBS analysis of pharmaceutical solid dosage forms, *Yves Mouget, Patrick Gosselin, Martine Tourigny, Simon Béchard, Pharma Laser Inc., Canada.*
Speed of analysis and minimal sample preparation make LIBS ideal for the analysis of pharmaceutical solid dosage forms for blend, content, and coating thickness uniformity. Inter-tablet %RSD values of less than 4% are easily achieved.

FB4 11:20am
Analysis by LIBS of complex solids, liquids and powders with an echelle spectrometer, *Pascal Fichet, Denis Menut, René Brennetot, Annie Rivoallan, CEA Saclay, France.*
One of the most promising approaches for the LIBS experiment involves the use of an echelle spectrometer. Quantitative results obtained with such apparatus on solids, liquids and powders will be described and compared with others coming from a Czerny Turner spectrometer

FB5 11:40am
Progress in LIBS analysis for military applications: Explosives detection, *Russell S. Harmon, Andrzej W. Miziolek, Kevin L. McNesby, ARL, USA; Thomas F. Jenkins, Marianne Walsh, Cold Regions Res. and Engineering Lab., USA.*
A broadband survey of explosives and explosive residues on snow and soils from Army firing ranges reveals characteristic spectra for different explosive types, suggesting a potential to develop a field-portable LIBS instrument for landmine/UXO detection.

FB6 12:00pm
Spark-induced breakdown spectroscopy (SIBS) field screening monitor for toxic metal detection in soil, *A.J.R. Hunter, R.T. Wainner, L.G. Piper, S.J. Davis, Physical Sciences Inc., USA.*
Spark-Induced Breakdown Spectroscopy (SIBS) is a recently developed analog of LIBS. We will present data acquired during applications of SIBS to measurement of toxic metals in soil, as well as methodology required for quantitative analysis.

12:20pm–2:00pm
Lunch Break

Room: Royal Palm III

2:00pm–3:00pm
FC ▪ LIBS Analysis of Particulate Matter
Simon Bechard, PharmaLaser Inc., Canada, Presider
Presider

FC1 2:00pm Invited
Single particle LIBS, *David W. Hahn, Jorge E. Carranza, Univ. of Florida, USA.*
LIBS is sensitive enough to measure aerosol elemental size and composition of individual particles. Single-shot LIBS analyses of aerosols raises new questions regarding shot-to-shot fluctuations and data precision, as well as issues involving the fundamental interaction between the laser-induced plasma and aerosol particles.

FC2 2:40pm
Monitoring of heavy metals in particulates suspended in flue gas by LIBS, *R. Yoshiie, M. Nishimura, H. Moritomi, Gifu Univ., Japan.*
Calibration lines for relative line intensities of iron and lead against their concentration ratios in particle samples, simulating fly ash, are presented. To generalize these calibration lines, plasma temperature was also investigated via Boltzmann plots.

Room: Royal Palm III

3:00pm–4:00pm
FD ▪ Laser Ablation and Desorption
Ulrich Panne, Tech. Univ. of Munich, Germany, Presider
Presider

FD1 3:00pm Invited
Influence of crater dimensions on laser induced plasma properties, *Richard E. Russo, Xianzhong Zeng, Samuel S. Mao, Chunyi Liu, Xianglei Mao, Lawrence Berkeley Natl. Lab., USA.*
Si emission lines were measured inside and outside of several craters. The spatial distribution of plasma temperature and electron number density were determined by measuring Stark broadening of the emission lines and the relative line-continuum ratio.

FD2 3:40pm
The effect of laser-induced crater depth in LIBS analysis and shock wave dynamics, *M. Corsi, G. Cristoforetti, M. Hidalgo, D. Iriarte, S. Legnaioli, V. Palleschi, A. Salvetti, E. Tognoni, Inst. per i Procesi Chimico, Italy.*
The influence of the crater depth on the laser-produced plasmas properties has been studied. The dynamics of the shock waves resulting from the laser-sample interaction inside and outside the craters and the results of in-depth LIBS analysis of metallic samples are discussed.

4:00pm–4:30pm
Coffee Break

Room: Royal Palm III

4:30pm–5:30pm
FE ▪ Imaging, Surface Mapping and Stratigraphy by LIBS
Demetrios Anglos, Inst. of Electronic Structure and Laser, Greece, Presider
Presider

FE1 4:30pm
Laser micro analysis of glass and tool steel, *K. Loebe, H. Lucht, A. Uhl, LLA Instruments GmbH, Germany.*
Micro analytical characterization of glass and tool steel is now possible by a new developed UV-laser microscope using LIBS. Coupled by a fiber optics to an Echelle spectrometer, it offers simultaneous qualitative and semi-quantitative multi-element-analysis.

FE2 4:50pm
Micro-LIBS and micro-Raman spectroscopic analysis of ancient pottery, *G. Cristoforetti, M. Corsi, M. Giuffrida, M. Hidalgo, D. Iriarte, S. Legnaioli, V. Palleschi, A. Salvetti, E. Tognoni, Inst. per i Processi Chimico, Italy; G. Boschian, S. Mazzoni, Univ. di Pisa, , Italy.*
Several samples of oriental colored pottery have been analyzed with micro-LIBS and micro-Raman technique in order to get information about the elemental composition and molecular structure of the pigments used.

FE3 5:10pm
Laser emission spectroscopy (LIBS) for plated layer thickness identification, *George Asimellis, Bruce Bromley, Stu Rosenwasser, Advanced Power Tech., Inc., USA.*
A LIBS instrument identifies layer thickness on steel core coins with alternating layers of Nickel, Copper, and Nickel. Layer thickness is determined by tracking the element concentration changes on successive shots.

6:00pm–10:00pm
Conference Social Event

Saturday
September 28, 2002

Room: Royal Palm III

9:00am–10:30am
Panel Discussion — Future of LIBS Sensor Technology and Applications I
V. Palleschi, Inst. per i Procesi Chimico, Italy, Presider

Presider

10:30am–11:00am
Coffee Break

Room: Royal Palm III

11:00am–12:30pm
Panel Discussion — Future of LIBS Sensor Technology and Applications II
L. Radziemski, Washington State Univ., USA, Presider

Presider

12:30pm–12:40pm
Closing Remarks
A. Miziolek, ARL, USA

Laser Induced Plasma Spectroscopy and Applications

Exotic LIBS

Wednesday, September 25, 2002

Vincenzo Palleschi, Inst. of Atomic and Molecular Physics, Italy,
Presider

WA
8:30am–10:10am
Room: Royal Palm III

Extreme LIBS

A.I. Whitehouse, J. Young and C.P. Evans
Applied Photonics Ltd, Unit 8 Carleton Business Park, Skipton, North Yorkshire BD23 2DE, U.K.
Tel.: +44 (0) 1756 708900, Fax., +44 (0) 1756 708909, email: mail@appliedphotonics.co.uk

Abstract: A summary of selected applications of Laser-Induced Breakdown Spectroscopy (LIBS) conducted for the nuclear power generation and spent-fuel reprocessing industries within the United Kingdom are presented. Various types of fibre-optic probe and telescope LIBS instrument, together with a description of the methods adopted for their deployment, are discussed.

OCIS codes: (300.6360) Laser spectroscopy; (280.0280) Remote sensing

Summary

Due to its ability to analyse materials remotely, LIBS is often claimed as being eminently suitable for applications involving hazardous materials or difficult-access environments. It could be argued that this "unique selling point" of LIBS has played an important role in helping many research groups obtain funding for their work. Eventually, of course, there comes a time when the research group concerned must deliver on its claims, the consequences of which may be such that the researcher is required to work in environments far less hospitable than the laboratory.

This presentation describes the experiences of one such group who had for many years been extolling the virtues of LIBS before being required to use it in a number of demanding applications within the nuclear industry. An overview of selected industrial applications of LIBS will be presented with an emphasis on the practical aspects of deploying the technology within a nuclear environment.

In-situ measurements of the copper content of 316H stainless-steel superheater bifurcation tubes within the pressure vessels of Advanced Gas-Cooled Reactor (AGR) nuclear power stations

A novel-design fibre-optic probe LIBS instrument incorporating a 75-metre armoured umbilical has been developed for use within the pressure vessels of Advanced Gas-Cooled Reactor (AGR) nuclear power stations [1]. The instrument was designed to remotely determine the copper content of 316H austenitic stainless-steel superheater bifurcation tubing with the aim of identifying components manufactured from a certain batch of steel. It was suspected that this batch of steel suffered from low-creep ductility, a condition that could result in premature failure of the bifurcation welds with the consequent risk of steam leaks. This represented a significant commercial threat to the operation of the reactors and hence identification of the suspect components was necessary.

It was believed that the suspect batch of steel exhibited higher than normal concentrations of copper and that this may help in the process of identification of suspect bifurcations. Compositional analysis of the steel could be used to measure the copper concentration but the severely restricted physical access to the bifurcations and the hostile environment of the reactor pressure vessel were such that removal of physical samples of the components for laboratory analysis was not feasible. The problem was exacerbated by the number of bifurcations requiring inspection, 528 in each of four reactors, and the limited time available to conduct a survey of each reactor. Inspections could only be carried out during a routine reactor outage, during which time the reactor is shut down and the pressure vessel opened up to allow man-access to the steam generators.

The environment within the pressure vessel is particularly demanding for the in-vessel inspection personnel. Ambient temperatures of up to 60°C, high noise levels, buffeting from the flow of cooling air, severely restricted physical access and confined working space placed severe physical demands on the in-vessel inspection team. The environment of the pressure vessel is classed in radiological terms as an R4/C3 area, indicating that radiation levels are relatively high and airborne radioactive contamination is possible. Specially-designed air-fed 'Hot-Suits' are used to provide protection for the vessel entrants against heat, noise and radioactive contamination. An umbilical is used to supply cooling and breathing air to the suit and to provide a communications link with the vessel entry controller and other vessel entrants. The descent into the vessel from the pile cap is made via a 15 metre vertical access ladder which leads to a circular walkway situated between the dome of the reactor and the twelve steam generators (figure 1). Between each steam generator is another vertical ladder leading down to the Sub-Boiler Annulus at the lowest part of the pressure vessel. After descending this ladder for about 4 metres, access to a superheater is made via a small hatch.

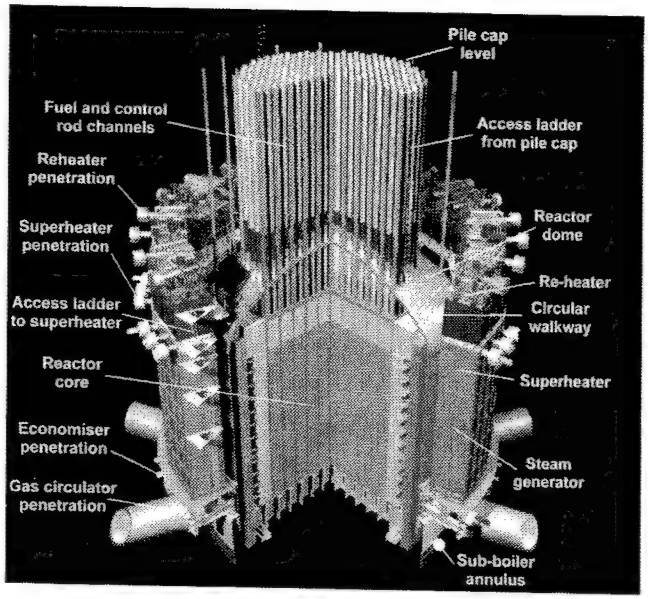

Fig. 1. CAD view of an Advanced Gas-Cooled Reactor (AGR) and associated steam generators

There is approximately 1 metre of headroom inside the superheaters, meaning that the inspection work must be carried out with the vessel entrant in a semi-prone position on top of the banks of bifurcations (figure 2). Each vessel entry period is limited to a maximum of 2 hours which, after allowing for the time taken to enter and exit the vessel, leaves little more than 1 hour to carry out the inspections. A 3-shift working pattern was adopted with the aim of completing a survey of a superheater within 2 to 3 shifts.

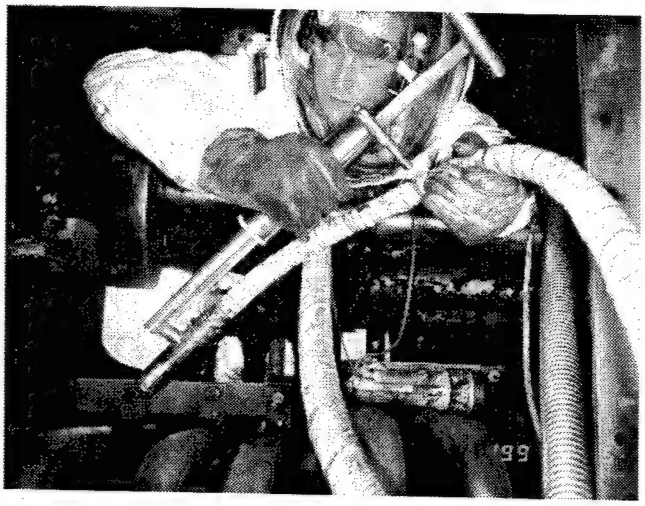

Fig. 2. Deployment of the LIBS probe within an AGR superheater

In-situ measurements of the chromium content of economiser tubes within the pressure vessel of an AGR nuclear power station

A modified version of the fibre-optic LIBS instrument described above was used to remotely determine the chromium content of mild-steel economiser tubing within the Sub-Boiler Annulus (SBA) of reactor 4 at Hunterston B station (see figure 1 for location of the SBA). The measurements were required as part of an inspection programme undertaken to identify tubes that had suffered damage through the effects of a process known as erosion-corrosion. Erosion-corrosion is a mechanical process affecting tubes whereby oxide crystals are removed from the surface of the tube wall either by high shear-stress or particles introduced via the flow. Erosion-corrosion has been found to be particularly associated with mild-steel tubing at elevated temperatures of 90-300°C [2].

Access to the SBA was achieved by removing one of the gas-circulators and installing a temporary air-lock and change-room structure within one of the gas circulator ports. The fibre-optic umbilical of the LIBS instrument was fed into the SBA via a ventilation duct situated adjacent to the air-lock. Temporary scaffold towers were erected within the SBA to facilitate access to the banks of economiser tubes located directly below the steam generators and approximately six metres above the floor level.

The LIBS instrument was deployed successfully at Hunterston B AGR power station in February 2001. Measurements of a number of tubes were carried out, the results of which indicated that the tubes examined were manufactured from steel having a chromium content of higher than 0.1% and hence were unlikely to be affected by erosion-corrosion. This finding was consistent with the results of previous video probe inspections confirming that the internal bore of the tubes had not been adversely affected by erosion-corrosion.

Non-invasive compositional analysis of radioactive contamination within a Hot-Cell environment

A transportable telescopic LIBS instrument has been used to perform non-invasive elemental analysis of a highly radioactive material by transmitting the laser beam through a 1-metre thick lead-glass shield window of a Hot-Cell. This simple method of deployment, illustrated schematically in figure 3, allowed the major elemental constituents of the radioactive material to be identified quickly, without breaching containment and without the need for additional equipment to be placed inside the Hot-Cell.

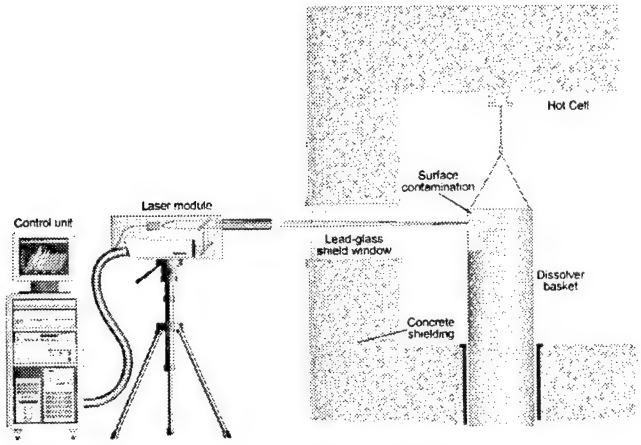

Fig. 3. Schematic diagram of a telescopic LIBS instrument deployed via the shield-window of a Hot-Cell

Identification of cooling water tubes and reinforcing bars within Magnox reactor pressure vessels using a telescope LIBS instrument

During a maintenance and repair programme at a Magnox nuclear power station in the UK, there was a requirement to drill a large number of bore-holes into the steel-reinforced concrete pressure vessels of the two reactors. The bore-holes, which were of 20 mm diameter and depth up to 1 metre, were to be used for anchor points for a reinforcing structure being added to the superheater penetrations. Within the vicinity of these penetrations, cooling water tubes are embedded in the structure to prevent the concrete from overheating. It was imperative not to damage these cooling water tubes when drilling the boreholes and hence a method was devised to automatically stop the drilling process in the event of contact with a metallic object. Due to the large number of reinforcing bars also present within the concrete structure, a method was required to distinguish between a cooling water tube and a reinforcing bar. Physical access to the component was severely restricted due to the diameter and length of the bore-hole, making the task of identification particularly difficult. As there was line-of-sight access to the steel component, a purpose-designed LIBS instrument was used to identify the component by detecting known differences in composition between the cooling water tubes and reinforcing bars.

References

1. A.I. Whitehouse, J. Young, I.M. Botheroyd, S. Lawson, C.P. Evans, J. Wright, "Remote material analysis of nuclear power station steam generator tubes by laser-induced breakdown spectroscopy," Spectrochim. Acta Part B, **56**, 821-830 (2001).
2. B. Poulson, "Complexities in predicting erosion-corrosion," Proc. Of Wear - Lausanne, **233-235**, 497-504 (1999).

Capabilities of LIBS for analysis of geological samples at stand-off distances in a Mars atmosphere

David A. Cremers[1], Roger C. Wiens[2], and Monty J. Ferris[1]
[1]*Advanced Diagnostics and Instrumentation, MS J565*
[2]*Atmospheric and Space Sciences, MS D466*
Los Alamos National Laboratory, Los Alamos, NM 87545
Tel: 505-665-4180; Fax: 505-665-6095:e-mail: cremers_david@lanl.gov

Rene Brennetot
CEA Saclay, Fuel Cycle Division, LALES DEN/DPC/SCPA Bâtiment 391, 91191 Gif sur Yvette France
Tel : (33) 1 69 08 77 53; Fax : (33) 1 69 08 77 38; e-mail : brennetot@carnac.cea.fr

Sylvestre Maurice
Midi Pyrenees Observatory
Tel : (33) 5 61 33 29 4;7 Fax : (33) 1 61 33 28 40; e-mail : maurice@ast.obs-mip.fr

1. Introduction

Through funding from NASA's Mars Instrument Development Program (MIDP), we have been evaluating the use of LIBS for future use on landers and rovers to Mars. Of particular interest is the use of LIBS for stand-off measurements of geological samples up to 20 meters from the instrument. Very preliminary work on such remote LIBS measurements, based on large laboratory type equipment, was carried out about a decade ago [1]. Recent work has characterized the capabilities using more compact instrumentation [2] and some measurements have been conducted with LIBS on a NASA rover testbed [3].

There is interest in LIBS for this application because of its many unique analysis capabilities compared to methods of elemental analysis used on previous missions and instruments being considered for near term flights. These are x-ray fluorescence (XRF) and the alpha proton x-ray spectrometer (APXS). Important LIBS advantages include: (1) Rapid analysis - i.e. each laser pulse generates one plasma and one measurement. (Many spectra may be averaged together, however, to increase accuracy/precision and to average out sample inhomogeneities.); (2) All elements (high and low z) can be detected; (3) Stand-off analysis capability – the laser pulse can be focused at a distance on a solid to generate the laser plasma for remote analysis [4]; (4) Surface cleaning – repetitive sampling at the same spot permits ablation through weathered surfaces to reach the underlying bulk rock and provides ejection of dust from a surface [2].

2. Experimental apparatus

Two configurations were used here. The first consisted of a large laboratory-sized laser (Spectra-Physics GCR-11) and spectrograph (Chromex 0.5 m) with a gated CCD detector (Andor Technology, InstaSpec V). This system was similar to that used in a previous study [2]. The second apparatus was a prototype LIBS instrument used on 2000/2001 field test rover [3] and for other field tests. It consists of a compact flashlamp-pumped Nd:YAG laser (80 mJ/pulse, 0.1 Hz, 1064 nm), an adjustable beam focusing system (6.4 cm diameter lens) to focus the pulses on remotely located samples and collect the plasma light. The collected light is transported to the detection system consisting of a compact echelle spectrograph (Catalina Scientific Inc., $\lambda/\Delta\lambda$=2500) and a gated-intensified array detector. Data analysis is provided by manufacturer-supplied software and software written in-house combining peak searches with calibration protocols.

3. Analysis requirements for Mars

This work is being carried out with emphasis on analysis requirements important to understanding Mars geology. Current knowledge is based on data from XRF on Viking and APXS on Pathfinder, from the SNC meteorites, and from remote sensing, (TES, Themis, and orbital gamma-ray spectrometry data). Only major element compositions have been obtained directly using XRF and APXS as TES and Themis can only infer elemental compositions. Minor and trace elements have been determined from the SNC meterorites, however. Uncertainties in major element concentrations have been large (Fe ~25% and Si ~10% [5]), which, along with the absence of mineralogical data, has left ambiguous whether the rocks were igneous or sedimentary [6]. In addition, the possible existence of weathered coatings on the rocks complicates the issue as the true composition of the underlying rock may not have

been measured: TES results suggest that much of the northern hemisphere is andesitic [7] but the data may also be interpreted as partially weathered basalt [8]. Detailed characterization of such coatings, if they exist, is very important not just to understand the underlying rock types, but also because of the wealth of information regarding atmosphere-surface interactions leading to weathering. Therefore, it is important that major elements be measured to ±10% and to have the capability to remove dust coatings and to depth profile through weathering rinds or coatings, at a spatial resolution of several microns.

Minor and trace element compositions are important in determining the provenance of rocks and dusts. For example, the global dust component likely arose from a combination of basaltic weathering plus a sulfur-rich component of either volcanic aerosol or hydrothermal origin. Major elements cannot distinguish between these components, but minor and trace element compositions should be completely diagnostic, as ratios such as Ba/Li or Zn/Li are predicted to vary by several orders of magnitude between proposed sources [9]. Likewise, minor and trace elements are important constraints on sedimentary processes. Therefore trace element detection of at least 10 species should be measurable with detection limits < 100 ppm to ±40%, including Ba, Li, Rb, Sr with detection limits ≤ 20 ppm. The ability to measure these separately in dust and in pristine rocks is required.

4. Matrix effects

The laser spark is known to exhibit both physical and chemical matrix effects. These can limit the ability to quantify a LIBS measurement, especially for complex matrices represented by geological samples. An example of the effect

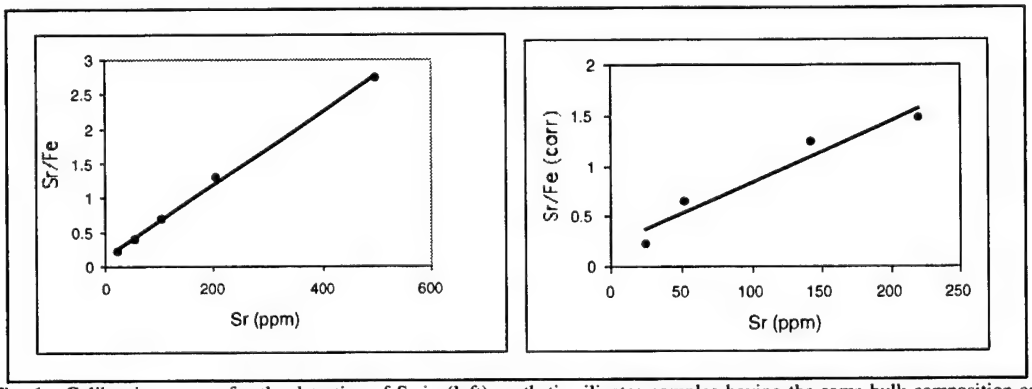

Fig. 1. Calibration curves for the detection of Sr in (left) synthetic silicates samples having the same bulk composition and (right) stream sediments with different bulk matrix compositions. The average RSD of measurements using the synthetic silicate and stream sediment samples were 5.5% and 12.3%, respectively.

of the matrix is shown in Figure 1. The data on the left refer to a calibration curve prepared using a set of synthetic silicate standards with a uniform bulk matrix composition but having significant variations in trace and minor elements. The data on the right correspond to stream sediment samples with variations in the concentration of major elements composing the matrix. These data were obtained with the samples placed in a 7 Torr CO_2 atmosphere at a distance of 19 m. Pulses of 80 mJ were used to interrogate the samples. It is clear that the bulk matrix effects the calibration for Sr as the data obtained using samples having different bulk compositions is significantly less correlated than the data obtained using samples having the same bulk compositions. Similar results showing greater differences between the two curves were obtained for other elements. All samples used here were finely ground powders of uniform size that were pressed into pellets. In terms of use on board a Mars lander or rover, the complete lack of sample preparation capability limits the ability to quantify even more. Therefore, study of the effect of the matrix both in terms of sample inhomogeneity and differences in bulk composition is important.

5. Detection Limits, Accuracy, and Precision

Measurement accuracy and precision are important for reasons described in Section 3. Representative values of these are listed in Table 1 for measurements taken at a distance of 2.3 meters using the compact LIBS prototype instrument and 14 certified standards as samples.

Table 1. Accuracy and precision

element	accuracy	precision
Al	4.4%	5.1%
Cr	7.7	5.6
Mg	3.2	5.2
Mn	4.2	3.8
Si	4.7	3.7
Sr	6.3	6.5

6. Other Detection Capabilities

In addition to geological targets, other targets are of interest such as ice (i.e. for missions that may focus on the Mars polar regions). The ability to detect ice is shown in Figure 2. Identification is via the OH bandhead emission at 306.4 nm. This spectrum was acquired at a distance of 3 meters with the ice sample in 7 Torr CO_2. In addition to the simple identification of ice as evidence of water, there is also interest in detecting dusts that may be mixed with the ice and have become stratified over time.

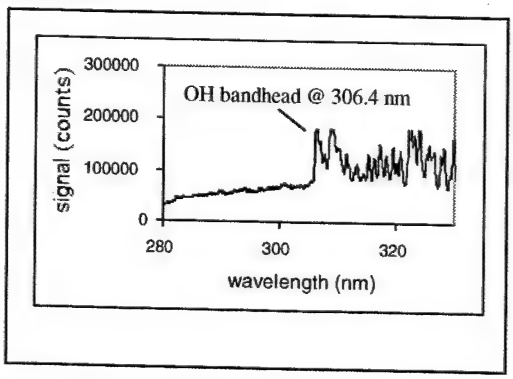

Fig. 2. LIBS spectrum acquired from an ice sample using the compact LIBS prototype instrument. The OH bandhead at 306.4 nm is clearly evident

7. References

[1] J.D. Blacic, D.R. Pettit, and D.A. Cremers, "Laser-Induced Breakdown Spectroscopy for Remote Elemental Analysis of Planetary Surfaces," in the Proceedings of the International Symposium on Spectral Sensing Research, Maui, HI, November 15-20 (1992).

[2] A.K. Knight, N.L. Scherbarth, D.A. Cremers, and M.J. Ferris, "Characterization of Laser-Induced Breakdown Spectroscopy (LIBS) for Application to Space Exploration," Appl. Spectrosc. **54**, 331 (2000).

[3] R.C. Wiens, R.E. Arvidson, D.A. Cremers, M.J. Ferris, J.D. Blacic, and F.P. Seelos,IV, "Combined remote mineralogical and elemental measurements from rovers: Field and laboratory tests using reflectance and laser induced breakdown spectroscopy," J. Geophys. Res., Planets, accepted for publication (2002).

[4] D.A. Cremers, "Analysis of Metals at a Distance Using Laser-Induced Breakdown Spectroscopy," Appl. Spectrosc. **41**, 572-57 (1987).

[5] J. Bruckner, G. Dreibus, R. Rieder, and H. Wanke H., "Revised data of the Mars Pathfinder Alpha Proton X-ray Spectrometer: Geochemical behavior of major and minor elements," Lunar Planet. Sci. XXXII, abstr # 1293, The Lunar and Planetary Institute, Houston, TX (2001).

[6] H.Y. McSween Jr., S.L. Murchie, J.A. Crisp, N.T. Bridges, R.C. Anderson, J.F. Bell, D.T. Britt, J. Bruckner, G. Dreibus, Economou T., A. Ghosh, M.P. Golombek, J.P. Greenwood, J.R. Johnson, H.J. Moore, R.V. Morris, T.J. Parker, R. Rieder, R. Singer, H. Wanke, "Chemical, multispectral, and textural constraints on the composition and origin of rocks at the Mars Pathfinder landing site," J. Geophys. Res. **104**, 8679-8715 (1999).

[7] J.L. Bandfield, V.E. Hamilton, and P.R. Christensen, "A Global View of Martian Surface Compositions from MGS-TES," Science **287**, 1626-1630 (2000).

[8] H.Y. McSween, "Basalt or andesite? A critical evaluation of constraints on the composition of the ancient martian crust." Lunar Planet Sci. XXXIII, 1062, The Lunar & Planetary Institute, Houston, TX (2002).

[9] H.E. Newsom, J. J. Hagerty, and F. Goff, "Mixed hydrothermal fluids and the origin of the Martian soil," J. Geophys. Res. (Planets), **104**, 8717-8728, (1999).

OPEN-PATH LASER INDUCED PLASMA SPECTROMETRY FOR THE STAND-OFF DETECTION AND FAST SCREENING OF SOLID SAMPLES

D. Romero[1], P.L. García[1], S. Palanco[1], J.M. Vadillo[1], J.M. Baena[2] and J.J. Laserna[1]

[1]*Department of Analytical Chemistry, Faculty of Science, University of Málaga, Campus de Teatinos s/n 29071, Málaga, Spain.*

[2]*Acerinox S.A., Villa de Palmones, 11397, Los Barrios, Cádiz*

laserna@uma.es

Abstract. LIPS has been applied for remote analysis (20-100 meters) of solid samples using an open path optical configuration. Several applications including hot stainless steel analysis, geochemistry or analysis of hostile environments is currently in progress.

Summary

Remote analysis process involves two general steps; sample excitation and chemical information collection by a suitable optical system. The whole process is performed without physical contact with the sample. Traditionally, laser remote analysis has been related with spectroscopic techniques based on light scattering methods as Rayleigh scattering, Mie scattering, Raman scattering, resonance scattering or other as fluorescence, absorption and differential absorption. Despite of the generic term, remote laser analysis is almost related to studies involving atmospheric chemistry and environmental applications. However, the development of analytical techniques to remotely extract the composition and structure of a certain sample under unfavorable situations (as hostile or corrosive environments) or sample inaccessibility (as in the case of cone penetrometers) must be considered as remote analysis as well.

In this contribution, LIPS has been investigated for remote analysis of solids placed at distances between 10 to 100 meters away from the spectrometer. An open-path configuration using a reflective Newtonian telescope to collect the plasma light (similar to those one used in LIDAR experiments) has been chosen. The stand off analysis of melted solids in terms of signal to noise ratios and reproducibility will be studied. Quantitative analysis of hot steel inside a laboratory furnace, an application impossible to be performed with current analytical technologies has been successfully performed.

Application of Doehlert experimental design for the optimization of LIBS analysis in Martian conditions

Rene BRENNETOT [1], Jean Luc LACOUR [1], Evelyne VORS [1], Pascal FICHET [1], Dominique VAILHEN [2], Sylvestre MAURICE [3] and Annie RIVOALLAN [1]

[1] *CEA Saclay, Fuel Cycle Division, LALES DEN/DPC/SCPA Bâtiment 391, 91191 Gif sur Yvette France*
Tel : (33) 1 69 08 77 53 FAX : (33) 1 69 08 77 38
e-mail : brennetot@carnac.cea.fr

[2] *CEA Saclay, Quality and Nuclear Safety Division, MQ /DSNQ Bâtiment 440, 91191 Gif sur Yvette France*
Tel : (33) 1 69 08 78 33 FAX : (33) 1 69 08 77 38
e-mail : vailhen@aquilon.cea.fr

[3] *Midi Pyrennees Observatory, 14 av Edouard Belin, 31400 Toulouse France*
Tel : (33) 5 61 33 29 47 FAX : (33) 1 61 33 28 40
e-mail : maurice@ast.obs-mip.fr

1. Introduction

Choosing a method of analysis to perform remote *in situ* analysis on Mars is no easy task. One method with great potential as a space exploration tool is Laser Induced Breakdown Spectroscopy (LIBS)[1]. LIBS has various advantages over more conventional methods such as alpha-X spectroscopy : 1) remote analysis up to 20 meters, 2) rapid analysis (few min), 3) detection of high and low Z elements including trace elements [1]. LIBS is a well known analytical technique which has been applied on many types of samples such as liquids [2], solid samples in hostile environment [3] and geological samples [4-7]. Yet, its qualification as a reliable analysis tool on Mars surface sets a series of new challenges.

A project called MALIS (Mars elemental Analysis by Laser Induced breakdown Spectroscopy) is under study to perform in situ geochemical analysis of Mars soils and rocks. To demonstrate the feasibility of LIBS in Martian conditions a better knowledge of the plasma emission is needed under Mars atmospheric conditions (Mars atmosphere is typically 5 - 12 mbar CO_2). Due to space limitations in terms of size, weight, and available power, it is important to characterize the method and to determine the best operating conditions to obtain in situ reliable analysis of Mars soils and rocks at stand of distance up to 20 meters. We use for the first time a Doehlert matrix design for LIBS optimization.

2. Experimental set up

To demonstrate the feasibility of LIBS for in situ analysis of Mars soils and rocks, a laboratory set-up (see figure 1) made with commercial components was used to determine the specific characteristics of the laser, the optical components, the detection system, that could be mounted on a rover.

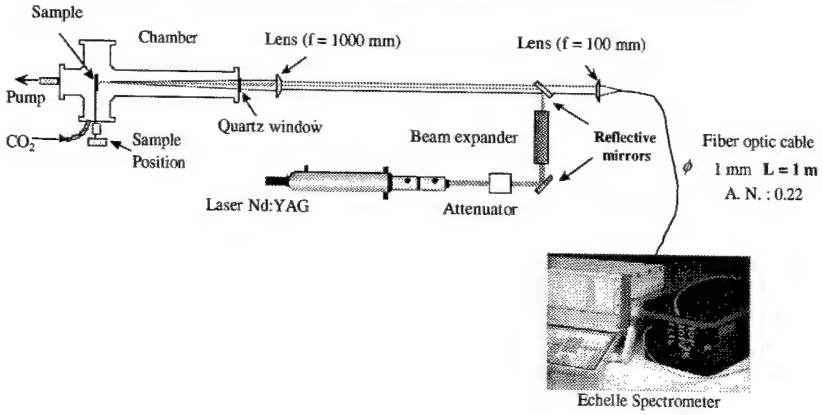

Figure 1 : MALIS experimental set up

The experimental set-up is composed of an ablation head (Nd:YAG laser, Quantel, France), a sample cell with CO_2 at a pressure between 5 and 12 mbar, an optical fiber for emission signal return and a detection system (echelle spectrometer ESA 3000, LLA, Germany). The spectral detection ranges from 200 nm to 780 nm with a resolution of $\lambda/\Delta\lambda$ = 10000. The Nd:YAG laser output is between 5 mJ to 40 mJ (depending on the laser wavelength used) per 5 ns pulse with a repetition rate of 10 Hz. Up to now, working distance is fixed at 1 m and the spot size on the sample is about 150 µm diameter for normal incidence.

3. Doehlert matrix design

Plasma emission is known to depend on many parameters such as laser wavelength, sample, angle of incidence of the laser beam, delay and duration of the measurement gate after the laser pulse, pressure of the surrounding gas... Due to such a number of factors, an optimization procedure based on a statistical design of experiments was chosen. Indeed a conventional experimental method consisting in varying the parameters one by one i) is really time consuming and ii) does not take into account the interactions between variables. Experimental designs based on statistical methods have already been conducted in ICP/AES [8].

In the first step, we used a screening design in order to eliminate factors with little or no effect.: the nature of ambient gas (CO_2 or air) at the same pressure showed no influence on LIBS signal (Martian atmosphere is CO_2 at 95%). The number of laser shots is determined by the characteristics of the laser to be used on Mars and the gate duration has to remain inferior to the plasma lifetime, previously determined to be less than 3 µs at Martian pressure with 2 mJ at 1064 nm [9].

The second step involved a Doehlert design with the remaining four factors : Laser energy, integration delay after the laser pulse, angle of incidence and pressure of CO_2. Much attention was focused on the laser energy used in these experiments. On Mars, energy consumption is strictly limited, due to in situ production by solar panels, which limits the laser output energy. The laser currently under construction for space qualification will deliver 40 mJ at 1064 nm. With an efficiency of 50% for second and third harmonic crystals the maximum energy available will be 20 mJ at 532 nm and 10 mJ at 355 nm. We wanted to test these 3 wavelength independently, each of them up to the maximum energy available on Mars. We thus performed 3 independent sets of Doehlert designs, one for each wavelength. The experimental design was built from the Doehlert matrix previously described in literature [10] and is shown in table 1. The sample studied was a glass with major composition : Si : 33 %, Na 10 %, Ca 7,5 %, Mg 1,6 %, O 46,34 %. Each experiment was repeated 5 times. Since 3 wavelength were independently tested, 315 planned experiments were performed in this second step.

N°	X1 (1064 nm)	X1 (532 nm)	X1 (355 nm)	X2	X3	X4
1	30 mJ	15 mJ	7.5 mJ	650 ns	30 °	8 mbar
2	40 mJ	20 mJ	10 mJ	650 ns	30 °	8 mbar
3	20 mJ	10 mJ	5 mJ	650 ns	30 °	8 mbar
4	35 mJ	17 mJ	8.5 mJ	953 ns	30 °	8 mbar
5	25 mJ	12 mJ	6 mJ	347 ns	30°	8 mbar
6	35 mJ	17 mJ	8.5 mJ	347 ns	30°	8 mbar
7	25 mJ	12 mJ	6 mJ	953 ns	30°	8 mbar
8	35 mJ	17 mJ	8.5 mJ	751 ns	55°	8 mbar
9	25 mJ	12 mJ	6 mJ	549 ns	6°	8 mbar
10	35 mJ	17 mJ	8.5 mJ	549 ns	6 °	8 mbar
11	30 mJ	15 mJ	7.5 mJ	852 ns	6°	8 mbar
12	25 mJ	12 mJ	6 mJ	751 ns	55°	8 mbar
13	30 mJ	15 mJ	7.5 mJ	448 ns	55°	8 mbar
14	35 mJ	17 mJ	8.5 mJ	751 ns	36°	11 mbar
15	25 mJ	12 mJ	6 mJ	549 ns	24°	5 mbar
16	35 mJ	17 mJ	8.5 mJ	549 ns	24°	5 mbar
17	30 mJ	15 mJ	7.5 mJ	852 ns	24°	5 mbar
18	30 mJ	15 mJ	7.5 mJ	650 ns	48°	5 mbar
19	25 mJ	12 mJ	6 mJ	751 ns	36°	11 mbar
20	30 mJ	15 mJ	7.5 mJ	448 ns	36°	11 mbar
21	30 mJ	15 mJ	7.5 mJ	650 ns	12°	11 mbar

Table 1 : Doehlert design with 4 factors for LIBS experiments in Martian conditions. X1 is the laser energy, X2 is the delay after laser pulse, X3 is the angle of incidence and X4 is the CO_2 pressure.

Doehlert design was preferred to other Response Surface designs (such as central composite designs) for the following reasons : i) compact (spherical) region of experimentation, ii) possibility of shifting the

design for sequential experimentation, a possibility which was eventually not used iii) (last but not least) all factors do not have the same number of levels : regulation of CO_2 pressure was limited to 3 levels.

4. Conclusions from Dohlert design results

The results, in term of peak height for two spectral lines Mg (II) at 279.553 nm and Ca (I) at 422.673 nm have been processed using the STATISTICA software [11]. Pareto diagram is used here to outline which factors have most effect on the LIBS signal. The results obtained for each wavelength are shown in figure 2. Interaction effects are noted with * and quadratic effect is noted quadra.

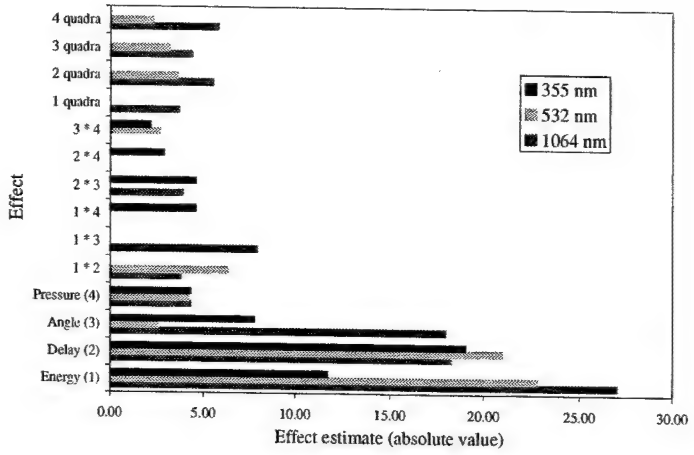

Figure 2 : Pareto chart of standardized effects for maximum of magnesium peak height at 279. 553 nm

From these designed experiments and subsequent statistical analysis, we determined the operating conditions that will give the best conditions for in situ geochemical analysis on Mars. The fitted response surface (second degree model with interactions) for magnesium and calcium maximum response is in good agreement with experimental data : coefficient of determination $R^2 = 0.948$, which is quite satisfactory.

This work supports the choices for the instrument to be used on Mars : i)1064 nm laser wavelength, ii) maximum energy available, iii) delay as short as possible taking into account auto absorption effect (300 ns), iv) angle of incidence less than 50 °.

Analysis have been also undertaken on two types of spectroscopic lines, atomic line from calcium and ionic line from magnesium, giving different behaviour. Results from another sample, a basalt from New Caledonia will be discussed too.

5. References

[1] A. K. Knight , N. L. Scherbarth, D. A. Cremers, and M. J. Ferris *Appl. Spectrosc., 54,* 331-340 (2000).
[2] P. Fichet., P. Mauchien, J. F. Wagner, and C. Moulin *Anal. Chim. Acta, 429,* 269-278, (2001).
[3] P. Fichet, P. Mauchien, and C. Moulin *Appl. Spectrosc., 53,* 1111-1117, (1999).
[4] M. C. Boiron, J. Dubessy, N. Andre, A. Briand, J. L. Lacour, P. Mauchien and J. M. Mermet *Geochim. Cosmochim. Acta, 55,* 917-923, (1991).
[5] D. Ohnenstetter and W. L. Brown *Contrib. Mineral. Petrol., 123,* 117-137, (1996).
[6] C. Fabre, M. C. Boiron, J. Dubessy and A. Moissette *J. Anal. At. Spectrom., 14,* 913-922, (1999).
[7] C. Fabre, M. C. Boiron, J. Dubessy, A. Chabiron, B. Charoy and T. Martin Crespo *geochim. Cosmochim. Acta, 66,* 1401-1407, (2002).
[8] M. Zougagh, P. C. Rudner, A. G. De Torres, J. M. Cano Pavon, *J. Anal. At. Spectrom., 15,* 1589-94, (2000).
[9] R. Brennetot, E. Vors, J. L. Lacour, P. Fichet, C. Fabre, J. Dubessy, A. Rivoallan, S. Maurice, R. C. Wiens, D. A. Cremers, LPSC XXXIII, 1178-1179, (2002).
[10] D. H. Doehlert, Appl. Stat., 19, 231-239, (1970).
[11] StatSoft, Inc. (2001). STATISTICA (data analysis software system), version 6. www.statsoft.com.

NOTES

Hyphenated Techniques

Wednesday, September 25, 2002

Mohamad Sabsabi, Natl. Res. Council of Canada, Canada,
Presider

WB
10:40am–12:20pm
Room: Royal Palm III

LIBS Using Dual-Laser Pulses

S. Michael Angel, The University of South Carolina, USA

An orthogonal, dual-beam geometry provides enhanced emission and material ablation for solid samples and has recently been extended to aqueous solutions. We are also investigating subpicosecond dual-pulse excitation.

Resonance-enhanced LIBS

K.M. Lo, S.L. Lui, X.Y. Pu, and N.H. Cheung
Department of Physics, Hong Kong Baptist University, Kowloon Tong, Hong Kong, PRC
nhcheung@hkbu.edu.hk

Abstract: Resonant photoexcitation of major species in the vapor plume generated plasmas with lower continuum background and stronger analyte emissions than non-resonant LIBS plasmas. When applied to solid and aqueous samples, orders of magnitude improvement in sensitivity was demonstrated.

OCIS codes: (140.3440) Laser-induced breakdown; (300.6210) Atomic spectroscopy; (300.2140) Emission spectroscopy

1. Introduction

While laser-induced breakdown spectroscopy (LIBS) is finding niche applications, it is also plagued by reproducibility and sensitivity issues. The problem arises from the intrinsically violent and chaotic nature of the LIBS process, which may be avoided if the laser energy is coupled to the sample vapor in more efficient and predictable ways than thermal breakdown. During the past years, we showed that one such scheme was photoresonant pumping when the laser wavelength was tuned to match the resonance absorption of the host specie in the vapor plume.

This technique of resonance-enhanced laser-induced plasma spectroscopy, or RELIPS for short, has been applied to solid as well as aqueous targets. In what follows, we will first outline its conceptual basis. We will then report our recent experimental findings that help elucidate its fundamental as well as its application aspects.

2. Conceptual basis of RELIPS

While real spectrochemical plasmas are complicated, a simplified computer model can still be illustrative. This simple model assumes a known amount of analyte atoms, such as sodium, in a homogeneous plasma. The plasma is assumed to be in local thermal equilibrium (LTE). The quantities to be computed are the plasma continuum background intensity, and the analyte emission intensity. The line-to-continuum ratio, which is the main concern in spectrochemical analysis, could then be computed.

Fig. 1 is a plot of the computed line-to-continuum ratio for three analyte lines, Na I 589-nm, Pb I 406-nm, and Cd I 229-nm, at a plasma electron density n_e of 10^{16} cm^{-3}. At higher n_e, the ratio dropped because

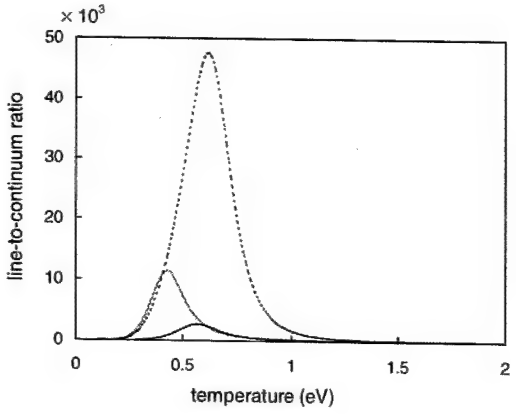

Fig.1. Computed line-to-continuum ratios for the Cd I 229-nm (dotted), Na I 589-nm (light), and Pb I 406-nm (dark) transitions, as functions of the plasma temperature. An electron density of 10^{16} cm^{-3}, an analyte density of 10^{14} cm^{-3}, and an instrumental line width of 0.2 nm were assumed.

the continuum background increased. At much lower n_e, LTE might not be valid. The three transitions were chosen because the Na I 589-nm transition is a typical 'soft' line while the Cd I 229-nm transition is

known to be 'hard'. The Pb I 406-nm transition is in between. As can be seen from Fig. 1, even for such disparate transitions, the line-to-continuum ratios were maximized when the temperature was in the narrow range of 0.5 ± 0.1 eV.

As is well known, LIBS plasmas are created too hot (> few eV) and the charge density too high (~ 10^{18} cm^{-3}). The neutral analytes are depleted by thermal ionization while the background emissions are too bright. The line-to-continuum ratio is therefore small, as evident from Fig. 1. The analyte signal will only emerge when the plasma temperature cools below 1 eV. Yet, LIBS plasma cannot be created cooler else the plume will not ignite [1].

Fortunately, plasmas may be created by alternative means. For example, full plasmas can be generated from the neutral vapors by tuning the laser wavelength to match a strong absorption line of the vapor atom. Excitation energy is converted efficiently and promptly to ionization. This kind of cool, photoresonant plasmas was demonstrated for vapors of alkali metals as well as other elements [2]; its use in RELIPS analysis will be reported below.

3. Experimental results and discussion

3.1 RELIPS analysis of refractory solids

For refractory targets, we showed that a two-pulse scheme worked well: The first 532-nm pulse generated the material plume and the second dye laser pulse conditioned the plasma [3]. Fig. 2 is a graphical summary of the performance of RELIPS. The spectra were generated by laser ablative sampling of pellets of KIO_3 doped with trace amounts of sodium as analyte. Trace (a) was produced by a minimally ablative dye laser pulse alone. Trace (b) was produced by the ablative 532-nm pulse alone. This may be likened to LIBS. Trace (c) was produced by the 532-nm pulse followed by an off-resonance (407 nm) dye laser pulse. Trace (d) is a RELIPS trace. It is similar to (c) except with an on-resonance (404 nm, K → K*) dye laser pulse. By optimizing the ambient gas, such as with 13 mbar of xenon, the enhancement was even more pronounced, as shown in trace (e). Detailed investigation of the plasma dynamics showed that resonant photoexcitation rather than photoionization was the key process responsible for its superior performance.

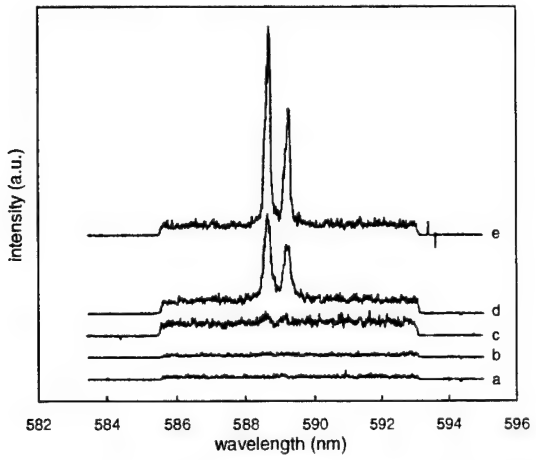

Fig. 2. Plume emission spectra generated by the RELIPS scheme. With (a) the dye laser alone; (b) the 532-nm laser alone; (c) the 532-nm laser followed by an off-resonance 407-nm dye laser pulse; (d) similar to (c) except with an on-resonance 404-nm dye laser pulse; (e) similar to (d) except the ambient gas was 13-mbar xenon instead of open air.

3.2. RELIPS analysis of aqueous samples

Since water is relatively volatile, a single laser pulse of the right wavelength can ablate as well as resonantly photoexcite the plasma plume. We showed that ArF laser has the right wavelength because vibrationally excited H_2O molecules resonantly absorb at 193 nm [4]. Relative to non-193-nm laser-induced plasmas, the ArF version was cooler and background emissions were much weaker. The mass detection limits were low enough to allow quantification of sodium and potassium in single blood cells [5].

The relative detection limits are listed in Table 1, together with non-193-nm results for easy comparison [6]. By using a double pulse approach, we have recently lowered the detection limit of Pb even further, to about 14 ppb (Fig. 3).

Table 1. Wavelength λ and Excited-State Energy E_k of the Analytical Lines, and the Limit-of-Detection for Various Elements

element	transition		limit-of-detection	
	λ (nm)	E_k (eV)	our work	Non-193-nm
Na I	589.0	2.10	0.4 ppb	7.5 ppb
Ca I	422.7	2.93	3 ppb	130 ppb
Ba II	455.4	2.72	7 ppb	6.8 ppm
Pb I	405.8	4.38	300 ppb	13 ppm

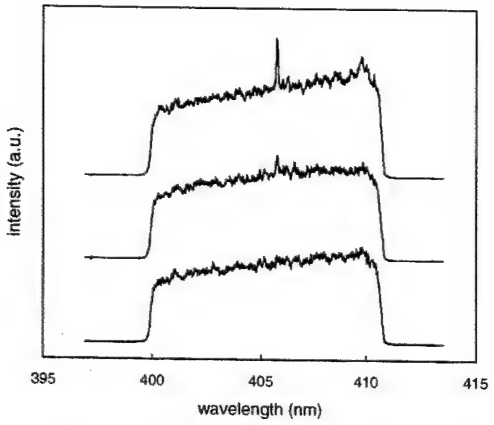

Fig. 3. Plasma emission spectra of aqueous samples containing none (bottom), 63 ppb (middle), and 125 ppb (top) of Pb.

4. Conclusion

We have demonstrated how cooler plasmas can be generated photoresonantly in a mild and tractable manner, which is very different from the violent explosions associated with thermal breakdown. The predictability and reproducibility of the process not only means superior detection limits, but also better-defined plasma properties, such as temperature, to aid spectrochemical analysis. We are presently applying RELIPS to more realistic problems. Nonetheless, we are only beginning to understand the fundamentals and more systematic investigations are underway. We look forward to sharing our latest results at LIBS2002.

[1] C.R. Phipps and R.W. Dreyfus, "Laser Ablation and Plasma Formation" in *Laser Ionization Mass Analysis*, A. Vertes, R. Gijbels, and F. Adams, eds. (Wiley: New York, 1993).

[2] R.M. Measures and P.G. Cardinal, "Laser ionization based on resonance saturation – a simple model description," Phys. Rev. A, **23**, 804-815 (1981).

[3] S.Y. Chan, and N.H. Cheung, "Analysis of solids by laser ablation and resonance-enhanced laser-induced plasma spectroscopy," Anal. Chem., **72,** 2087-2092 (2000).

[4] W.J. Kessler, K.L. Carleton, and W.J. Marinelli, "Absorption coefficients for water vapor at 193 nm from 300 to 1073 K," J. Quant. Spectrosc. Radiat. Transfer, **50,** 39-46 (1993).

[5] C.W. Ng, and N.H. Cheung, "Detection of sodium and potassium in single human red blood cells by 193-nm laser ablative sampling: A feasibility demonstration," Anal. Chem. **72,** 247-250 (2000).

[6] K.M. Lo and N.H. Cheung, "ArF laser-induced plasma spectroscopy for part-per-billion analysis of metal ions in aqueous solutions," to appear in June 2002 issue of Appl. Spectrosc.

Spectroscopic characterization of plasmas produced by dual-laser ablation

V.S. Burakov, A.F. Bokhonov, M.I. Nedel'ko, N.A. Savastenko, N.V. Tarasenko
Institute of Molecular and Atomic Physics National Academy of Sciences of Belarus.
70 Scaryna Ave., 220072 Minsk, Belarus
tarasenk@imaph.bas-net.by

Abstract: Based on the results of spectroscopic diagnostics a role of laser-surface and laser-plasma interactions in enhancement of line emission from plasma produced by the sequence of two laser pulses at different wavelengths is discussed.

OCIS Codes: 140.3440: 300.2140

Laser-induced plasma spectroscopy (LIBS) is recognized as a fast, real-time method for elemental analysis normally without the need for sample preparation. Presently, in order to improve the sensitivity and precision of LIBS different approaches are being investigated. One of them is double-pulse laser ablation, which provides more efficient production of analyte species in excited states [1,2] For further development and optimization of double-pulse approach it is important the detail understanding the main processes leading to better coupling of laser pulse energy to the target and ablated matter. In this paper based on the results of spectroscopic diagnostics the role of laser-surface and laser-plasma interactions in enhancement of line emission from plasma produced by the sequence of two laser pulses at different wavelengths is discussed. The main attention is focused on the processes of laser-induced resonance ionization of ablated atoms and photoelectron emission from the preliminary irradiated target surface.

The second harmonic of the Nd-YAG (532 nm, 10 ns, 1 - 5 J/cm^2) laser and excimer XeCl (308 nm, 10 ns, 1 J/cm^2) laser with different temporal delays between pulses were employed for ablation. The laser beams were focused on the surface of the samples (Al, graphite) placed in the chamber under vacuum and gas (air, helium) environments.

Spectroscopic characterization of the ablated plume was performed by the time resolved emission spectroscopy and laser-induced fluorescence methods. The plasma emission spectra (300 - 700 nm) were recorded and compared for different ablation regimes (single pulse and double pulse in coincidence and in sequence at various delays between pulses and laser fluences). The major species including neutral, ionized and some molecular species were identified. The particles within the plume were observed by using Rayleigh scattering method.

The experiments demonstrated increased plasma emission, higher degree of particle atomization and a higher proportion of ions in dual-pulse ablation regime compared to the plasma produced by one laser. The optimal pulse separations were found both for atomic and ionic lines. The results of spectroscopic measurements were confirmed by ion probe analysis of the ionic content in the plume. Probe measurements revealed a strong enhancement of photoelectron emission from the preliminary irradiated target surface. The interpretation of results obtained is based on the wavelength dependence of laser-plasma (inverse bremsstrahlung absorption and photoionization) as well as laser-surface interaction processes.

Besides, the definite reduction in number of particulate formed in laser ablation plasma was obtained by the use of the second laser under conditions of suitable temporal delays. This result may be explained in terms of heating and fragmentation of the blowoff material produced in the plume by the first laser.

The results obtained are used for improvement of quantitative data of LIBS-based analysis of metal in environmental samples.

1.L.St-Onge, V.Detalle, M.Sabsabi, 2002, Spectrochim. Acta B 57, 121
2. J.D.Wu and N.H.Cheung , 2001, Appl. Spectroscopy 55. 366

Resonance-enhanced laser-induced plasma spectroscopy: time-resolved studies and ambient gas effects

S.L. Lui and N.H. Cheung
Department of Physics, Hong Kong Baptist University, Kowloon Tong, Hong Kong, PRC
nhcheung@hkbu.edu.hk

Abstract: The dynamics of resonance-enhanced LIBS plasmas in various ambient gases was investigated by time-resolved studies. Results suggest that a larger plume volume was heated in the resonance case. Together with the right ambient gas, the plasma temperature could be sustained to enhance the analyte signal.

OCIS codes: (140.3440) Laser-induced breakdown; (300.1030) Absorption spectroscopy; (300.2140) Emission spectroscopy

1. Introduction

In resonance-enhanced laser-induced plasma spectroscopy (RELIPS), a second laser pulse of frequency that matches the resonance absorption of the host specie in the vapor plume is used to reheat the cold plasma. It has been demonstrated that RELIPS can successfully increase the analytical sensitivity by at least an order of magnitude [1,2]. In order to further improve the limit of detection (LOD), the basic mechanism of RELIPS is investigated by time-resolved study.

LIBS signal was affected by the type and the pressure of the ambient gas around the plasma [3,4]. It was found that the main reason for the signal decay was the cooling of the plasma. In other words, signal can be enhanced if the plasma temperature can be sustained.

In this presentation, we will first outline our experimental technique. Time-resolved signal of the resonance case will then be compared against the non-resonant one. Finally, the cooling effect of different ambient gases at different pressures will be reported.

2. Experimental section

The second harmonic of the Nd:YAG laser was used to ablate a potassium iodate matrix. The matrix contained 35 ppm of sodium, and 55 ppm of lithium was added as the reporter element. Thirty nanoseconds later, a dye laser pulse, which was tuned to match the resonance frequency of K atoms ($4\ ^2S_{1/2}$ to $5\ ^2P_{3/2}$), was focused on the plume. The fluence of the Nd:YAG laser was 800 mJ cm^{-2}, which was above the ablation threshold. The fluence of the dye laser was 460 mJ cm^{-2}, which was marginally ablative.

The sample was placed inside a closed chamber that was filled with different ambient gases (N_2, He, Ar, and Xe) to different pressures. The plasma spectra were recorded by an intensified charge-coupled device with gate width set to 5 μs for time-integrated study and 50 ns for time-resolved studies.

The plasma temperature was determined from the intensity ratio of the Li 610.3 and 670.8-nm line, while the electron density was obtained from the Stark width of the Li-670.8-nm line.

3. Results and discussion

The performance of RELIPS under different ambient conditions is shown in Figure 1, where the sodium doublet emitted by the plume is displayed. By comparing trace (b) and trace (d), which corresponded to the on and off-resonance respectively, the effect of resonance enhancement was demonstrated. Trace (c) through (e) showed the effects of air pressure on RELIPS signal. The signal was weakest in vacuum (~0.01mbar), and peaked at ~350 mbar. The effects of ambient gas on RELIPS signal were illustrated in trace (f), 50 mbar argon, and (g), 13 mbar xenon. Compared with the open-air trace (c), enhancement by the heavy inert gases is evident.

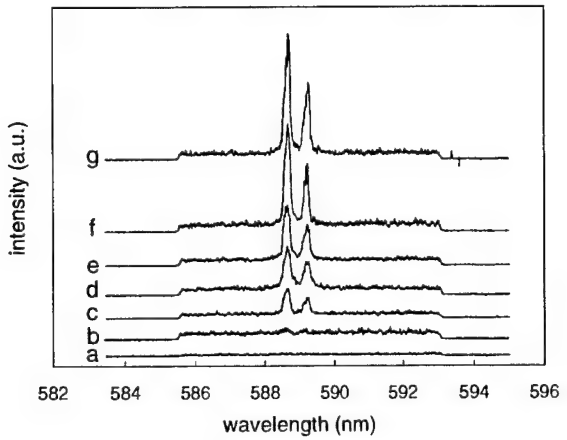

Fig. 1. Sodium doublet signal generated by RELIPS under different conditions: (a) 532-nm laser alone; (b) 532-nm laser followed by an off-resonance 407-nm dye laser pulse; (c) 532-nm laser followed by an on-resonance 404-nm dye laser pulse, in vacuum; (d) to (g) were similar to (c) but was done in: (d) open air; (e) 350mbar air; (f) 50mbar argon; and (g) 13 mbar xenon.

3.1 On vs off-resonance

Time-resolved spectra were captured for both on and off-resonance. The time origin, t = 0 ns, referred to the onset of the Nd:YAG laser pulse. The dye laser was fired at t = 30 ns. From Fig. 3a, the resonance-enhanced signal of sodium (open circles) was four times stronger and lasted longer than the off-resonance case (crosses). An instantaneous rise in signal and electron density (not shown) was not observed at t = 30 ns. Photoionization was therefore not the dominant process. Rather, the boost of the signal and electron density (not shown) happened at t = 45-50 ns. This suggests that superelastic collision between electrons and excited species might play an important role in heating the plasma.

The on-resonance plasma temperature lasted longer than the off-resonance case (Fig. 3b). The off-resonant temperature was only transiently measurable because of the weak 610-nm line. This could be attributed to a smaller heated volume in the non-resonance case. This smaller heat reservoir meaned a faster cooling rate.

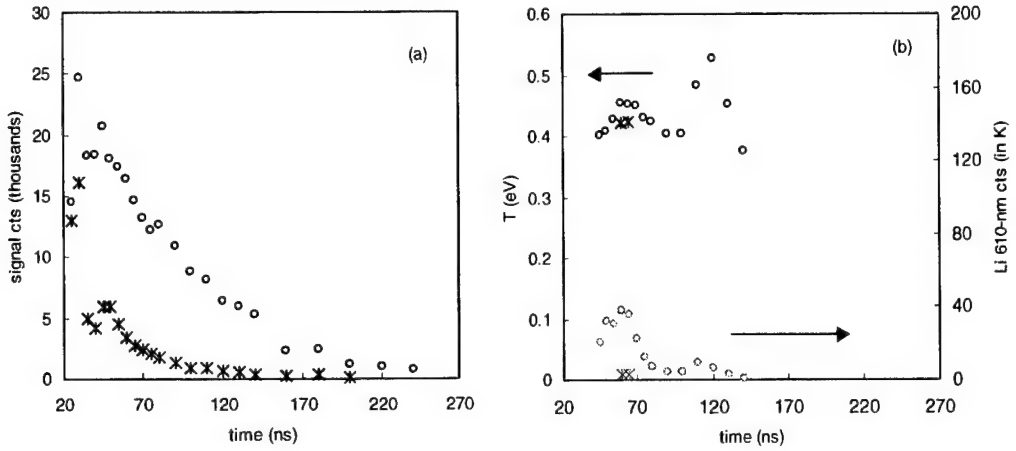

Fig. 2. Time-resolved plume emissions generated under conditions identical to that of traces (b) and (d) in Fig. 1, except the air pressure was 350 mbar. The on-resonance (circles) and off-resonance (crosses) results were shown together for comparison. Fig. 2a shows the sodium signal intensity while Fig. 2b plots the plasma temperature and the Li 610-nm line intensity (lighter symbols).

3.2 Pressure and ambient gas effect

Because the signal decay is due mainly to plasma cooling, an understanding of the cooling process is helpful. Energy transfer to the ambient gas was characterized by evacuating the sample chamber or filling it with various gases. Fig 3(b) showed the plasma temperature in 350-mbar air (open circles), 13-mbar xenon (crosses) and vacuum

(triangles). It was observed that the differences in temperature were small and could not explain the difference in Na signals shown in Fig. 1. However, the electron density in vacuum was significantly lower (Fig. 3a). This suggested that without the ambient gas confinement, the free expansion of the plasma caused a dilution of the Na atoms, which, in turn, lowered the Na signal.

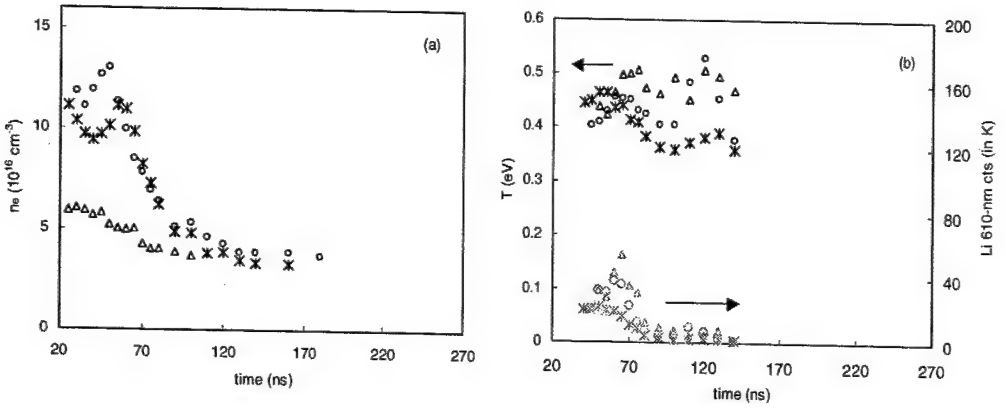

Fig. 3. Effect of pressure and ambient gas on time-resolved RELIPS signal: Plume emissions captured under conditions identical to that of the on-resonance data shown in Fig. 2, at 350-mbar air (open circles), vacuum (triangles) and 13-mbar xenon (crosses): Fig 3a shows the electron density determined from the Stark widths of the Li 610 and 670-nm lines. Fig 3b shows the plasma temperature and the intensity of the Li 610-nm line (lighter symbols).

The enhancement of signal in argon and xenon can be attributed to better thermal insulation. Heat loss in plumes was due to the collisional energy transfer between the plume species and the surrounding molecules. Because of a larger mass difference, the energy transfer efficiency between the heavy noble gases and the lighter plume species is poor [5]. Thus the plasma temperature can last longer.

4. Conclusion

The decay of LIBS signal is mainly due to air-cooling. However, cooled plasmas can be resonantly rekindled to drastically increase the analyte signal. With appropriate ambient gas at suitable pressure, heat loss can be reduced. Our findings point to the possibility of laser-customized plasmas for increased analytical sensitivity. Currently, we are pursuing the mechanisms of photoresonant excitation of plasmas, as well as application to realistic problems.

1. S.Y. Chan and N.H. Cheung, "Analysis of solids by laser ablation and resonance-enhanced laser-induced plasma spectroscopy," Anal. Chem., **72**, 2087-2092 (2000).
2. J.D. Wu and N.H. Cheung, "Resonance-enhanced laser-induced plasma spectroscopy for multi-element analysis in laser ablative sampling," Appl. Spectrosc., **55**, 366-370 (2001).
3. Yasuo Iida, "Effects of atmosphere on laser vaporization and excitation processes of solid samples," Spectrochimica Acta, Part B, **45B**, 1353-1367 (1990).
4. Y.I. Lee, T.L. Thiem, G.H. Kim, Y.Y. Teng and J.Sneddon, "Interaction of an excimer-laser beam with metals. Part III: Then effect of a controlled atmosphere in laser-ablated plasma emission," Appl. Spectrosc., 46, 1597-1604 (1992).
5. Zel'dovich, Ya. B. and Raizer, Yu. P., "Physics of shock waves and high temperature hydrodynamic phenomena," Academic Press: New York, 1966.

NOTES

New LIBS Methodologies and Instrumentation: I

Wednesday, September 25, 2002

Kevin McNesby, US Army Res. Lab., USA,
Presider

WC
2:00pm–3:40pm
Room: Royal Palm III

Long Term Assessment of LIBS Instrumentation in an Industrial Environment

D. Body and B.L. CHADWICK[1,2]

[1]Cooperative Research Centre for Clean Power From Lignite
8/677 Springvale Rd. Mulgrave, 3170 Australia
[2]Laser Analysis Technologies
23/200 Canterbury Rd. Bayswater, 3153 Australia

bruce.chadwick@cleanpower.com.au
phone 61 3 8542 0800 fax 61 3 9561 0710

Abstract: Testing of daily coal samples at commercial power stations using LIBS instrumentation and standard acid-extraction, AAS analysis has revealed excellent correlation ($R > 0.9$) between the two methods over 18 months of operation.

1. Introduction

It has been nearly 40 years since it was first noted that the plasma emission of a high-power laser irradiating a material contains sufficient spectroscopic information for the elemental analysis of that material. In the intervening period there have been numerous investigations, application demonstrations, and instrument variations reported by researchers, technologists and instrument manufacturers world-wide using the technique that has become known as laser-induced breakdown spectroscopy (LIBS).

In the wider context LIBS is an elemental analysis technology that is an alternative to established analysis methods that include X-ray fluorescence, atomic absorption spectroscopy, atomic emission spectroscopy (ICP, arc-spark, glow discharge ...), and neutron activation analysis. Relative to these established technologies LIBS is only a minor influence on elemental analysis applications such as the assessment of commercially mined and manufactured materials. LIBS can only grow in importance if it achieves wider industry acceptance as a viable alternative for materials analysis. This acceptance can only be gained by proving the technology achieves the same level of precision and accuracy as alternative methods over extended periods in commercial applications – while offering the users specific benefits such as faster analysis and wider elemental range. This paper describes such a proving study where LIBS instruments (developed by the authors) have been placed in commercial coal-fired power stations for an 18 month comparative investigation.

LIBS was chosen as the analysis tool in this application owing to its ability to detect the low atomic number elements that are difficult to detect using alternative direct analysis techniques for solid materials (notably XRF). The sensitivity of the technique to low analyte concentrations is also a distinct advantage. At the time of the development the lack of integrated analysis systems in the commercial marketplace led to the development of the instrument described in this paper. The instrument designs have since been commercialized by a private company [1].

2. Instrument Design

The LIBS instrument is an integrated analysis system comprising excitation laser, optical spectrographs, gated CCD detectors, and is fully software controlled [2,3]. Coal and mineral samples are received from the mines and are crushed and mixed prior to analysis. For moist materials only light crushing is required, however for hard materials samples are crushed to ~100 μm to obtain both accurate and precise analysis results. The crushed samples are loaded into sample holders that allow pressing of the sample and direct transfer into the analyser without further handling.

The laser energy is adjusted according to the samples being analysed, with moist brown coals requiring the full laser energy of 90 mJ. Drier black coals and ashes generally require less laser energy. The laser is focussed onto the samples which are located on a fast translation stage that moves the sample between successive laser pulses, thereby exposing a fresh region of the sample to each successive laser pulse. This reduces any matrix effects between laser pulses induced by sample/laser interaction.

Key to the successful operation of the device is its parallel processing design comprising multiple spectrographs and CCD detectors. Four spectrographs and detectors are used to cover the wavelength range of 180 - 850 nm. This proprietary design allows simultaneous determination of all detectable elements thereby reducing analysis time and analysis errors resulting from sample heterogeneity.

The plasma ignition is accompanied by a period of bright broadband fluorescence associated with thermal emission and electron-ion recombination in the plasma. Delaying the spectral acquisition approximately 1 μs after the laser pulse allows the broadband emission to subside and the elemental fluorescence to be observed. Each of the CCD detectors is electronically gated (i.e has a fixed exposure time) to achieve the required delay between plasma ignition and recording of the spectrum. Software controlled timing circuitry controls the firing of the laser pulse and the spectrum acquisition.

3. Coal Analysis Examples

The performance of the technology is well demonstrated in the analysis of a low-ash lignite from the Yallourn mine in Victoria, Australia. This coal has just 1.6 % ash content (dry basis) and 67% moisture content. Detectable elements in this lignite variety include C and H in addition to inorganic components such as Al, Na, Fe, Mg, Ca, Si and K.

The reproducibility and accuracy of the measurement can be ascertained from measurements on multiple samples of the same material. As can be seen from Table 1 the accuracy and reproducibility for the principal inorganic components is excellent.

Table 1. Analysis results of a low-ash Yallourn (Australia) lignite (SD = standard deviation).

Sample	% Na 589nm	% Ca 422.7nm	% Mg 285nm	% Fe 275nm	% Al 309nm
1	0.023	0.046	0.082	0.137	0.015
2	0.023	0.047	0.085	0.132	0.013
3	0.023	0.045	0.087	0.138	0.014
4	0.023	0.048	0.080	0.136	0.020
5	0.023	0.048	0.087	0.128	0.016
6	0.024	0.045	0.080	0.140	0.016
Mean	0.023	0.047	0.084	0.135	0.016
SD	0.001	0.002	0.003	0.004	0.003
Standard Analysis	0.024 (0.005)	0.041 (0.005)	0.089 (0.005)	0.11 (0.005)	0.011 (0.005)

4. Long Term Assessment

Since mid 2000 two prototype Spectrolaser units have been installed at Loy Yang and Hazelwood power stations, located in Victoria, Australia. One of the power stations (Loy Yang) has conducted further independent evaluation using comparative testing to standard, wet-chemical techniques. To the best of our knowledge this is one of the first reports of long-term, independent testing of such laser-based technology in a commercial, analysis application.

Prior to commencing the evaluation the instrument was calibrated using the prepared standards made from blending high- and low-ash coals. At the power station at least four samples were collected from different points in the conveyor system every weekday and measured by the Spectrolaser. As a standard practice duplicate measurements are made for each sample and the results averaged for reporting purposes. Since a large number of samples (>1500) are taken over an extended period, each of which is analyzed in duplicate by two alternative methods, the test provides a comprehensive accuracy and repeatability test for the LIBS instrument. For example, over a one-month

period (approximately 90 analyses of different coal samples) the comparison between LIBS and the AAS analyses is excellent and within the uncertainty of 0.01% in the acid-extraction, AAS technique.

Table 2 Example of a monthly average measurements for Na, Al and Ca

Element	Monthly Average Measurement (%)		Δ %
	LIBS	AAS	
Al	0.125	0.135	0.01
Na	0.090	0.092	0.002
Ca	0.034	0.044	0.01

Correlation between the two methods over extended periods has likewise been proven the efficacy of LIBS in this application. For example, Na below yields a correlation of 0.91 over 1500 measurements during the 18 months of operation. Similar levels of accuracy are also observed for Ca and Al measurements over the period.

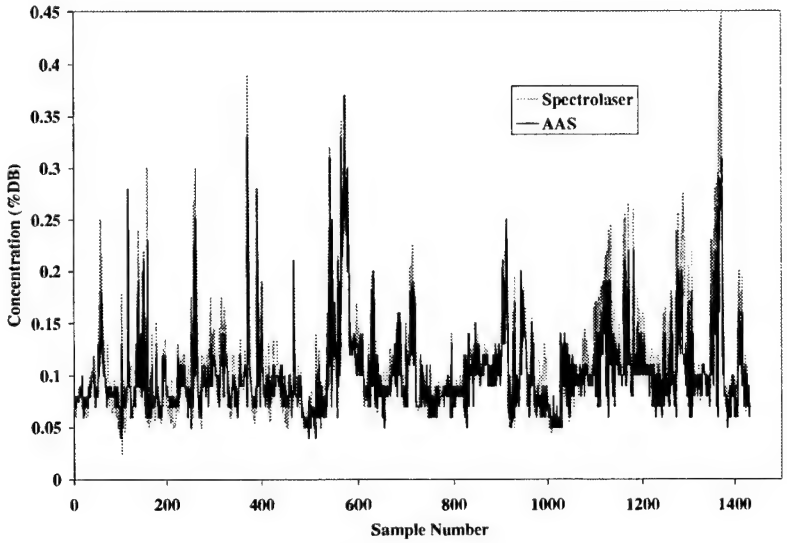

Fig. 1 Comparison for Na measurements in coal using LIBS and AAS over 18 months (~1500 measurements)

5. Conclusions

For the power stations using this technology, the forecast analytical cost savings are in the vicinity of US$100,000 per year enabling the power station to recover the capital cost of the equipment within nine months. In addition, the rapid analysis enables further savings via better supervision of plant operations resulting in potentially fewer unscheduled shut-downs. Since elemental analysis is a generic quality control measure it is expected that there are numerous other potential applications for the technology where similar cost savings and operational improvement can be obtained.

6. References

1. Laser Analysis Technologies, www.laseranalysis.com
2. D. Body and B. L. Chadwick "A Simultaneous Elemental Analysis System using Laser Induced Breakdown Spectroscopy", Rev. Sci. Instrum. **72** ,1625-1629 (2001)
3. D. Body and B. L. Chadwick "Optimization of the spectral data processing in a LIBS simultaneous elemental analysis system" Spectrochem. Acta B **56**, 725-736 (2001).

Geiger photodiode spectrometer for compact, lightweight LIBS instrumentation

R. A. Myers and A. M. Karger
Radiation Monitoring Devices, Inc., 44 Hunt Street, Watertown, MA 02472-4699
rmyers@rmdinc.com, akarger@rmdinc.com

D. W. Hahn
Department of Mechanical Engineering, University of Florida, P. O. Box 116300, Gainesville, FL 32611-6300
dwhahn@ufl.edu

Abstract: We will discuss a unique spectrometer based on an array of Geiger photodiodes resulting in enhanced performance of laser induced breakdown spectroscopy instrumentation. These compact, silicon-based detectors eliminate the need for post amplification electronics and allow detection of single photons at room temperature.

OCIS codes: (040.1240) arrays; (040.5160) photodetectors; (140.3440) laser-induced breakdown

1. Background

Laser induced breakdown spectroscopy (LIBS) utilizes atomic emission spectroscopy in a laser-induced microplasma to identify atomic species present in an individual aerosol or surface particle. It also can yield quantitative measurements of constituent species enabling direct, simultaneous measurements of particle mass and elemental composition, as demonstrated during preliminary experiments [1]. The LIBS approach to elemental analysis provides:

- Rapid, near real-time analysis;
- Simultaneous multi-element monitoring;
- Identification of both high and low Z elements;
- Discrimination between weathered layers and bulk properties; and
- Standoff detection.

When power densities exceed several GW/cm^2, a high-temperature, high-electron-density laser spark, or microplasma, is formed. The temperature of this plasma, initially, is very hot (10^4 to 10^7 °C). At such a high temperature any sample material is vaporized and ionized. As the plasma cools, ionization reduces but the neutral atoms are continually excited at the elevated temperatures producing atomic emission transitions. The plasma lifetime might be several hundred microseconds, with the first 10 to 20 μs consisting of the large background continuum and little atomic emission.

Typically, a fiber optic or lens collects the return light from the plasma and couples it into a spectrum analyzer. Each atomic species emits a very precise set of atomic lines so that time-resolved spectral analysis of these emissions yields a fingerprint of the species present in the sample. Scientists use an optical grating and high-resolution spectrometer to separate the spectral signatures from the background. Wavelengths of the atomic emissions range from 190 to 850 nm. Because the precise transition of the atomic emission competes with a broad background, the signal-to-noise (s/n) of the system is strongly dependant on the resolution of the spectrometer.

Recently, it has been shown that the standoff measurement capabilities and ablative nature of the LIBS instrument would provide an extremely useful tool for, among other studies, space and planetary exploration [2]. This and other applications require compact, robust and sensitive electro-optical components. Most often, intensified charge coupled devices (ICCD) are used at the output of the spectrometer in LIBS instrumentation. The format might be a linear array for a traditional linear grating spectrometer, or an n x n array coupled to an echelle system. While the ICCD is highly sensitive and allows high speed gating, the intensifier is fragile, requires cooling, has relatively low quantum efficiency and the real-time analysis is limited by the readout rate of the CCD.

2. Geiger Photodiodes

The avalanche photodiode (APD) is a solid-state alternative to photomultiplier tubes (PMT) and ICCD detectors. It is unique among solid-state radiation detectors in that it has internal gain. In its simplest form, an APD is a p-n junction formed in a silicon wafer, structured so that it may be operated near the breakdown voltage under reverse bias. When either photons or charged particles are absorbed in the silicon, electron-hole pairs are generated and are accelerated by the high electric field. These electrons gain sufficient velocity to generate free carriers by impact ionization, resulting in internal current gain. Compared to conventional solid-state sensors, the APD produces relatively large output pulses, along with improved s/n [3,4]. APD gains of up to 10,000 at room temperature have been achieved in devices where the output is proportional to the input.

Geiger photodiodes (GPD) (**Figure 1**) are APDs operating in the photon counting mode and are most often used when single photon sensitivity is required. Geiger mode operation is accomplished by applying an external bias, which is above the breakdown voltage of the APD p-n junction. This breakdown voltage is usually much lower than the high voltages that are needed for other photodetectors such as PMTs. The high internal electric field at the p-n junction results in extremely high gains and a nonlinear output. The GPD can achieve gains of up to 10^9 [5,6]. This highly amplified signal relaxes the requirements on subsequent electronics resulting in improved s/n performance and the ability to detect single photon events without cooling. In addition, the GPD, like most silicon-based devices, is robust and has high quantum efficiencies at wavelengths from 200 to 1000 nm. Until recently, this photon counting device has only been available in a single-element format. However, Radiation Monitoring Devices, Inc. (RMD) has developed a multi-element GPD with individually addressable pixels for array applications, including LIBS.

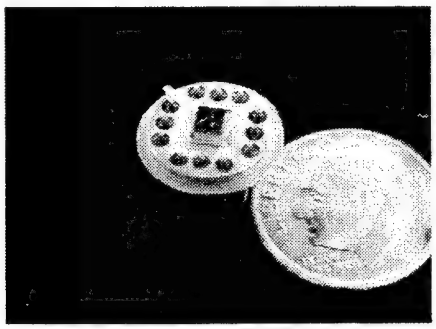

Fig. 1. T0-8, 12-pin package for the GPD. Bonding wires connect the individual pixels to the posts and a ceramic standoff isolates the chip from the package. The test pattern on the array contains 117 individual pixels with diameters ranging from 10 to 110 μm.

3. LIBS and Geiger Photodiodes

The GPD output can be coupled to a simple circuit to achieve digital TTL pulses in response to a detection event. This simplifies the computer interfacing and readout requirements. For LIBS applications, we use an active quenching design to decrease the reset time by several orders of magnitude [7]. Once the avalanche is initiated, the discriminator output triggers a fast solid state switch to rapidly reduce the bias across the GPD. After the avalanche is quenched, the switch reverses polarity and recharges the bias across the GPD, resetting it for the next event detection. Active quenching circuits developed at RMD have improved the maximum count rate of these photodiodes by more than two orders of magnitude. Counts rates of over 20 MHz have been achieved (**Figure 2**). For applications where the gate time is 200 μs, the dynamic range approaches 12 bits. The data stream also provides temporal information of the breakdown process rather than a single integrated readout.

We have been able to utilize this GPD readout system as part of a LIBS instrument. The focus was on creating a high-speed readout for a multi-pixel device. We have demonstrated that it is quite feasible to use these circuits to monitor low concentrations of atomic vapor (**Figure 3**). We have also shown that the circuit will work with a system using a nitrogen or Nd:YAG laser as the excitation source. It is also important to realize that the detector sensitivity starts from single photon detection, so it is relatively simple to extend the dynamic range by reducing the incoming signal with filters or a smaller aperture.

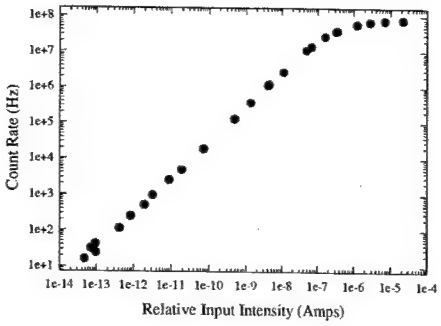

Fig. 2. GPD count rate as a function of the relative incident intensity. The data shows a linear response over six decades of operation.

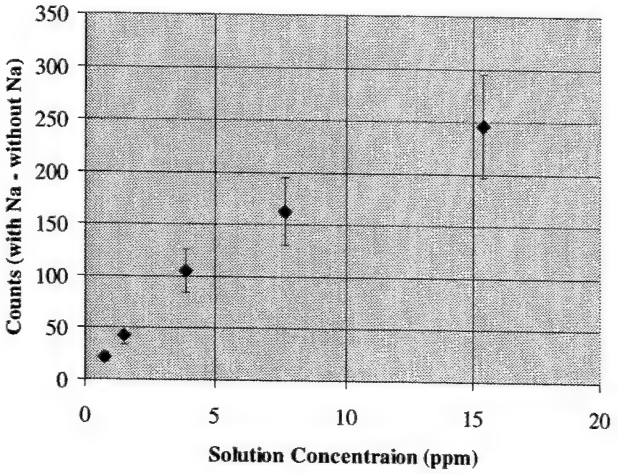

Fig. 3. Plot of GPD signal vs. sodium concentration. The background, which was recorded prior to each change in sodium concentration, is subtracted from each data point. The counting duration was 500 μs with a 60-μs delay following the laser pulse. The data was recorded at the University of Florida using a Nd:YAG source to excite sodium vapor.

4. References:

1. D. W. Hahn, W. L. Flower and K. R. Hencken, "Discrete Particle Detection and Metal Emissions Monitoring Using Laser-Induced Breakdown Spectroscopy," Appl. Spectrosc., **51**, 1836-1844, 1997.
2. A. K. Knight, N. L. Scherbarth, D. L. Cremers and M. J. Ferris, "Characterization of Laser-Induced Breakdown Spectroscopy (LIBS) for Application to Space Exploration," Appl. Spectrosc., **54**, 331, 2000.
3. R. Farrell, F. Olschner, E. Frederick, L. McConchie, K. Vanderpuye, M. R. Squillante and G. Entine, "Large Area Silicon Avalanche Photodiodes for Scintillation Detectors," Nucl. Inst. And Meth., **A288**, 137, 1990.
4. R. Farrell, K. Vanderpuye, L. Cirignano, M. R. Squillante and G. Entine, "Radiation Detection Performance of Very High Gain Avalanche Photodiodes," Nucl. Inst. And Meth., **A353**, 176, 1994.
5. R. Redus and R. Farrell, "Gain and Noise in Very High Gain Avalanche Photodiodes: Theory and Experiment," in Hard X-Ray/Gamma Ray and Neutron Optic Sensors and Applications, R. B. Hoover and F. P. Doty, eds., Proc. SPIE 2859, p. 288 (1996).
6. S. Vasile, P. Gothoskar, R. Farrell, and D. Sdrulla, "Photon Detection with High Gain Avalanche Photodiode Arrays," IEEE Trans.Nucl.Sci., **NS-45**, 720 (1997).
7. R. G. W. Brown, R. Jones, J. G. Rarity and K. D. Ridley, "Characterization of Silicon Avalanche Photodiodes for Photon Correlation Measurements. 2: Active Quenching," Appl.Optics, **26**, 2383 (1987).

Fiber Optic Modular Spectroscopy and Its Application to LIBS

Roy A. Walters
Ocean Optics, Inc., 4202 Metric Drive, Winter Park, FL 32792, RoyW@OceanOptics.com

Jeremy B. Rose
Ocean Optics, Inc., 4202 Metric Drive, Winter Park, FL 32792, JeremyR@OceanOptics.com

Abstract: The application of miniature fiber optic modular spectroscopy to LIBS allows for great flexibility in data retrieval. A spectrometer with 200 nm to 980 nm range and 0.1 nm resolution observing only one laser event has been commercialized.

Optimization of Laser-Induced Breakdown Spectroscopy for Liquid Samples at Millijoule Pulse Energies

Mike Taschuk, Ying Tsui, Robert Fedosejevs
Department of Electrical and Computer Engineering, University of Alberta, Edmonton, Alberta Canada T6G 2V4
Phone: 1 (780) 492-3905, Fax: 1 (780) 492-1811; E-mail: mtaschuk@ee.ualberta.ca

Abstract: A study is being carried out investigating the capabilities of laser-induced breakdown spectroscopy for analysis of water samples at pulse energies from sub-millijoule to 100 mJ per pulse. The sub-millijoule energy regime for LIBS of water samples is not well investigated, and optimal conditions need to be identified. Optimization of the limit of detection of contaminants in water requires detailed characterization of the plasma evolution, the line emission and the sources of background noise. Pulse energies from 3 mJ to 100 mJ focused with a 30 cm lens have been tested for Na in water, resulting in detection limits from 200 ppm to 2 ppm respectively. Scaling to sub-millijoule energies using shorter focal length lenses is currently under investigation.

OCIS codes: (140.3440) Laser-induced breakdown, (300.6360) Spectroscopy, laser

1. Introduction

A study is being carried out investigating the capabilities of laser-induced breakdown spectroscopy for analysis of water samples at pulse energies from sub millijoule to 100 mJ per pulse – a range lower than the pulse energies traditionally used in LIBS studies of liquid samples. Even at these energies one can easily produce focal spot intensities on the order of 10^{10} Wcm^{-2} as required to exceed the breakdown threshold of the surface of water. Extending LIBS to sub millijoule energy regimes will improve the industrial applicability of the technique, as low cost, high repetition rate lasers can be integrated into small or portable LIBS systems. However, the sub millijoule energy regime for LIBS is not well investigated, and optimal conditions need to be identified.

One of the main factors determining the detection of contaminants in water is the optimization of conditions to maximize the signal to noise ratio. Initially the plasma is too hot for efficient emission of UV and visible emission lines and one must wait until expansion cooling has created the optimum conditions for atomic line emission. In order to maximize the sensitivity the spatial and temporal dependence of the plasma expansion from a water jet target into air has been measured, leading to the identification of optimum gating time and observation position for contaminant elements such as sodium and aluminium. Detailed studies of the expansion of the emission region into air have been undertaken, and compared with theoretical shock wave models. The temperature and density of the plasma are derived from theoretical models of the blast wave expansion into air. In order to compare results from different experimental conditions and from different groups it is important to measure the line emission in absolute units. Careful calibration of the experimental set-up has been undertaken, facilitating comparison with both simulation and other experimental groups.

Another equally important factor in the limit of detection for any element is the characterization of the background noise level in the region of the spectral measurement. Contributions to background noise come from continuum radiation, weak spectral lines of other elements, and dark current in the detector channels. Based on the characterization of the signal and noise scaling it is possible to predict the limits of detection for a wide variety of conditions. Single shot detection limits for sodium have been observed ranging from a few parts per million up to the order of a part per thousand, depending on the laser pulse energy. Scaling laws for the limit of detection as functions of energy have been characterized and are discussed.

2. Experimental Details

For the experiments presented here, a frequency tripled (355 nm) Nd:YAG laser (Continuum Powerlite - 9010) with 10 ns pulses (FWHM) was used. For initial characterization, a 30 cm focal length lens was used in order to give a relatively uniform beam spot. The beam profile is elliptical, with best focus beamwaist approximately 55 μm by 45 μm. However, for very low energies (<~3 mJ/pulse), a shorter focal length lens is required in order to achieve sufficient intensities for breakdown.

The spectrometer used is a 0.5 m focal length f/7 spectrometer (Spectra Pro 500, Acton Research) equipped with an intensified multichannel array detector (OMA 1455 G, Princeton Instruments). A high-resolution grating (1200 lines/mm), blazed at 500 nm, is used for the wavelength range above 350 nm.

3. Plasma Characterization

Using a 1 dimensional spherical expansion plasma model [1], the initial conditions of the plasma can be calculated. With a 45 mJ pulse focused by a 30 cm lens, the initial plasma temperature is approximately 30 eV, with an expansion velocity of $3.3*10^6$ cms^{-1} for the initial interaction period. The subsequent density and temperature of the expanding plasma can be modelled by the Taylor/Sedev blast wave model, and compared to experimental measurements. The optimum conditions within the plasma for spectral emission can be correlated with these blast wave parameters, and ideal conditions for LIBS emission will be explored.

Detailed studies of the plasma dynamics have been undertaken in order to identify the optimum location in spacetime for viewing of the plasma, and to better understand the physical conditions under which the optimum signal to noise ratios can be achieved. In our experiments, a high-resolution space time study of the line emission from a contaminant in water is performed. An example of this work is presented in Figure 1. The dotted lines presented in Figure 1b represent the Taylor/Sedev blast wave model for a strong shock wave in air (right) and in water (left). The emission occurs from the region inside the predicted blast wave boundary in air. Within the expanding blast wave region there are large temperature and density gradients and thus it is expected that there will be a region of optimum conditions for emission of a particular wavelength of line radiation.

The measured expansion in air agrees with blast wave theory. The observed expansion of the emission region into the water jet is complicated by optical distortion of the emission due to rippled edges of the water jet. Thus, at points between -0.5 and 0.0 mm, the signal is observed through the water jet, which may distort the apparent expansion.. Even so the observed emission region agrees approximately with the predicted propagation of the strong shock into the water.

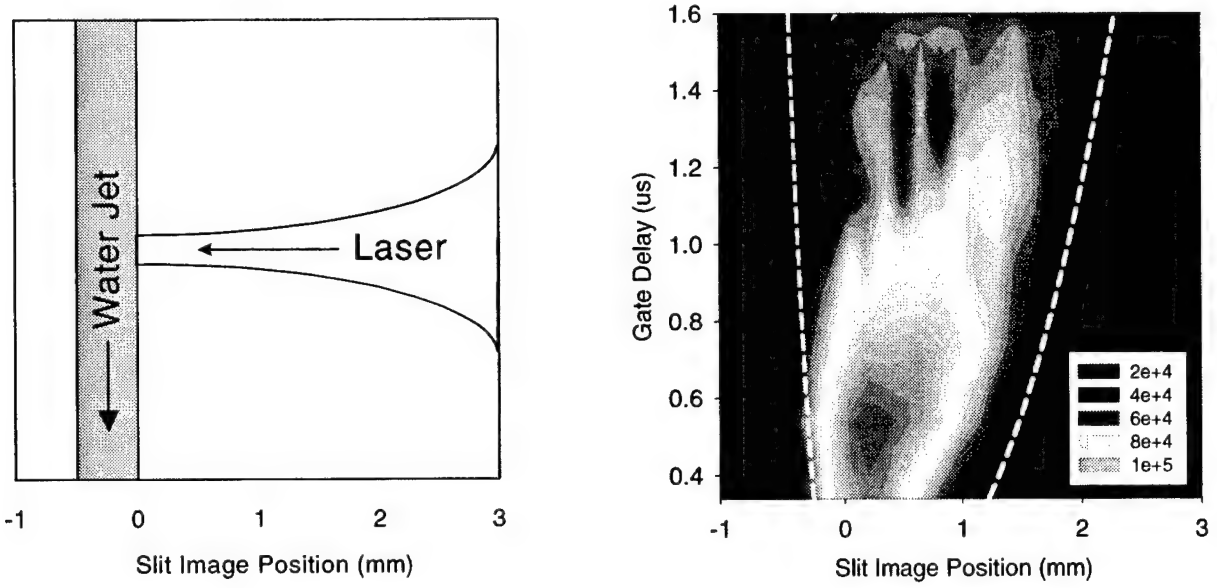

Fig. 1. (a) Schematic view of the experimental set-up. The water jet extends from –0.5 mm to 0 mm. The laser enters from right, and interacts with the water jet at a position of zero in space and time (b) Space time evolution of LIBS sodium emission at 589nm from plasma from a water jet. The dotted lines indicate the predicted blast wave propagation for strong shock waves in air (right) and water (left). Experimental conditions: 45 mJ/pulse, 200 ns Gate Width, 10 μm entrance slit on the spectrometer.

4. Limit of Detection

Liquid samples have two key advantages over solids: they are more homogenous than normal solids, and arbitrary concentrations in the ppm region can easily be prepared. In the present experiments, the signal strengths and background noise as functions of concentration have been characterized. The intersection of the signal strength with the 3σ level of background noise determines the detection limit, as can be seen in Figure 2. As expected, the signal from the sodium is linear with concentration, until it descends below the noise level. Pulse energies from 3 mJ to 100 mJ focused with a 30 cm lens have been tested for Na in water, resulting in detection limits from 200 ppm to 2 ppm respectively. With shorter focal length lenses one can achieve breakdown and emission at energies below a millijoule.

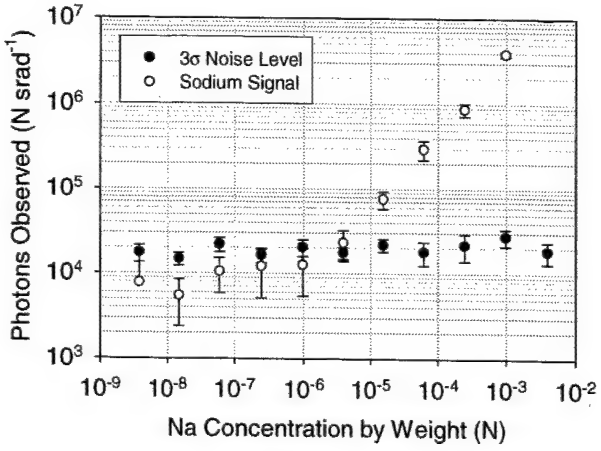

Fig. 2. Limit of detection of Na in distilled water. In this case, the LOD is 3 ppm. Experimental conditions: 45 mJ/pulse, 16 μs Gate Width, 1 μs Gate Delay, 10 μm slit.

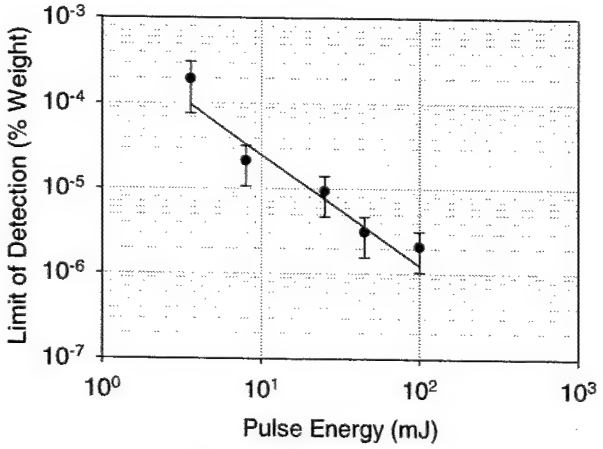

Fig. 3. Energy Scaling of limit of detection for sodium in water as a function of pulse energy using a 30cm focussing lens. The line is a least squares fit to the data.

5. Conclusion

A study is being carried out investigating the capabilities of laser-induced breakdown spectroscopy for analysis of water samples at pulse energies from sub millijoule to 100 mJ per pulse – a range lower than the pulse energies traditionally used in LIBS studies of liquid samples. The sub millijoule energy regime for LIBS of water samples is not well investigated, and optimal conditions need to be identified. It is expected that the present results may lead to improvements in the industrial applicability of LIBS, as low cost high repetition rate lasers can then be integrated into portable LIBS systems. Optimization of the limit of detection of contaminants in water requires detailed characterization of both the plasma line emission and the sources of background noise. The late time density and temperature of the expanding plasma can be derived using the Taylor/Sedev blast wave model, and spectral emission correlated with plasma conditions. The LIBS emission occurs from the region inside the predicted blast wave boundary in air. Pulse energies from 3 mJ to 100 mJ focused with a 30 cm lens lead to measurable emission from Na in water, resulting in detection limits from 200 ppm to 2 ppm respectively and the use of shorter focal length lenses allow signals to be detected even with sub-millijoule pulses..

6. Reference

[1] P. Mora, Phys. Fluids, 25, 1051, 1982.

NOTES

New LIBS Methodologies and Instrumentation: II

Wednesday, September 25, 2002

Russell Harmon, US Army Res. Lab., USA,
Presider

WD
4:10pm–5:30pm
Room: Royal Palm III

Quantitative Elemental Analysis of Metal Alloys by Laser Induced Breakdown Spectroscopy using Multivariate Calibration

Scott R. Goode, Richard Hoskins, Stephen L. Morgan
Department of Chemistry and Biochemistry, The University of South Carolina, Columbia SC 29208
Phone: 803-777-2601 FAX: 803-777-9521 Email: goodc@sc.edu, slmorgan@sc.edu

Abstract: Laser induced breakdown spectroscopy has enjoyed acceptance as an analytical tool in many areas despite its spectral interferences. We demonstrate here the application of multivariate calibration for quantitative elemental analysis of metal alloys.

OCIS codes: (300.6210) Spectroscopy, atomic (070.5010) Pattern recognition and feature extraction

1. Introduction

The ability of LIBS to predict accurate concentrations in metallic samples has been limited by matrix effects from the bulk of the sample. Solid samples and standards must be matrix matched to insure accurate results. For example, determination of chromium in high temperature alloys usually requires a series of high temperature alloy standards of known chromium concentration. Chromium calibrations using standards of a different type of alloy will not provide satisfactory quantitative results.

Multivariate calibration using principal component regression enables modeling of emission dependence on multiple analytes while taking multiple matrix effects into account. We have successfully applied multivariate calibration curve to the determination of several elements in metal alloys.

2. Experimental

Metal alloy samples were placed in a simple mount that allowed x-y positioning under computer control. The computer also controlled the z-axis by moving the focusing lens as needed. Emission was collected by an Echelle spectrometer with an intensified charge couple device (ICCD) camera (1).

Adventitious calibration was performed by taking standard alloy samples of widely varying, but known, composition (Table 1).

Three spectra of five steel alloys of composition were obtained by LIBS over a three day period. The echellograms were converted to spectra and then to ASCII data files. Intensities from twenty wavelengths selected wavelength in the range from 352.44 nm to 532.90 nm were selected for multivariate calibration. These files were analyzed by principal component regression (2) to produce multivariate calibrations for the five known elements.

Table 1. Composition of reference materials.

Standard	Ni	Fe	Mn	Cr	Cu
NBS845	0.28	83.523	0.77	13.3	0.065
NBS846	9.11	69.14	0.53	18.35	0.19
NBS850	24.8	46.88		22.13	24.9
NBS1204	70.6	3.1	0.41	12.75	0.056
BS3941	0.019	98.2918	0.8	0.068	0.053

3. Results and discussion

Figure 1 shows a plot of the 15 spectra over the 20 selected wavelengths in the calibration set. The spectral region chosen contains the 20 strongest lines in the spectrum observed from the BS 3941 standard (Table 1). These samples consist of a wide range of elemental compositions; for example, nickel varies for 0.28 to 70.6%, and iron ranges from 3.1 to 98.3%. The alloy spectra show obvious differences from their variation in compositions.

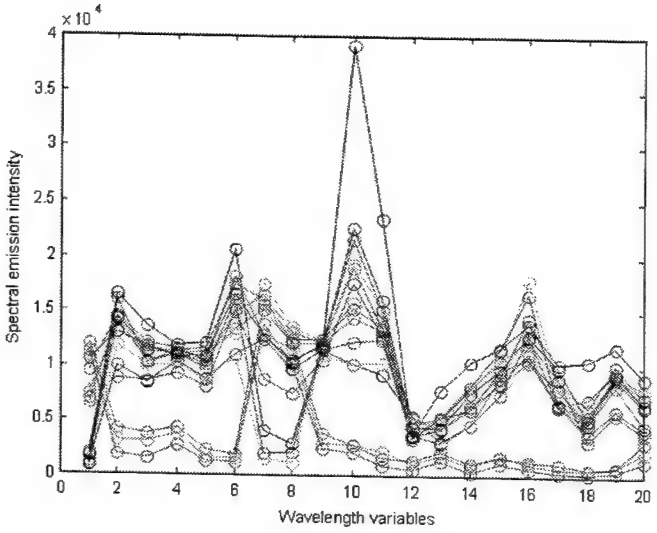

Figure 1. LIBS emission spectra for 15 alloy standards over 20 selected wavelengths (352.44 nm to 532.90 nm).

Principal component analysis indicated that 7 principal components are needed to evaluate nickel concentrations and 5 principal components are needed to evaluate iron concentrations. Plots of predicted versus measured composition for nickel and iron are shown in Figure 2. Figure 2A shows the calibration curve for nickel in the five alloys shown in Table 1. Fig. 2B shows the multivariate calibration results for iron. As mentioned above, LIBS analyses were performed in triplicate over a three day period; each set of three replicates are indicated in the plots below.

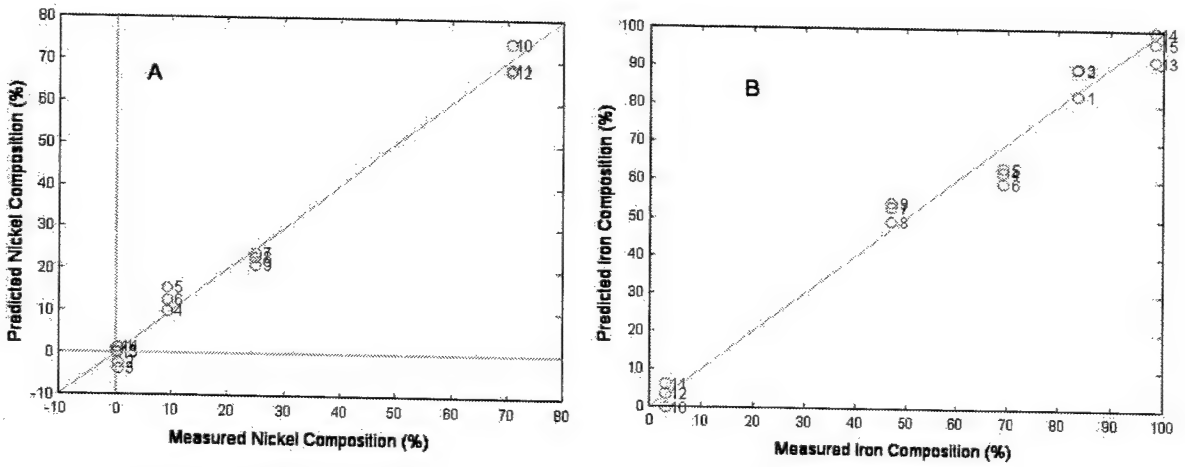

Figure 2. Multivariate calibration in metal alloys for (A) nickel composition (% w/w); and (B) iron composition (% w/w).

4. Conclusions

Multivariate calibration offers a valuable tool for accomplishing quantitative calibrations for elements in metal alloys. The ability of principal component regression to model multiple analyte compositions for a set of five alloys has been demonstrated.

5. References

1. Goode, S. R., Morgan, S.L., Hoskins, R., Oxsher, A. "Identifying alloys by laser-induced breakdown spectroscopy with a time-resolved high resolution echelle spectrometer," *J. Anal. At. Spectrom.* **2000**, *15*, 1133-1138.
2. W. J. Egan, W. E. Brewer, and S. L. Morgan, "Measurement of carboxyhemoglobin in forensic blood samples using UV/VIS spectrometry and improved principal component regression," *Appl. Spectrosc.* **1999**, *53*(2), 218-225.

Shooting slurries: sampling is the name of the game

D. Michaud, E. Proulx, J.G. Chartrand and L. Barrette
COREM, 1180 de la Minéralogie, Québec, Canada, G1N 1X7
daniel.michaud@corem.qc.ca

1. Introduction

COREM is a research consortium dedicated to provide the mining and mineral beneficiation industry with practical solutions to process and quality control needs. Laser-Induced Breakdown Spectrometry (LIBS) is viewed as a means of monitoring the chemical composition of process flow material, both on-line and in real-time, with minimal or no sample preparation. Upon applying the technology, though, to real-world situations, sampling is readily identified as a critical issue [1]. It is the purpose of this paper to report and discuss the problem of analyzing slurries with LIBS.

2. Experimental setup

The lasers used were Q-switched Nd:YAGs, model CFR-200, supplied by BigSky Laser Technologies; used at 1064 nm, pulses of circa 10 ns and 150 mJ could be focused to 0.5 mm^2 on target. The Czerny-Turner-type spectrometer used was a TRIAX 550, from Jobin-Yvon-Spex; it has a 550 mm focal length and a numerical aperture of f/6.4. A diffraction grating of 2400 l/mm, blazed at 250 nm was used for the present work. Emission spectra were recorded with an ICCD camera, from Andor Technology; with 690 x 128 elements of 26 x 26 μm, windows of about 12.5 nm in width could be viewed from a total spectral range of 180 nm to 850 nm.

For exploratory purposes, experience in analyzing slurries has driven us to establish three standard shooting conditions. These are: 1) one laser with 150 mJ pulses; 2) two simultaneous and co-linear lasers summing up to 300mJ; and 3) two cascaded lasers: an initial 100 mJ pulse followed 2 microseconds later with a 150 mJ pulse shot co-linearly to the first. A 2 μs delay is programmed before starting to record the emission from the plasma. Laser firing was initially done at a frequency of 1 Hz.

3. Prior work

Work was carried out earlier which demonstrated the practicability of measuring Si (along with C, Ca, Mg and Al) on-line in iron ore slurries [2]. These slurries, at 75% solids content, were high iron concentrates and the Fe signal was used as an internal standard. With an industrial-sized sampler, a precision of 0.2% was obtained (2-sigma at the 95% confidence level) on material containing between 0.4% and 5% silica. Shooting mode was cascaded lasers. Striving to push the work further in the laboratory, with a downscaled sampler-recirculator, results lacked reproducibility and calibration curves exhibited poor linearity.

4. Qualitative observations

The first (downscaled) laboratory recirculating system consisted of a closed circuit containing two funnels, one on top of the other, and a peristaltic pump. The pump merely took the exiting material from the lower funnel and dropped it in the upper funnel. The laser aimed at the 4.6 mm diameter free-falling

slurry column between the funnels. A number of detrimental phenomena were observed during operation, among which: sedimentation and channeling in the funnels, flotation, bubble pumping, pulsed flow, etc. Manual stirring inside the funnels, to tentatively homogenize the circulating slurry, only exacerbated signal instabilities because it put lumps of sedimented iron-rich material back into motion, especially in the upper-funnel. Also, the precise locations of the slurry entry point in the upper funnel and of both funnels relative to each other affected the results in a non-repeatable manner.

Looking into these problems, a new sampler geometry was devised (see Figure 1). It consists of a reservoir with a mechanical stirrer, a double-head peristaltic pump, a "laboratory" faucet (shaped like an upside-down J) and a rigid receiver tube. One end of the receiver tube slips tight over the tip of the faucet; the other end returns the slurry to the reservoir. The laser aims the 8 mm diameter free-falling slurry column through a hole in the receiver tube at a point situated 5 mm below the tip of the faucet. Around the strike point, downward aspiration is provided to evacuate nebulized material resulting from the laser impact: this enabled to raise the shooting frequency to 2 Hz without experiencing pre-hits on splashed material (see also reference [3] for a related geometry). The upside-down-J-shaped faucet is important to ensure good flow quality (minimizing exiting turbulences). The sampler is engineered in such a way that dismantling and reassembling sets it in a unique and repeatable geometry.

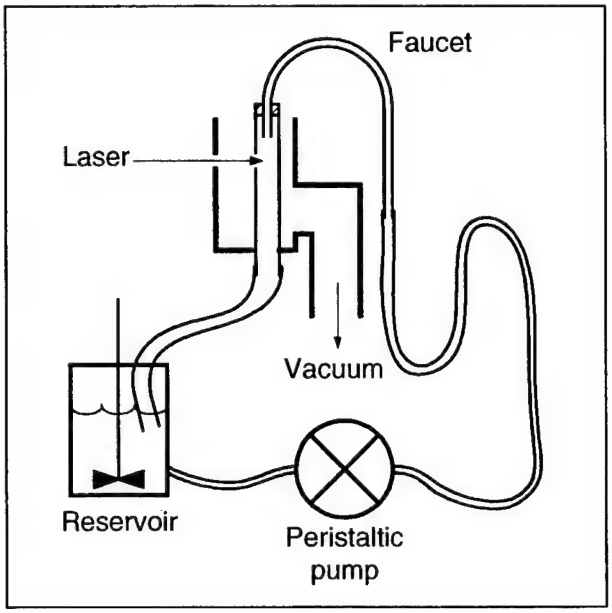

Fig. 1. Schematic of the slurry recirculator

5. Quantitative observations

Throughout the development of the sampler, two variables were specifically monitored: the signal stability (short term variance of Si at 288.16 nm and Fe at 282.55 nm) and the Si/Fe ratio. Said variables were greatly affected by any geometric change in the layout. Although signal stability, in a specific setup, could be observed in the short term, any disturbance of the sampler (even a specimen change) could sway the Si/Fe ratio out of due calibration. By way of a rigid geometry, long term stability and repeatability were obtained (circa ±5% on the ratio). Flow rate, inside the range from 2 to 5 L/min was found irrelevant.

Shooting too close to the tip of the faucet increased the variance of the signals; a distance of 5 mm was found to be most suitable. The horizontal position of the strike point on the slurry column was found to hold crucial influence on the Si/Fe ratio; the ratio was maximum when aiming the center but rapidly dropped by 50% when striking just 1 mm on either side (with original 4.6 mm spout). Using a larger slurry column and integrating a visor in a rigid hardware assembly solved this problem.

The new slurry sampler-recirculator was tested on similar material as done in the former work. Using cascaded lasers, the 2-sigma precision was established at 0.08% and linearity (R^2) scored 0.997. Shot to shot stability of signals yielded ±14% for Fe and ±29% for Si; these standard deviations shrink to 3.7% and 4.7%, respectively, when using 50-shots averaged measurements. The sum of lasers firing mode gave even better results, with 0.05% precision, 0.996 for R^2 and stability of 10% for both Si and Fe (2.5% on 50-shots measurements). This means that in a slurry (75% solids) containing between 0.4% and 5% silica per weight, a variation of only 0.05% in silica could be monitored; it is worth mentioning that our industry partners were hoping for a 0.10% sensitivity.

6. Conclusion

The sampling question is a key issue to sound LIBS measurements. Analyzing slurries (as well as suspensions, solutions and liquids in a general sense) with LIBS may suffer dramatic sampling inconsistencies. Thoughtful design of the slurry recirculator at the laboratory scale has enabled to increase sensitivity and signal stability significantly. The new sampler has been used to circulate high density iron ore slurries (which tend to sediment), low density graphite slurries (which tend to float) and iodine solutions successfully. Investigations are now oriented to studying the effect of %water in slurries and up-scaling the apparatus to industrial needs.

References

[1] Kenneth J. Grant, George L. Paul and James A. O'Neill, "Quantitative elemental analysis of iron ore by laser-induced breakdown spectroscopy", Appl. Spec. **45**, 701-705 (1991).

[2] Louis Barrette and Simon Turmel, "On-line slurry monitoring for real-time process control of pellet making processes using laser-induced breakdown spectroscopy: graphitic vs. total carbon detection", Spectrochim. Acta B **56**, 715-723 (2001).

[3] Susumu Nakamura, Yoshiro Ito, Kazuhiro Sone, Hitoshi Hiraga and Ken-Ichi Kaneko, "Determination of an iron suspension in water by Laser-Induced Breakdown Spectroscopy with two sequential laser pulses", Anal. Chem. **68**, 2981-2986 (1996).

Optimal Boiler Control through Real-time Monitoring of Unburned Carbon in Fly Ash Using Laser Induced Breakdown Spectroscopy

Miki Kurihara[1], Koji Ikeda[2], Yoshinori Izawa[2], Yoshihiro Deguchi[3] , and Hitoshi Tarui[4]

1) *Power Plant Engineering Department, Nagasaki Shipyard & Machinery Works, Mitsubishi Heavy Industries, Ltd.*
2) *Control & Electrical Systems Engineering Section, Power Plant Engineering Department, Nagasaki Shipyard & Machinery Works, Mitsubishi Heavy Industries, Ltd.*
3) *Applied Physics Laboratory, Nagasaki Research & Development Center, Mitsubishi Heavy Industries, Ltd.*
5-717-1 Fukahori-machi, Nagasaki, 851-0392, Japan
Tel: +81-(0)95-834-2322, Fax: +81-(0)95-834-2165, E-mail: deguchi@ngsrdc.mhi.co.jp
4) *Thermal Power Engineering Sec., Thermal Power Dept., Thermal & Nuclear Power Div., Tohoku Electric Power Company Inc.*

Abstract: A laser induced breakdown spectroscopy (LIBS) technique has been applied to detect the unburned carbon in fly ash, and an automated LIBS unit has been developed and applied in a 1000MW pulverized coal fired power plant for real-time measurement of unburned carbon in fly ash. Good agreement was shown between measurement results from the LIBS method and those from the conventional method(JIS 8815), with a standard deviation of 0.27%. This result confirms that measured unburned carbon in fly ash using LIBS is accurate enough for the boiler control and boiler control in optimized way is possible using the value of unburned carbon content in fly ash.

1. Introduction

Operating characteristics of coal-fired boilers are heavily influenced by factors such as differences in fuel properties and furnace surface dirtiness of heat transfer surfaces. Accordingly, in order to achieve optimal control of multiple coal fired boilers, it is necessary to accurately monitor the state of combustion, which is constantly changing, and to automatically adjust the control parameters[1]. The research presented here focused on the quantity of unburned carbon in fly ash as an indicator of the combustion state, considering the measured value as a basis for optimal and stable boiler combustion control, as well as fly ash quality control. As conventional analytical methods have required at least 20 minutes and have been conducted offline, it has not been possible to use the quantity of fly ash as a control indicator. With recent advances in laser measurement technology, however, the composition of solids can be assessed in real time. Our research applied this LIBS technique[2] in the development of apparatus for real-time measurement of unburned carbon in fly ash. Measurements taken by the apparatus were also integrated into the control system of a boiler with the objective of achieving optimal and stable combustion and operation of the boiler. By controlling the rotating speed of a mill rotary separator basis on the measured unburned carbon content, it was demonstrated that boiler control in optimized way is possible using the value of unburned carbon content in fly ash.

2. LIBS Measurement of Unburned Carbon in Fly Ash

The main components of fly ash are Si, Al, Fe, Ca, and carbon[3]. The carbon content in the fly ash can be calculated using the emission intensities of Si, Al, Fe, Ca, and carbon from the following equation.

$$\text{Unburned Carbon in Fly Ash} = \frac{f\ \alpha_C I_C/I_{Si}}{1 + f\ \alpha_C I_C/I_{Si} + f\ \alpha_{Al} I_{Al}/I_{Si} + f\ \alpha_{Fe} I_{Fe}/I_{Si} + f\ \alpha_{Ca} I_{Ca}/I_{Si}} \quad (1)$$

Here, I_i (J/s) is the emission intensity of species i, α_i is a variable factor related to species i, which contains the plasma temperature and pressure correction factors. These parameters have to be determined under the experimental operating conditions used in the power plant monitoring location[4].

The measurement apparatus consists of the MLIBS-UC2002 prototype developed by Mitsubishi Heavy

Industries, Ltd., and is composed of a measurement head box containing the laser device and a control box containing the measurement control device. The LIBS apparatus was installed at the economizer (ECO) outlet of Unit 1 at the Haramachi thermal power plant (1000MW pulverized coal fired power plant), operated by Tohoku Electric Power Co., Inc. The unburned carbon measurement range for this apparatus is 0~10%, and measurement results corresponding to a 1~5 minute moving average were transmitted to the boiler control system every 15 seconds to facilitate processor-controlled operations. Measured unburned carbon values were processed by means of new circuitry built into the boiler control unit.

3. Measurement Results of Unburned Carbon in Fly Ash

Our apparatus for the measurement of unburned carbon in fly ash was installed in December 1999, and was in operation through January 2001. Over ten types of coal were used during the operating period. Figure 2 presents a comparison between our measurement results and those obtained by using the standard method (JIS M8815). Simultaneous plots are shown for multiple types of coal. Good agreement is shown between measurement results from the LIBS method and those from the standard method, with a standard deviation of 0.27%. This comparison confirms that measured unburned carbon in fly ash is accurate enough for the boiler control and it is not affected by the type of coal when using the LIBS technique. Figure 3 presents examples of measurement results of unburned carbon in fly ash. Results for low fuel ratio coal are indicated by (a), with stable results having been obtained for unburned carbon value measurements. The transition from high to low fuel ratio coal is indicated by (b), and the difference in unburned carbon in fly ash resulting from the switchover can be seen in the corresponding measurement results.

4. Optimal Boiler Control Test Results

Optimal boiler control using measurement results for carbon in fly ash can be accomplished in various ways, including mill rotary separator speed and O_2 concentration. Separator speed was used in the current context to verify boiler controllability. Optimal control circuitry based on unburned carbon content was added to the existing boiler control circuitry, and separator speed was adjusted in conjunction with the measured values of unburned carbon provided by the LIBS apparatus. Figure 4 shows examples of control results based on unburned carbon. Unburned carbon setting values were varied from 2% to 1%, and then to 3%, and control characteristics at the actually measured values were observed. Average measured values changed from 2.3% to 2.0%, and then to 2.4%, confirming that control of unburned carbon content was possible with the new control circuitry. The difference between the setting values and the actual values are due to interference between the unburned carbon control logic and the existing multiple coal fired boiler control logic (attempting to maintain appropriate mill load based on mill current), which effectively limited the range of speed control. The speed of the rotary separator was raised through real-time unburned carbon control, and the value of unburned carbon was reduced, thereby increasing at-site efficiency (i.e., boiler efficiency) and enabling fly ash quality control. Conversely, increasing the unburned carbon value would reduce auxiliary power, such that operations could be performed in consideration of total plant running costs.

From the perspective of lowering total running costs, fan electric power could also be reduced. In this case, operations would be based on reducing the O_2 setting, and the use of unburned carbon values measured in real time could be used as an effective indicator for ascertaining the combustion state of the boiler.

5. Conclusion

An apparatus enabling real-time measurement of unburned carbon in fly ash was developed, and control results using measurement values from this apparatus were confirmed to be effective in optimal and stable boiler combustion control, as well as fly ash quality control. Future work will include applications such as the low O_2 setting, and the use of unburned carbon values measured in real time could be used as an effective indicator for ascertaining the boiler efficiency improvement.

References

[1] I. Moriyama, T. Sonoda, M. Kurihara, K. Yamamotomo, and N.Takahashi, M.H.I. Technical Review , Vol.35, No.1, (1998), p.22-25.

[2] Y. Deguchi, S. Iwasaki, K. Yoshikawa, H. Moritomi, and K. Matsumoto, IMEKO2000, Proceedings Volume II, (2000), p.179-184.

[3] D.K. Ottesen, L.L. Baxter, L.J. Radziemski, J.F. Burrows, Energy & Fuels, Vol.5, NO.2,(1991), p.304-312.

[4] M. Noda, Y. Deguchi, S. Iwasaki , and N. Yoshikawa, Spectrochimica Acta B, Vol.57,NO.4 ,(2002) p.701-709.

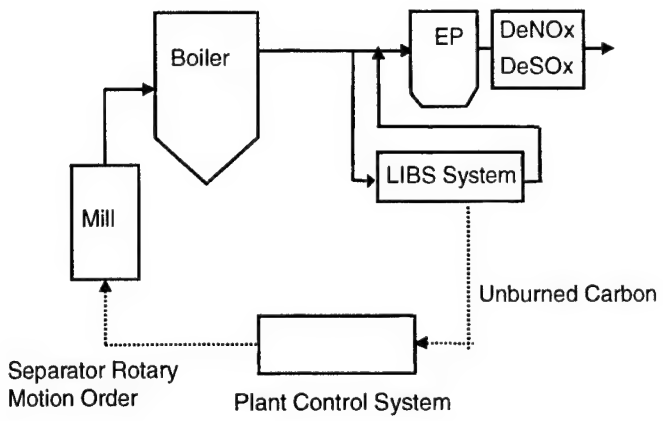

Figure 1 Unburned Carbon Measurement Systems for Optimal Boiler Control

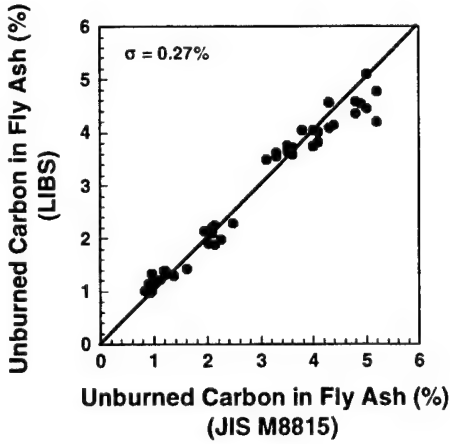

Figure 2 Comparison between LIBS and JIS M8815

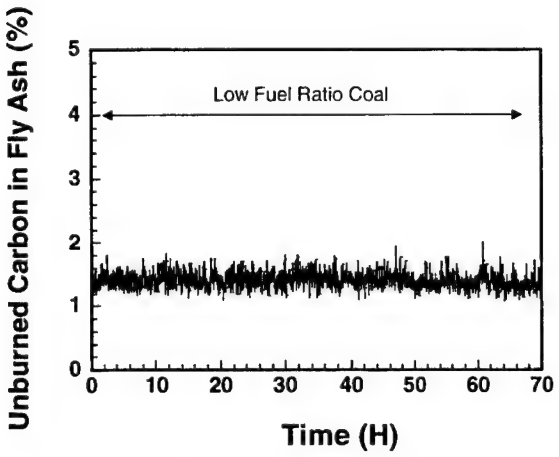

(a) Low Fuel Ratio Coal

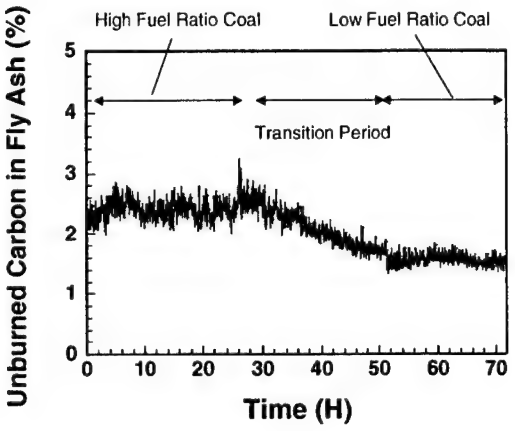

(b) Transition from High to Low Fuel Ratio Coal

Figure 3 Measurement Examples of Unburned Carbon in Fly Ash

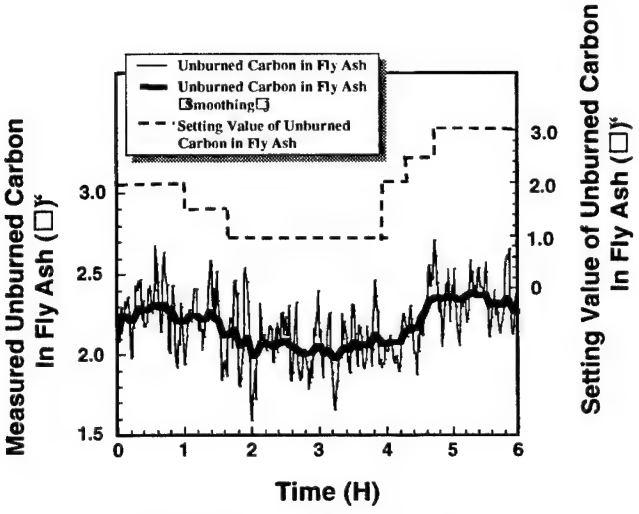

(a) Unburned Carbon Control Result

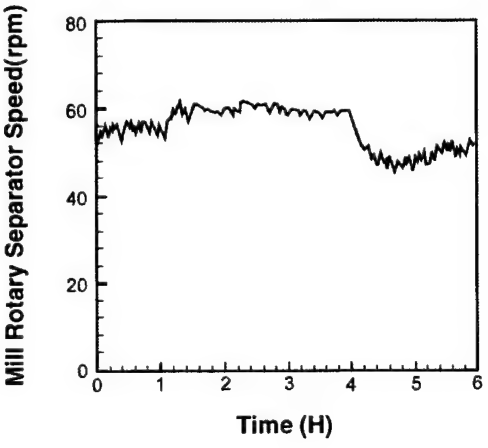

(b) Change of Mill Rotary Separator Speed

Figure 4 Examples of Unburned Carbon Control Results

On-line analysis of liquid samples by laser induced plasma spectroscopy (LIPS)

M. Sabsabi[1], R. Heon[1], J.M. Lucas[2], L. St-Onge[1], V. Detalle[1], A. Hamel[1]
[1] National Research Council Canada, Industrial Materials Institute
75, Boul. de Mortagne, Boucherville, Quebec, J4B 6Y4 Canada
[2] Noranda Technology Centre
240 Hymus Boul., Pointe Claire, Quebec, J9X 5B6 Canada
Email: mohamad.sabsabi@nrc.ca

Abstract: A LIPS monitor for real-time analysis of aqueous and other liquids has been developed. This system enables the laser to sample a fresh surface while preventing problems associated with the laser liquid interaction. We outline its successful laboratory and on-line industrial operation.

OCIS codes: (120.1880) Detection; (160, 3710) liquid, (140,3440) laser induced breakdown, (300.2140) Emission

1.0 Introduction

LIPS is a technique in which a laser pulse is focused onto a surface, or into a gas, to form a hot microplasma. The plasma light is spectrally and temporally resolved to obtain the sample's composition. Quantitative and qualitative analysis by LIPS has generally been applied to solids, with much less attention being paid to liquids [1-3]. This is largely due to the fact that analysis of liquid by existing analytical techniques is well established, and does not call for the laborious preparatory steps often needed for solids. However, since the reliable on-line analysis of liquids required to meet demands for improved control of industrial processes is often is difficult to achieve by conventional techniques, there is growing interest and publication in LIPS for liquids. Thus LIPS has been proposed for monitoring various elements in liquids, including molten metal, during industrial processing, as an alternative to sampling for subsequent laboratory analysis. Direct monitoring provides many advantages over discrete sampling, including the ability to adjust the process in real time according to analysis results.

In our development of an industrial LIPS instrument the following technical issues were addressed to produce a viable system. We needed to minimize the frequent cleaning of exposed optical components (focusing lens or window) to remove accumulated matter ejected and splashed from the monitored sample by incident laser pulses. Moreover, under some conditions, the miniature shock waves associated with vaporization of liquid samples create aerosols above the liquid surface, which disrupt both the incident laser beam and light returning to the spectrometer. The shock waves also tend to induce waves on the liquid surface, which increase shot-to-shot signal variation, and thus decrease measurement precision. Furthermore, it appears that laser pulses may induce bubbles inside liquids that are transparent at the laser wavelength. These bubbles may reach the surface being analyzed and change the characteristics of the laser-induced plasma, thereby affecting measurement reproducibility.

To overcome the problems associated with plasmas generated from liquid samples, a variety of LIPS configurations have been applied in experiments on liquids, including, plasma formation on the surface [2-5], in the bulk liquid [6], on droplets [7], and on liquid jets [8]. Most of the papers published focused on the detection of trace elements in the liquid, and almost none to our knowledge were devoted to the analysis of analyte elements present at high concentrations (> 10%). We are also not aware of industrial application of on-line LIPS analysis to aqueous solutions.

In this paper, we outline application of a new configuration to overcome the problems mentioned above, and describe its use in the quantitative analysis of both low (ppm) and high concentration (%) levels of analyte elements in liquids. Also, we provide an example of application of our LIPS system to the on-line measurement of residual metal concentrations in aqueous liquid in an industrial plant, and compare results with laboratory analysis.

2.0 Results and discussion

Figure 1 shows the experimental setup used in our laboratory for the LIPS analysis of liquid. The plasma is generated on the surface of the liquid by focusing Nd:YAG laser pulses (8 ns, 300 mJ, 1064 nm).

Light collected from the plasma emission through a quartz window (see Figure 1) above the liquid is focused into a fiber optic cable, and thus conveyed to a spectrometer coupled to an intensified CCD detector. For quantitative analysis by LIPS, elements are monitored by the measurement of spectral peak intensities, with lines selected to be proportional to species concentrations. Line intensities are affected by several parameters. In particular, they are highly dependent on the degree of vaporization and ionization, both of which can change as a function of laser wavelength, laser fluence, pulse-to-pulse variability, sample surface morphology, ambient gas pressure, and ambient gas species. When the bubbles created inside the liquid by the laser pulse burst at the surface, or the waves induced on the surface by the laser pulse are not dissipated, they change the angle of incidence between the laser beam at the liquid surface. This in turn, can change the fluence of the laser, and hence line intensity. Also, aerosols created by the laser-liquid interaction absorb the laser beam, and partially prevent the laser from reaching the sample surface. This absorption can change the reproducibility of the measurement by affecting the energy delivered to the sample.

In our instrument, the droplets and aerosols generated by the laser pulse are deflected from the optical path by a nearby air jet or air exhaust fan. Furthermore the liquid flow sweeps away laser induced bubbles below its surface, and thus prevents them from reaching the point of laser impact. Also, the form in the cell promotes a stable liquid surface by breaking the wave generated by the laser pulse. We thus improve measurement reproducibility and accuracy by enabling the laser to sample a stable and even liquid surface. Provision is made for easy removal of the protective window for cleaning deposits from any residual spray during on-line measurement. A second optical window above the removable window completes isolation of the sample region from the laser and other sensitive components. If necessary, added protection from infiltration of corrosive fumes, or other contamination, into the enclosure housing the laser and other optics may be provided by purging with instrument air. An example of industrial on-line application of this configuration will be given in the presentation, and the results compared with those obtained by conventional laboratory analysis.

For the LIPS analysis of analyte at high concentrations we studied aqueous solutions with calcium in the range of 10-20%. Our results indicate that the successful analysis depends on the selection of analyte lines. We show that analysis is feasible using weak lines that are not self absorbed by the plasma. Since self absorption of lines depends in part on the population of lowest level of the line, the selection should avoid also those related to metastable levels.

Table 1 compares results obtained for the Ca 393.3 nm line in an aqueous solution. It shows how measurement reproducibility obtained by focusing laser pulses onto the solution's surface is enhanced by an air removal blower. The table also shows how liquid flow further improves measurement reproducibility. This combination of blower and liquid flow permits continuous analysis with a reproducibility, based on 100 laser shots, of better than 2%.

Liquid	Blower	Net Amplitude Ca 393.3 nm	Std. Dev'n	SD/Amp %
Flowing	On	9630	1220	12.6
Flowing	Off	5715	3314	58.0
Stationary	Off	5180	4030	77.9
Stationary	On	9883	3439	34.9

Table 1: Comparison of the reproducibility of single shot laser measurements with and without air blowing and liquid motion

3.0 Conclusion

In this paper we have described a new LIPS analysis configuration which overcome problems associated with plasma generated by laser pulses at liquid surfaces, and thereby achieves better than 2% reproducibility. Our system was used in the laboratory for quantitative analysis of analyte elements in water at both low (ppm), and high (5 - 25%) concentrations. Continuous on-line measurement of residual metal in aqueous solution at an industrial plant is also described.

References

1. R. Knopp, F.J. Scherbaum, J.I. Kim, Fresenius J. Anal. Chem. **355**, 16 (1996)
2. O. Samek, D.C.S. Beddows, J. Kaiser, S.V. Kukhlevsky, M. Liska, H. Telle, J. Young, Opt. Eng. **39,** 2248 (2000).
3. P. Fichet, P. Mauchien, J.F. Wagner, C. Moulin, Anal. Chim. Acta **429**, 269 (2001).
4. C. Arca, A. Ciucci, V. Palleschi, S. Rastelli, E. Tognoni, Appl. Spectrosc., **51**, 1102 (1997)
5. L.M.Berman, P.J. Wolf, Appl. Spectrosc. **52**, 438 (1998).
6. D.A. Cremers , L. Radziemski, T.R. Loree, Appl. Spectrosc. **38**, 721 (1984)
7. D.E. Poulain, D.R. Alexandre, Appl. Spectrosc. **49**, 569 (1995)
8. S.Nakamura,Y. Ito, K. Sone, H.Hiraga, K. I. Kanedo, Anal. Chem. **68**, 2981 (1996).

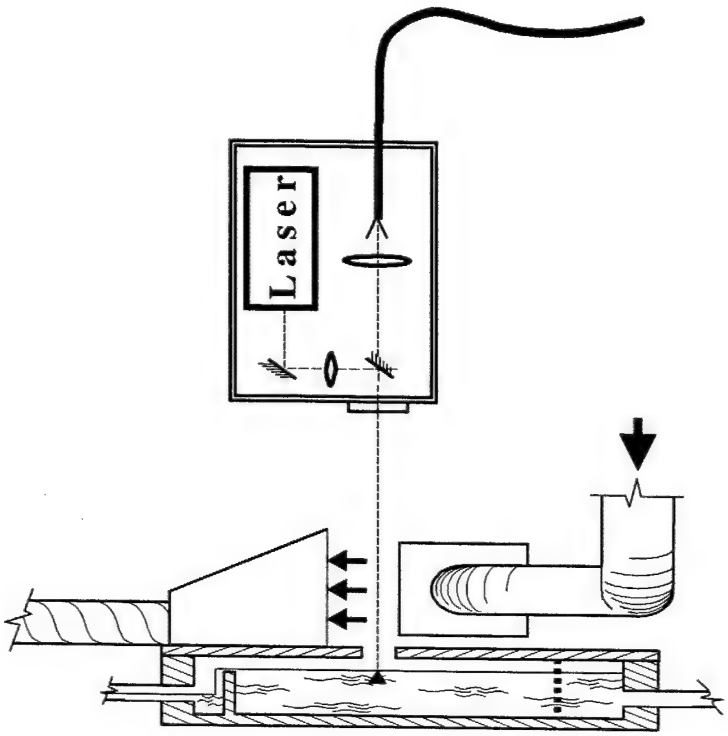

Figure 1: LIPS setup for liquids analysis

NOTES

LIBS for the Environment and Art

Thursday, September 26, 2002

Mohamed Harith, Cairo Univ., Egypt,
Presider

ThA
8:30am–10:10am
Room: Royal Palm III

ENVIRONMENTAL APPLICATION OF LASER INDUCED BREAKDOWN SPECTROSCOPY

Jagdish P. Singh and Virendra N. Rai*
Diagnostic Instrumentation and Analysis Laboratory
Mississippi State University
205 Research Boulevard, Starkville, MS, 39759-7704 (USA)
Tel: 662-325-7375, e-mail:singh@dial.msstate.edu, * on leave from CAT, Indore-452013, India

ABSTRACT

Laser induced breakdown spectroscopy (LIBS) has the capability to perform rapid, online and real time analysis of materials in difficult and harsh environmental conditions. The application of LIBS, as a multi metal continuous emission monitor for off gases, in the analysis of soil and nuclear waste, is presented.

1. INTRODUCTION

Laser induced breakdown spectroscopy (LIBS) is a laser based diagnostics technique for measuring the concentration of various elements in the test medium [1-2]. In the LIBS technique, a pulsed laser beam is focused at the test point to produce a spark. The spark in the focal region generates high-density plasma, which atomizes and excites various atomic elements in the test volume. Atomic emission from the plasma is collected with the help of a collimating lens and sent to the detection system. The intensity of the atomic emission lines observed in the LIBS spectrum is then used to infer the concentration of the atomic species. LIBS has been used to analyze solid, liquid, gas and aerosol samples even if it is present in a harsh and difficult environmental conditions [2]. It can significantly reduce the time and cost associated with the sample preparation required by the conventional analytical techniques and is therefore a promising technique for environmental monitoring and process control. LIBS has been applied to many environmental situations. The application of LIBS in environmental monitoring and in industrial process control is reviewed.

2. ENVIRONMENTAL APPLICATION

2.1 Off-Gas Emission

The detection of trace elements in the off gas from waste processing is very important for public health. LIBS has been used to perform in-situ off gas measurements by focusing the laser beam on the gas stream through a window and collecting the signal through an optical fiber. Neuhauser et al. [3] tested an on line lead (Pb) aerosol detection system with aerosol diameters ranging between 10 and 800 nm. A detection limit of 155 $\mu g\ m^{-3}$ was found. LIBS has been demonstrated as a process monitor and control tool for waste remediation [4]. The toxic metal from three plasma torch test facilities have been monitored and was found that LIBS can be integrated with a torch-control system to minimize toxic metal emission during plasma torch waste remediation. The possibility of using metal hydride to calibrate metals in off gas emission was investigated [5]. A static sample cell was used to perform LIBS experiment on metal hydrides and was found that the LIBS signal was affected by gas composition, gas pressure and laser intensity. It was also found that LIBS signal intensity for metal hydrides changes with time.

The use of LIBS as continuous emission monitor (CEM) requires the quantitative trace level determination of the toxic metals. The LIBS system developed in DIAL was successfully used to monitor the concentration of selected toxic metals in near real time [6]. The concentration of Be and Cr were measured at all the tested metal levels. The concentration of Cd was measured during medium as well as and high metal feed tests whereas the concentration of Pb was measured at only high concentrations. It was found that the LIBS system can be used as a CEM to monitor only the concentration of Be, Cr and Cd. However, a further improvement in the sensitivity of this system is needed to get a better limit of detection for Pb, Hg, As and Sb.

2.2 Soil, Concrete and Paint

Detection of contaminated soil and concrete is another important area of research for LIBS. Yamamoto et al. [7] have used a portable LIBS system to detect toxic metals in soil. The detection limit of

Ba, Be, Pb and Sr in soil was reported as 265, 9.3, 298 and 42 ppm, respectively. Cremers et al. [8] have detected Ba and Cr in soil using an optical fiber probe. Limit of detection of 26 ppm and 50 ppm were found for Ba and Cr, respectively. The effect of matrix has been studied in soil sample. The LOD for Pb an Ba in a sand matrix were found as 17 and 76 ppm (by weight), respectively with a precision of 7% RSD or less. In the soil, the detection limit were 112 and 63 ppm for Pb and Ba respectively with 10 % RSD precision. The LIBS signal was affected by chemical speciation as well as matrix composition. LIBS accuracy can be degraded if calibrations are not matrix specific.

Pakhomov et al. [9] has applied the LIBS for the detection of Pb in contaminated concrete. A time resolved LIBS spectra was recorded for the quantitative measurement of the Pb content in concrete. Pb calibrations were obtained for different delay times using the ratio of the integrated emission line of lead (405.78 nm) to an oxygen line (407.59 nm). They found the absolute Pb signal was independent of the laser pulse energy for laser energy between 250 and 400 mJ. Based on the analysis of the sensitivity of the lead measurements at different delay times, they derived a best lead detection limit of 10 ppm in concrete at an optimum delay time of 3.0 μs. Similarly Pb in the paint is a potential health threat, specially to children. Yamamoto et al. [7] has successfully demonstrated the feasibility of using LIBS to determine Pb in the paint surface

2.3 Radioactive Elements

LIBS has also been used to monitor the level of radioactive elements in a process stream. Watcher and Cremers [10] found a detection limit of 100 ppm for uranium in solution. LIBS is preferable to other radiological measurements because nuclear detector may not be able to differentiate the radionuclides U, Pu and Np. The LIBS spectra of U, Pu an Np was recorded in a globe box and the emission lines suitable for the detection of these radioactive elements were identified [11]. Their preliminary studies shows that LIBS is suitable for the measurement of radioactive elements in waste stream. LIBS has also been used as a tool for detection of radiation embrittlement [2] in a nuclear power plant by determining the copper concentration in A533b steel. As copper is a key impurity contributing to radiation embrittlement, the Cu concentration in the steel is an indicator of radiation embrittlement and of expected material lifetime.

3. IMPROVEMENT IN THE SENSITIVITY OF LIBS

Technetium (Tc) is a radioactive element, which is encountered during the processing of nuclear waste. An effort is in progress to make the technetium monitor which needs an improvement in the sensitivity of LIBS technique. Various techniques have been used to improve the sensitivity of LIBS, such as application of magnetic field, double pulse excitation and the use of purge gas around the liquid jet .An enhancement of 1.5-2 times in the emission from the laser produced plasma was obtained using a steady magnetic field of ~5 kG. The magnetic field system used in this experiment is easily available and is simple to handle. The enhancement factor depended mainly on the nature of target material (solid or liquid) as well as on the transition probability of the elements [12]. Saturation (decrease) in the signal was also noted towards higher laser energy in the absence as well as in the presence of a magnetic field. Saturation became pronounced in the presence of a magnetic field in both types of samples for higher laser energy. Simple analysis of plasma emission in the presence of a magnetic field explained the experimental findings of enhancement in emission and showed that this enhancement depended mainly on the plasma β (ratio of plasma kinetic energy to magnetic energy) parameter. No enhancement in plasma emission was possible, when the plasma beta was high due to high plasma temperature and high plasma density. A correlation between an enhancement in the plasma emission and deceleration in the plasma expansion was noted through plasma β. As the plasma decelerated under the effect of a magnetic field the emission from it started increasing. A model was presented here to explain the phenomenon well, which showed that emission was mainly dependent on plasma β, which is a function of plasma density, its temperature and the external magnetic field. It was noticed that the consideration of other plasma parameters and their temporal evolution in the model would make the model more versatile.

In another experiment ssystematic studies of the emission from magnesium plasma produced under the double laser pulse excitation were performed [13]. The inter-pulse separation between lasers was varied from 0 to 20 μs. The measurements showed an enhancement in the emission by a factor of more than six times for the inter pulse separation of 2-3 μs. It was noted that increasing the inter-pulse separation between the lasers made neutral magnesium line emission dominant over the ion line emission. Observation

of maximum enhancement in emission at 2-3 μs inter-pulse intervals indicates that an optimum expansion of pre-plasma was necessary for better absorption of the second laser. Ultimately it provided an increased plasma volume, which contributed to the enhancement of emissions. An increase in the background emissions, just after the interaction of second laser pulse with pre-formed plasma, indicated about the increase in plasma temperature due to its better absorption. An increase in plasma temperature could have increased the ablation of the target material, which could have finally increased the density of the emitting volume of the plasma. These observations indicated that an increase in the emitting plasma volume, plasma temperature and ablation of the sample material after second laser pulse contributed towards enhancing the emission from the plasma. Enhancement in the emission from the plasma was found directly related with improvement in its sensitivity.

4. CONCLUSION

It was found that LIBS can work as a process monitor and provides online and real time information about the concentration of toxic and hazardous elements in different types of matrices. Further improvement in its sensitivity will make this technique even more useful.

ACKNOWLEDGMENT

This work was supported by U.S. Department of Energy cooperative agreement No. DE-FC26-98FT-40395.

REFERENCES

1. L. J. Radziemski, D. A. Cremers (Ed.), "Spectrochemical analysis using plasma excitation," in: Laser Induced Plasmas and Applications, Marcel Dekker, NewYork, NY, 1989, ch. 7, pp 295-325.
2. F. Y. Yueh, J. P. Singh and H. Zhang, Laser-induced breakdown spectroscopy: Elemental analysis. Encyclopedia of Analytical Chemistry, John Wiley & Sons, Ltd. Vol. **3** 2065-2087 (2000).
3. R. E. Neuhauser, U. Panne, R. Niesner, G. A. Petrucci, P. Vavalli, N. Omenetto, "On line and in-situ detection of lead aerosols by plasma spectroscopy and laser excited atomic fluorescence spectroscopy," Anal. Chim. Acta, **346,** 37-48 (1997).
4. J. P. Singh, F. Y. Yueh, H. Zhang, R. L. Cook, "Study of laser-induced breakdown spectroscopy as a process monitor and control tool for hazardous waste remediation," Process control Quality, **10,** 247-258 (1997).
5. J.P.Singh, H. Zhang, F.Y.Yueh and K.P. Carney, "Investigation of the effects of atmospheric conditions on the quantification of metal hydrides using laser-induced breakdown spectroscopy," Appl. Spectrosc. **12,** 764-773 (1996).
6. H. Zhang, F. Y. Yueh and J. P. Singh, "Laser-induced breakdown spectrometry as a multi metal continuous emission monitor," Appl. Opt. **38**, 1459-1466 (1999).
7. K.Y. Yamamoto, D. A. Cremers, M.J. Ferris and L.E. Foster," Detection of metals in the environment using a portable laser-induced breakdown spectroscopy instrument," Appl. Spectrosc. **50,** 222-233 (1996).
8. D. A. Creamers, J. E. Barefield, A. C. Koskelo," Remote elemental analysis by laser-induced breakdown spectroscopy using fiber optic cable," Appl. Spectrosc. **49**, 857-860 (1995).
9. A. V. Pakhomov, W. Nichols, J. Borysow, "Laser-induced breakdown spectroscopy for detection of lead in concrete," Appl. Spectrosc. **50**, 880-884 (1996).
10. J. R. Watcher and D.A. Cremers, " Determination of uranium in solution using laser-induced breakdown spectroscopy," Appl. Spectrosc. **41**, 1042-1048 (1987)
11. J.P. Singh, F.Y. Yueh, H. Zhang and K.P. Carney," A preliminary study for the determination of uranium, plutonium and neptunium by laser-induced breakdown spectroscopy, " Rec. Res. Dev. Appl. Spectrosc. **2**, 59-67 (1999).
12. V. N. Rai, A. K. Rai, F. Y. Yueh and J. P. Singh, " Laser-induced breakdown spectroscopy of liquid and solid sample in the presence of magnetic field," Laser application to Chemical and Environmental Analysis, Technical Digest (OSA) FA31-FA33 (2002).
13. V. N. Rai, F. Y. Yueh and J. P. Singh, " Laser-induced breakdown spectroscopy of liquid sample with double pulse excitation," 223rd ACS National meeting, Orlando, Fl. April 7-11 (2002), Appl. Optics (Communicated).

Environmental Monitoring of Total Carbon and Nitrogen in Soils using Laser-Induced Breakdown Spectroscopy

Madhavi Martin, Stan Wullschleger, Charles Garten Jr., and Anthony Palumbo
Environmental Sciences Division, Oak Ridge National Laboratory, Oak Ridge TN, 37831-6038
(865)-574-7828, (865)-576-8646, martinm1@ornl.gov

Abstract: We have successfully demonstrated the technique of laser-induced breakdown spectroscopy (LIBS) in the determination of the total concentration of carbon and nitrogen in soils. We have obtained a linear calibration curve for carbon in 15 soil samples directly correlated to the soil combustion technique.

OCIS codes: (140.3440) Lasers and laser optics

Introduction

Carbon reservoirs at the earth's surface comprise the atmosphere, biomass, and organic and inorganic carbon in soils, lakes, rivers and ocean surfaces. These reservoirs interact with the atmosphere and affect its CO_2 content. Knowledge that CO_2 is stored within and exchanged between the atmosphere and vegetation and soils has lead to the suggestion that soils and vegetation could be managed to increase their uptake and storage of CO_2, and thus become 'land carbon sinks'. Uncertainty in the scientific understanding of the causes, magnitude and permanence of the land carbon sink is of utmost concern and hence in need of instrumentation and technology development to accurately measure baseline amounts of carbon sequestered in land masses[1]. Soil organic matter (SOM) is the sum total of all organic carbon containing substances in soils. SOM influences plant growth through its effects on the physical, chemical, and biological properties of soils. SOM consists of humic substances that are amorphous, dark-colored, complex, polyelectrolyte-like materials[2]. The very complex structure of humic and fulvic acid makes is difficult to obtain a spectral signature for all soils in general[3]. The percentage of the humus that occurs in the various humic fractions varies considerably from one soil type to another. The humus of forest soils is characterized by a high content of fulvic acids while the humus of peat and grassland soils is high in humic acids.

Laser spectroscopic techniques are well established for their versatility in environmental chemical analysis because they offer real-time monitoring capabilities with high analytical sensitivity and selectivity [4]. FT-IR, FT-Raman, dispersive Raman, surface-enhanced Raman, and ^{1}H-NMR spectroscopies [5,6] have been applied to investigate molecular changes in SOM. These techniques are valuable for in-laboratory research. However, to take an instrument or technology into the field requires another level of research and development to ensure ruggedness, stability, reliability, small footprint, and calibration algorithms that have been tested for a variety of matrices. The choice of particular laser technique is decided by the specific problem at hand. For example, in the elemental characterization of airborne particles, if simultaneous *in situ* multielement determination is desired then laser-induced breakdown spectroscopy (LIBS) is the technique of choice. We have applied this technique to the determination of total carbon and nitrogen in various soils[7].

The LIBS technique

The ability of LIBS to provide rapid multielemental microanalysis of bulk samples (solid, liquid, gas, aerosol) in the parts-per-million (ppm) range with little or no sample preparation has been widely demonstrated. LIBS induces the vaporization of a small volume of sample material with sufficient energy for optical excitation of the elemental species in the resultant sample plume. The vaporized species then undergo de-excitation and optical emission on a microsecond time scale, and time-dependent ultraviolet-visible spectroscopy fingerprints the elements associated with the spectral peaks. LIBS is typically a surface analytical technique, with each laser pulse vaporizing microgram or submicrogram sample masses. However, the rapidity of sampling (typically 10 Hz laser repetition rate) and ability to scan a sample surface, ablate a hole into a solid sample with repeated laser pulses, for depth profiling or focus the laser spark below the surface of a liquid sample permits more versatile analyses and provides sufficient statistics for bulk sampling. The greatest advantage of LIBS is its capability for remote chemical analysis of samples with minimal handling and little or no sample preparation, which minimizes generation of waste to the microgram per pulse of ablated material. Although calibration standards are required for quantitative analysis, the generation of a single calibration curve will suffice for analysis of samples in a similar matrix.

Experimental setup

The experimental setup employs a Spectra Physics™ laser, model INDI-50. This is a Q-switched Nd: YAG laser that has output wavelengths at the fundamental wavelength of 1064-nm, frequency doubled to 532-nm, and frequency quadrupled to 266-nm. For these experiments, we used the 266-nm laser wavelength with 23 mJ/pulse as the excitation energy. The laser pulsewidth is 6-8 ns and the repetition rate is 10 Hz. All the processes such as plasma formation, emission, gated detection, data collection, and analysis are completed within 100 milliseconds until the next pulse arrives in the sample volume. The pulsed laser beam is focused onto a soil sample that has been pressed into a pellet. The light emitted by the resulting plasma is collected by an optical collection system situated at ~ 45° angle to the axis of the sample and the laser excitation beam and is delivered to an Acton Research Inc. spectrometer (SpectraPro-500) via a carbon-core fiber-optic cable bundle. The resolved spectrum is detected by an intensified charge coupled device (ICCD) built by Andor Technology with the ICCD delayed and gated by a Stanford Research Systems model SRS535 delay generator. Figure 1 shows the characteristic elemental carbon peak that occurs at 247.9 nm.

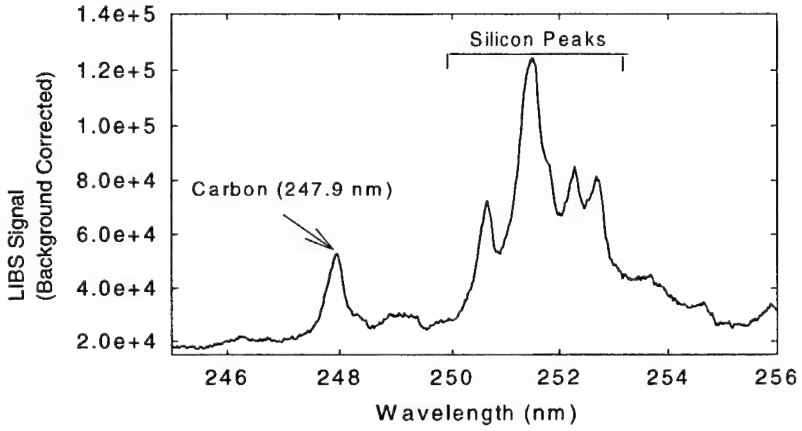

Figure 1. LIBS Signal for Carbon in Soil

The numerous peaks around 252 nm wavelength are silicon peaks, with silicon very abundant in most soils.

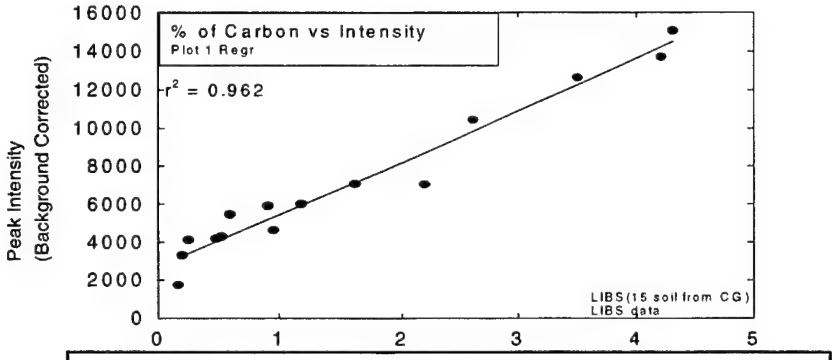

Figure 2. LIBS Calibration Curve for Soil Carbon Content

The LIBS signal as a function of carbon content in different soil samples is shown in figure 2. From the data shown in figure 2, it is observed that the linearity of the calibration extends from < 0.2 % to > 4 % of carbon contained in

15 soil samples. These fifteen soils were obtained from Oak Ridge National Laboratory's, Natural and Accelerated Bioremediation Research (NABIR) Field Research Center (FRC).

We have also taken four different soils from SW Virginia mined lands and have analyzed each soil at least twenty times using LIBS to obtain the standard deviation in those soils for the carbon and nitrogen concentrations, and compared to LECO carbon-nitrogen-2000 elemental analyzer. The data for the same soils was obtained before and after acid washing of the soils. It has been observed that after acid washing the amount of total carbon signal decreased significantly (50%-60%), while the amount of nitrogen remained within the percentage of standard deviation before being washed in acid. This is to be expected since the acid washing of the soils eliminates the inorganic carbon and will not affect the organic carbon (bound to the nitrogen in the soils).

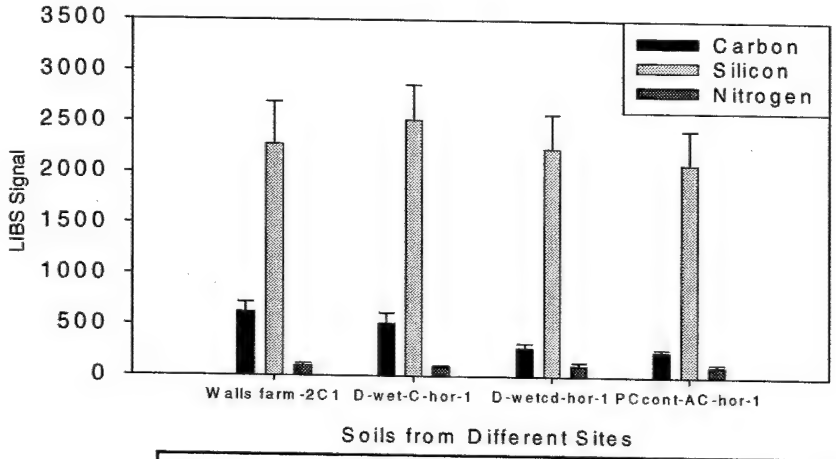

Figure 3. Concentration of carbon, silicon, and nitrogen in the four soils from SW Virginia mined lands.

Conclusions

In this research we have shown LIBS to be a viable technique in the determination of total carbon and nitrogen concentrations. The variability has been reduced by increasing the number of spectra over which the data is averaged. In case of certain soils the ratio C/Si can be used to reduce this variability. The LIBS technique can be used to determine the total concentration of carbon and nitrogen *in situ* in field measurements.

References

1. D. Read, D. Beerling, M. Cannell, P. Cox, P. Curran, J. Grace, P. Ineson, Y. Malhi, D. Powlson, J. Shepherd, and I. Woodward, *The role of land carbon sinks in mitigating global climate change,* 1-27, The Royal Society, London, 2001.

2. M. Schnitzer and U. Khan, *Humic Substances in theEnvironment*, 2-3, Marcel Dekker, New York, 1972.

3. F. J. Stevenson, *Humus Chemistry*, 1-25, John Wiley and Sons, New York, 1982.

4. S. J. Weeks, H. Haraguchi, and J. D. Winefordner, "Improvement of Detection Limits in Laser-Excited Atomic Fluorescence Flame Spectrometry," Analytical Chemistry, **50**, 360-68, 1978.

5. O. Francioso, S. Sanchez-Cortes, V. Tugnoli, C. Ciavatta, L. Sitti, and C. Gessa, "Infrared, Raman, and Nuclear Magnetic Resonance (^{1}H, ^{13}C, and ^{31}P) Spectroscopy in the Study of Fractions of Peat Humic Acids," Appl. Spectrosc., **50** (9), 1165-1174, 1996.

6. T. Wang, Y. Xiao, Y. Yang, and H. A. Chase, "Fourier Transform Surface-Enhanced Raman Spectrof Fulvic Acid from Weathered Coal Adsorbed on Gold Electrodes," J. Environ. Sci. Health, A **34** (3), 749-765, 1999.

7.Madhavi Martin, Stan Wullschleger, and Charles Garten Jr., "Laser-induced breakdown spectroscopy for environmental monitoring of soil carbon and nitrogen", Proceed. SPIE, 4576: 188-195.

Acknowledgements

We would like to acknowledge Bonnie Lu in analyzing the fifteen soils by LECO technique. Research sponsored by the Laboratory Directed Research and Development Program of Oak Ridge National Laboratory, managed by UT-Battelle, LLC, for the U.S. Department of Energy under Contract No DE-AC05-00OR22725.

Ambient Measurements of Inorganic Species in an Urban Environment Using LIBS

[1]Gregg Lithgow, [2]Allen L. Robinson, [1]Steven G. Buckley*

[1]Department of Mechanical Engineering, University of Maryland, College Park, MD
* = Corresponding Author; 301-405-8441, buckley@eng.umd.edu

[2]Department of Mechanical Engineering, Carnegie Mellon University, Pittsburgh, PA

Abstract:

Urban environments contain high levels of particulate matter of a variety of forms. The University of Maryland (UMCP) has been participating in a large-scale multi-University effort to characterize urban particulate matter in Pittsburgh, PA. This "Aerosol Supersite" project, sponsored by the U.S. EPA and the U.S. Department of Energy, brings together a number of aerosol measurement technologies to characterize the size, organic and inorganic constituents, and ionic character of the urban aerosol. UMCP has been working to employ LIBS for inorganic species concentrations measurements in the ambient aerosol.

We present temporal analysis of species measurements made at the Pittsburgh Supersite. These measurements, made over a two-week period, illustrate both the power of the LIBS analysis for on-line aerosol analysis, and several sampling challenges that it was necessary to overcome to allow the measurements to work out correctly. These include the sampling configuration, the sample cell design, and the sample flow characteristics. Measurements made with an echelle spectrometer and with a traditional grating spectrometer, both coupled to ICCD cameras, reveal difficulties with the particular echelle spectrometer used for on-line aerosol measurements.

LIBS : A new tool in archaeometry?

K. Melessanaki, S. Kotoulas, A. Petrakis, A. Hatziapostolou, D. Anglos
Foundation for Research and Technology-Hellas (FO.R.T.H.), Institute of Electronic Structure and Laser, P.O.Box 1527, GR 71110 Heraklion, Crete, Greece
Tel. +30 810 391154, Fax +30 810 391318, e-mail: anglos@iesl.forth.gr

S. Ferrence, P. P. Betancourt
Department of Art History, Temple University, Philadelphia, PA 19122, USA

Abstract: Our experience with the development and use of a transportable, user -friendly LIBS instrument designed for use in the museum, the conservation laboratory or even at the excavation site is described and the potential of LIBS in archaeometry is discussed.

OCIS codes: (140.3440) Laser induced breakdown; (300.6210) Atomic spectroscopy

1. Introduction

The compositional analysis of ancient artefacts is essential to archaeologists and historians in their efforts to extract information about the use and origin of archaeological objects as well as the materials that were used. In addition, important technological insight is provided by means of systematic chemical and structural analysis, about the techniques of manufacture and processing.

Indeed a wide variety of analytical techniques and instrumentation are being used extensively in the study of archaeological and art objects including, for example, polarized light optical microscopy and Scanning Electron Microscopy (SEM), X-Ray Fluorescence (XRF), Proton Induced X-Ray Emission (PIXE), X-Ray Diffraction (XRD), Neutron Activation Analysis, Inductively Coupled Plasma coupled to Optical Emission or Mass Spectrometry (ICP-OES, ICP-MS) and Raman Microscopy [1-6]. In many cases accurate analytical measurements are obtained with the techniques mentioned above, however, several issues arise, which relate to the need for sampling (and also sample preparation) of sensitive and valuable objects or the need of transportation of samples or objects to specialized analytical laboratories, a task often subject to strict regulations.

In this respect the need of compact, portable instrumentation for the analysis of archaeological objects becomes obvious and Laser-Induced Breakdown Spectroscopy (LIBS) appears as a potential alternative to other spectroscopic, mass spectrometric, or X-ray techniques used in art conservation and archaeology. It is a practically non-destructive as well as rapid elemental analysis technique with the critical advantage of being applicable in situ, thereby avoiding sampling and sample preparation. Indeed, LIBS has been used for the analysis of pigments in easel paintings, icons, polychromes and pottery [7-12] and demonstrates the prospects of the technique to become a useful analytical tool in art and archaeology. Furthermore quantitative LIBS analysis leading to absolute concentration values for each element is ideal for the accurate compositional characterization of the materials analyzed [11-12].

This paper presents in brief our experience from the development, integration and use of a compact, transportable, user-friendly LIBS instrument, which was designed for use in the museum, the conservation laboratory or even at the excavation site to provide on-site, rapid, analytical information about the qualitative and semi-quantitative elemental composition of a wide variety of materials aiding the quick characterization of archaeological objects and/or samples.

2. Instrumentation and Measurement

2.1LIBS instrument

Following tests with a laboratory prototype, constructed in the first phase of this project, we proceeded with the integration of the components of the final instrument in one bench-type, independent unit (H: 90 cm, W: 80 cm, D: 65 cm), which could be transported on wheels. The components used for the LIBS instrument were quite standard and included: a compact Q-switched Nd;YAG laser, operating at 1064 nm, and its power supply unit, a medium size grating spectrograph, an intensified CCD detector and a home-made pulser to provide proper gating, a platform on a XYZ translation stage for mounting samples, a small color camera for accurate sample viewing and aiming purposes and a personal computer for instrument control and data analysis.

The laser, beam guiding optics and viewing camera, were housed in a sub-unit, mounted on the top surface of the instrument along with the sample platform stage. The PC monitor and keyboard were also placed on the top surface. The rest of the components were housed in the main body of the instrument. All components and measurements are controlled through a unified user-friendly software environment, which in addition provides the user the ability to perform data analysis.

2.2 Measurements

For the analysis, each sample/object is placed on the translation stage and the spot to be analysed (ca. 100-200 microns diameter) is positioned at the focal point of the focusing lens with the aid of the viewing camera. Emission spectra are recorded for a single laser pulse, their resolution being ca. 0.4 nm. In cases a depth profiling study is carried out, spectra are acquired separately for each one of several successive laser pulses. Elements are identified through the analysis routine of the instrument's software on the basis of the characteristic wavelength values of the emission lines from various elements while the option of overlaying acquired spectra with reference ones for a variety of materials is also available.

3. Results and discussion

Measurements were carried out at the INSTAP Study Center for Eastern Crete (Pahia Ammos, Crete), where the LIBS instrument was moved. A broad variety of archaeological findings were examined including painted and glazed pottery, vitreous materials (glass, feience), different types of metal objects, and jewellery. In most cases, LIBS analyses were carried out in order to identify pigments on pottery sherds or characterize metal alloys. It has to be noted at this point that analysis of the objects examined, in a specialized analytical laboratory, would require special permits for moving and/or sampling each one of these objects. Obviously the presence of an analytical instrument on site (i.e. in the archaeological conservation and study laboratory or the museum) overcomes the obstacles outlined above. In addition, the speed of LIBS analysis makes it ideal for performing routine, rapid, on site analysis of archaeological objects.

To indicate the type of information drawn through LIBS analysis, three examples are briefly described. In the first case, examination of a glazed pottery sherd is shown, focusing on analysis of the bright yellow glaze, used to decorate the interior and exterior rim of a ceramic bowl. On the basis of the LIBS spectrum, the glaze was found to contain Pb, Ca, and Cr. The combined presence of lead and chromium suggests that chromium yellow (lead chromate, $PbCrO_4$) has been used. Chromium yellow, a synthetic pigment, was introduced as a colouring agent ca. 1818. This implies that the pottery analysed dates not before the early 19th century, which is in fact in agreement with the excavation data as the sherd was found close to the surface of the area excavated. This type of information suggests that LIBS can be employed, in certain cases, to determine/confirm the date of certain types of pottery.

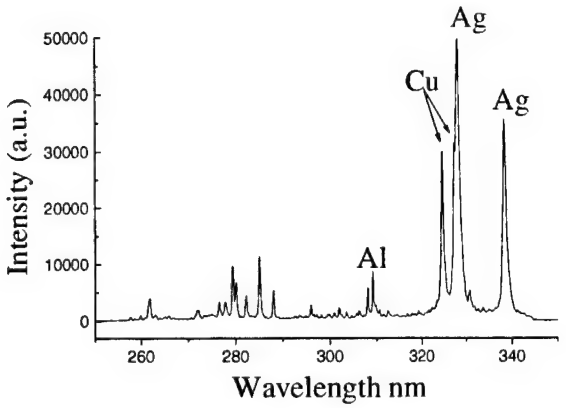

Fig. 1. LIBS spectrum on the flat side of rivet from Minoan dagger.

In a different case a copper rivet (cylindrical piece used to hold the blade within the wooden handle of a dagger), dated from the Late Minoan IB period (ca. 16th C. BC), was examined. It was found to be composed of copper by probing representative points around the cylindrical surface. While taking additional spectra on the flat sides of the rivet a surprising result was found. Intense emission from silver

was recorded in the LIBS spectrum (Fig. 1). This indicates the presence of silver on the exposed flat sides of the rivet, possibly from a silver coating. This rivet is the first of its type found on the excavation site of Pseira island.

Finally, several pieces of jewellery (golden beads, ear rings, rings etc.) from the Late Minoan IIIA period (ca. 14th C. BC) were analysed showing different relative intensities of emission lines of Au, Ag and Cu suggesting variable proportions in the composition of these main components in the alloys used. These results indicate that LIBS analysis can quickly provide information on the qualitative and semi-quantitative elemental content of different metal objects and aid their characterization and classification. Quantitative analysis by LIBS is also possible using proper reference samples or alternative approaches, such as the one recently used for the quantitative analysis of precious metal alloys [13].

4. Conclusions

The results presented in this paper demonstrate the advantages of LIBS analysis in obtaining elemental analysis information about the materials used for making and decorating ancient pottery or metal artefacts. An important aspect of LIBS is the speed of analysis, which can allow the quick examination of a large number of samples in the field, at a museum, or at an excavation site. Compact and user-friendly instrumentation could make a powerful tool for the analysis of a large variety of materials leading to quick characterization and classification of archaeological findings.

5. References

E. Ciliberto and G. Spoto (Eds.), *Modern analytical methods in art and archaeology; Chemical Analysis, A series of monographs on analytical chemistry and its applications*, vol. 155, J.D. Winefordner (Ed.), (Wiley, New York 2000).

P. Mirti, "Analytical techniques in art and archaeology", Ann. Chim. **79**, 455-477 (1989).

M. Mantler, M. Schreiner, "X-ray fluorescence in art and archaeology", X-Ray Spectrometry **29**, 3-17 (2000).

W. Noll, R. Holm, L. Born, "Painting on ancient cwera,ics", Angew. Chem. Int. Ed. **14**, 602-613 (1975).

C. P. Swann, S. Ferrence, P. P. Betancourt, "Analysis of Minoan White Pigments Used on Pottery from Palaikastro", Nucl. Instr. And Meth. In Phys. Res. B **161-163** ,714-717 (2000).

R.J.H. Clark, "Raman Microscopy: Application to the identification of pigments on Medieval Manuscripts", *Chem. Soc. Rev.* **24**, 187-199 (1995).

D. Anglos, "Laser-induced breakdown spectroscopy in art and archaeology", Appl. Spectrosc., **55**, 186A-205A (2001),.

L. Burgio, R. J. H. Clark, T. Stratoudaki, D. Anglos, M. Doulgeridis, "Pigment identification. A dual analytical approach employing laser induced breakdown spectroscopy (LIBS) and Raman microscopy", Appl. Spectrosc. **54**, 463-469 (2000).

K. Melessanaki, V. Papadakis, C. Balas, D. Anglos, "Laser Induced Breakdown Spectroscopy (LIBS) and Hyper-spectral Imaging Analysis of Pigments on an Illuminated Manuscript", Spectrochim. Acta Part B **56**, 2337-2346 (2001).

D. Anglos, K. Melessanaki, V. Zafiropulos, M. J. Gresalfi, J. C. Miller, "Laser-induced breakdown spectroscopy for the analysis of 150-year old daguerreotypes", Appl. Spectrosc. **56**, 423-432 (2002).

I. Borgia, L. M. F. Burgio, M. Corsi, R. Fantoni, V. Palleschi, A. Salvetti, M. C. Scuarcialupi, E. Tognoni, "Self-calibrated quantitative elemental analysis by laser-induced plasma spectroscopy: application to pigment analysis" J. Cult. Heritage**1**, S281-S286 (2000).

Y. Yoon, T. Kim, M. Yang, K. Lee, G. Lee, "Quantitative analysis of pottery glaze by laser induced breakdown spectroscopy", Microchemical Journal **68**, 251-256 (2001).

M. Corsi, G. Cristoforetti, V. Palleschi, A. Salvetti, E. Tognoni, " A fast and accurate method for the determination of precious alloys caratage by laser induced plasma spectroscopy", Eur. Phys. J. D: Atom. Mol. Opt. Phys. **13**, 373-377 (2001).

6. Acknowledgments

The authors wish to thank the Institute for Aegean Prehistory (INSTAP) and the Foundation for Research and Technology-Hellas (FORTH-IESL) for funding and collaboration on this project. Technical support, in the instrument construction phase, by the machine and electronics shops at FORTH-IESL is gratefully acknowledged. The authors would also like to thank S. Chlouveraki and T. Brogan of the INSTAP Study Center of Eastern Crete for making all the necessary arrangements for the analysis of objects/samples.

NOTES

LIBS in Life Sciences and Materials

Thursday, September 26, 2002

Amy Hunter, Physical Sciences Inc., USA,
Presider

ThB
10:40am–12:20pm
Room: Royal Palm III

Biomedical applications of laser-induced breakdown spectroscopy

Helmut H. Telle
Department of Physics, University of Wales Swansea, Singleton Park, Swansea SA2 8PP, United Kingdom
Telephone: +44-1792-295847, fax: +44-1792-29532, e-mail: h.h.telle@swansea.ac.uk

Abstract: Applications of laser-induced breakdown spectroscopy to the analysis of biological and medical samples are surveyed, and possible spatial resolution information (lateral and/or depth) will be discussed. Samples include calcified tissue, soft tissue and bio-fluid materials.

1. Introduction

Laser Induced Breakdown Spectroscopy (LIBS) offers a simple and fast method of elemental analysis: in principle, any material - solid, liquid or gaseous - can be analyzed, and no or only very little sample preparation is needed. Detection limits are in favorable cases of the order of a few parts per million (ppm). While this may be inferior to other methods of analysis one has to keep in mind that LIBS analysis can be undertaken directly from an (untreated) sample, often *in situ* and at "remote" locations, and even *in vivo* analysis may be possible, when dealing with living organisms. For example, when considering the role of mineral nutrition and metabolism in the context of maintaining human health, the knowledge on the presence or absence of key elements is of vital importance: for excess concentration – often still minute – toxic effects may be encountered for specific elements; on the other hand, the presence of some trace elements may be of vital importance, i.e. deficiencies can be indicative of an illness.

While the success of LIBS in the qualitative and quantitative analysis of solids is now unquestioned, a search of the published literature reveals that only very few investigations address non-ferrous materials. In particular, publications about using LIBS on bio-matrix materials are still relatively few. Overall, this is not very surprising, due to a range of reasons. Firstly, biological tissue samples – "hard" calcified tissue and "soft" cell materials – are normally less "tough" in their texture than metals or minerals. Thus, the ablation process "destroys" the sample area much more rapidly, which results in poor statistics and reproducibility. Secondly, in many cases, biological samples are rather inhomogeneous. Again, this makes selectivity, statistics and reproducibility of results difficult. Thirdly, traces of specific elements in the biomass are often of most interest at concentration levels, which are close top or below the detection limits of LIBS. And finally, more often than not molecular species are of vital importance in biology, and normally these are beyond the capabilities of LIBS. Here we address a selection of different types of samples.

2. Investigation of calcified bio-samples

Mineralized tissue, i.e. bones and teeth – and other bio-minerals – have been found to be excellent "archives" related to living habits, nutrition and exposure to changing environmental conditions. They maintain much of the "biological signature" from the living phase over a long time, revealing e.g. the uptake of contaminants from the surrounding environment during defined periods.

LIBS compositional analysis has been used to determine e.g. the temporal / spatial evolution of trace element concentrations in bones and teeth, and whether tooth material is healthy or not (see e.g. Samek et *al* [1]). Continuously tracking the spectral analysis during the progress of ablation, information about the spatial (lateral and depth) distribution of elements in teeth and bones can be obtained *in vitro*, or even *in vivo*. It is possible to link the quantitative results from our LIBS analysis to e.g. environmental influences (*in vitro* studies of tooth or bone sample cross sections) and dental disease states (*in vivo* monitoring).

Finally, studies of marine life have been used in environmental monitoring (see e.g. Raith *et al* [2]). Marine species accumulate elements first in their soft tissues, from where it precipitates into the calcified parts. Thus, elemental composition of calcified tissue should reflect the water and nutrient composition, including pollutants. Specifically, the "hard" shells of mussels provide a time-base record of pollution. The shell samples discussed here were sampled from Swansea Bay, a shallow bay on the South Wales coast.

3. Investigation of "soft" tissue materials with cell structure

It should be noted from the outset that only very few LIBS studies of „soft" tissue have been carried out to date. This should not come as a surprise since by its matrix nature human and animal cell tissue are very rapidly distroyed by the laser ablation process, and due to the in general very high water content spectral emission from elements in

the tissue is severely affected. Recently, our research team has carried out a few measurements to analyse soft tissues, namely nails and skin (Samek *et al* [3]). As for the calcified tisssue, *Ca* was an abundant component in the spectra. However, the sensitivity of LIBS was found not to be sufficient to detect various potentially toxic trace elements. Other groups also carried out LIBS studies on cell tissue, namely to detect some trace elements in or on skin, or to monitor elements present in abundance, such as *Ca* and/or *H*.

When tracing the nature of cell materials, frequently molecular information is required for identification. For this task LIBS does therefore seem to be relatively unsuitable because normally the ablated sample material is fully atomised. On the other hand, particular elements are accumulated predominantly in different cell types, or they are abundant „finger print" elements. We are currently exploring the feasibility to use LIBS to distinguish between different pollen; this may be of great advantage to determine whether particular alergens, causing e.g. hay feaver, are present in abundance. Evidently, a similar approach is being pursued at present by a number of army research laboratories, to test LIBS for its suitability to detect e.g. chemical and biological warfare agents. A discussion of this aspect of LIBS will be included in the presentation.

4. Investigation of bio-fluids

The detection and quantification of many light elements and heavy metals within liquid samples is pertinent to industrial processing, waste management and environmental monitoring. To date LIBS approaches have achieved only limited success when applied to sensitive, quantitative analysis of liquids; test arrangements have utilized static liquid pools, aerosols or droplets, or liquid streams. In general, for *in situ* measurements detection limits of 1-100ppm for light metal elements were realized, while heavy metals are rather more elusive, some of them having been found to be undetectable even at concentration levels as high as 1,000ppm.

A very promising approach for sensitive and reliable LIBS analysis of liquid samples has been realized e.g. by Van der Wal *et al* [4]). In their approach the analyte solution is evaporated upon an amorphous graphite substrate; subsequently, LIBS analysis of the substrate surface follows. In this manner on, the trace element identification within the liquid is transformed into a solid surface analysis measurement, with the advantage of the much greater flexibility and high sensitivity associated with LIBS solid surface analysis. Detection limits of the order 10-100ppb have been achieved for many of the important elements in aqueous samples.

In our laboratory we have followed a similar approach to develop a liquid-to-surface transfer LIBS analysis procedure, which lends itself for the screening of bio-fluid samples. In this implementation, the liquid (blood) sample is transferred to a standard filter paper (instead of the amorphous graphite substrate used by Van der Wal *et al*). The particular example highlighted here is that of the potential screening of blood for traces of *Rb* by LIBS (in combination with LIFS), as a possible analysis technique to trace the effect of illegal doping drugs. Since *Rb* is mainly bound to the erythrocytes, any *Rb* signal above the (normally low) background concentration can be related to the athlete's read blood cell count. A semi-quantitative result can be achieved rapidly, in principle, within less than a few minutes, in contrast to the tedious blood cell counting procedures currently used in drug abuse testing which take a few hours to complete.

In summary, LIBS analysis of liquid samples, dried on carbon substrates, offers greatly improved detection limits over LIBS applied to the *in situ* liquid itself. Preparation time is minimal, and the volume of sample is minuscule. Consequently, the method may easily be applied to screening of liquid environmental and biological samples, including e.g. the analysis of urine or blood samples, but rather importantly the analytical results are nearly "instantaneous", and because of the portability of modern LIBS systems may be described as being "*in situ*".

5. References

1. O. Samek, M. Liska, J. Kaiser, D.C.S. Beddows, H.H. Telle and S.V. Kukhlevsky, "Clinical application of laser-induced breakdown spectroscopy to the analysis of teeth and dental materials". J. Clin. Laser Med. Sur., **18**, 281-289 (2000).

2. Raith, W.T. Perkins, N.J.G. Pearce, and T.E. Jeffries, "Environmental monitoring on shellfish using UV laser ablation ICP-MS". Fresenius J. Anal. Chem., **355**, 789-792 (1996).

3. O. Samek, M. Liska, J. Kaiser, V. Krzyzanek, D.C.S. Beddows, A. Belenkevitch, G.W. Morris and H.H. Telle, "Laser ablation for mineral analysis in the human body: integration of LIFS with LIBS". in *Biomedical Sensors, Fibers and Optical Delivery Systems*, (eds. F. Baldini, N.I. Croitoru, M. Frenz, I. Lundstrom, M. Miyagi, R. Pratesi and O.S. Wolfbeis) *Proc. SPIE*, **3570**, 263-271 (1998).

4. R.L. Van der Wal, T.M. Ticich, J.R. West and P.A. Householder, "Trace metal detection by laser-induced breakdown spectroscopy". Appl. Spectrosc., **53**, 1226-1236 (1999).

Fast identification of urinary tract stones via laser induced breakdown spectroscopy

Mohamad. A. Azooz*, H. Imam, and M.A. Harith
National Institute of Laser Enhanced Science (NILES), Cairo University, Egypt
* *Fellow of urology department, student's Hospital, Cairo University*
mharithm@hotmail.com

Abstract: Laser-induced breakdown spectroscopy has been used to identify five types of the most commonly known urinary stones. Specific combinations of spectral lines were selected as the finger print lines for each stone type.

OCIS codes: (300.2140) Emission spectroscopy; (170.7230) Urology

1. Introduction

During the last four decades the widespread of laser applications opened new frontiers in many scientific as well as applied fields. In medicine, among many other important applications, the ability of laser energy to travel through fine flexible quartz fibers without appreciable energy loss has offered a very useful tool in endoscopies in surgery, cardiology, ENT and urology. Applications of laser in urology for stone disintegration are well known since (1971) [1]. Recently, the technique of laser induced breakdown spectroscopy (LIBS) has made remarkable progress towards being a field deployable analytical technique [2]. In conventional LIBS, few tens of milli-Jouls of Q-switched laser light pulse of duration less than ten nanoseconds are focused on the sample. At temperatures in the range 7000-10000 K the molecules in the target vapor dissociates to its atomic constituents, and the process continues to produce a plasma plume consisting of electrons, excited and ionized atoms. Each atomic species has its unique characteristic emission spectrum. Analyzing the collected LIP emission spectrum provides us with qualitative information about the target material elemental composition.
In the present work we report on a detailed study of LIBS application for in vitro qualitative identification of five typical types of urinary calculi.

2. Experimental

Forty- eight stones of human urinary tract origin that have been removed by various urological procedures were used in the present investigations. The calculi were of five different types and have different sizes. The stones type and composition was known from previous analysis by conventional infrared spectrometry (see table 1). Breakdown of the target material is produced by focusing the laser light (100mJ, 7 ns at λ = 1064nm) via a quartz convex lens of focal length 100 mm on the target such that the sample surface is 3 mm higher than the focal plane of the focusing lens to avoid breakdown in air.
Time resolved measurement of the evolved plasma emission is essential to avoid the overwhelming bright continuum emission in the early stages of the laser induced plasma lifetime. The spectra were collected and analyzed using an echelle spectrometer (Mechelle 7500 Multichanell Instruments, Sweden) coupled to a gatable ICCD camera (DiCAM-Pro-PCO Computer Optics, Germany). Fig. 1 is a three-dimensional display showing the effect of gating the ICCD camera at different delay times on the overall spectral features and on the improvement of S/N ratio. The average of 250 emission spectra per sample each of duration 2.5 μs and delayed 1.5 μs from the laser pulse were used for all samples throughout the present study. On each urinary stone sample measurements were performed at 5 different positions on the surface, separated by distances 1-2mm, depending on the stone size. At each position 50 laser shots were fired at a rate of 1 Hz, i.e. each sample takes a total measuring time of less than 5 minutes. 10 to 20 minutes were required for complete spectral lines identification adopting the data base library of Gram/32 software. This means that a total time of 15 to 25 minutes is required for a single stone identification, which is extremely short time compared with the conventional or even other laser based analytical techniques.

Table 1: Composition and finger print lines of each type of stones

Stone types	Finger Print Lines (FPL)
I - Struvite Mg NH_4PO_4	Magnesium: Mg (I) 516.7, 517.3 and 518.4 nm Phosphorous: P (I) 253.4, 253.6, 255.3 and 255.5 nm Nitrogen: N (band I, II) 478.8 – 495.9 nm
II- Uric acid $C_5 H_4N_4O_3$	Carbon: C (I) 247.8 nm Hydrogen: H (I) 656.3 nm Nitrogen: N (band I) 740.6 – 746.8 nm
III-Calcium oxalate monohydrate Ca C_2O_4 H_2O	Carbon: C (I) 247.8 nm Calcium: Ca (II) 370.6 and 373.7 nm
IV-Tricalcium phosphate [$Ca_3(PO_4)_2$]	Calcium: Ca (II) 315.9, 317.9, 370.6 and 373.7 nm Phosphorous: P (I) 253.4, 253.6, 255.3 and 255.5 nm
V- Calcium oxalate monohydrate with tricalcium phosphate Ca C_2O4 H_2O+ 7[$Ca_3(PO_4)_2$]	Carbon: C (I) 247.8 nm Calcium: Ca (II) 315.9 and 317.9 nm Phosphorous: P (I) 253.4, 253.6, 255.3 and 255.5 nm

3. Results

As shown in table 1, specific spectral lines of three elements have been chosen as the finger print lines FPL characterizing three calculi groups, namely struvite, uric acid, and calcium oxalate monohydrate with tricalcium phosphate. Spectral lines of only two elements have been selected as FPL for the identification of calcium oxalate monohydrate and tricalcium phosphate stones. Figure (1) depicts a typical total emission spectrum in the spectral wavelength range 200-900 nm of the struvite stones (Mg NH_4 PO_4 $6H_2O$), which represent a 25% of the total number of the investigated calculi. The spectrum represents the average of the spectra collected at five different positions on the sample as mentioned before. For struvite stones, spectral lines of magnesium, phosphorus and Nitrogen were the FPL that are shown on the zoomed segments of the same figure.

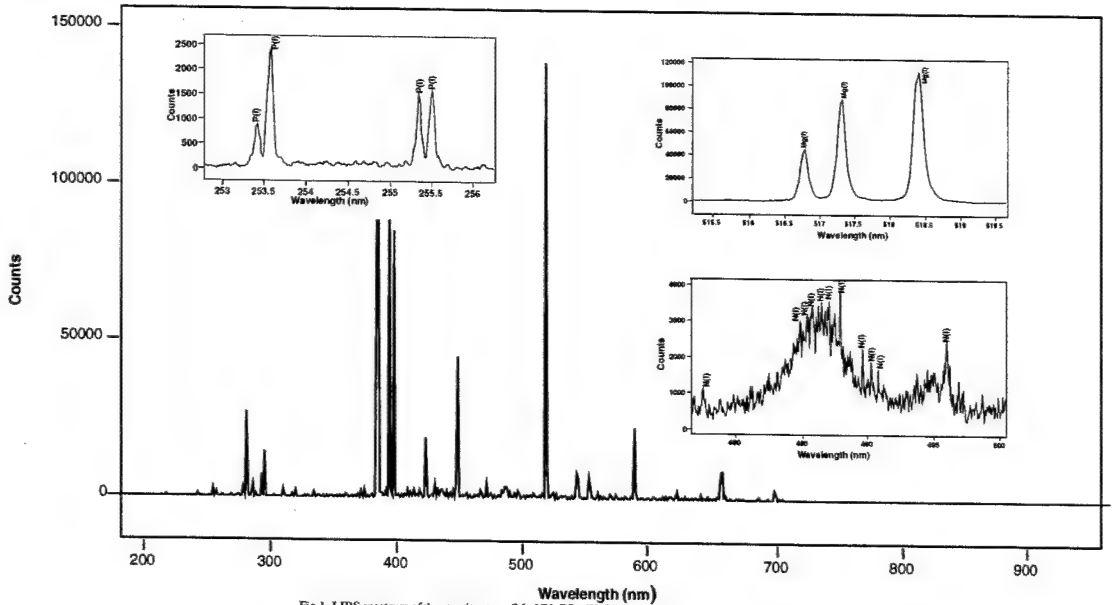

Fig.1. LIBS spectrum of the struvite stone (Mg NH_4 PO_4 $6H_2O$), with zoomed segments of the chosen finger print lines (FPL)

The presence of such group of spectral lines in the collected LIBS spectrum is taken as a clear evidence of the stone identification as struvite calculus and this has been confirmed in all samples of the same type.

Fortunately, the matrix effect has been positively utilized in the present work. Because of the fact that same element spectral lines differs on different matrices, we noticed that the spectral lines of the nitrogen appearing on the emission spectra of sturvite in the range 493 – 497 nm do not appear in the spectra of the uric acid. Another nitrogen spectral lines in the blue spectral region between 482 and 488 nm are characteristic of the uric acid. Fig. 2 shows a typical spectrum with zoomed FPL segments for uric acid stone.

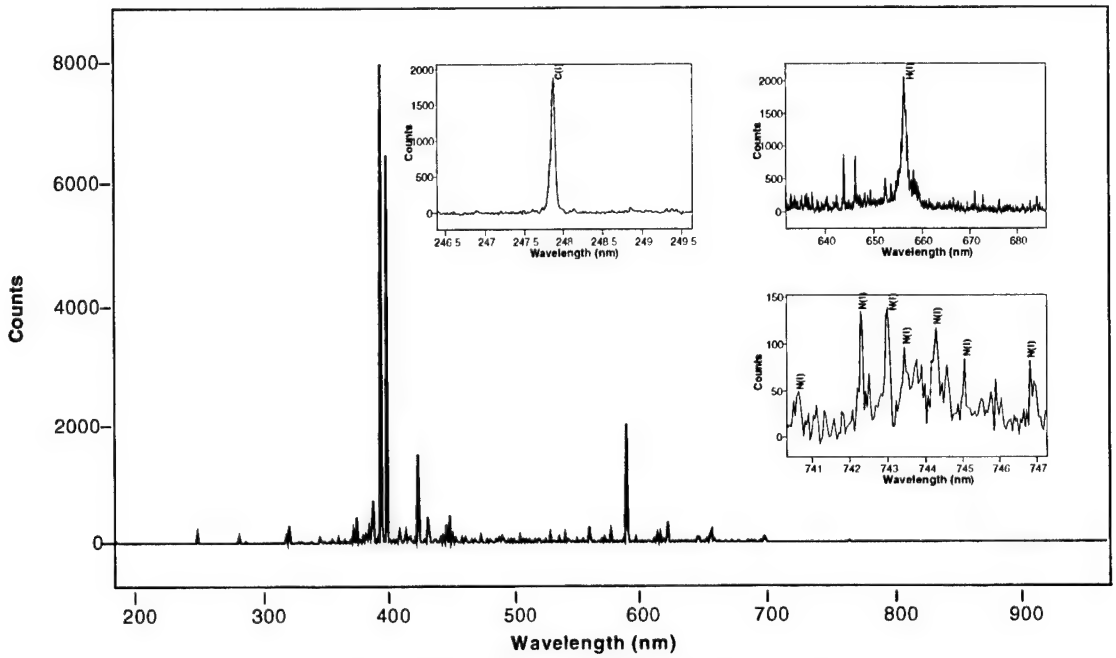

Fig. 2. LIBS spectrum of Uric acid stone ($C_5H_4N_4O_3$) with zoomed segments of the finger print lines (FPL)

The method proved to be very successful for urinary stones identification. The main advantages of the LIBS technique of being multi-elemental, rapid and needs no or very little sample preparation makes it a good candidate for application in operation rooms in clinics. Despite the accurate results obtained by the other conventional methods such as XRF, AAS and ICP, they are applicable only in vitro [3]. Exploiting fiber optics in suitable endoscopic systems to deliver the laser pulse and receive the emission from the plasma for analysis, it is foreseen to use LIBS in vivo applications in urology. Further studies are however recommended to cover the other types of stones.

4. References

1- J.F. Ready, "Effects of High-power Laser Radiation", Academic press, New York , (1971)

2- M. Corsi, V. Palleschi, E. Tognoni, Proceedings of 1st. International Conference on Laser Induced Plasma Spectroscopy and Applications, Tirrenia, Pisa, Italy, LIBS 2000 , Special issue of Spectrochimica Acta B,**56**, 565-1034 , (2001).

3- D. Bauerle, "Laser processing and chemistry", Springer Verlag, New York, (1996)

Investigation of the analysis of pellet samples by laser-induced breakdown spectroscopy: application to steel making slags

C. Aragon
Departamento de Fisica, Universidad Publica de Navarra, Campus de Arrosadia, E-31006 Pamplona, Spain
carlos.aragon@unavarra.es

J.A. Aguilera
Departamento de Fisica, Universidad Publica de Navarra, Campus de Arrosadia, E-31006 Pamplona, Spain
j.a.aguilera@unavarra.es

F.Peñalba
Fundacion INASMET, Mikeletegui Pasalecua 2, E-20009 San Sebastian, Spain
fpenalba@inasmet.es

Abstract: Experimental factors affecting laser-induced breakdown spectroscopy applied to steel making slags are investigated. Laser plasmas generated with pellet samples prepared from oxides (CaO, Fe_2O_3, SiO_2, Al_2O_3) and metallic Fe are characterized by emission spectroscopy.

OCIS codes: (140.3440) Laser-induced breakdown; (300.2140) Emission spectroscopy

1. Introduction

One of the main advantages of laser-induced breakdown spectroscopy (LIBS) is its applicability to field and on-line analysis. However, previously to its field application, the technique has to be tested in laboratory conditions using reference samples. In several applications, the use of pellets obtained by milling and pressing the materials of interest is a relatively fast and simple way to prepare the reference samples. Some of the early applications of LIBS began with the analysis of pellets, as the analysis of iron ore [1] and the trace elemental analysis of environmental samples, as sand and soil [2]. In these applications, at present time, the analysis can be performed or is in the way to be realized with field instruments based in the LIBS technique. In this way, Barrette et al. [3] have recently reported the on-line determination of C, Si, Ca, Mg and Al in an iron ore slurry of a pelletizing plant. Also, Wainner et al. [4] have developed a portable system for field analysis of Pb contamination in soils and paint, with similar performance to that of a laboratory instrument.

In the steel industry, an interesting application of LIBS is the analysis of the slags formed in the furnaces [5]. The knowledge of the slag composition is crucial for the control of the steel production process. In this application, also, the use of pellets obtained from milled slag and analyzed by standard methods is a simple way to obtain reference samples. However, the complexity of the composition of slags, which are formed by a mixture of various oxides (CaO, FeO, Fe_2O_3, SiO_2, MnO, MgO), including also some amount of metallic Fe, makes that special difficulties appear in the quantitative analysis of slag pellets [6].

The aim of this work is to investigate the factors affecting the analysis of pellet samples by LIBS, including the experimental conditions as well as the sample preparation procedures, with the objective of obtaining improved conditions for the analysis of slag pellets. Laser-induced plasmas are generated using pellets prepared with pure materials present in the slags. These plasmas are characterized using emission spectroscopy in order to select the best experimental conditions for slag analysis.

2. Experimental

Laser-induced plasmas are generated using a Nd:YAG laser (wavelength 1064 nm, pulse width 4.5 ns, repetition rate 20 Hz). The pulse energy is selected by using an optical attenuator. The laser beam is focused by a lens at right angles to the sample surface, which is placed in air at atmospheric pressure. During the measurements, an air flow is directed towards the region of plasma formation. The samples are placed in a device that allows precise positioning as well as the rotation of the sample. The light emitted by the plasma is collected in a fiber optic cable and guided to the entrance of a monochromator with 0.5-m focal length. The spectra of the plasma emission are detected using a charge-coupled device (CCD) detector, preceded by an image intensifier that provides temporal resolution. Two

types of samples are used in the experiments. On one side, slag samples generated at a steel making plant are milled, and the resulting power is pressed to obtain pellets. On the other side, reference pellet samples are obtained from pure materials that are present in slags (CaO, Fe_2O_3, SiO_2, Al_2O_3, metallic Fe). The pressure in the pellet preparation is varied to determine its effect in the laser-induced plasmas.

3. Results and discussion

2.1 Selection of spectral lines

The spectral lines selected in a LIBS experiment determine the features of the calibration curves obtained and, therefore, the figures of merit of the analysis. In slag analysis, the main interest is a high sensitivity at the whole range of the elemental concentrations, more than the capability for trace determination. Therefore the analytical lines have been selected in order to obtain linear calibration curves. Line selection has been carried out applying the results of a previous work [7], in which a method to predict the relevance of self-absorption was reported. Also, some intense lines have been used in order to characterize the laser-plasmas by the number of atoms of the elements of interest.

2.2 Effect of sample rotation

The formation of a crater during the LIBS measurements is found to be of special importance for intensities and their dispersion when pellet samples are used. Fig. 1. shows the variation of the Fe and Ca line intensities with the number of previous shots for the laser plasmas generated with a stationary (top) and with a rotating (bottom) slag pellet. In each plot, the data correspond to three measurements at different positions in the sample. It is found that, by rotating the pellet sample, the intensity variation is slower, which leads to a decrease in the dispersion of the measurements.

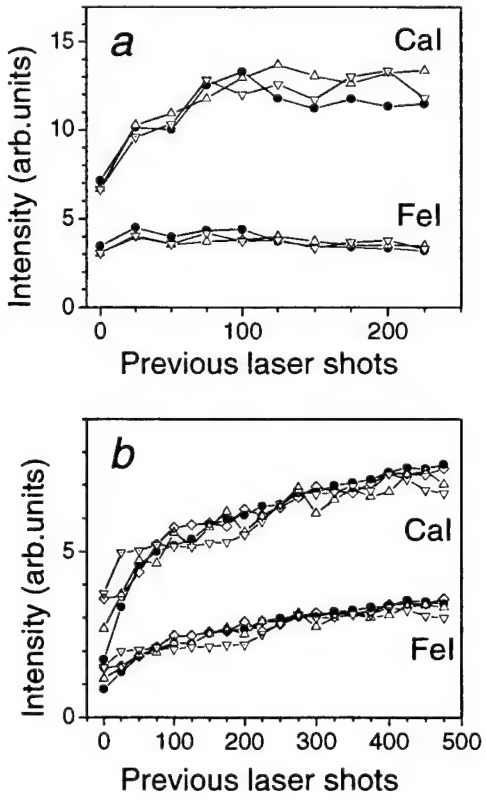

Fig. 1. Variation of the lines 534.95 nm Ca I and 534.95 nm Fe I with the crater formed by the previous laser shots for the laser-induced plasmas generated with a slag pellet: (a) stationary sample, (b) rotating sample.

2.3 Effect of particle size and pressure during sample preparation

Pellet samples have been prepared varying the particle sizes of the materials used and the pressure during pelletization. The characteristics of the laser-induced plasmas generated are compared and the implications for the LIBS analysis are discussed.

2.4 Effect of sample composition

Starting from the main materials present in slags, pellets have been prepared with different compositions in order to investigate the matrix effects that affect slag analysis by LIBS.

1. K. J. Grant, G. L. Paul and J. A. O'Neill, "Quantitative elemental analysis of iron ore by laser-induced breakdown spectroscopy", Appl. Spectrosc. **45**, 701-705 (1991).
2. R. Wisbrun, I. Schechter, R. Niessner, H. Schröder and K. L. Kompa, "Detector for trace elemental analysis of solid environmental samples by laser plasma spectroscopy", Anal. Chem. **66**, 2964-2875 (1994).
3. L. Barrette and S. Turmel, "On-line iron-ore slurry monitoring for real-time process control of pellet making processes using laser-induced breakdown spectroscopy: graphitic vs. total carbon detection", Spectrochim. Acta Part B **56**, 715-723 (2001).
4. R. T. Wainner, R. S. Harmon, A. W. Miziolek, K. L. McNesby and P. D. French, "Analysis of environmental lead contamination: comparison of LIBS field and laboratory instruments", Spectrochim. Acta Part B **56**, 777-793 (2001).
5. R. Noll, H. Bette, A. Brysch, M. Kraushaar, I. Mönch, L. Peter and V. Sturm, "Laser-induced breakdown spectrometry – applications for production control and quality assurance in the steel industry", Spectrochim. Acta Part B **56**, 637-649 (2001).
6. J. A. Aguilera, C. Aragon, P. Aguirre and F. Peñalba, "Application of laser-induced breakdown spectroscopy to the analisis of steelmaking slag", in Progress in analytical chemistry in the steel and metals industries proceedings, to be published.
7. C. Aragon, J. Bengoechea and J. A. Aguilera, "Influence of the optical depth on spectral line emision from laser-induced plasmas", Spectrochim. Acta Part B **56**, 619-628 (2001).

On-line detection of heavy metals and brominated flame retardants in technical polymers with laser-induced breakdown spectrometry

M. Stepputat, R. Noll
Department of Laser Metrology, Fraunhofer Institute of Laser Technology (ILT), Steinbachstraße 15, D-52074 Aachen, Germany
Phone: ++49 (0) 241 89 06 0, Fax: ++49 (0) 241 89 06 121, E-mail: noll@ilt.fraunhofer.de

Abstract: A LIBS analyzer for the automatic detection of heavy metals and brominated flame retardants in moving end-of-life waste electric and electronic equipment (EOL-WEEE) pieces collected for recycling is presented. An autofocusing unit with an adjustment range of 50 mm has been incorporated to allow measurements with varying distances to the sample surface. Detection limits in the range of 100 µg/g were achieved for the elements Cd, Hg, Pb, Cr and Sb in moving samples. The classification results achieved during tests of the LIBS analyzer at a conveyor belt of a pilot sorting system for EOL-WEEE are presented.

OCIS codes: (000.0000) General

1. Introduction

During the recycling process of end-of-life waste electric and electronic equipment (EOL-WEEE), downgrading of valuable technical polymers has to be avoided by separating the collected material in fractions of high purity. Most EOL-WEEE pieces are doped with several additives to improve their mechanical, electrical and chemical properties. Common additives are flame retardants, antioxidants, light stabilizers, fillers, dyes and pigments. Their concentration varies typically from traces to several percent [1].

Waste pieces containing brominated flame retardants (BFR) and additives with heavy metals have to be automatically identified and removed from the waste stream to be recycled. This is due to the significant environmental problems during the waste management phase caused by these substances. To establish an economically feasible recycling process which meets these requirements, high speed automatic sorting systems performing the identification of both the polymer and the detection of the critical additives at a rate of several parts per second are required. In the scope of the European project »Sure-Plast« (BRPR-CT98-0783) a prototype automatic identification and sorting line has been set-up and evaluated for material specific sorting of EOL-WEEE pieces. The detection unit of this automatic sorting line is a multi-sensor system for the rapid identification of the polymer matrix and the detection of the contained additives. It comprises three spectroscopic modules based on LIBS (= laser-induced breakdown spectroscopy), NIR (= near infrared spectroscopy) and MIR (= mid-infrared spectroscopy). This paper focuses on the LIBS analyzer developed by Fraunhofer ILT and its application for the detection of heavy metals and brominated flame retardants in moving EOL-WEEE pieces.

2. LIBS analyzer for on-line detection of additives

The task of the LIBS analyzer is the rapid quantification of heavy metal and halogen concentrations in EOL-WEEE pieces moving at a speed of 0.5 m/s to 1.0 m/s on a belt conveyor. The major problem is the large variation in size and shape of the real waste EOL-WEEE pieces such as monitors, telephones and keyboards. To provide a reduced dependency of the measuring distance on the sample shape, the samples pass the sensor on a tilted belt conveyor sliding on the side panel of the conveyor. The LIBS measurement is carried out through a gap in the conveyor side panel. The LIBS detection of heavy metals is focused on Pb, Cr, Cd and Hg found in pigments, nucleating agents and heat stabilizers. Brominated flame retardants are detected via Br and additionally via Sb as a component of their widely used synergist Sb_2O_3.

The set-up of the LIBS module is shown in Fig. 1. The Nd:YAG laser generates laser bursts consisting of two laser pulses with a total energy of 360 mJ at a repetition rate of 30 Hz. The laser pulses are focused onto the sample surface by the autofocusing optics. The emission of the laser-induced plasma is picked up by a fiber optics at a distance of 130 mm to the far end of the measuring range and is guided to a Paschen-Runge polychromator.

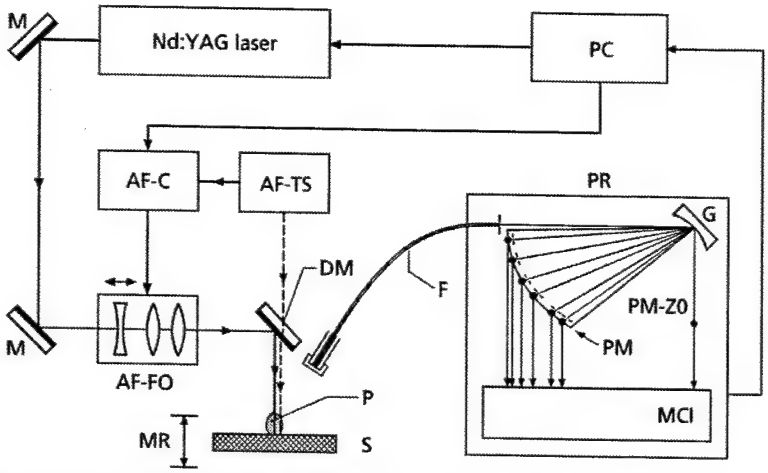

Fig. 1. Set-up of the LIBS analyzer. PC = personal computer, PR = Paschen-Runge polychromator, G = grating, PM = photomultiplier, PM-ZO = photomultiplier for the 0th order, MCI = multi-channel integration electronics, F = fiber optics, P = plasma, S = sample, MR = measuring range, DM = dichroic mirror, M = mirror, AF = autofocusing unit, AF-TS = triangulation sensor, AF-C = controller, AF-FO = focusing optics.

In the Paschen-Runge polychromator, spectral emission lines with wavelengths in the range of 228 nm to 828 nm and the 0th order signal are detected by photomultiplier tubes. The photomultiplier signals are processed by the multi-channel integration electronics MCI , where they are integrated during a gate of 20 µs after a delay of 800 ns with respect to the plasma generation by the laser burst. The integrated values are digitized and transmitted to the control PC for further data processing.

Owing to the surface topology of the real waste samples, the distance from the focusing optics to the sample surface varies while the EOL-WEEE pieces pass the LIBS analyzer on the belt conveyor. To compensate for these distance variations and to keep the analyzing laser focused on the sample surface, an autofocusing unit for LIBS was developed which provides a measuring range of 50 mm, see Fig. 1.

In the autofocusing unit, a laser triangulation sensor measures the distance of the focusing optics to the sample surface with a fixed frequency of 50 Hz. The autofocus control processes the distance values provided by the triangulation sensor into the control signal for the variable focal length optical system with an average focal length of about 220 mm.

Using static focusing, the LIBS signals show a strong dependency on the deviation from the optimum distance to the sample surface [2]. This dependency cannot be compensated by referencing the LIBS signal to the 0th order signal. However, using dynamic focusing with the autofocusing unit, the LIBS signals referenced to the 0th order are constant within 5 % over a measuring range of 50 mm. An example is shown in Fig. 2, where the referenced Pb I 405.78 nm LIBS signals acquired with static and dynamic focusing are compared for varying distances between the focusing optics and the sample.

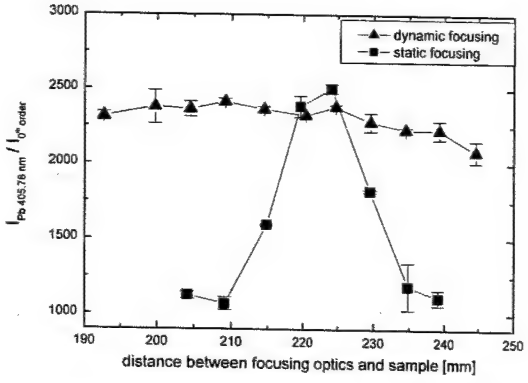

Fig. 2. Comparison of Pb I 405.78 nm LIBS signal referenced to 0th order with static and dynamic focusing.

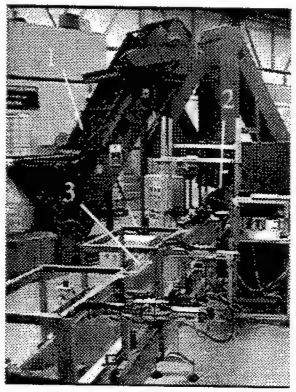

Fig. 3. Prototype automatic identification and sorting line for EOL-WEEE at Bilbao/Spain. 1 = singularization unit, 2 = measuring systems, 3 = sorting equipment.

3. Results

The limits of detection (LOD) determined for the investigated heavy metals and halogens with a laboratory set-up using static focusing and the LODs determined for the on-line LIBS analyzer at the pilot sorting plant using dynamic focusing are shown in Table 1. According to the enduser of the Sure-Plast project, EOL-WEEE pieces containing higher concentrations of heavy metals than 100 µg/g will be refused for recycling by manufacturers.

Table 1. Limits of detection (LOD) for the investigated elements in ABS samples. LOD calculated by the 3s-criterion. (n. d. = not determinable)

element	λ [nm]	static focusing LOD [µg/g]	dynamic focusing LOD [µg/g]	required LOD [µg/g]
Cd	228.80	20	96	100
Cr	425.43	11	73	100
Pb	405.78	24	140	100
Hg	253.65	102	60	100
Sb	259.80	45	80	100
Br	827.24	14438	n. d.	5000

The required detection limit of 100 µg/g is achieved for the elements Cd, Cr, Hg and Sb, both using static focusing in a laboratory set-up and using dynamic focusing in on-line measurements. The lower sensitivity of the on-line LIBS analyzer with dynamic focusing attributes to additional disturbing influences during operation at the pilot sorting plant. Here, the LOD of Pb was 140 µg/g and the LOD of Br was higher than the available concentrations of the reference samples used for calibration.

The on-line classification performance of the LIBS sensor was evaluated with 160 measurements on 40 real waste monitor samples. The reference analysis for the concentration of heavy metals and halogens in these monitor housings was provided by inductively coupled plasma atomic emission spectrometry (ICP-OES). For sorting, the determined element concentrations were classified into four categories: a) 0 – 100 µg/g, b) 100 – 1000 µg/g, c) 1000 – 2000 µg/g, d) > 2000 µg/g. The results of the classification obtained for samples without surface preparation moving on the belt conveyor with a velocity of about 0.5 m/s are summarized in Table 2. The classification result for mercury cannot be regarded since no mercury concentration > 1 µg/g was found in the real waste EOL-WEEE monitor housings with ICP-OES. For Sb, Cd, Pb and Cr, high classification ratios of up to 95% are achieved during the on-line measurements at the pilot sorting plant.

Table 2. Results of the on-line LIBS analyzer at the pilot sorting plant with real waste EOL-WEEE monitor housings moving at a velocity of 0.5 m/s.

	Sb	Cd	Pb	Cr	Hg*
no. of correct classifications	152	135	152	152	(160)
no. of total classifications	160	160	160	160	160
percentage of correct classifications [%]	95	84	95	95	(100)

4. References

[1] *Ullmann's Encyclopedia of Industrial Chemistry*, Vol. A 20 (VCH Publishers Inc., 1992)

[2] A. Cremers, D. J. Romero, "An evaluation of factors affecting the analysis of metals using laser-induced breakdown spectroscopy (LIBS)", in Remote Sensing, Proc. SPIE 644, 7-12 (1986).

Fundamentals of LIBS: I

Thursday, September 26, 2002

Nicolo Omenetto, Joint Res. Ctr., Italy,
Presider

ThC
2:00pm–3:40pm
Room: Royal Palm III

The potential of LIBS in spectrochemical analysis

Kay Niemax, ISAS, Germany

The potential and limitations of LIBS for element analysis of solid samples are discussed. Particular attention will be paid to possible systematic errors in LIBS-analysis and how to reduce them.

Experimental and theoretical investigation of the early stage of laser induced plasma produced by the interaction between a KrF excimer laser and a metallic titanium target.

A. De Giacomo,
Dipartimento di Chimica, Via Orabona 4, 70126 Bari, Italy, Tel. +39-080-4674314, Fax +39-080-4674457, E-mail: adg@centrolaser.it
G. Colonna
IMIP-CNR , Via Orabona 4, 70126 Bari, Italy, Tel +39-080-5443563,Fax+39-080-5442024, E-mail: cscpgc08@area.ba.cnr.it
A. Casavola
Dipartimento di Chimica,Via Orabona 4, 70126 Bari Italy,Tel +39-080-5442052,Fax+39-080-5442024,E-mail:casavola@chimica.uniba.it
O. De Pascale
IMIP-CNR , Via Orabona 4, 70126 Bari, Italy, Tel +39-080-5443563,Fax+39-080-5442024, E-mail: depascale@centrolaser.it

1. Introduction. The interaction of laser beam with solid matter and the consequent plasma generation has been studied for many years [1]. Nevertheless the great efforts to exploit the laser matter interaction for material processing and diagnostic purposes, many aspects still need to be elucidated and clarified. In particular the plasma induced by ultraviolet and visible nanosecond laser is successfully employed for thin film deposition of a wide range of classical and novel materials (PLD) [2] and for in situ qualitative elemental analysis (LIBS) [3].

In both these applications is really important to understand the composition and the temporal evolution of species in the plasma. The classical approach in the study of laser-induced plasma (LIP) is based on the assumption of Local Thermodynamic Equilibrium (LTE).

In LIP all the energy is delivered during the laser pulse (tenths of ns) and then the system evolves spontaneously for few microseconds. The most part of initial energy is converted in kinetic energy so that the LIP expands with supersonic velocities (10^7-10^5 cm s^{-1}). In these conditions the velocity of expansion can change plasma parameters in a shorter time respect to that necessary for the establishment of elementary processes balances [1]. The knowledge of the deviations from LTE is really important to understand the constraints and the corrections on theory to be taken into account for practical applications [4].

The aim of this work is the investigation by emission spectroscopy of the basic aspects of the plasma generated by the interaction between a KrF excimer laser and a metallic target of titanium at low pressure. In this work, experimental observation and theoretical model have been employed to discuss fundamental concepts of the LIP in order to understand the main processes that must be taken into account for the analysis of this kind of plasma.

2. Experimental. The experimental set-up has been described in details in previous work [5] and consists of a vacuum chamber with rotating holder for target and quartz windows for laser input and for the emission spectra detection, a spectroscopic system and a vacuum system. The laser source is a KrF excimer laser at 248 nm (Lambda Physic LPX350) with a pulse width of 30 ns and an adjustable repetition rate between 1 and 150 Hz. Using mirror and lens the laser beam is directed through a quartz window into the vacuum chamber and focused onto the target at 45° from the surface normal. In these experiments the energy density of the laser beam has been fixed at 5 J/cm^2 with a rectangular spot 2.00 X 2.42 mm^2 and a repetition rate of 5 Hz.

The spectroscopic system is made by an optical fiber (diameter of 0.6mm) connected to the input slit of a high-resolution monochromator (HR 640, Instruments S.A., division Jobin Yvon) and an intensified charge coupled device (ICCD, Jobin Yvon cv3000) for the

detection of spectra. The plume image is focused on a virtual plane by a short focus quartz lens (6 cm). The optical fiber is placed on a micrometric XYZ table so that is possible to move the entrance of the optical fiber in the virtual plane where is focused the plume image with a 1:1 magnitude. This configuration allows detecting a portion of plume with a spatial resolution that has the same dimension of the optical fiber entrance. The signal of a fast photodiode, detecting the laser reflection of the diaphragm, is the main trigger for the ICCD. To avoid the intrinsic delay of the electronic system (80 ns) a 25 m long optical fiber is used so that the transmission of emission light to the detection system is delayed of 83 ns. A gate width of 40 ns has been chosen in the experiment for maximizing the spectral line intensity while maintaining a good temporal resolution. To optimize the signal-to-noise ratio and the spectra reproducibility, the detection of spectra is carried out by averaging 5 sets of 10 signal accumulations. By this acquisition mode the fluctuations of spectra are under 7% at the experimental conditions applied in this work.

The spectroscopic investigation of the LIP has been carried on in the visible range at the maximum vacuum allowed by our vacuum system 10^{-5} Torr. In order to neglect the angular dispersion of LIP the measurements has been performed along the propagation axis at distance from the target surface shorter or comparable to the spot dimension.

The evolution of LIP species by temporally and spatially resolved OES at different distance from the metallic titanium target has been studied. Two non- resonance lines with high emission coefficients and with similar energy have been selected: 399.86 nm and 401.23 nm, corresponding to the species Ti I and Ti II respectively. On the other hand atomic and ionic state distribution functions has been studied by Boltzmann plot technique.

3. Theoretical. The theoretical model basically describes the plume expansion via fluid dynamic equations along the plume axis in the one-dimensional approximation, being based on the observation that the angular dispersion of the plume is small in vacuum. Euler equations consist of mass momentum and energy continuity equations, completed with an equation to calculate the mass fraction of each species (c_i) [6]. To investigate the effects of finite rate coefficients on the plume expansion, we include in the fluid dynamic model the following processes:

(a) ionization by electron impact (direct process)

(b) three body recombination (inverse process)

$$Ti_k(E_k) + e^-(\varepsilon) \underset{K_0^I}{\overset{K_0}{\rightleftarrows}} Ti^+ + e^-(\varepsilon') + e_b^-(\varepsilon'')$$

(c) radiative recombination

$$Ti^+ + e^-(\varepsilon) \xrightarrow{K_1} Ti_k + h\nu$$

The ionization rate coefficients have been calculated considering a Maxwellian electron energy distribution and a Boltzmann distribution of the excited level of atoms at the gas temperature (thermal rates), and the ionization cross sections have been obtained by Grizinskii model. The recombination rate has been calculated by detailed balance principle.

The coupling between fluid dynamic and kinetic equations involves an "operator splitting" technique. As a first step, we solve the Euler equations in the free flow approximation and then, in the same time interval, we solve the kinetic equations locally to update the concentration values. This approach is valid for small temperature variations.

4. Discussion. The comparing of experimental values of atomic and ionic number density ratio ($N_{Ti\ II}/N_{Ti\ I}$), obtained by Boltzmann plot analysis, with the one obtained by Saha equation at the same electron number density and temperatures, are reported in table 1. It leads to the conclusion that the departure from the equilibrium state can be attributed to the violation of the balancing between the processes of ionization and three bodies recombination.

Table.1: Results of Boltzmann plot analysis.

	Ti I		Ti II		Experimental	Calculated
Delay (ns)	T ± 800 (K)	$q(N_{Ti\ I})$ ± 0.5	T ± 800 (K)	$q(N_{Ti\ II})$ ±0.5	$N_{Ti\ II}/N_{Ti\ I}$	$N_{Ti\ II}/N_{Ti\ I}$
50	11800	-30.2	11200	-25.4	66.885	9.50
100	8700	-28.6	8850	-23.3	113.29	1.00
150	8800	-28.6	8600	-23.2	127.35	1.16
200	9600	-29.0	8950	-23.9	96.93	2.52

Moreover in experiments a characteristic delay between the atomic and ionic maximum of temporal emission profiles has been observed. To investigate these deviations and to explain the experimental observations we apply the theoretical model described before, to the emission temporal profiles at different distances from the target.

Fig.1 (a) and (b) shows a comparing between experimental and theoretical results of Ti I and Ti II temporal evolution at 1 and 2 mm. We can observe a good agreement at all the distances examined in this work. Some differences arise after 2 mm as a consequence of the radial component of velocity and the experimental curves are broader than them obtained by calculation. By the analysis of theoretical model it results that deviation from LTE can be attributed to the prevailing of three bodies recombination process over the ionization process.

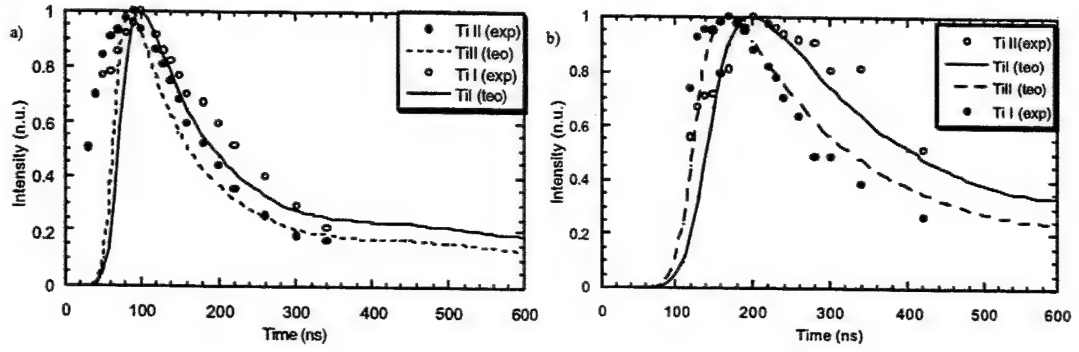

Fig.1. Examples of the comparison between experimental and calculated TOF at (a) 1 mm and (b) 2 mm.

5. References:

[1] M. Capitelli, F. Capitelli, A. Eletskii, Non-equilibrium and equilibrium problems in laser-induced plasmas, Spectrochim. Acta Part B, 55 (2000) 559-574.

[2] P.R. Willmott and J.R. Huber, Pulsed laser vaporization and deposition, Reviews of Modern Physics 72, No1 (2000) 315-328.

[3] A. Ciucci, M. Corsi, V. Palleschi, S. Rastelli, A. Salvetti, E. Tognoni, New Procedure for Quantitative Elemental Analysis by Laser Induced Plasma Spectroscopy, Applied Spectroscopy, 53 (8), (1999) 960-964.

[4] A. De Giacomo, V. A. Shakhatov, G.S. Senesi and S. Orlando, Spectroscopic investigation of the technique of Plasma assisted Pulsed Laser ablation of titanium dioxides, Spectrochimica Acta B, 56 (2001), 1459-1472.

[5] A. De Giacomo, V. A. Shakhatov, O. De Pascale, Optical emission spectroscopy and modeling of plasma produced by excimer laser ablation of titanium oxides, Spectrochimica Acta B 56 (2001), 753-776.

[6] G. Colonna, A. Casavola, M. Capitelli, Modelling of LIBS plasma expansion, Spectrochim. Acta Part B, 56 (2001), 567-586.

Laser-induced breakdown: pressure and temperature dynamics

C. G. Parigger
Center for Laser Applications, The University of Tennessee Space Institute, Tullahoma, TN 37388
Phone: 931-393-7338, Fax: 931-454-2271, E-mail: cparigge@utsi.edu
http://www.utsi.edu

I. G. Dors
The University of New Hampshire, Space Science Center, Durham, New Hampshire 03824
E-mail: ivan.dors@unh.edu
http://www.unh.edu

Abstract: Fluid Physics phenomena following laser-induced breakdown are computed and compared with experimental records. Comparison of computational and experimental results give insight into the dynamics of the temperature and pressure profiles during the decay process.

OCIS codes: (140.3440) Laser-induced breakdown; (350.5400) Plasmas; (280.1740) Combustion diagnostics

1 Introduction

Laser-induced optical breakdown results in the generation of a micro-plasma (laser-spark) and formation of a shock wave, followed by fluid physics phenomena[1, 2, 3]. The initial hot plasma temperature distribution can be inferred by laser spectroscopy methods. The expansion and subsequent cooling of the plasma causes spatially dependent temperature and pressure gradients.

2 Experimental Method

Shadow graph measurements in and near the focus can shed light on the typical post-breakdown effects. Shadowgraphs of optical breakdown in air were recorded by the use of a standard video camera, and by the use of a 308-nm back-light radiation source (XeCl eximer laser, 10 ns pulse width). Figure 1 illustrates the results.

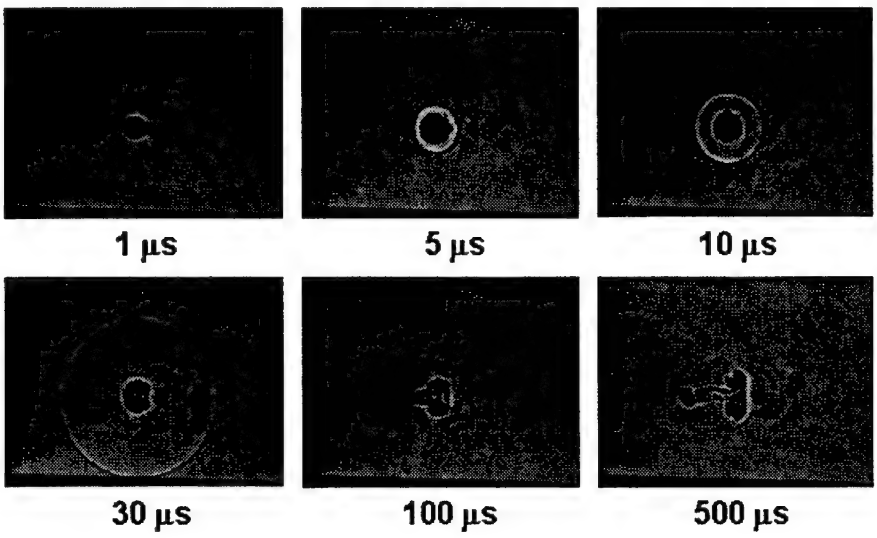

Fig. 1. Shadow graph images for 50 mJ breakdown pulses. The backlight source was operated at 80 Hz; therefore, a superposition of images at two time delays is shown: (i) at the indicated delay, and (ii) at the indicated delay plus 12.5 milliseconds.

The selected images were taken at delays of up to 500 microseconds after the laser spark gerenation, which was induced by a Coherent 40-100 Infinity Nd:YAG laser. These images show the development in time of the ignition kernel as well as the development in time of the shockwave, including reflected shock-waves[4].

3 Computational Method

The CFD-ACE software package[5], along with laser-spark specific modules, was used to solve the unsteady fluid transport equations for an axisymmetry geometry. The initial laser spark temperature distribution was characterized to simulate a post-breakdown profile. The developed computational model includes a kinetics mechanism that implements plasma equilibrium kinetics in ionized regions, and non-equilibrium, multi-step, finite-rate reactions in non-ionized regions. Figure 2 illustrates typical computational results.

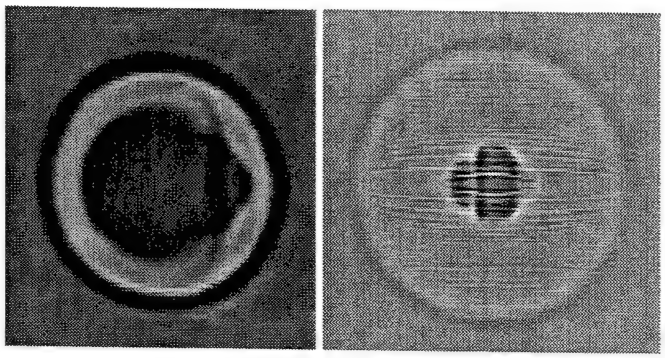

Fig. 2. Experimental (left) and computationally predicted (right) shadowgraphs 5 μs after optical breakdown of air.

4 Results and Comparison

The computational model time-accurately predicts the dynamics of the temperature and pressure field during laser spark decay. The computationally predicted fluid phenomena show qualitative agreement with the measured flow patterns[6]. Detailed quantitative comparisons, however, are believed to resolve some of the interesting behavior near the initial location of the laser spark, which are important in the study of laser-spark ignition[1, 2, 3, 7].

5 Acknowledgments

The authors thank Drs. Y.-L. Chen, G. Guan, J.W.L. Lewis and D.H. Plemmons for their interest and contributions to this work. This work is in part supported by the National Science Foundation under Grant No. CTS-9512489, a UTSI graduate research assistantship, and a NASA space grant fellowship.

References

1. I. G. Dors, "Laser Spark Ignition Modeling," Ph.D. dissertation, The University of Tennessee, 2000, http://etd.utk.edu:90/2000/DorsIvan.pdf.
2. Y. Chen, "Laser-Induced Gas Breakdown and Ignition," Ph.D. dissertation, The University of Tennessee, 1998.
3. David H. Plemmons, "Laser-Spark Ignition and the NH Radical," Ph.D. dissertation, The University of Tennessee, 1996.
4. C.G.Parigger, D.H. Plemmons, J.W.L. Lewis, G. Guan, and Y.L. Chen, "Visualization of Laser-Induced Plasma," private communications, 1996, http://view.utsi.edu/cparigge/airimages.html
5. CFD Research Corporation, Huntville, Alabama, http://www.cfdrc.com.
6. I.G. Dors and C.G. Parigger, "Computational Modeling of Temperature Dynamics During Laser Spark Decay in Air," Opt. Express (submitted for publication, 2002).
7. Y.A. Chen and J.W.L. Lewis, "Visualization of laser-induced breakdown and ignition," Opt. Express **9**, 360-372 (2001), http://www.opticsexpress.org/abstract.cfm?URI=OPEX-9-7-360.

SEMIEMPIRICAL MODEL OF AN OPTICALLY THICK LASER INDUCED PLASMA

I.B. Gornushkin, C.L. Stevenson, B.W. Smith, N. Omenetto and J.D. Winefordner
Department of Chemistry, University of Florida, Gainesville, FL 32611

A semiempirical model is developed for an optically thick inhomogeneous laser induced plasma (LIP). The model describes the time evolution of the plasma continuum and specific atomic emission after the laser pulse has terminated and interaction with the target material has ended. Local thermodynamic equilibrium (LTE) is assumed, allowing application of the collision-dominated plasma model and standard statistical distributions. Calculations (see Figure) are performed for a two-component Si/N system.

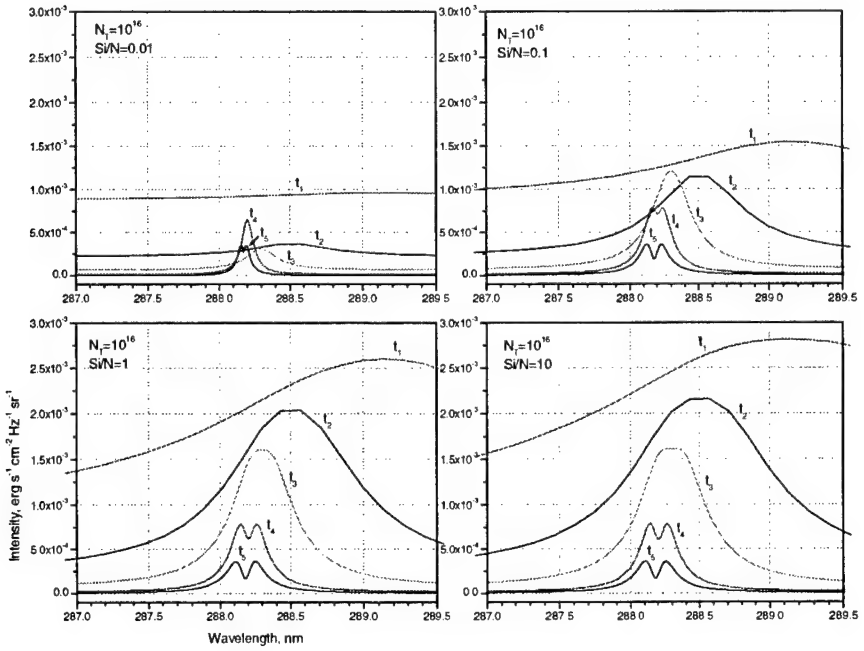

Figure. Calculated emission profiles for early LIP consisting of 10\+(16) Si and N atoms in proportions from Si/N=0.01 to Si/N=10. Times t1-t5 correspond to the values of 1, 1.5, 2, 3, and 4 in rel. units.

The model input parameters are the number of plasma species (or plasma pressure) and the atomic ratio of silicon to nitrogen, which ranged from 0.01 to 10. Functions are introduced which describe the evolution of temperature and size of the plasma. All model inputs are measurable in the experiment. The model outputs are spatial and temporal distributions of atom, ion, and electron number densities, evolution of an atomic line profile and optical thickness, and the resulting absolute intensity of plasma emission in the vicinity of a strong non-resonance atomic transition. Practical applications of the model include prediction of temperature, electron density and the dominating broadening mechanism. The model can also be used to choose the optimal line for quantitative analysis.

Fundamentals of LIBS: II

Thursday, September 26, 2002

Stanley Michael Angel, Univ. of South Carolina, USA,
Presider

ThD
4:10pm–5:30pm
Room: Royal Palm III

Spatial characterization of laser-induced plasmas by deconvolution of spatially resolved spectra

J.A. Aguilera
Departamento de Fisica, Universidad Publica de Navarra, Campus de Arrosadia, E-31006 Pamplona, Spain
j.a.aguilera@unavarra.es

C. Aragon
Departamento de Fisica, Universidad Publica de Navarra, Campus de Arrosadia, E-31006 Pamplona, Spain
carlos.aragon@unavarra.es

J. Bengoechea
Departamento de Fisica, Universidad Publica de Navarra, Campus de Arrosadia, E-31006 Pamplona, Spain
jb23249@zurron.unavarra.es

Abstract: A numerical procedure has been developed to deconvolute the lateral integrated spectra of a laser-induced plasma. Three-dimensional distributions of emissivity, temperature, electron density and relative atom density have been obtained for an iron plasma.

OCIS codes: (140.3440) Laser–induced breakdown; (300.2140) Emission spectroscopy

1. Introduction

For the development of the analytical applications of laser-induced breakdown spectroscopy (LIBS), the characterization of the laser-induced plasmas (LIPs) has a great importance. As it is known, LIPs are spatially inhomogeneous and have a fast temporal evolution. Then, their characteristic magnitudes (temperature, electron density and atom and ion densities) have spatial distributions that change with time. It is possible to obtain these distributions from spectroscopic measurements if the experimental system has spatial resolution. In last years, many works dedicated to the determination of these spatial distributions in LIPs have been published. In some of them, one-dimensional systems have been employed to measure the time integrated temperature and electron density along the axial direction [1,2]. In other works, temporal resolution was also used, and a study of the evolution of the axial distribution of the temperature and the electron density was carried out for plasmas generated with different targets and gas surrounding pressures [3,4]. Also, two-dimensional imaging of the LIP emission has been used to determine the intensity distributions [5-7]. In these works, the intensity was wavelength-integrated, so it was not possible to obtain the temperature and electron density distributions.

In previous works of our group [8,9], time-resolved spectra of LIP emission with spatial resolution in the lateral direction, parallel to the sample surface, were obtained for an iron sample and different pressures of the ambient gas. From these spectra, intensity distributions of Fe I lines, integrated along the line of sight, were measured. Assuming local thermodynamic equilibrium (LTE) and applying the Boltzmann relation, temperature distributions, also integrated along the line of sight, were deduced. The distributions of the electron density along the lateral direction were determined from the measurement of the line width of a Fe I line broadened by the Stark effect.

In the present work, a numerical inversion method has been used to deconvolute the spectra measured with lateral resolution, with the purpose of obtaining synthesized spectra along the radial direction (from the center to the edge of the plasma in a direction parallel to the sample surface). Based in these radial spectra, the distributions of line emissivity, temperature, electron density and relative atom density along the radial direction have been obtained. By repeating the process while varying the height above the surface, maps of the distribution of these plasma magnitudes have been deduced and, therefore, the three dimension spatial characterization of the LIP has been performed. In this way, an iron plasma has been characterized for different time gates, as a continuation of the iron plasma study carried out in previous works. The LIPs studied have been generated in air and argon atmospheres.

2. Experimental

The experimental system configuration was similar to that employed in previous works [8,9]. The laser used to generate the plasma was a Nd:YAG laser (wavelength 1064 nm, pulse with 4.5 ns, repetition rate 20 Hz, pulse energy 100 mJ), focused at right angles to the sample surface. The plasma emission was analyzed by using an

imaging monochromator of 0.5 m focal length and an intensified CCD detector with 5 ns temporal resolution. An image of the LIP was formed onto the entrance slit of the monochomator by a lens of 50 mm focal length. The entrance slit was placed parallel to the sample surface. In this way, spectra from different positions along the lateral direction were recorded simultaneously at different CCD rows. In these spectra, the emission was integrated along the line of sight. A vacuum chamber with a pumping system was employed to create the surrounding atmosphere.

3. Results

2.1 Deconvolution procedure

For an inhomogeneous spectroscopic source, the observed spectra are composed necessarily by the emission, integrated along line of sight, from plasma regions that have different characteristics. Assuming that the source has cylindrical symmetry and that it is optically thin, it is possible to obtain the emissivity as a function of the radial distance starting from the lateral observed intensities [10]. For this purpose, it is necessary to carry out a process of mathematical deconvolution that separates the contributions of different regions to the integrated emission. In this work, the cylindrical symmetry of a LIP with the axis along the laser beam direction (perpendicular to the sample surface) has been assumed. A computer program has been developed to perform the numerical deconvolution, supposing that the LIP is formed by cylindrical layers of constant emissivity. The numerical process progress from the edge of the LIP to the center. In one iteration, the emissivity of a layer is calculated taking into account the contribution to the intensity of all the external layers. The deconvolution process has been carried out for each wavelength of the spectrum (CCD channel); in this way, the spectra emitted at the different radial positions (emissivity vs. wavelength) have been obtained. Repeating the process for the different distances to the sample, the deconvoluted spectra of the LIP with tree-dimension resolution have been obtained.

2.2 Spatial distribution of LIP parameters

From the spectra obtained, maps of line emissivity have been measured for selected Fe I lines. Assuming that the LIP is in LTE, the temperature has been determined by the Boltzmann method for each point where the line emissivity had been measured. In this way, spatial distributions of temperature have been obtained. The electron density distributions have been obtained from the measurement of the line width of the Fe I line at 538.34 nm, which is broadened by the Stark effect.

From the knowledge of the distributions of temperature and emissivity, the distribution of the relative density of atoms can be easily deduced if LTE and optically thin conditions are assumed. In this work, the relative density distribution of iron atoms has been obtained.

The results obtained for the emissivity, the temperature, the electron density and the relative atom density are presented as a function of the radial position and the axial distance in two-dimensional maps for different time gate and plasma atmosphere conditions.

1. K. J. Grant and G. L. Paul, "Electron temperature and density profiles of excimer laser-induced plasmas", Appl. Spectrosc. **44**, 1349 (1990).
2. Y.-I. Lee, S Sawan, T. L. Thiem, Y.-Y. Teng and J. Sneddon, "Interaction of a laser beam with metals. Part II: space-resolved studies of laser-ablated plasma emission", Appl. Spectrosc. **46**, 436 (1992).
3. S. S. Harilal, C. V. Bindhu, V. P. N. Nampoori and C. P. G. Vallabhan, "Temporal and spatial behavior of electron density and temperature in a laser-produced plasma from $YBa_2Cu_3O_7$"Appl. Spectrosc. **52**, 449 (1998).
4. B. C. Castle, K. Visser, B. W. Smith and J. D. Winefordner, "Spatial and temporal dependence of lead emission in laser-induced breakdown spectroscopy", Spectrochim. Acta Part B **52**, 1017 (1997).
5. D. B. Geohegan, "Effects of ambient background gases on YBCO plume propagation under film growth conditions: spectroscopic, ion probe, and fast photographic studies" in: Laser Ablation of Electronic Materials: Basic Mechanisms and Applications, E. Fogarassy and S. Lazare, eds. (North-Holland, Amsterdam, 1992), p. 73.
6. R. A. Al-Wazzan, J. M. Hendron and T. Morrow, "Spatially and temporally resolved emission intensities and number densities in low temperature laser-induced plasmas in vacuum and in ambient gases", Appl. Surf. Sci. **96-98**, 170 (1996).
7. F. Kokai, K. Takahashi, K. Shimizu, M. Yudakasa and S. Iijima, "Shadowgraphic and emission imaging spectroscopic studies of the laser ablation of graphite in an Ar gas atmosphere", Appl. Phys A **69**, S223 (1999).
8. E. M. Monge, C. Aragon and J. A. Aguilera, "Space- and time-resolved measurements of temperatures and electron densities of plasmas formed during laser ablation of metallic samples", Appl. Phys. A **69**, S691 (1999).
9. J.A. Aguilera and C. Aragon, "Temperature and electron density distributions of laser-induced plasmas generated with an iron sample at different ambient gas pressures", Appl. Surf. Sci., in press (2002).
10. H.R. Griem, Plasma spectroscopy (McGraw-Hill, 1964).

Temporal and spatial evolution of a laser induced plasma from a steel target

M.Corsi, G.Cristoforetti, M.Hidalgo, D.Iriarte, S.Legnaioli, V.Palleschi, A.Salvetti and E.Tognoni

Istituto per i Processi Chimico - Fisici CNR - Via Moruzzi 1, 56124 PISA (ITALY)
http://www.ifam.pi.cnr.it - e-mail: *gabriele@ifam.pi.cnr.it*

Abstract: Temporally and spatially resolved measures of emission lines by a photomultiplier and shadow images by a frame camera were used to study the dynamical evolution of different elements in a steel plume in air produced by a Q-switched Nd:Yag laser.

OCIS codes: (140.3440) Laser-induced breakdown; (300.6500) Spectroscopy, time-resolved

Introduction

Although the LIBS technique in the recent years has already improved in its reliability and many applications of this technique have been proposed, it is important to go further into the comprehension of plasma evolution for modeling the phenomenon and optimizing the experimental conditions and timing for LIBS analysis. Understanding the spatial distribution of the different elements in the plume and its evolution with time it's essential to select the most suitable region of the plasma from which collecting the emissions in order to obtain the best signal to noise ratio and to make a reliable quantitative estimate of the target composition. Many studies have been focused on the morphology of the plasma obtained by laser ablation [1-6] but it is still difficult to have an organic view of the argument since the experimental parameters can be very different (laser energy, ambient gas, target material, focusing distance, etc.). The aim of this work is investigating on plasma morphology in air.

Experimental Set-up

The laser pulse (a Q switched Nd:YAG laser delivering about 70 mJ in 8 ns pulses at the fundamental frequency) was normally focused (focal length 100 mm) on the sample surface, a stainless steel containing Fe, Cr and Ni as major elements. The experiments were carried out in air, in order to gather useful information for the many existing or potential applications of the LIBS technique for in situ analyses. We examined the plasma dynamics by two different techniques: firstly we analysed the temporal evolution of emission lines in different regions of the plume, then we compared the results with the images of the plasma obtained by the shadowghraphic technique. In the former configuration an optical fiber collected the signal in the direction normal to the axis of the plume after a magnification X4 and sent it to a 1m-focal length spectrometer (equipped with a 1200 grooves/mm grating). At the exit slit a photomultiplier was mounted and the signal evolution of the chosen emission lines was displayed and averaged on a digital oscillograph. We choose emission lines both from elements contained in the target (Fe I 3719, Cr I 4289, Cr II 3667) and from the air (N I 7468). The steps of spatial sampling used were of 1 mm, corresponding to a plasma slice of 0.25 mm. In the latter configuration a white light from a flash back-illuminated the plasma. The images were taken with a frame camera at different times. Both the measurements were done focusing the laser beam 5 mm under the target surface (case a) and on the surface (case b) obtaining plumes of very different shape.

Results

As clearly visible in Fig.1, the time evolution of the signal, as recorded by a photomultiplier tuned on a emission line, is the superposition of a first peak due to continuum emission, which decays rapidly in 1-2 μs, and a second peak coming from the line observed. So, each emission peak was obtained by subtracting the continuum signal (acquired at a wavelength close to the emission line) from the total signal (as shown in the inlay in Fig.1).

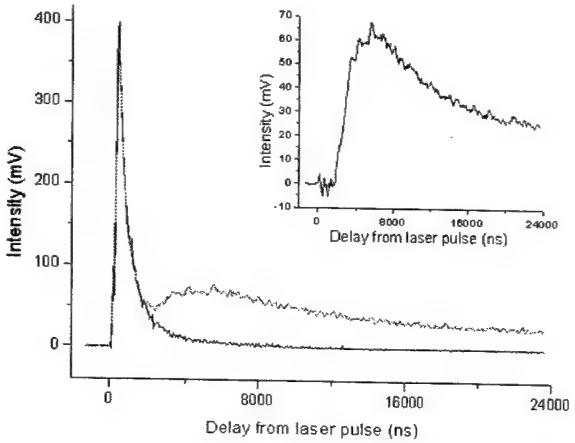

Fig.1. Temporal profile of Fe I at 3719 A (blue line) obtained after subtracting the continuum (black line) from the total signal (red line)

From a first inspection of the signals obtained, we noted a hump in the decay of some lines (not showed in figure), which apparently moves forward with time. This feature, already observed by Wu et al. [7], could be due to the distribution of matter inside the expanding plasma (e.g. it could be due to the arrival of the core of the plasma after the first front). In order to analyse the dynamics of the plasma we studied the starting time of each line for each position, obtained by fitting the rising front.
Results for the case a), where the shape of the plasma is quite flat on the surface, are plotted in Fig.2: the starting time of all the lines is represented for each position in the plume.

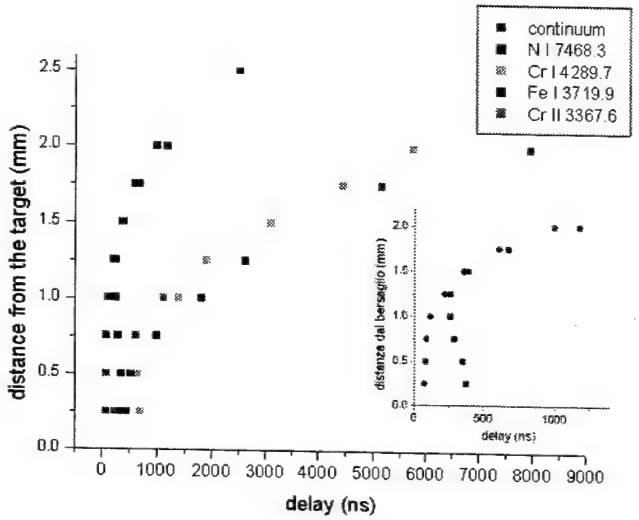

Fig.2. Starting times of emission lines and continuum at different distances from the target. In the inlay, comparison between starting times of continuum and nitrogen

From the plot it is evident that in each position of the plume the continuum and the nitrogen emissions arrive and appear earlier than emissions from elements ablated from the target. Estimating the maximum velocity of continuum front (from a fit of the curve with a power function) we obtain a value of $1.2 \cdot 10^6$ cm/s while for the front of Cr I line we obtain $1.5 \cdot 10^5$ cm/s. This is confirmed by a typical spatial profile of emission lines as shown in Fig.3 (delay = 1 μs), where the peak intensity is normalized at the maximum value. It's evident that nitrogen and continuum emissions come also from regions of the plume more distant from the target than Cr I, Cr II and Fe I lines. This is explainable with the hypothesis that the shockwave, produced in front of the plasma, heats the air it reaches. So, the air molecules can be

dissociated and ionized just from this temperature enhancement or because the heated air becomes thick to laser radiation in the early nanoseconds of plasma life, as in the mechanism of laser supported shock wave, and the laser radiation absorption causes the ionization of air (which then expands and cools in the following evolution after the laser pulse is ended). As a matter of fact, the air starts to emit immediately after the passage of the shockwave.

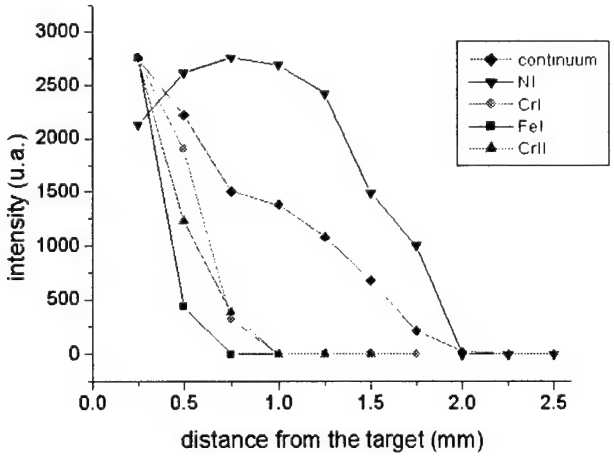

Fig.3. Spatial profile of line emissions along the normal to the target

It's interesting the comparison of the starting times of continuum and nitrogen as shown in the inlay in Fig.2. Close to the target the shockwave heats the air so much than the nitrogen is probably mostly ionized and we can see NI emission only after ca 200 ns; going away from the target surface, the shockwave, after the laser pulse ended, is less and less efficient in heating the air, until nitrogen is just weakly ionized or not ionized at all and the starting times of continuum and nitrogen coincide. This interpretation is confirmed from other observations where N II lines are visible just in the first 200 ns of plasma life. In the case b), where the plasma is approximately hemispheric, the results are similar but with some interesting deviation. The continuum and nitrogen emissions, as before, precede the target elements ones and their front moves with a velocity slightly higher than in case a). In this case, however, the front of the target elements moves very faster than in case a) ($V_{max} \approx 5-7 \cdot 10^5$ cm/sec) so that the two fronts are very close. This probably happens since in case a) the portion of surface interested from the beam is larger and the fluence is lower; then in the strong point explosion theory the shockwave velocity is weakly dependent from laser fluence ($V \propto E^{1/5}$) while the rear plasma velocity depends much more from the energy that each particle ablated receives.

The images of the plume obtained with the shadowgraph technique confirmed these interpretations showing the shockwave and plasma fronts, with velocity consistent for case a) and b) with the previous found. We are still working to extrapolate from the experimental data information on the spatial dishomogeneities between the target elements in the plasma.

References:

[1] V.Bulatov, L.Xu and I.Schechter, "Spectroscopic Imaging of Laser-Induced Plasma" Anal. Chem., **68**, 2966 (1996)
[2] Y.Lee, K.Song, H.Cha, J.Lee, M.Park, G.Lee and J.Sneddon, "Influence of Atmosphere and Irradiation Wavelength on Copper Plasma Emission Induced by Excimer and Q-switched Nd:YAG Laser Ablation", Appl. Spectrosc., **51**, 959 (1997)
[3] M.Milan and J.J.Laserna, "Diagnostics of silicon plasmas produced by visible nanosecond laser ablation", Spectrochim. Acta, **56B**, 275 (2001)
[4] R.A.Al-Wazzan, J.M.Hendron and T.Morrow, "Spatially and Temporally resolved emission intensities and number densities in low temperature laser-induced plasmas in vacuum and in ambient gases", Appl. Surf. Sci., **96-98**, 170 (1996)
[5] R.A.Multrari, L.E.Foster, D.A.Cremers and M.J.Ferris,"Effect of sampling geometry on elemental emission in laser-induced breakdown spectroscopy" Appl. Spectrosc., **50**, 1483 (1996)
[6] D.B. Geoghan and A.A.Puretzky, "Laser ablation plume thermalization dynamics in background gases: combined imaging, optical absorption and emission spectroscopy, and ion probe measurements", Appl. Surf. Sci., **96-98**, 131 (1996)
[7] J.D.Wu, Q.Pan and C.Chen, "Investigation of the Dynamics of Copper Plasma Generated from a Laser-Ablated Target Using Optical Emission Analysis", Appl. Spectrosc., **51**, 883 (1997)

Study of the influence of Er:YAG and Nd:YAG wavelengths upon LIBS measurements under air or helium atmosphere

V. Detalle, M. Sabsabi, L. St-Onge, A. Hamel and R. Heon

National Research Council Canada, Industrial Materials Institute,

75 de Mortagne Blvd., Boucherville, Quebec, J4B 6Y4 Canada

1.0 Introduction

Laser-induced breakdown spectroscopy (LIBS) is now recognized as a useful analytical tool for elemental analysis. However, to obtain a quantitative analysis using LIBS, one needs to control several parameters that can strongly affect the measurements. These parameters are for example, the amount of ablated and vaporized material, the property of plasma to absorb/reflect the delivered energy and the degree of ionization that can change as a function of laser wavelength and irradiance, the ambient gas nature and pressure, and the sample surface morphology. If all these parameters are set, and accounting for slight laser shot-to-shot variations in terms of laser beam energy and spatial profile, the spectral line intensities will generally be proportional to the elemental concentration.

The choice of these different parameters is critical and depends on the application. On one hand, control of these parameters leads to a reproducible and stable measurement. On the other hand, allowance should be given for flexibility in these parameters in order to optimize the sensitivity for particular elements.

Two of the most important experimental parameters for the LIBS performance are the laser wavelength and the surrounding atmosphere. Historically, different kinds of laser have been used for LIBS experiments. The LIBS experimentalist could not choose any laser wavelength but just those that the technology allowed. For first LIBS developments,Brecht and Cross in 1962 [1] described a LIBS experiment using a ruby laser at 694 nm with 50 ns pulse duration. Then, in the 70s three commercially manufactured LIBS microanalysers (Mark III Jarell-Ash, LMA 10 VEB Carl Zeis and JLM 200 JEOL) were proposed using a ruby laser [2]. However, due to the difficulty of controlling the pulse-to-pulse stability, the technique was not viewed as a technique of reference for the analysis of solids; the pulsed-laser technology was not sufficiently ripe. The next phase of LIBS development started with the apparition of the Nd:YAG and excimer lasers in the eighties. Since then, many UV, visible and NIR laser wavelengths were available. It was possible to vary the wavelength and to study how that could affect the LIBS measurements.

Nowadays, with the wide variety of laser systems available in terms of wavelength (with OPO systems the whole range of wavelengths is available) and pulse duration, one is able to study and search more systematically the best conditions for LIBS implementation. In addition, the surrounding atmosphere plays a key role in the

development of the plasma and can change LIBS performance. The atmosphere can be reduced in the majority of cases to a simple gas puff blown at the moment of laser-sample interaction.

Most of the LIBS work published was concerned with laser wavelength of Nd: YAG at 1064 nm and its harmonics or with eximer laser wavelengths mainly in the UV and less attention was paid to the generation of laser induced plasma by wavelength available in the infra-red IR (>1 μm). For example, the Er: YAG laser has the advantage of providing a 2.94 μm wavelength for which certain materials (polymeric or organic) are more absorbing. Moreover, the absorption of plasma by inverse Bremsstrahlung (varying as λ^2) makes it possible to induce a different behaviour in terms of excitation. In this work, Nd: YAG and Er:YAG lasers, with 1.06 and 2.94 μm wavelengths, were used for LIBS analysis of solids. Using air or He buffer gases, the influence of the wavelength on the laser-produced plasma was studied.

2.0 Results and discussion

In our experiments, the Er:YAG laser source supplied energy of 25 mJ/pulse (with pulse duration of 170 ns) and the laser beam was focused on the target using a lens with 10-cm focal length, yielding a spot diameter of 250 μm. The Nd:YAG source was used with the same fluency, but the pulse duration was 6 ns. We chose to carry out a comparison in terms of spectrochemistry and plasma characterization. We studied aluminum alloys in order to compare our results with previous work [3,4]

Spectra obtained with either Nd:YAG or Er:YAG lasers are presented in Fig. 1.

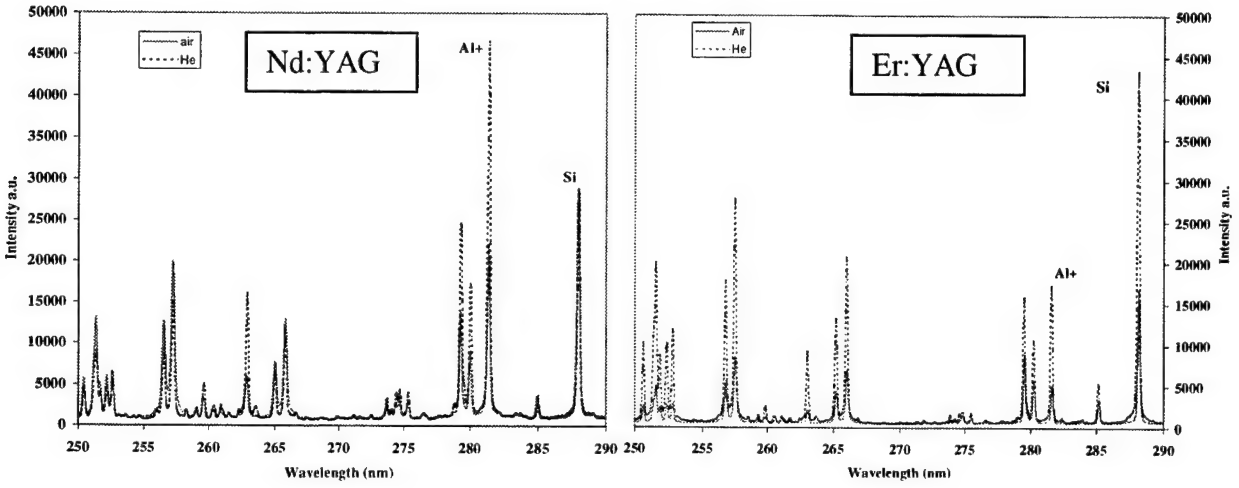

Figure 1: Study of buffer gas effect using two wavelengths in aluminum alloys.

The signal integration conditions have been optimized separately for the two wavelengths in terms of delay and width. The coupling between Er:YAG or Nd:YAG radiation and helium buffer gas seems to be significantly different. In the two cases, the 281.62 nm aluminum ion line intensity increases by at least a factor of 2. But the Si 288.16 nm line increases only with Er:YAG excitation. In order to understand the evolution of physical parameters,

we studied the excitation temperature of the plasma. Figure 2 shows the difference observed between the He and air buffer gas conditions, with Er:YAG excitation.

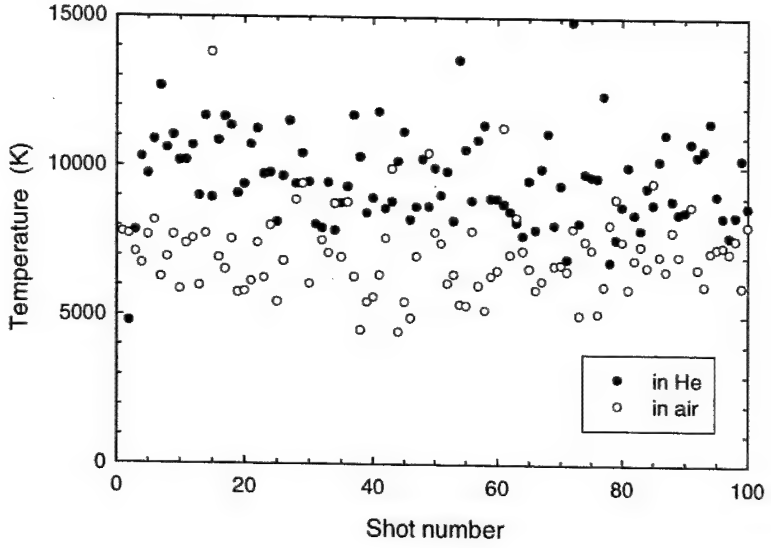

Figure 2 : Excitation temperature measurements for individual Er:YAG shots, based on Boltzmann plot calculation using Fe lines (aluminum alloy with 0.61% Fe), with 0.5 µs delay and 1 µs integration.

The He buffer gas induces an increase of 2500 K of the excitation temperature, giving a partial explanation for the increased line intensities shown in Fig. 1.

3.0 Conclusion

In summary we have carried out a comparison of the influence of two different wavelengths, 1.06 and 2.94 µm for Nd:YAG and Er:YAG lasers, respectively. This was performed under He or air environments in terms of plasma properties and spectrochemical analysis of several elements in aluminum alloys. The results show that these parameters induce important variations in the generated plasma, in terms of temperature and analytical measurements.

This study was performed in order to allow a better comprehension and control on the implementation of laser-induced breakdown spectroscopy.

[1] F. Brecht and L. Cross, Appl. Spectrosc. **16**, 59 (1962).

[2] L. Moenke-Blankenburg, Laser Micro-analysis (J.Wiley Interscience, New-York, 1989).

[3] V. Detalle, R. Heon, M. Sabsabi and L. St-Onge, Spectrochim. Acta Part B **56**, 1011-1025 (2001).

[4] L. St-Onge, V. Detalle and M. Sabsabi, Spectrochim. Acta Part B **57**, 121-135 (2002).

Plasma Morphology and Matrix Effects Interrelation in LIBS Analysis

Israel Schechter, Valery Bulatov and Rivie Krasniker

Department of Chemistry, Technion - Israel Institute of Technology, Haifa 32000, Israel
israel@techunix.technion.ac.ill, phone:972-4-8292579, fax:972-4-8292579

Extended Abstract: Matrix effects limit the performance of LIBS in absolute elemental analysis, since the spectral intensity of an emission line at a given concentration depends on the matrix. On the other hand, several characteristics of the plasma morphology depend on the matrix as well. Therefore, understanding the interrelation between plasma morphology and the matrix effects may result in releasing LIBS analysis from the necessity of obtaining independent information on the sample matrix. Preliminary results indicate that morphological data, which can be readily obtained, may provide the necessary information on the most important matrix characteristics, such that the proper calibration plot can be utilized for obtaining the required concentration. Moreover, once the interrelations between the matrix effects and plasma morphology have been established, one can utilize this information for performing sophisticated LIBS analysis. For example, the organic carbon content of soils can be distinguished from the total carbon, using a specific emission line, which is affected be the organic content. This way, the matrix effect is utilized for obtaining analytical information that could not be obtained by traditional LIBS.

OCIS codes: (120.6200) Spectrometers and spectroscopic instrumentation

Poster Session

Thursday, September 26, 2002

ThE
8:00pm–10:00pm
Room: Royal Palm III

Laser-induced breakdown spectroscopy for quantitative analysis of Aluminum alloy

Awadhesh K. Rai[1], Fang Yu Yueh and Jagdish P. Singh[2]

Diagnostic and Analysis Laboratory, Mississippi State University, 205 Research Boulevard, Starkville, MS 39759
[1]Department of physics, G. B. Pant University of Agriculture and Technology, Pantnagar-263145, India.
[2] Corresponding author, Singh@Dial.msstate.edu Phone 662 325 7375

Abstract

LIBS spectra of molten Al alloys were recorded inside the melt and used to obtain the calibration curves for the minor elements. The methods to improve the measurement precision of LIBS application were studied and presented.

Analysis of alluvial soils for environment survey by micro LIBS (μLIBS)

Denis MENUT[1], Philippe LE COUSTUMER[2], Jean Luc LACOUR[1], Pascal FICHET[1], Annie RIVOALLAN[1]

1 - CEA Saclay, Fuel Cycle Division, LALES DEN/DPC/SCPA Bâtiment 391, 91191 Gif Sur Yvette France
Tel. : (33) 1 69 08 77 52 FAX. : (33) 1 69 08 77 38
e-mail : MENUT@carnac.cea.fr

2 – BORDEAUX 1 UNIVERSITY, Department of Applied Geosciences Bâtiment 18 Recherche Geologique, Avenue des Facultes, 33405 Talence CEDEX France
Tel. : (33) 5 56 84 87 98 FAX. : (33) 5 56 80 71 38
e-mail : plc@Inet.fr

The chemical composition of a material gets fundamental importance for numerous tasks of process control and quality assurance in industrial production and environmental technology [1, 2]. The Laser Analysis and Surface Study Laboratory of the CEA Saclay in collaboration with the Department of Applied Geoscience from Bordeaux I University tried to evaluate the capability of the micro Laser Induced Breakdown Spectroscopy (μLIBS) for application in environmental field. First samples provided come from alluvial sediments catched at different locations along Garonne bed river (south east of France). These researches aim at controlling the heavy metal transport and understanding processes involved into the Garonne river mud. The same samples were analysed at Bordeaux I University by SEM/X-EDS and ICP/AES after dilution. Qualitative surface mapping analysis by μLIBS have been performed with the use of Fe and Mn lines in an Al, Si and Ca matrix. Those elements of interest (Fe & Mn) are considered to be the vehicule of the pollutant (Ni, Zn, Cd, Pb, etc) transport mechanism. Multi elemental surface mapping reconstruction has allowed to obtain a composition approach of the different micro texture observed on the sample surface.

The second sample studied come from volcanic ash material where the statistical distribution of the elements observed should allow an approach of the geological phenomenon induced during the volcano eruption.

In the case of microanalysis by LIBS, the most important feature is the lateral resolution of the measurements and its control during the experiment duration. This has been done in our laboratory by the use of a combination of a laser microprobe based on a modified optical microscope and a powerful XY driver moving very quickly and precisely. A standard optical microscope set-up is used with optical component treated at the laser wavelength. At the beginning of the optical path the laser beam goes through a diaphragm and is focused on the sample surface using a refractory microscope objective. A CCD camera is placed above the microscope in order to control and adjust the sample position along rapid translation stage. The CCD is designed to cover a visible image of the sample surface about 200 μm x 200 μm. Samples are positioned and fixed with screws on the XY driver monitored at 20 Hz (laser shot frequency) with a 3 μm displacement (with a repeatability < 10 %) between consecutive laser shots. For the plasma analysis, a 3 m long optical fiber whose entrance is placed as close as possible from it guides the emission on the entrance slit of a Czerny-Turner spectrometer equipped with a pulsed Intensified CCD camera. A basic personal computer controls both the moving stage but also the ICCD camera. The pulsed laser and ICCD camera are electronically enslaved with the XY drivers that governs all the experimental set-up after the experiment starting. Moreover, on a fixed part of the microscope, a small tube is locked to add the Ar buffer gas flow near the point where plasma is generated. It is well know that Ar flow increase the magnitude of the plasma emission and reduce self absorption process. The μLIBS system do not required sample preparation nor evacuation. The spectral record is instantly digitised and stored, allowing a very rapid quantitative surface mapping can be performed at atmospheric pressure (see figure 1).

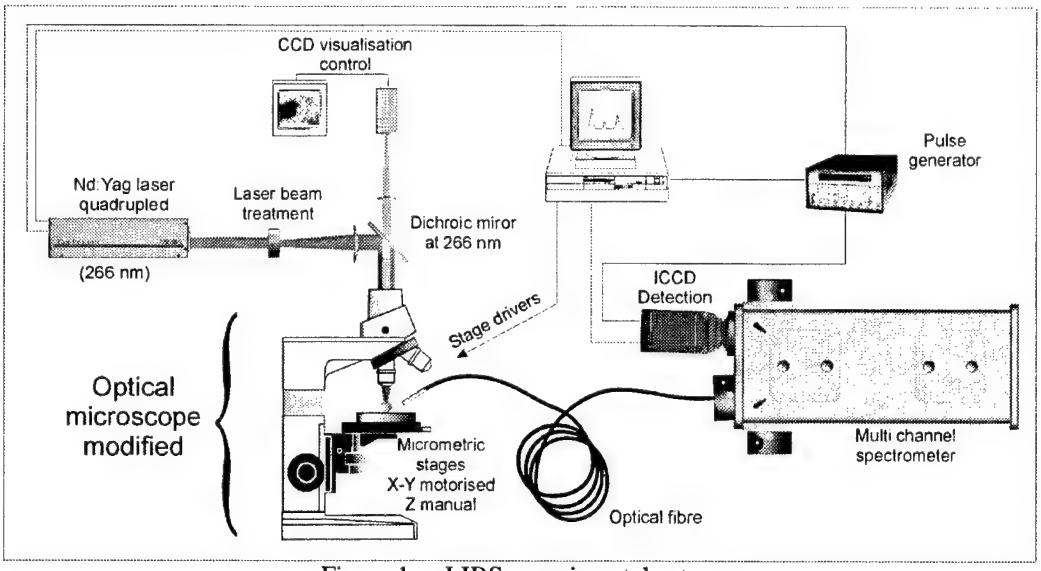

Figure 1 : µLIBS experimental set-up

The µLIBS device described in this paper is under patent [3] and applied to characterise as an example very small aggregates on samples surfaces. With a spatial resolution of the laser microprobe of 3 µm combined with a well-controlled displacement of 3 µm, it is obvious that at least one entire crater among three consecutive craters can describe qualitatively and quantitatively the composition of a 10 µm wide aggregate (see figure 2). Each crater formed and analysed are obtained with a single laser shot (see figure 2). For a typical surface analysis by µLIBS, every plasma emission is recorded and the experimental set-up allows the surface investigation with a repetition rate of 20 Hz. Therefore, it takes about half an hour to record the emission of 32 000 separated craters corresponding to a rectangular area of 600 x 480 µm with a lateral resolution of 3 µm. In the case of quantitative surface analysis, the elemental detection sensibility is not dependant of the acquired repetition rate.

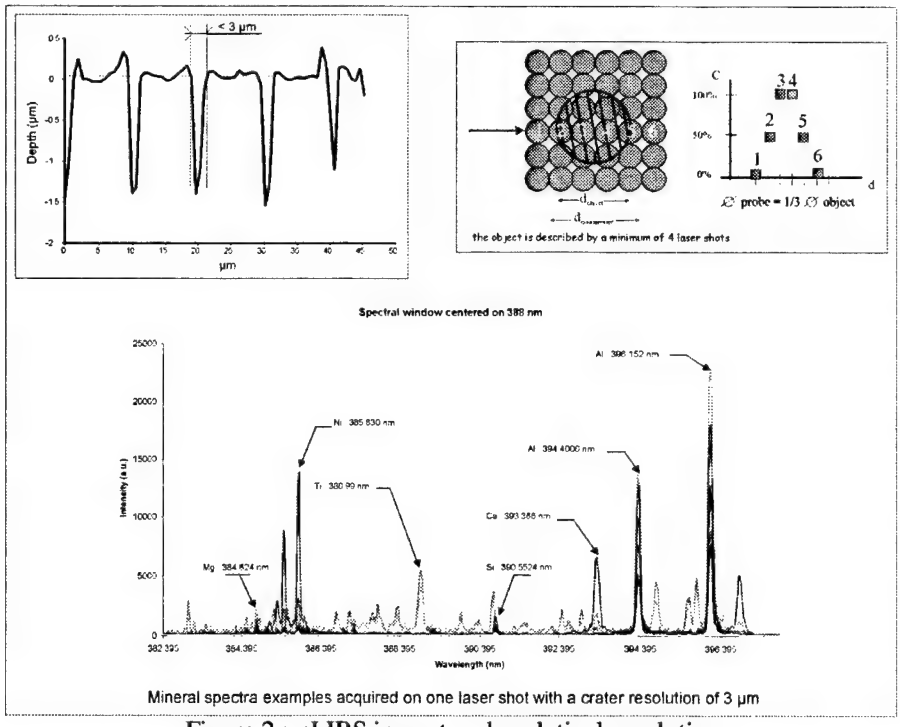

Figure 2 : µLIBS impact and analytical resolution

The µLIBS system developed has been mainly applied on ceramics before and after heating to investigate the inter-elementary diffusion during there industrial process. Steel and aluminium alloy samples have been also studied. Another application was performed on mineral samples with the detection of low atomic number component such as Li [4] and C, H, O, N [5]. The Li is, for example, an important geochemical tracer for geological fluids and solids. The Li was detected in oxides forms as a solid state but also in fluid inclusions. In this study on environmental samples, the µLIBS the detection of light such O but also heavy element such ac Ni or Cr. On the two kinds of samples (alluvial and volcanic), a chemical distribution map of the different elements as been acquired fastly (see figure 3). They put into an evidence that the chemical distribution of the elements is heterogeneous and some elements are associated such Al-Si-Ca (see figure 3) or Ti-Mg (see figure 4). This result agree with the mineralogy of the sample which contains carbonate (calcite and aragonite) and silicate minerals (feldspath). The analysis of the trace elements (Mn, Ti, Ni) is also possible (see figure 5).

In conclusion, the µLIBS delivers in few minutes a powerful information on the chemistry of the material : elementary distribution of the majors but also for the trace elements at different scales (10 µm or 3 µm). Using the Image Analysis is will be possible to get a chemical map showing the association of the elements which is function of the mineralogy. The next step will be focused on the quantitative aspect of the technic.

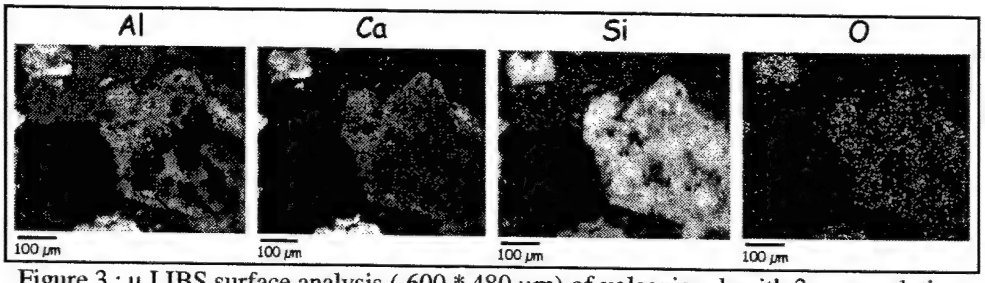

Figure 3 : µ LIBS surface analysis (600 * 480 µm) of volcanic ash with 3 µm resolution.

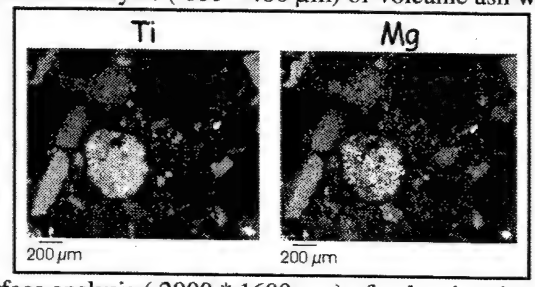

Figure 4 : µLIBS surface analysis (2000 * 1600 µm) of volcanic ash with 10 µm resolution.

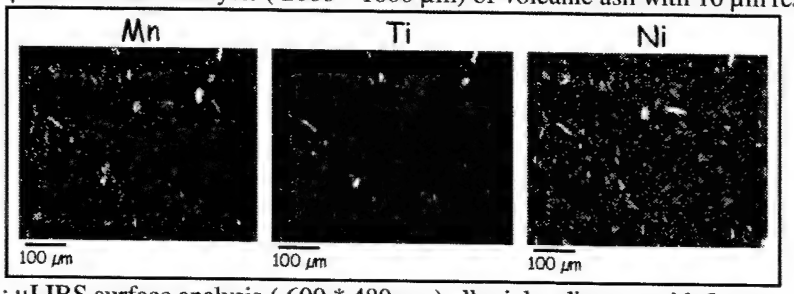

Figure 5 : µLIBS surface analysis (600 * 480 µm) alluvial sediments with 3 µm resolution.

References :

1. Fichet, P. ; Mauchien, P. ; Moulin, C. (1999) Appl. Spectrosc. 53, 1111-1117.
2. Radziemski, L.S. and Cremers, D.A. (1989) Laser-Induced Plasmas and Applications. New York, Marcel Dekker.
3. European Patent Office N°00978635.5-2204 ; 2001.
4. Fabre, C. ; Boiron, M.C. ; Dubessy, J. ; Catelineau, M. ; Banks, D.A. (2002) Chem. Geol. 182, 249-264.
5. Tran, M, Sun, Q, Smith, B. W., Winefordner, J. D. (2001) J. Anal. At. Spectrom 16, 628-632.

A LIBS spectral database obtained in Martian conditions with an echelle spectrometer for in situ analysis of Mars soils and rocks

Cecile FABRE [1], Rene BRENNETOT [2], Pascal FICHET [2], Evelyne VORS [2],

Jean Luc LACOUR [2], Jean DUBESSY [1], Marie-Christine BOIRON [1], Annie RIVOALLAN [2],

Sylvestre MAURICE [3], David CREMERS [4], Roger WIENS [5]

[1]CREGU UMR G2R 7566,BP 239, 54501 Vandoeuvre les Nancy France
Tel : (33) 3 83 91 38 14 FAX : (33) 3 83 91 38 01
e-mail : cecile.fabre@g2r.uhp-nancy.fr
[2] CEA Saclay, Fuel Cycle Division, LALES DEN/DPC/SCPA Bâtiment 391, 91191 Gif sur Yvette France
Tel : (33) 1 69 08 77 53 FAX : (33) 1 69 08 77 38
e-mail : brennetot@carnac.cea.fr
[3] Midi Pyrenees Observatory
Tel : (33) 5 61 33 29 47 FAX : (33) 1 61 33 28 40
e-mail : maurice@ast.obs-mip.fr
[4] Chemical and Advanced Diagnostics, Los Alamos National Laboratory (MS J565, Los Alamos, NM 87545 USA
Tel : 505-665-4180 FAX : 505-665-6095
e-mail : cremers_david@lanl.gov
[5] Space and Atmospheric Sciences, Los Alamos National Laboratory (MS D466, Los Alamos, NM 87545 USA
Tel : 505-667-3101 FAX : 505-665-7395
e-mail : rwiens@lanl.gov

1. Introduction

LIBS method is well-known for its numerous advantages such as 1) rapid analysis, 2) simultaneous multi-elemental detection, 3) detection of high and low z elements, 4) ability to drill onto the sample up to several hundreds of micrometers and 5) stand-off analysis capability [1, 2].

A project called MALIS (Mars elemental Analysis by Laser Induced breakdown Spectroscopy) is under study to perform in situ geochemical analysis of Mars soils and rocks. To demonstrate its feasibility, a laboratory set-up is tested in order to determine the specific characteristics of the laser, the optical components and the detection system that could be mounted on a rover [3]. Thus, the achievement of a LIBS spectral database under Mars atmospheric conditions seems to be of major importance to observe the actual sensitive emission lines for each element of interest without any interference and to ensure a reliable recognition of elemental composition of rock and soil in Mars atmospheric conditions.

2. Experimental set up

Current development has already optimized experimental analysis (under CO_2 atmosphere: 5 and 12 mbars) using Doehlert matrix design to study the influence of major parameters on LIBS signal [3]. This work has permitted to choose the instrument that will be used on Mars: 1064 nm for laser wavelength (Nd:YAG laser), 40 mJ energy output, short delay and angle of incidence lower than 50°. The spectral detection covered ranges from 200 nm to 780 nm with a resolution of $\lambda/\Delta\lambda$= 10000 using an Echelle spectrometer detection system (ESA 3000, LLA, Germany). It can be noticed that up to now, working distance is fixed at 1 m and the spot size on the sample is about 150 µm diameter for normal incidence, but future working distance is expected to be 15 m.

3. Mars applications

In-situ geochemical data of Mars rock and soil compositions are essential to determine which kind of rocks exists on the planet and to have access to the possible geological processes that they are issued from (volcanism, sedimentary, alteration processes...). These in-situ data are complementary and important for the analysis and the interpretation of orbital chemical and mineralogical data. The global Martian dust is supposedly a mixture of andesitic rocks (Mars Pathfinder data, [4]), basaltic rocks and a salt component. However, the presence of andesitic rocks has recently been challenged by the suggestion that these rocks are basalts with weathered surface coatings [5]. To answer this question it is essential to determine the composition of major elements such as Na, Mg, Al, Si, K, Ca, Ti, Fe, Mn and O. Carbon and sulfur are also important to discriminate different processes such as sedimentary or alteration,

respectively. Moreover, it is essential to detect N, Cl and P to clearly identify nitrates, chlorine and phosphates. Concerning trace elements, we can already include Ba, Sr, Pb, Li, Cs and Rb as useful for indicating alteration processes.

4. Experimental procedure

To enlarge the choice of the analyzed elements and for the reproducibility of the experiment, we have decided to work on different synthetic silicate glass standards, specially produced in our laboratory. These silicate glasses are prepared from carbonates ($CaCO_3$, Na_2CO_3, K_2CO_3...), oxides (Li_2O...) or chlorides ($PbCl_2$...) in a SiO_2 matrix. After decarbonation (600°C), the powders are twice heated in an oven (Fisher Bioblock Scientific, France) to a temperature up to 1600°C (depending on compositions) in platinum crucibles during ten minutes to reach liquid state [6]. When glasses are still liquid, they are directly soaked on a copper tablet or in water. Between the two heating stages, the glasses are finely crushed to homogenize the composition. The synthetic glass compositions are analyzed by electron microprobe to check the element content homogeneity at the microscopic scale and by bulk analysis (ICP-MS or ICP-AES) to obtain light element concentrations (such as lithium) and trace elements.

5. Standard compositions

The different glass standard compositions have been chosen based on the in-situ Mars surface chemical compositions obtained for major and trace elements (Mars Pathfinder, Viking, [5], [7]) and in relation to analysis realized on SNC meteorites (Shergottites, Nakhlites, Chassigny [8]). Major elements are Si, Na, Fe, Al, Mg, Ca, Ti and K (from 1 to 50 oxide weight%) and trace elements include halogen, alkali, metal or lanthanide elements (Cl, P, Ni, Sr, Ba, Eu, La, Li…) (see Table 1).

Element	concentration	Element	concentration
Na_2O	3%	Cs	500 ppm
FeO	15 %	Ba	500 ppm
MgO	4 %	Pb	500 ppm
Al_2O_3	25 %	Ce	500 ppm
SiO_2	50 %	Gd	500 ppm
K_2O	1 %	Th	500 ppm
CaO	7 %	S	500 ppm
TiO	5 %	Eu	500 ppm
P	500 ppm	Zr	500 ppm
Cl	500 ppm	Sn	500 ppm
Cr	500 ppm	Nb	500 ppm
Mn	500 ppm	La	500 ppm
Ni	500 ppm	Sm	500 ppm
Rb	500 ppm	Co	500 ppm
Sr	500 ppm	Li	500 ppm

Table 1: Starting values for each selected element for the first run of silicate glass standards.

The first step of this work is the synthesis of several standards displaying a single element in a SiO_2 matrix, in order to select the most appropriate emission lines that will be used for the LIBS calibration. To estimate precisely the potential of the LIBS instrument and the detection limits, different series of glass standards have been realized decreasing the element content from the starting values down to few ppm. It is also important to estimate the detection limit for each element expected in Mars conditions and to get first quantification.

The second step is the addition of several elements in the SiO_2 matrix, to identify the possible interference between the optical emission lines (figure 1). Indeed, the samples with very high abundance of some transition elements (Fe, Mn, Ti...) which are intended to be analyzed at the Mars surface are likely to increase detection limits due to interference from their numerous emission lines.

The last standards are natural samples which can be considered as "Mars analogue" rocks or soils, specially collected to cover all of the rocks supposed to be observed on Mars surface. They will be also used to check the validity of LIBS calibration of quantitative element content and to test the estimated detection limits. In addition, homogeneous minerals such as olivine or pyroxene of known compositions (analyzed by global method, ICP-AES) will be tested. As analytical procedure requires several tests on the same object to obtain a good repeatability, the laser spot size could be a limitation aspect (150 µm), because it is relatively difficult to sample enough large homogeneous minerals.

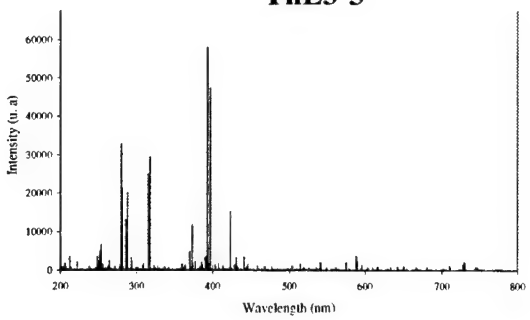

Fig 1: Total LIBS spectrum obtained on standard silicate glass. (1064 nm, 40 mJ, 50 shots integrated)

Different igneous rocks were collected: boninite (Figure 2) and troctolite from New Caledonia, referenced standard basalt (BR and BE-N, CRPG, Nancy, France, [9]), pillow-lava from Central-Indian dorsal with or without hundred microns depth altered crust (to examine the laser drilling onto the sample and to record the different LIBS spectra during the process, [10]) and andesite (which has higher SiO_2 than basalt) from California. Powdered glasses will be analyzed to simulate powder and dust and also, analogue Mars dust from Hawaiian Mauna Kea volcano will be specifically tested [11].

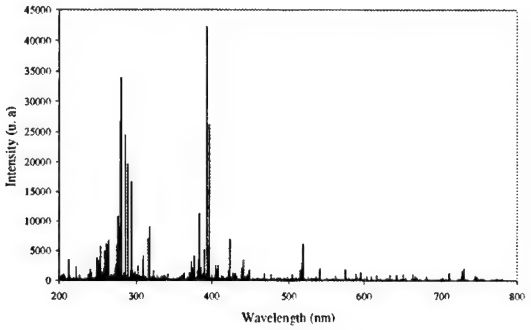

Fig 2: LIBS spectrum of boninite (1064 nm, 40 mJ, 50 shots integrated).

6. Conclusion and perspectives

All of these different standards from mono to multi-elementary compositions have finally permitted to collect numerous reference emission spectra to develop a complete LIBS spectra database. It will be possible using LIBS analysis to obtain quantitative data of compositions, from several to hundreds of ppm in Mars atmospheric conditions. The final aim of this LIBS database is the reconstruction of the chemical and mineralogical composition of rock using major element concentrations and the CIPW normalization.

Regarding the requirements imposed by a spatial project such as MALIS (e.g. low weight, miniaturization instrument, and high spectral resolution), the LIBS prototype can be considered as a future suitable portable instrument. Indeed, the powerful advantages of this industrial instrument will permit rapid acquisitions of direct quantification of element in rocks or metals using standoff analysis, allowing numerous applications such as ore prospecting, cartography or hazardous product analysis [12].

7. References

[1] S. Palanco, J. M. Baena, J. J. Laserna, Spectrochim. Acta 57B, 591, (2002)
[2] A. K. Knight, N. L. Scherbarth, D. A. Cremers, M. J. Ferris, Appl. Spectrosc. 54, 331, (2000)
[3] R. Brennetot, J. L. Lacour, E. Vors, P. Fichet, A. Rivoallan, S. Maurice *LIBS2002*, this volume (2002).
[4] H. Y. Mc Sween *Lunar & Planetary Science XXXIII* (2002).
[5] R. Rieder, T. Economou, H. Wänke, A. Turkevich, J. Crisp, J. Brückner, G. Dreibus, H. Y. Mc Sween Jr. *Science, 278,* 1771-1774 (1997).
[6] C. Fabre, M. C. Boiron, J. Dubessy, A. Chabiron, B. Charoy and T. Martin Crespo *Geochim. Cosmochim. Acta, 66,* 1401-1407 (2002).
[7] R. V. Morris, D. C. Golden, J. F. Bell, T. D. Sheffer, A. C. Scheinost, N. W. Hinman, G. Furniss, S. A. Mertzman, J. L. Bishop, D. W. Ming, C. C. Allen, D. T. Britt *J. Geoph. Research E : Planets, 105,* 1757-1817 (2000).
[8] C. Meyer *Mars Meteorite Compendium,* http://www-curator.jsc.nasa.gov/curator/antmet/mmc/mmc.htm (1998).
[9] D. Ohnenstetter and W. L. Brown *Contrib. Mineral. Petrol.*, 123, 117-137. (1996).
[10] J. M. Nafziger PhD Thesis, 259 (1995).
[11] R. V. Morris, D. C. Golden, D. W. Ming, T. D. Sheffer, L. C. Jorgensen, J. F. Bell, T. G. Graff, S. [10] A. Mertzman *J. Geoph. Research E : Planets, 106,* 5057-5083 (2001)
[12] J. P. Singh, F. Y. Yueh, H. Zhang, R. L. Cook *Process control and Quality, 10,* 247-258. (1997)

Laser-induced plasma spectroscopy in near vacuum ultraviolet using ordinary spectrograph and ICCD

Saara Kaski, Heikki Häkkänen and Jouko Korppi-Tommola
Department of Chemistry, P.O. BOX 35, FIN-40014 University of Jyväskylä
saara.kaski@jyu.fi

Abstract: An experimental setup to measure laser-induced plasma emission spectra with an ordinary Czerny-Turner spectrograph and intensified charge-coupled device in the near vacuum ultraviolet down to 130 nm is described. Spectra of bromine, chlorine and iodine were recorded to demonstrate the performance of the setup.

OCIS codes: (140.3440) Laser-induced breakdown; (300.6540) Spectroscopy, ultraviolet

1. Introduction

Laser-induced plasma spectroscopy (LIPS) measurements are most often done in the visible and ultraviolet region. However, there are several important elements that have strong emission lines in the near vacuum ultraviolet (VUV) *i.e.* 110-190 nm. For example emission lines of halides Cl, Br and I are rather weak in the visible and are traditionally detected in the near-infrared [1-4], but most intensive lines of halides are in the near VUV.

Detection of the plasma emission in the VUV region is limited by absorption of ambient atmosphere. To avoid this a suitable gas purge or vacuum techniques have to be used. In LIPS measurements using vacuum ultraviolet spectrographs and VUV transparent sample chambers, emission lines in this region have been detected [5-7]. VUV lines have also been measured using Czerny-Turner spectrograph with gas purge, but shortest wavelengths reached with such an approach have been around 180 nm [8-10].

In this work we describe a simple setup for near VUV measurements that may be used down to 130 nm. It consists of an ordinary Czerny-Turner spectrograph, an intensified charge-coupled device (ICCD) and a gas purge arrangement. Also fiber optics input was tested.

2. Experimental

The LIPS setup used is described in detail elsewhere [11]. Modifications to the previous setup are shortly described here. A KrF excimer laser (Optex, Lambda Physik) operating at 248 nm with ~10 mJ pulse energy was used to create plasma. Emission of the plasma was detected by using an ICCD detector equipped with a magnesium fluoride (MgF_2) input window (Andor DH520) or an ICCD detector having a quartz input window (Instaspec V, Oriel). A 150-mm Czerny-Turner spectrograph (Acton Research Corp.) was purged with Ar or N_2 to prevent atmospheric absorption. The sample was placed approximately 10 mm away from the slit of the spectrograph. Because the plasma was generated close to the slit, gas flow through the spectrograph slit towards the plasma was sufficient to purge the optical path between the plasma plume and the spectrograph (setup I in Fig. 1.).

The optical fiber used in the setup II of Fig. 1. was a 1-m long UV grade fused silica bundle. The gas flow from the spectrograph slit kept the optical path transparent for VUV emission between the fiber output and the slit. The fiber head was ~10 mm away from the plasma and the optical path between the plasma and the fiber was purged through the fiber head cover (setup II in Fig. 1.). ICCD with quartz input window was used in these measurements since emission below 180 nm is not transmitted in UV-grade fused silica.

Sample tablets were pressed from pure (>99%) potassium salts of chlorine, bromine and iodine. For fiber optics experiments sample tablet of enriched ore consisting of several elements (*e.g.* Cu, Fe, S, Si) was used.

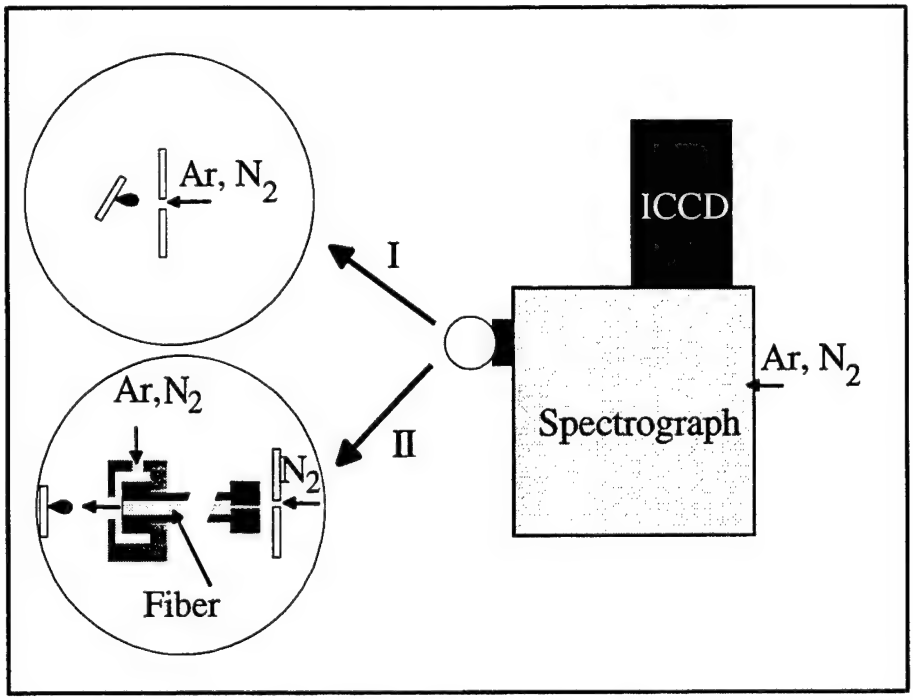

Fig. 1. Schematic diagram of the near VUV setup consisting of an ordinary spectrograph and an ICCD detector. Setup I presents purge system for measurements down to 130 nm and setup II shows purge system for fiber optics measurements.

3. Results

The performance of the setup I of Fig. 1. using ICCD with MgF_2 optics was demonstrated by measuring spectra of chlorine, bromine and iodine. Fig. 2. shows the spectrum of chlorine down to ~130 nm. Emission line intensities have been reported to be enhanced in argon buffer [12]. This is also shown in the near VUV when spectra of chlorine under argon (A) and nitrogen (B) purges are compared (Fig. 2.). A few nitrogen lines were detected in the spectra when nitrogen purge was used. When setup I and ICCD detector with quartz input window was used, emission lines down to 164 nm could be detected, although their intensities were rather low.

Fig. 3. demonstrates the removal of atmospheric absorption when using nitrogen purge and fiber optics detection (setup II of Fig. 1.). Spectrum A was measured from an enriched ore sample with and spectrum B without nitrogen purge. The spectra were normalized to the line at 189 nm in order to allow comparison of the two spectra.

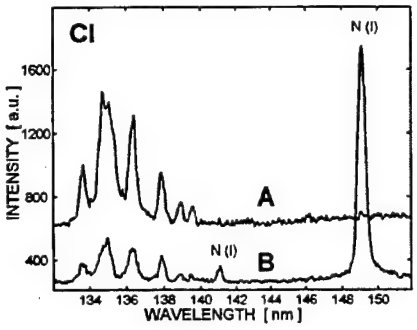

Fig. 2. Influence of the purge gas to the line intensities. The chlorine lines measured in argon (A) and nitrogen (B) purge with single laser pulse.

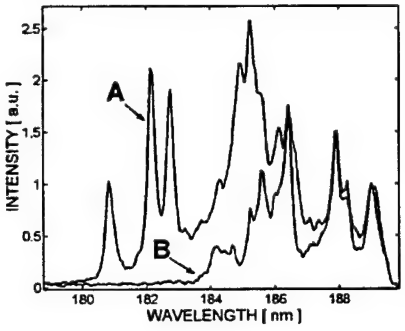

Fig. 3. The influence of atmospheric absorption in the spectrum measured with (A) and without (B) nitrogen purge between the sample and the fiber optics.

4. Conclusions

Neither vacuum ultraviolet spectrographs nor sample chambers filled with gas are necessarily needed for measurements in the near VUV. An ordinary Czerny-Turner spectrograph can be used to detect emission lines down to 130 nm by using argon or nitrogen purge. The samples can be kept in ambient air, when purge gas flows from the spectrograph towards the sample, assuming that the plasma plume is not too far from the slit. It was demonstrated in the VUV that argon purge enhances emission line intensities of the LIPS spectrum. Nitrogen emission lines may be used as an internal standard in the measurements when nitrogen purge is used. Chlorine lines near 130 nm could be detected with ICCD detector equipped with a MgF_2 window. With an ordinary ICCD detector emission lines down to 164 nm could be recorded. Fiber optics allows detection of emission down to 180 nm. If there were fibers for vacuum ultraviolet region, gas purge would enable remote measurements in the near VUV region, as well.

5. References

1. M. Tran, Q. Sun, B. W. Smith, J. D. Winefordner, "Determination of F, Cl and Br in solid organic compounds by laser-induced plasma spectroscopy.", Appl Spectrosc **55,** 739-744 (2001).
2. L. Dudragne, Ph. Adam, J. Amouroux, "Time-resolved laser-induced breakdown spectroscopy: application for qualitative and quantitative detectuin of fluorine, chlorine, sulfur and carbon in air.", Appl Spectrosc **52,** 1321-1327 (1998).
3. D. A. Cremers and L. J. Radziemski, "Detection of chlorine and fluorine in air by laser-induced breakdown spectrometry.", Anal Chem **55,** 1252-1256 (1983).
4. C. Haisch, R. Niessner, O. I. Matveev, U. Panne, N. Omenetto, "Element-specific determination of chlorine in gases by laser-induced breakdown spectroscopy (LIBS).", Fresenius J Anal Chem **356,** 21-26 (1996).
5. M. Hemmerlin, R. Meilland, H. Falk, P. Wintjens, L. Paulard, "Application of vacuum ultraviolet laser-induced breakdown spectrometry for steel analysis -- comparison with spark-optical emission spectrometry figures of merit.", Spectrochim Acta B **56,** 661-669 (2001).
6. R. Noll, H. Bette, A. Brysch, M. Kraushaar, I. Monch, L. Peter, V. Sturm, "Laser-induced breakdown spectrometry -- applications for production control and quality assurance in the steel industry.", Spectrochim Acta B **56,** 637-649 (2001).
7. V. Sturm, L. Peter, R. Noll, "Steel analysis with laser-induced breakdown spectrometry in the vacuum ultraviolet.", Appl Spectrosc **54,** 1275-1278 (2000).
8. A. González, M. Ortiz, J. Campos, "Determination of sulfur content in steel by laser-produced plasma atomic emission spectroscopy.", Appl Spectrosc **49,** 1632-1635 (1995).
9. C. Aragón, J. A. Aquilera, F. Penalba, "Improvements in quantitative analysis of steel composition by laser-induced breakdown spectroscopy at atmospheric pressure using an infrared Nd:YAG laser.", Appl Spectrosc **53,** 1259-1267 (1999).
10. C. J. Lorenzen, C. Carlhoff, U. Hahn, M. Jogwich, "Applications of laser-induced emission spectral analysis for industrial process and quality control.", J Anal Atom Spectrom **7,** 1029-1035 (1992).
11. H. Häkkänen, J. Houni, S. Kaski, J. Korppi-Tommola, "Analysis of paper by laser-induced plasma spectroscopy.", Spectrochim Acta B **56,** 737-742 (2001).
12. W. Sdorra and K. Niemax, "Basic inverstigations for laser microanalysis: III Application of different buffer gases for laser-produced sample plumes.", Mikrochim Acta **107,** 319-327 (1992).

Laser-induced breakdown spectroscopy: analysis of OH spectra

C. G. Parigger
Center for Laser Applications, The University of Tennessee Space Institute, Tullahoma, TN 37388
Phone: 931-393-7338, Fax: 931-454-2271, E-mail: cparigge@utsi.edu
http://www.utsi.edu

G. Guan
Microparticle Photophysics Laboratory (MP ^{3}L), Polytechnic University, Brooklyn, New York 11201
E-mail: guanguoming@yahoo.com
http://www.poly.edu/microparticle

J. O. Hornkohl
Center for Laser Applications, The University of Tennessee Space Institute, Tullahoma, TN 37388
E-mail: jhornkoh@utsi.edu
http://www.utsi.edu

Abstract: Measured laser induced emission spectra of the OH radical subsequent to laser-induced optical breakdown in air are analyzed to infer spectroscopic temperature by use of Monte Carlo simulations.

OCIS codes: (140.3440) Laser-induced breakdown; (350.5400) Plasmas; (280.1740) Combustion diagnostics

1 Introduction

Applications of laser-induced breakdown include laser spark ignition[1]. Typically, it is of interest to investigate the onset of ignition. The presence of specific radicals may be used for determining the occurrence of combustion. Here, laser-induced optical breakdown spectroscopy (LIBS) methods are used in the study of post-breakdown phenomena in air. Following 1064-nm Nd:YAG breakdown, OH radical emissions dominate the recorded spectra in the wavelength range of 305 to 322 nm, some 40 to 300 μs after the laser pulse.

2 Computational Methods

Analysis of superposed spectra is performed by combining the program NEQAIR (Non-Equilibrium Air Radiation) with BESP (Boltzmann Equilibrium Spectrum Program)[2]. Accurate line-strength files from BESP[3] are used to elaborate the measured spectroscopic data including extensive Monte Carlo simulations[4]. For the process of the Monte Carlo simulation, new sets of synthetic data are generated by adding a random number to each measured data point,

$$y_j' = y_j + x * y_{mean} * R(), \tag{1}$$

where y_j is measured data and y_{mean} is the mean value of $\{y_j\}$. $R()$ is a generator function for the random number with a normal probability distribution. x is a constant factor and may be estimated from the differences between the measured and fitted data; x amounts to typically 10 to 15 %. A least-square merit function is used to determine the averages, variances and correlations for (i) temperature, (ii) background, and (iii) line-width.

3 Results

The OH $A^2\Sigma^+ \rightarrow X^2\Pi_i$ transition is investigated experimentally and computationally by using BESP and line-strength files. The temperature range of interest is between 2000 and 6000 K, for spectral resolutions of typically 32 cm^{-1}. Despite such low resolution, highly resolved spectroscopic data are found to be required

in the data analysis. The Monte Carlo simulations are performed in the wavelength range of 305 to 322 nm, with error magnitude $x = 0.2$. Figure 1 shows the obtained results for the spectroscopic temperature versus time delay.

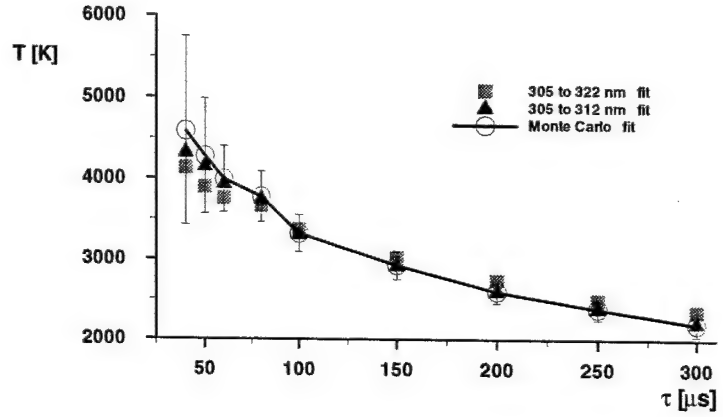

Fig. 1. Spectroscopic temperature and its variance versus time delay from optical breakdown, induced by use of Coherent Infinity 40-100 Nd:YAG 1064-nm radiation of 3.5 ns pulse width, focused to typical peak intensity in air of 10^{13} W/cm^2, at a frequency of 10 or 100 Hz. The squares and triangles show the result of the spectroscopic fits with BESP, the circles show the results from the Monte Carlo simulation.

The primary errors are due to background emissions, shot-to-shot variations and unknown line profiles. According to NEQAIR results, the background emissions are negligible for temperatures below 3500 K, and the shot-to-shot variations of the radiating plasma are the dominant contributions to the errors in the measured spectral intensity.

4 Conclusions

Applications of the NEQAIR program and the BESP allowed us to perform a detailed analysis of OH spectra following laser-induced optical breakdown. The measured background emissions show a strong correlation with temperature while the line profile is weakly correlated with temperature. The variance of the spectroscopic temperature is proportional to the magnitude of the variation of the data. Monte Carlo simulations appear to be important for LIBS, and analysis of spectra should be alleviated by use of clustered computers[5].

5 Acknowledgments

The authors thank Drs. Y.-L. Chen, I.G. Dors, J. Drakes, D.R. Keefer, J.W.L. Lewis, W. Qin, and D.H. Plemmons, for their interest and contributions to this work. This work is in part supported by the National Science Foundation under Grant No. CTS-9512489, in part by a grant of High Performance Computer (HPC) time from the Department of Defense HPC Center, AEDC at Arnold AFB, on the Origin 2000 computer, in part by UTSI and UTSI's Center for Laser Applications, and a UTSI graduate research assistantship.

References

1. I. G. Dors, "Laser Spark Ignition Modeling," Ph.D. dissertation, The University of Tennessee, 2000, http://etd.utk.edu:90/2000/DorsIvan.pdf, and see references therein.
2. J.W.L. Lewis, C.G. Parigger, J.O. Hornkohl, and G. Guan, "Laser-induced Optical Breakdown Plasma Spectra and Analysis by use of the Program NEQAIR," in *AIAA Proceedings of the 37th Aerospace Sciences Meeting & Exhibit*, (AIAA, Reno, 1999) paper AIAA-99-0723, and see references therein.
3. J.O. Hornkohl, "BESP," private communications, 2002, http://view.utsi.edu/besp.
4. G. Guan, "On the Analysis of Emission Spectra and Interference Images," Ph.D. dissertation, The University of Tennessee, 1998.
5. C.G. Parigger, "Grid Clusters," private communications, 2001, http://tell11.utsi.edu.

Laser-induced breakdown spectroscopy: molecular spectra with BESP and NEQAIR

C. G. Parigger
Center for Laser Applications, The University of Tennessee Space Institute, Tullahoma, TN 37388
Phone: 931-393-7338, Fax: 931-454-2271, E-mail: cparigge@utsi.edu
http://www.utsi.edu

J. O. Hornkohl
Center for Laser Applications, The University of Tennessee Space Institute, Tullahoma, TN 37388
E-mail: jhornkoh@utsi.edu
http://www.utsi.edu

Anna M. Keszler
Chemical Research Center, H-1025 Budapest, Hungary
E-mail: akeszler@chemres.hu
http://www.chemres.hu

László Nemes
Chemical Research Center, H-1025 Budapest, Hungary
E-mail: nemesl@chemres.hu
http://www.chemres.hu

Abstract: Diatomic molecular spectra are modeled and compared with measured spectra to infer temperature and species density by use of the programs BESP (Boltzmann Equilibrium Spectrum Program) and NEQAIR (Non Equilibrium Air Radiation).

OCIS codes: (140.3440) Laser-induced breakdown; (350.5400) Plasmas; (300.6390) Molecular Spectroscopy

1 Introduction

Highly excited molecular recombination spectra are typically observed subsequent to laser-induced optical breakdown of gases. Specifically, optical breakdown plasma generated by nominal nanosecond-pulsed, focused in laboratory air, Nd:YAG infrared laser radiation of 1 to 100 TW/cm^2 intensity shows well-demarcated progressions and sequences of molecular emission spectra. Such spectra can be readily recorded using time-resolved laser spectroscopy methods some 10 to 100 μs after the laser spark, showing spectroscopic temperatures of typically 6000 Kelvin. Several orders of magnitude less-intense Nd:YAG radiation of some 0.1 to 1 GW/cm^2, when focused on a solid target, also generates highly excited molecular spectra in the plasma plume emanating from the target. Analysis of superposed spectra by use of programs such as NEQAIR allows us to infer temperature and species density[1]. Detailed spectroscopic analysis, however, of selected diatomic molecules is accomplished with the program BESP[2] that utilizes accurate line-strength files.

2 Computation of Diatomic Spectra with BESP

The theoretical model and simulation used is based on computing the polarization- and angle-averaged, spontaneous-emission intensity of a specific, isolated molecular transition[3]. The BESP program makes use of so-called line-strength files for a molecular transitions of interest. For isolated molecular transitions, the Franck-Condon factors are found by numerically solving the radial Schrödinger equation, and the Hönl-London factors are obtained by numerical diagonalization of the rotational and fine-structure Hamiltonian. For high temperature and high density breakdown spectra, and for typical gate-width times and gate-delays used in time-resolved measurements of recombination spectra, thermal equilibrium of vibrational and rotational modes is assumed. For the computation of a diatomic spectrum, typically the temperature and spectral resolution is specified, and in turn, non-linear fitting routines may be used to infer the spectroscopic temperature.

3 Swan Spectrum

The C_2 Swan band emissions ($d\,^3\Pi \leftrightarrow a\,^3\Pi$) have been measured in spectroscopic investigations of laser-induced optical breakdown in gases[4]. The interest of the Swan band system however is extended to both pure and applied diatomic spectroscopy. Figure 1 shows Swan spectra that were recorded during nano-particle generation using LIBS.

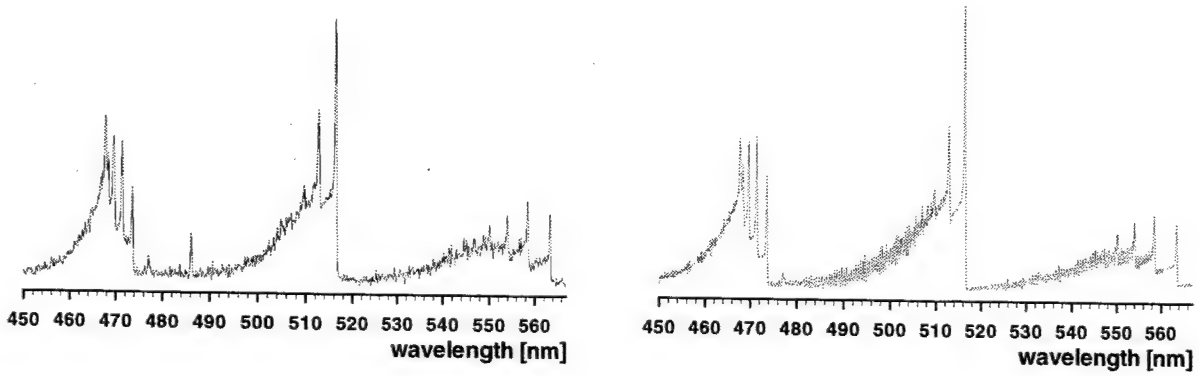

Fig. 1. Recorded (left) and fitted (right) LIBS spectra of the C_2 Swan band $\Delta\nu = +1, 0, -1$ progression, showing a spectroscopic resolution (FWHM) of 0.27 nm for the synthetic spectrum. The spectroscopic temperature of T=6400 K was inferred with BESP.

Here, the Quantel Brilliant 10 Hz pulsed, Q-switched Nd:YAG laser radiation was focused onto a graphite rod to intensity levels of some 0.1 to 1 GW/cm^2. The illustrated Swan spectrum was recorded by use of the Ophir Optronics Wavestar U spectrometer and Ophir Optronics Wavestar software. A relatively long exposure time of several seconds was selected to collect average spectra from the plasma plume emanating from the graphite target. Particularly strong C_2 Swan bands were observed when CO_2 was used as as ambient gas. The inferred C_2 Swan band temperature was between 3500 and 9000 K for various experimental conditions.

4 Conclusions

Synthetic NEQAIR96 spectra are particularly useful for initial analyses of molecular spectra that are recorded subsequent to laser-induced optical breakdown. Detailed analysis of selected diatomic spectra, such as the Swan spectra, is best accomplished by using line-strength files and the program BESP.

5 Acknowledgments

The authors thank Drs. I.G. Dors, G. Guan, J.W.L. Lewis and D.H. Plemmons for their interest and contributions to this work. This work is in part supported by UTSI's Center for Laser Applications and by the Hungarian OTKA Foundation under contract number T032549.

References

1. J.W.L. Lewis, C.G. Parigger, J.O. Hornkohl, and G. Guan, "Laser-induced Optical Breakdown Plasma Spectra and Analysis by use of the Program NEQAIR," in *AIAA Proceedings of the 37th Aerospace Sciences Meeting & Exhibit*, (AIAA, Reno, 1999) paper AIAA-99-0723, and see references therein.
2. J.O. Hornkohl, "BESP," private communications, 2002, http://view.utsi.edu/besp.
3. J.O. Hornkohl, C. Parigger and J.W.L. Lewis, "Temperature Measurements from CN Spectra in a Laser-Induced Plasma," J. Quant. Spectrosc. Radiat. Transfer, **46** 405 (1991).
4. C. Parigger and D. H. Plemmons and J. O. Hornkohl and J. W. L. Lewis, "Spectroscopic temperature measurements in a decaying laser-induced plasma using the C_2 Swan system," J. Quant. Spectrosc. Radiat. Transfer, **52** 707 (1994).

Laser-Induced Breakdown Spectroscopy used to Detect Palladium metal Dispersed in Cellulose Membranes

Madhavi Martin
Environmental Sciences Division, Oak Ridge National Laboratory, Oak Ridge TN, 37831-6038
(865)-574-7828, (865)-576-8646, martinm1@ornl.gov

Barbara Evans, Hugh O'Neill, and Jonathan Woodward
Chemical Sciences Division, Oak Ridge National Laboratory, Oak Ridge TN, 37831-6194
(865)-241-3185, (865)-574-1275, evansb@ornl.gov

Abstract: Metals dispersed in membranes have been used as active electrodes in fuel cell technology. Laser-induced breakdown spectroscopy (LIBS) was used to detect palladium in cellulose membranes. Different concentrations of palladium solution were used in the uptake of palladium into cellulose films. We have correlated the palladium concentration in various cellulose membranes to the standard laboratory technique of atomic absorption spectroscopy (AAS).

OCIS codes: (140.3440) Lasers and laser optics

Introduction

The cellulose synthesized by bacteria of the genus *Gluconoacetobacter* is a gel-like skin or pellicule formed at the surface of the culture medium. Although chemically identical to plant cellulose, being composed of β–1,4-linked glucose chains, bacterial cellulose differs in its high hydration, up to two hundred fold its weight of water, and its netlike microstructure. The special properties of this cellulose enable it to catalyze deposition of palladium nanoparticles from solution inside the hydrated cellulose matrix (Evans et al., submitted). Such palladium-treated cellulose can be easily dried to thin membranes for application in membrane electrode assemblies and other electronic devices (Evans et al., patent pending).

The ability of LIBS to provide rapid multielemental microanalysis of bulk samples (solid, liquid, gas, aerosol) in the parts-per-million (ppm) range with little or no sample preparation has been widely demonstrated (Martin et. al.,). LIBS induces the vaporization of a small volume of sample material with sufficient energy for optical excitation of the elemental species in the resultant sample plume. The vaporized species then undergo de-excitation and optical emission on a microsecond time scale, and time-dependent ultraviolet-visible spectroscopy fingerprints the elements associated with the spectral peaks. LIBS is typically a surface analytical technique, with each laser pulse vaporizing microgram or submicrogram sample masses. However, the rapidity of sampling (typically 10 Hz laser repetition rate) and ability to scan a sample surface, ablate a hole into a solid sample with repeated laser pulses, for depth profiling or focus the laser spark below the surface of a liquid sample permits more versatile analyses and provides sufficient statistics for bulk sampling. Although calibration standards are required for quantitative analysis, the generation of a single calibration curve will suffice for analysis of samples in a similar matrix. We have previously demonstrated the technique of LIBS for sample vaporization and optical emission in the detection of RCRA metals (e.g., Hg, Cr, Pb, V, Ni, and Cu) present in aerosols for use in continuous emission monitoring from smoke stacks (Martin and Cheng).

Preparation of the metal doped cellulose membranes

The cellulose-producing bacterium *Gluconoacetobacter hansenii* (ATCC 10821, formerly classified as a strain of *Acetobacter xylinus*) was cultivated in rich medium for 7 to 10 days (Schramm and Hestrin, 1954). The gel-like cellulose pellicules that were produced were harvested and cleaned by soaking in boiling distilled water for 2 h, followed by 18 h in 1% sodium hydroxide. The hydroxide was neutralized with acetic acid. The cellulose samples were soaked in several changes of distilled water to removed salts from the neutralization, then stored in 20% ethanol. Palladium was deposited by incubation of purified cellulose with 0-10 mM ammonium hexachloropalladate solution in water for 2 h at 90°C. Black particles of palladium formed throughout the cellulose matrix. The samples were soaked in several changes of distilled water to remove residual hexachloropalladate. Dried samples of

palladium-treated and control cellulose were prepared by drying the cellulose pellicules to a thin membranes on a laboratory gel drier with application of vacuum.

Experimental setup

The experimental setup employs a Spectra Physics™ laser, model INDI-HG. This is a Q-switched Nd: YAG laser that has output wavelengths at the fundamental wavelength of 1064-nm, frequency doubled to 532-nm, and frequency quadrupled to 266-nm. For these experiments, we used the 266-nm laser wavelength with 20 mJ/pulse as the excitation energy. The laser pulsewidth is 6-8 ns and the repetition rate is 10 Hz. All the processes such as plasma formation, emission, gated detection, data collection, and analysis are completed within 100 milliseconds until the next pulse arrives in the sample volume. The light emitted by the resulting plasma is collected by an optical collection system situated at ~ 45° angle to the axis of the sample and the laser excitation beam and is delivered to an Acton Research Inc. spectrometer (SpectraPro-500) via a carbon-core fiber-optic cable bundle. The resolved spectrum is detected by an intensified charge coupled device (ICCD) built by Andor Technology with the ICCD delayed and gated by a Stanford Research Systems model SRS535 delay generator.

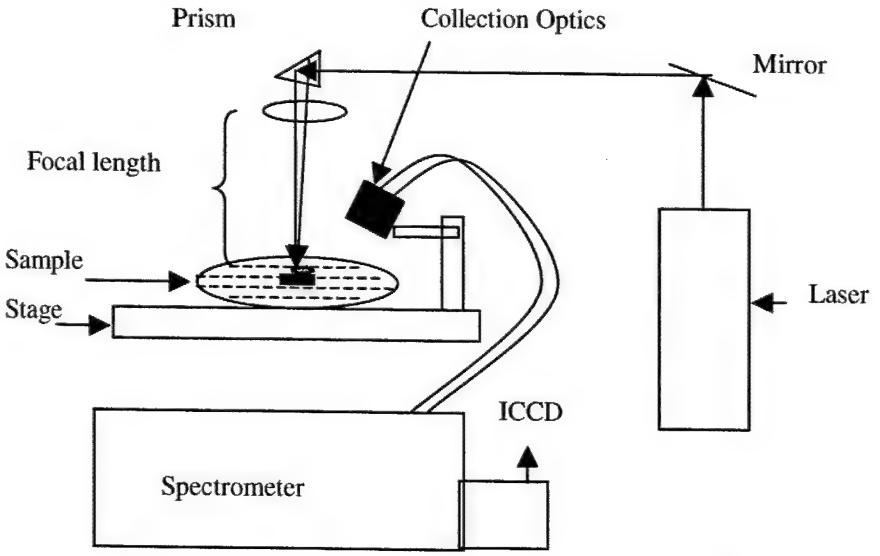

Figure 1. Schematic of the LIBS Experimental Setup

The typical spectrum for metallic palladium deposited on a cellulose membrane starting with a 10 mM solution of $[(NH_4)_2PdCl_6]$ is shown in figure 2. This shows that we can combine chemical analysis and imaging of the

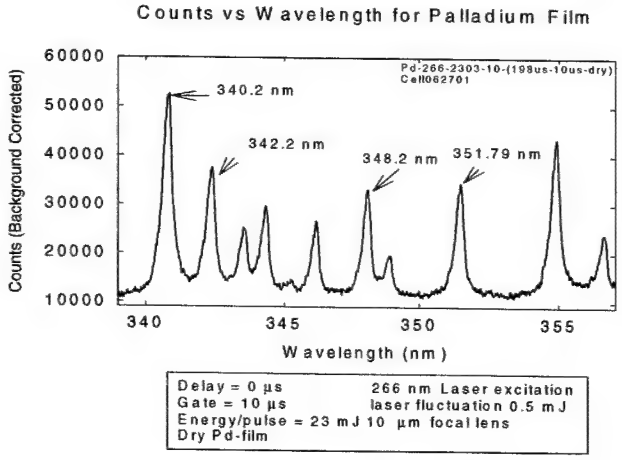

Figure 2. LIBS spectra obtained from Pd metal incorporated in a cellulose film.

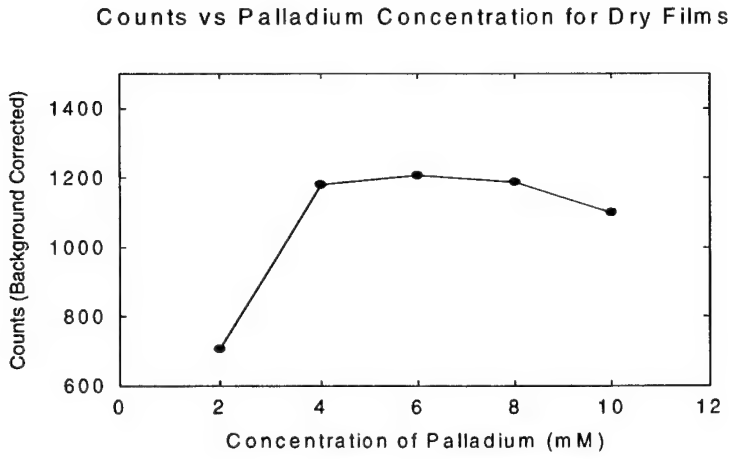

Figure 3. Calibration of the LIBS signal to the concentration of Pd

membranes to obtain complete information of the sample under test. Numerous cellulose membranes with varying concentrations of palladium were used to construct the calibration curve shown in figure 3. The concentrations of Pd in the cellulose membranes tested with the LIBS method were 2, 4, 6, 8 and 10 mM. There seems to be a decrease in the deposition of palladium metal by the bacteria when the concentration of $[(NH_4)_2PdCl_6]$ solution goes above 8 mM. It has been correlated to the calibration curve obtained for the same samples that were used to obtain the calibration curve using a well-established laboratory technique of atomic absorption spectroscopy (AAS).

Conclusions

We have demonstrated successfully that LIBS can be a viable technique in the determination of total Pd concentrations present in specially synthesized cellulose membranes. We have also tested this technique for the detection of silver metal-doped cellulose membranes. We have compared this to a standard technique of atomic absorption spectroscopy.

References

Martin, M. Z., M. D. Cheng, and R. C. Martin, "Aerosol Measurement by Laser-Induced Plasma Technique: A Review," *Aerosol Sci. and Technol.*, **31**(6) (1999) 409-421.

Martin, M. Z., and M. D. Cheng (2000), "Detection of Chromium Aerosol Using Time-Resolved Laser-Induced Plasma Spectroscopy," *Appl. Spectrosc.*, **54**, 1279.

Hestrin, S., Schramm, M. (1954) "Synthesis of cellulose by *Acetobacter xylinum* : Preparation of freeze-dried cells capable of polymerizing glucose to cellulose", *Biochem. J.* **58:** 345-352.

Evans, B. R., O'Neill, H. M., Malyvanh, V. P., Lee, I., Woodward, J. "Palladium-bacterial cellulose membranes for fuel cells", *Biosensors and Bioelectronics* (submitted).

Evans, B. R., O'Neill, H. M., Malyvanh, V. P., Woodward, J., "Metallization of Bacterial Cellulose for Electrical and Electronic Device Manufacture", ID 0869, (Patent Pending).

Supersensitive Detection of Na in Water Using Dual-Pulse Laser-Induced Breakdown Spectroscopy

Akira Kuwako, Yutaka Uchida and Katsuji Maeda
Toshiba Corporation, 8, Shinsugita-cho, Isogo-ku Yokohama 235-8523, Kanagawa, Japan
akira.kuwako@toshiba.co.jp

Abstract: Laser-induced breakdown spectroscopy has been applied to detect Na in water. Laser-induced breakdown was formed by dual-pulse and crossed beam Nd:YAG lasers on a water film. To improve the detection sensitivity, fluorescence intensity dependence on timing between laser pulses, delay time of fluorescence detection timing, gate width of fluorescence detection period, and laser energy were investigated. Under the optimized conditions, the detection limit of Na in water was achieved in the range of 0.1ppb. The developed system is applicable for quick and supersensitive detection of Na atoms in water.

OCIS codes: (140.0140) Lasers and optics, (140.3440) Laser-induced breakdown, (300.0300) Spectroscopy, (300.6500) Spectroscopy, time-resolved

1. Introduction

Laser-induced breakdown spectroscopy (LIBS) has been investigated extensively with a view to establishing it as a practical method for chemical analysis for specimens in various states, namely gas, liquid, and solid[1-2]. However, the technique has been developed mainly for solid samples and much less attention has been paid to liquid samples. In many industrial fields, real-time and in-situ analysis of water contamination is desirable, but conventional chemical analysis methods are impracticable. For power plants, the highly sensitive detection of Na in circulating condensed water is important to detect the leakage of seawater. Using the conventional LIBS technique, the detection limit of Na in water has been reported to be 80ppb[3], a value larger than the leak detection criterion (0.1ppb). In order to enhance the fluorescence intensity, dual-pulse LIBS has been applied and the effectiveness has been reported[4]. Additionally, the authors have applied a technique in which LIBS is combined with laser-induced fluorescence spectroscopy (LIFS) for Fe detection[5-6] and the detection limit of 0.5ppb was achieved. In the system, laser-induced breakdown was formed by dual-pulsed beams which were crossed on a water film. In the work reported in this paper, taking into account the above-mentioned features of laser analysis, a method combining dual-pulse and crossed beam LIBS (DPX-LIBS) was applied for the analysis of NaCl solution. The optimized conditions of DPX-LIBS for detection of Na in water were investigated and the detection limit was evaluated.

2. Experimental

The DPX-LIBS system is shown schematically in Fig.1. Two Q-switched Nd:YAG lasers (Surelite SLI-10, Hoya-Continuum) were controlled independently by delay generators (Stanford Instruments Model DG535) and operated under the following conditions: fundamental wavelength (1064nm) @10Hz, 3.5ns pulse width (FWHM), 100-200mJ/pulse. Each laser beam, divided into two beams and composed into dual and coaxial beam by a half mirror, was focused by a quartz lens (f=100mm) on the surface of the water film in a test cell at 45 degrees. The energy of individual laser pulse was almost a quarter of total laser energy. The irradiation cell has a circulation loop of sample solution, prepared by diluting a standard solution of NaCl for chemical analysis, and a water film was formed by a spray nozzle. The water film was adjusted to the position at which the intensity of emission of Na:589nm line showed the maximum value. The cell has 7 quartz windows (D=50mm) for laser irradiation and/or fluorescence detection and the body was made of PTFE block to ensure no solution remained. The fluorescence from breakdown plasma was collected and focused on the incident surface of an optical fiber by a lens (f=100mm, D=100mm) and led to a spectrometer (HR320, Jovin Yvon). The spectrometer has effective aperture: F/4.2, a 1200 g/mm holographic grating blazed at 500nm, and ICCD (DH501-18F-01, Andor) or photomultiplier (R928 Hamamatsu) for detector. The photomultiplier signals were accumulated by digital oscilloscope (Tektronix TDS684A, 1GHz,5GS/s). All fluorescence data obtained by ICCD or photomultiplier were collected for ten seconds and evaluated by averaging and subtracting background.

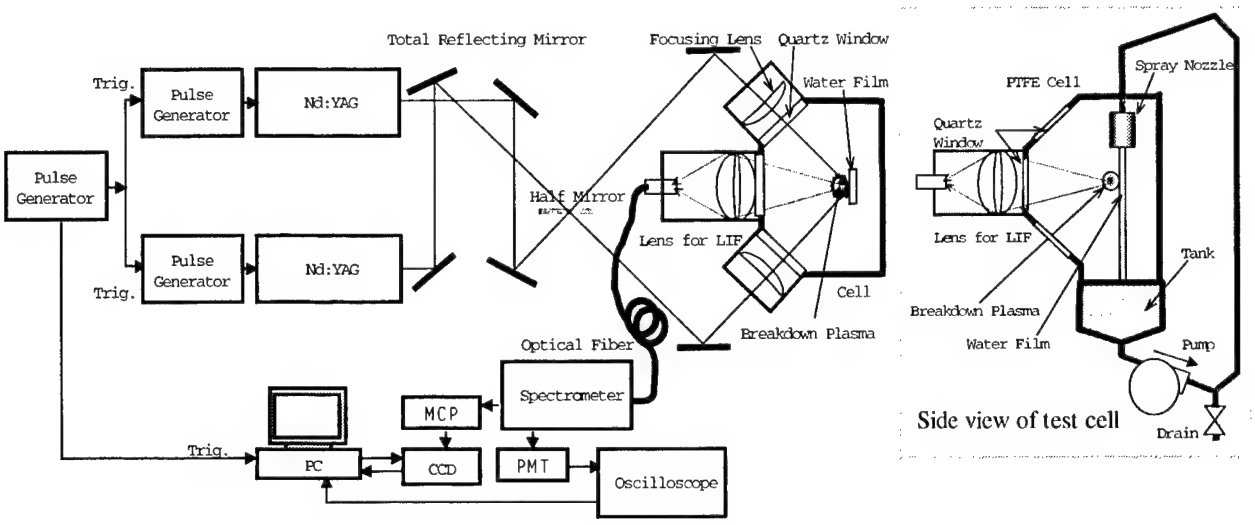

Fig.1 The experimental setup.

3. Results and discussion

In order to improve the detection efficiency, it is important to optimize the following conditions.

T1: Timing between laser pulses
T2: Delay time of fluorescence detection timing
T3: Gate width of fluorescence detection period
P : Total laser energy

In order to investigate the temporal characteristics of breakdown plasma by DPX-LIBS, the T1 and T2 dependence on the intensity of Na:589nm emission line was observed. Figure 2 shows the T2 dependence of fluorescence intensities and S/N values observed under several T1 conditions at total laser energy of 201mJ. Signal to noise value (S/N) is defined by the ratio of peak intensity to fluctuation level of background. From these results, the maximum fluorescence intensity was nearly obtained under T1=8μs and T2=8μs conditions. Furthermore, under high laser energy conditions at 287mJ and 372mJ, similar behavior of fluorescence intensity was observed.

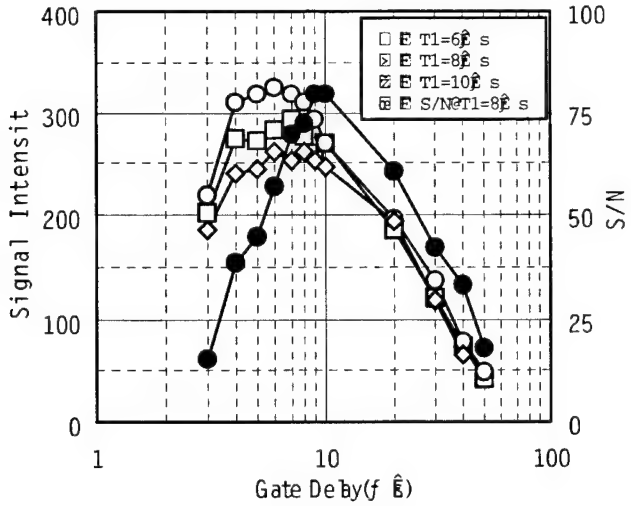

Fig.2 Dependence of delay time (T2) of fluorescence detection timing under various timing between laser pulses using 100ppb Na solution sample.

At the same time, the temporal changes of fluorescence were measured by photomultiplier at 589nm and larger intensity of fluorescence and much longer fluorescence lifetime were observed in the DPX-LIBS case than those in the case of single laser irradiation. We suppose that these phenomena are caused by the enhancement of Na atom re-excitation during the collision between the two expanding plasmas. From the decay behavior of the fluorescence, the gate width of the fluorescence detection period (T3) was selected as 100μs for high S/N condition. As to the laser energy dependence on the fluorescence intensity, at the higher laser energy irradiation, the larger fluorescence intensity was observed, but S/N showed saturation. Therefore, for sensitive detection of Na, we supposed the total laser energy should be less than 400mJ. Under the optimized conditions obtained in this work, the fluorescence intensity of Na:589nm emission line was measured for several Na concentration samples. Figure 3 shows the concentration dependency of fluorescence intensity and a typical spectrum of Na:589nm emission line obtained by 1ppb solution. From these results, linear correlation between concentration and fluorescence intensity was obtained and the detection limit of Na in water is estimated to be in the range of 0.1ppb in our system.

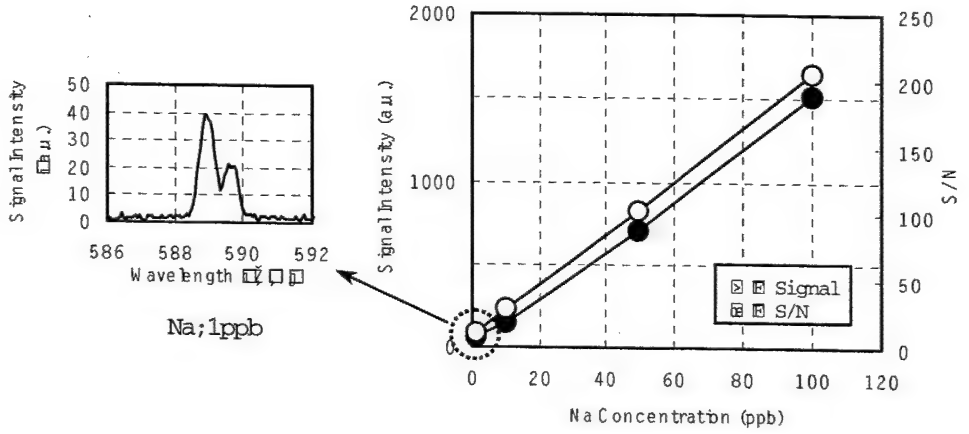

Fig.3 Intensity of Na:589nm emission line by ICCD vs. Na concentration in water sample under irradiation at 372mJ.

4. Conclusions

Dual-pulse and crossed beam LIBS (DPX-LIBS) has been applied to detect Na atoms in water. To improve the detection sensitivity, fluorescence intensity dependence on timing between laser pulses, delay time of fluorescence detection timing, gate width of fluorescence detection period, and laser energy were investigated and optimized. Under the optimized conditions, the detection limit of Na in water was achieved in the range of 0.1ppb in our system. Furthermore, in order to obtain higher detection efficiency at lower laser energy, optimization of power ratio for individual pulse will be evaluated. In either case, the developed system is applicable for quick and supersensitive detection of Na atoms in water.

5. References

1.L.J.Radziemski,R.W.Solarz and J.A.Paisner,Eds. "Laser Spectroscopy and Its Application", (Dekker,New York,1987)
2. D.A.Cremers, "The Analysis of Metals at a Distance Using Laser-Induced Breakdown Spectroscopy", Appl. Spectrosco.Vol.41,No.4,572-578(1987)
3.O.Samek,et al, "Application of laser-induced breakdown spectroscopy to *in situ* analysis of liquid samples", Opt.Eng.Vol.39,No.8,2248-2262(2000)
4.D.N.Stratis,et al., "Effect of Pulse Delay Time on a Pre-ablation Dual-Pulse LIBS Plasma", Appl.Spectrosco.Vol.55,No.10,1297-1303(2001)
5.M.Nakane,et al., " Analysis of Trace Metal Elements in Water Using Laser-Induced Fluorescence for Laser-Breakdown Plasma ", Proc.SPIE,Vol.3935,127-131(2000)
6.K.,Arakawa,et al., "Trace Element Analysis by LIB & LIF Spectroscopy(2)", Proc. of Fall Meeting of Atomic Energy Society of Japan,Vol.I,98(2000)

Laser-induced breakdown spectroscopy: Balmer series H-beta measurements

C. G. Parigger

Center for Laser Applications, The University of Tennessee Space Institute, Tullahoma, TN 37388

Phone: 931-393-7338, Fax: 931-454-2271, E-mail: cparigge@utsi.edu

http://www.utsi.edu

D. H. Plemmons

Current address: Plemmons Consulting, 404 Crest Drive, Lynchburg, TN 37352

E-mail: dhplemmons@aol.com

Abstract: Balmer series H_β emission profiles are measured in a pulsed laser-induced breakdown micro-plasma. The line widths are used to infer electron number densities during the plasma decay.

OCIS codes: (140.3440) Laser-induced breakdown; (350.5400) Plasmas; (020.3690) Line Shapes and Shifts; (300.6210) Atomic Spectroscopy

1 Introduction

In dense plasmas with traces of hydrogen, electron number densities can be determined from measured full-widths at half maximum of the the Balmer series. Electron temperatures can be inferred from Balmer series Boltzmann pots. Time-resolved laser spectroscopy techniques are used to characterize the temporal evolution of the electron number density and temperature of a micro-plasma generated in pure hydrogen gas[1]. Previously, we reported the temporal evolution of the hydrogen micro-plasma, generated with Continuum YG680S Nd:YAG 1064-nm, 7.5-ns pulse width, laser radiation focused into H_2 gas[2, 3]. Electron number densities in the range 10^{16} to $10^{19}/\text{cm}^3$ were found in the analysis of the Stark broadened hydrogen-alpha line profiles, with a corresponding electron temperature range of 7,000 to 100,000 K. Here, we discuss the results of electron number density measurements from the Balmer series hydrogen-beta line profiles.

2 Experimental Method

Measurement of the H_β line profile poses several additional challenges and limitations compared to H_α line profile measurements. First, for otherwise identical plasma conditions, the H_β line width is approximately a factor of five wider than the H_α line. Second, the spectral proximity of other Balmer series lines such as H_γ and H_δ inhibits the use of H_β profiles early in the plasma decay. Third, measured intensity asymmetries in the peaks and spectral profiles lessen the application of H_β profiles in micro-plasma characterization early in the plasma decay. And fourth, for the H_β FWHM to be useful as a density diagnostic the electron number density should be approximately less than $5 \times 10^{17}/\text{cm}^3$.

The experimental arrangement for detailed hydrogen-beta line profile investigations is largely identical to the one used for the time-resolved hydrogen-alpha measurement[2]. The H_β profiles were recorded by use of an intensified EG&G linear diode array detector and a Jarrell Ash 1/4 m crossed Czerny Turner spectrometer. The usual sensitivity correction, wavelength calibration, and slit deconvolutions were applied in the analysis aided by the EG&G optical multi-channel analyzer (OMA) and a personal computer.

3 Results

The inferred electron number densities from H_β line profiles agree with the values found from H_α line profiles early in the plasma decay, i.e., for time delays between 0.2 and 0.5 μs from laser-induced optical breakdown. The electron number density of 1.8×10^{17} is found for a time delay of 0.5 μs, subsequently the obtained results differ for H_α and H_β profiles. The ratio of the electron number density discrepancy, $(n_e)_{H_\alpha} / (n_e)_{H_\beta}$, amounts to 1.2, 2.0, and 5.4, for time delays of 0.75 μs, 1.5 μs, and 2.5 μs, respectively. Figure 1 shows the results for the electron number density versus time delay from the laser pulse.

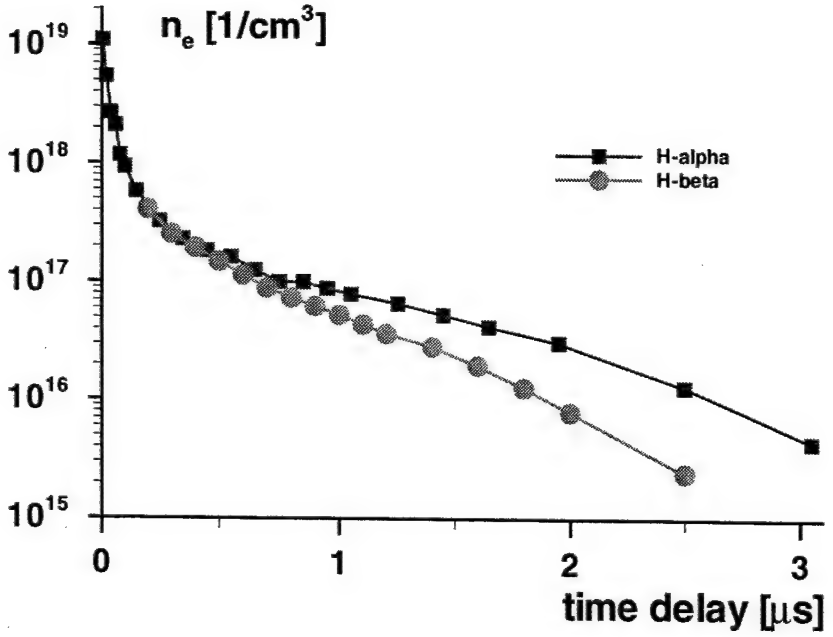

Fig. 1. Comparison of electron number densities obtained from H_α (squares) and H_β (circles) line profiles, following laser-induced optical breakdown in a cell containing H_2 gas at a pressure of 810 Torr. The Nd:YAG laser radiation was focused to typically 1400 GW/cm^2, or more than ten times larger than the nanosecond breakdown threshold of hydrogen gas for 1064-nm radiation.

The theoretical results[4] indicate that one can expect an electron density accuracy of at best 5% for H_β and 20% for H_α. Therefore, the above ratios of the electron number densities show that the results differ significantly. The magnitudes of the disparities at later times, and increasing with time, suggest the occurrence of spatially inhomogeneous micro-plasma.

4 Conclusions

A comparison of electron number density results using H_α and H_β line widths shows that the results are consistent at earlier time delays from the laser pulse, but differ at later time delays. Further two-dimensional, time-resolved experiments are recommended to address the differences in the inferred number densities from the Balmer Series H_β line profiles. In addition, a more sophisticated modeling is indicated to account for line profile asymmetries at high electron number densities.

5 Acknowledgments

The authors thank Dr. J.W.L. Lewis, Mr.'s N.W.Wright, F. Schwartz, and J.O. Hornkohl for their interest and contributions to this work. This work is in part supported by UTSI and UTSI's Center for Laser Applications, and a UTSI graduate research assistantship.

References

1. D.H. Plemmons, "Electron Density and Temperature Determination of a Laser-Induced Plasma in Hydrogen Gas," M.S. thesis, The University of Tennessee, 1994, and see references therein.
2. C. Parigger, J.W.L. Lewis, and D.H. Plemmons, "Electron Number Density and Temperature Measurement in a Laser-Induced Hydrogen Plasma," J. Quant. Spectrosc. Radiat. Transfer, **53**, 249 (1995).
3. C. Parigger, D.H. Plemmons, and J.W.L. Lewis, "Spatially and Temporally Resolved Elecron Number Density Measurements in a Decaying Laser-Induced Hydrogen Plasma Using Hydrogen-alpha Line Profiles," Appl. Opt. **34**, 3325 (1995).
4. H.R. Griem, *Spectral Line Broadening by Plasmas* (Academic Press, Inc., New York and London, 1974).

Quantum Degeneracy and Line Emission in LIBS Plasmas

V. G. Molinari, D. Mostacci, F. Rocchi, M. Sumini
INFM-BO and Laboratorio di Montecuccolino, DIENCA,Bologna University, Italy
via dei Colli 16, 40136 Bologna (BO), Italy
tel. +39-051-6441711, fax +39-051-6441747
domiziano.mostacci@mail.ing.unibo.it

Abstract: The effect of quantum degeneracy on collisional excitation is investigated, and its effect on line emission evaluated for application to quantitative spectroscopy in LIBS. Response matrix techniques are used to evaluate sensitivity to quantum degeneracy.

Summary.

In calculating averaged plasma parameters a maxwellian distribution for electrons or ions is generally assumed: when degeneracy is accounted for, however, signficant changes may be introduced in those averages.

In a previous work [1] the authors derived a correction to the electron distribution function accounting for quantum degeneracy in the interaction of an electromagnetic wave with a plasma. With this distribution function the dispersion relations valid for the transversal component of the electric field wave were obtained, these showing the importance of degeneracy effects. Since in the early stages of the time evolution of a LIBS plasma the electron component is in a weakly degenerate state the above mentioned correction can play a significant role in the description of the plasma at the beginning of its formation. The correction to the distribution function was at first order in the Sommerfeld parameter ρ which gives information about the degeneracy degree of the plasma.

In this work an analogous first order in ρ corrected distribution function is used to calculate collisional excitation rates to be used in predicting line emission from LIBS plasmas. Using response matrix techniques the influence of degeneracy on line emission and hence on spectroscopic quantitative evaluations is investigated.

[1] F. Rocchi, V. G. Molinari, D. Mostacci, M. Sumini, Dispersion Relations in weakly degenerate plasmas, Spectrochimica Acta Part **B** 56 (2001), 599-608.

Combination of nanosecond and femtosecond pulses in dual-pulse LIBS of solids and aqueous solutions

Jonathan Scaffidi, Jack Pender, Univ. of South Carolina, USA; Bill Colston, Lawrence Livermore Natl. Lab., USA; S.R. Goode, S.M. Angel, Univ. of South Carolina, USA.

Abstract: Signal enhncement, limits of detection, and relevance to environmental concentrations for metals and metal ions in aqueous solution using combined 1064 nm nanosecond and 800 nm femtosecond pulses in dual-pulse LIBS will be presented.

SPATIO-TEMPORAL STUDY OF LASER INDUCED PLASMA ON WATER SURFACE OF IONIC SOLUTIONS

J. Ben Ahmed[1], Z. Ben Lakhdar[2], G. Taieb[1]

[1]Laboratoire de Photophysique Moleculaire du CNRS, Universite de Paris XI, Orsay, France.
[2] Laboratoire de Spectroscopie Atomique, Moleculaire et Applications, Universite El Manar, Tunis,
* *Corresponding author. E-mail : guy.taieb@ppm.u-psud.fr*

ABSTRACT

Results of a spatio-temporal study of laser induced plasma on the surface of water solutions of Ca^{++} and Mg^{++} are given. An initial electronic temperature T_e of 28000K is observed at t= 500 ns in the plasma center where the electronic density is equal to 1.25 10^{18} cm^{-3}.

SUMMARY

Spectroscopic study of laser induced plasma have been carried out by recording the intensity evolution of some line emission of *CaII, CaI, MgII, MgI* and H_α with time and with axial distance from the plasma center. The plasma was produced directly on surface of water solutions of Ca^{++}, and Mg^{++} by focusing the pulses of the second harmonic of a Nd-YAG laser (10 ns duration, 70 mj energy and 2 Hz repetition rate). The plasma was imaged on the entrance slit (100µm) of the monochromator by a lens, the spatial resolution obtained by an horizontal displacement of this lens, and temporal behavior of the emission with 10 ns resolution measured by a digital oscilloscope and processed by computer using Labview language.

1. Electronic temperature

The plasma temperature T_e is determined by measuring the relative population of *CaII* states and by using a Saha-Boltzmann analysis [1]. The establishment of the local thermodynamic equilibrium in the plasma is assumed, the validity of this assumption being supported by verifying the criteria proposed by Griem [2]. In the plasma center, the value of T_e is 28000K at t=500ns, and decreases to 21000K at t=4000ns (Figure 1). The figures 2a-2d show the spatial evolution of the temperature from the plasma center at different delay from the end of the laser pulse : the temperature maximum is observed in center, and decreases in the plasma edge.

2. Electronic density

The electronic density N_e is an important parameter used to describe the plasma environment, and it is crucial for the establishing of the thermodynamic equilibrium. N_e is usually measured from the Stark broadening of emission lines [3-5]. In this work, the electronic density is deduced from Stark broadening of some atomic lines (H_α and *CaI*) : we have compared the experimental width with the theoretical data for the same T_e determined as mentioned above: an initial electronic density of 1.25 10^{18} cm^{-3} is observed in the whole plasma at t=500 ns after the laser impulsion, and decreases with time following an exponential decay with a decay constant τ= (1200±50) ns (Figure 3) ,this value is bigger then

that observed in the case of plasma induced in bulk [6] . The spatial variation of the electronic density is not significant within the experimental error.

Other measurements made at different interval time will be reported. The kinetics of the apparition of the excited species observed and their spatial distribution at different distance from the center of the plasma has been studied by using an electron-ion recombination model [7].

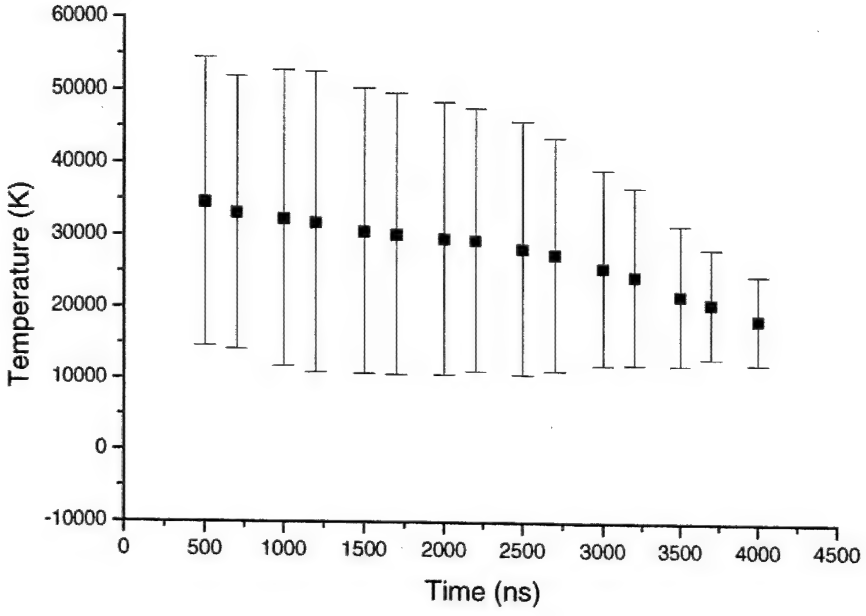

Figure 1:Evolution of electronic temperature with time in the plasma center

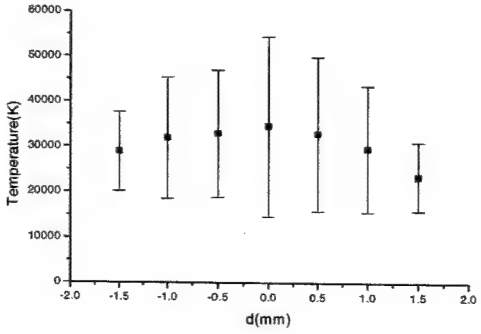

Figure 2 a

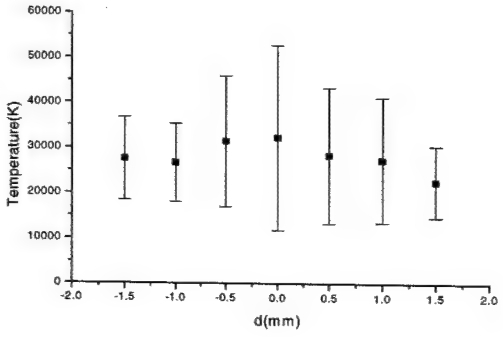

Figure 2 b

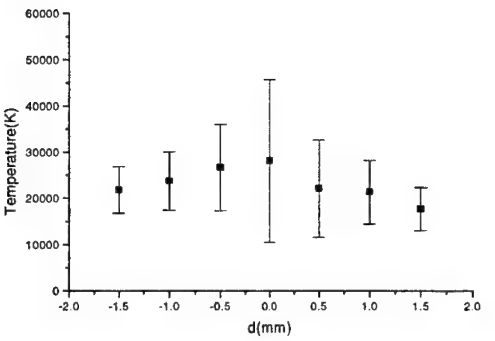

Figure 2 c

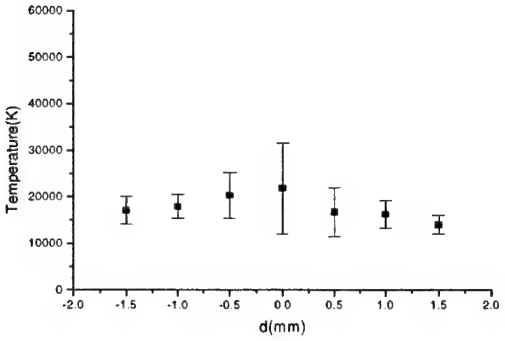

Figure 2 d

Figures 2 a –2d : Evolution of the electronic temperature with the displacement from the plasma center at different delay after the laser pulse;
2a t=500ns, 2b t=1000ns, 2c t=2500ns and 2d t=3500ns.

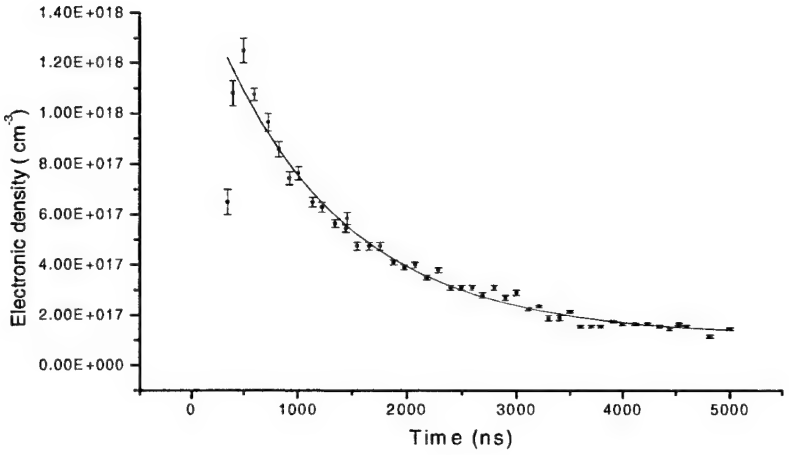

Figure 3: Evolution of electronic density with time in the plasma center

References

[1] S. Vaquie, «L'arc electrique». CNRS Edit. (2000).
[2] H. R. Griem, «Plasma spectroscopy», McGraw-Hill, NewYork, 1964
[3] [S. Sahal-Brechot, Astron.Astrophys, **1,** 91 (1969)
[4] S. Sahal-Brechot, Astron.Astrophys, **2**, 322 (1969)
[5] M. Baranger, Phys.Rev.**111**, 494 (1958)
[6] D. A. Cremers, L. J. Radziemski and T. R. Loree, Appl. Spectrosc. **38,** 721 (1984)
[7] J. Ben Ahmed, Z. Ben Lakhdar and G. Taieb, Kinetics of laser induced plasma on water surface, submitted.

LIBS analysis of lichens as bioindicators of environmental pollution

A. Tozzi, R.Barale

Dipartimento di Scienze dell'uomo e dell'ambiente

Università degli Studi di Pisa Via Volta 6, 56100 Pisa, Italy

G.Cristoforetti, M.Corsi, M. Hidalgo, D.Iriarte, S.Legnaioli, V.Palleschi, A.Salvetti and E.Tognoni

Istituto per i Processi Chimico-Fisici Consiglio Nazionale delle Ricerche, via Moruzzi 1, 56124 Pisa , Italy

michela@ifam.pi.cnr.it

Abstract: The concentration of pollutants in the epiphytic lichen *Xanthoria parietina* was measured with Laser-Induced Breakdown Spectroscopy technique. The analysis shown a very good agreement between the pollutant distribution and the location of the sampling sites.

OCIS codes: (010.1120) Air pollution monitoring; (300.0300) Spectroscopy

1. Introduction

Monitoring of air pollution with living organisms (bio-monitoring) is based on evaluation of ecological variation induced on the environment by the pollution. These variations are reflected on organisms as morfo-structural modification, accumulation of pollutting substance from the environment (heavy metals) and variation of the faunistics and floristics biocoenosis.

Organisms react to pollution in two ways, corresponding to two main groups of biomonitoring techniques:

- bioindication techniques, measuring morphologic, physiologic, genetic, ethologic modifications at community, population or individual level in pollution-sensitive organisms;
- bioaccumulation techniques, measuring the concentrations of substances in pollution-resistant organisms that absorb and accumulate them from the environment.

Lichens can be used as biomonitors of air pollution because they are higly dependent on atmospheric sources for nutrients, they don't have a defensive structure and do not shed plant parts as readily as vascular plants.

These organisms are well known to accumulate and retain a variety of contaminants and are the most widely used biomonitors, with many articles published [1-4].

Sampling was localized in the province of Pisa in the area named "Leather District", with many tanneries and industries connected with tannery process.

2. Methods

In each site, lichen samples were taken from the side of the trunk of isolated trees, 1.5-1.9 m above the ground, following the guide-lines of the Italian National Agency for Environmental Protection.

Only the outermost of the lichens thallus (3 mm) were analyzed and the pure sample was then homogenized with potassium bromide in a ceramic mortar for making a pellet suitable for the laser analysis.

The samples have been analyzed with the following LIBS apparatus: the pulse of a Nd:YAG laser (HY400 Lumonics, delivering a maximum of 0.4 J in 8 ns at a wavelength of 1064 nm), is focused over the sample surface by means of a lens of 100 mm focal length.The LIBS signal is collected with quartz optics and sent by optical fiber to a Czerny-Turner spectrometer (Jobin-Yvon THR1000, grating 1200 grooves/mm). The spectral signal is collected by an optical multichannel anlyzer (IRY 1024 Princeton Instruments Inc.).

The LIBS spectra, covering the range from 2000 to 6000 Å, have been analized with a dedicated spectral software, developed at IPCF laboratory, using CF-LIBS technique [5].

We have compared the concentrations of Al, Ca, Cr, Fe, Mg, Na, P, Si, Ti, Zn in the lichens coming from the different sampling sites.

3. Results

The contamination data of the revealed elements have been treated using multivariate analisys. The dendrogram obtained shows two groups with similar pollution source; both of the groups have been further subdivided in two subgroups.

Fig. 1. Dendrogram with the clusterization of the heavy metals detected

Group 1 (Fe, Si)

Fe and Si form this group. Both of them are widely present in Earth's crust, therefore indicating wind-borne soil and rock dust contamination.

Industrially, iron is used like mordant in dyeing plants and in the ink and pigment industry. Iron and silica are in two separated groups because their areal distribution is different, but the tipology of the site where they are rivelated is almost identical, i.e. along dusty roads.

Group 2 (Al, Cr, Mg, Na, P, Ti, Zn)

It is costituited from element whose origin is prevalently deriving from human activities. It is divided in two subgroups: the source of aluminium pollution is either natural (Al is the third element in the Earth's crust) or from human activities (tawing), the other element are prevalently indicator of human activities (tanning, traffic, agriculture).

This first attempt to use the LIBS technique for the analysis of the heavy metals in lichens has shown a very good agreement between the laboratory data and the distribution of the pollutants in the research area. In fact Phosphorous and Zinc, used in agricolture as fertilizer and plant protection products, are shown by LIBS to be present in higher concentration in cultivated zones; silica is mostly present in zones near open fields or characterized by high levels of dust. On the other hand sodium, an element widely used for industrial bleaching and common soap, is mainly distributed in city areas and industrial zones.

The Cr has an anomalous distribution, because the maximum was revealed in a site far from tanneries, but the second high value was in the same site where whether Na or Al (used in tanning and tawing) have their maximum values.

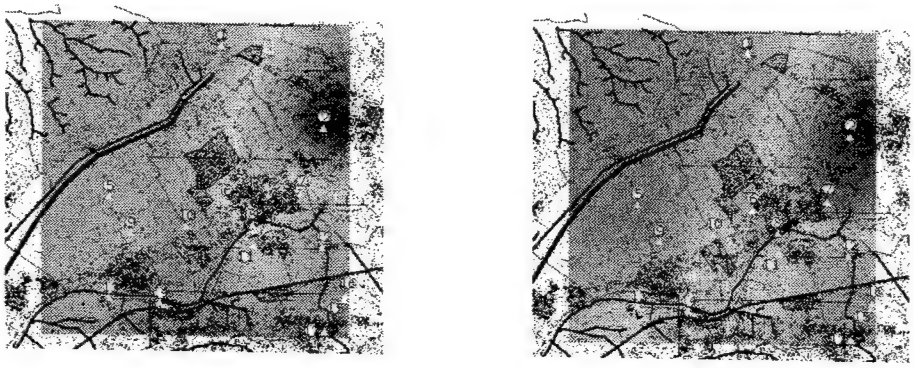

Fig. 2. Geographical distribution of aluminum (left) and sodium (right) as derived by the LIBS analysis of lichens.

References

T.H. Nash, V. Wirth, "Lichens, bryophytes and air quality" Bibl. Lichenol. **30,** 1-298 (1988)

P.L.Nimis, S. Andreussi,, E. Pittao, "The performance of two lichen species as bioaccumulators of trace metals" Sci Total Environ. **275**, 43-51 (2001)

R. Scerbo, T. Ristori, L. Possenti, L. Lampugnani, R. Barale, C. Barghigiani "Lichen (Xanthoria parietina) biomonitoring of trace element contamination and air quality assesment in Pisa Province (Tuscany, Italy)" Sci. Total Environ. **286**, 27-40 (2002)

S. Loppi, "Environmental distribution of mercury and other trace elements in the geothermal area of Bagnore (Mt. Amiata, Italy)" **45**, 991-995 (2001)

A. Ciucci, M. Corsi, V. Palleschi, S. Rastelli, A. Solvetti, E. Tognoni " New procedure for quantitative elemental analysis by Laser Induced Plasma Spctroscopy" Appl. Spectrosc. **53**, 960-964 (1999)

Single element recognition and quantitative analysis using a minimalist laser-induced breakdown spectroscopy system

H.H. Telle* **and G.W. Morris**

Department of Physics, University of Wales Swansea, Singleton Park, Swansea, SA2 8PP, United Kingdom

** Corresponding author - tel: +44-1792-295847, fax: +44-1792-29532, e-mail: h.h.telle@swansea.ac.uk*

O. Samek and M. Liška

Institute of Physical Engineering, Brno University of Technology, Technicka 2, Brno, Czech Republic

Abstract: We report on a simple set-up for laser-induced breakdown spectroscopy including an avalanche photodiode detector (gating by delayed bias voltage or frustrated total internal reflection modulator) and a narrow bandwidth interference filter for wavelength selection.

1. Introduction

Laser-induced breakdown spectroscopy (LIBS) is becoming a handy tool for (multi) trace element analysis and material recognition. For this, typical analysis systems comprise a spectrometer (traditionally Czerny-Turner instruments were/are used, but next-generation Echelle instruments are now becoming increasingly popular) and a time-gated, usually intensified light detector (typically an IPDA array detector or an ICCD cameras). For applications that require the detection of only a single element in the analyte, at any one time, such a full standard LIBS detection system may be seen as a "costly overkill".

Here we report on a substantial simplification of a LIBS set-up for single element analysis, in which a narrow bandwidth interference filter replaces the spectrometer, and instead of a gated, intensified array detector a single avalanche photo diode device is used.

2. Experimental set-up

Commonly a LIBS set-up is made up of a pulsed laser source to generate the plasma, a light delivery / collection system, and a spectrometer with suitable spectral dispersion, coupled to a time-gated detector. The overall principle of the set-up described here follows this general recipe.

The ablation laser was identical to that used in most of our LIBS experiments, namely a small Nd:YAG laser (Quantel "*Brilliant*"), operating at its fundamental wavelength and providing pulse energies in the range 15-150mJ. Its radiation is focused onto the target by a lens of focal length f=150mm.

The plasma emission was collected / collimated using a single, plano-convex collection lens. The (parallel) light beam passed through a narrow bandwidth interference filter (IF) for wavelength selection. Naturally, the bandwidth which can be realized, by using a standard IF, is normally inferior to that of even a small spectrometer. Off-the-shelf IFs in general have a bandwidth of $\Delta\lambda$=10nm. For a few wavelengths ultra-narrow filters with $\Delta\lambda$=2nm, or even $\Delta\lambda$=1nm are avaialble; modern coating techniques also allow to easily fabricate such ultra-narrow filters at any required custom wavelength. Hence, provided that the spacing between lines in a particular LIBS spectrum is larger than the filter bandwidth, IFs may provide sufficient resolution to carry out elemental analysis. In our test measurements, we have utilized IFs with bandwidth $\Delta\lambda$=10nm and $\Delta\lambda$=2nm. After passage through the filter, the light was focused onto the detector diode by a second plano-convex lens. Note that the collimation procedure for the beam path through the IF is required since the filter transmission maximum is a function of the angle of incidence. On the other hand, this angular dependence in turn allows to "tune" the transmission wavelength to a certain degree.

The detector diode was an avalanche photodiode system (Hamamatsu, *C5460-1*), with a built-in amplifier / current-to-voltage converter. Time-gating (essential for most LIBS applications) was possible only to a certain degree, by applying the high-voltage bias to the avalanche diode with a delay of a few microseconds relative to the LIBS plasma generation (laser-light scattering and the strong initial Bremsstrahlung could completely saturate the detector), thus providing a reasonable delayed temporal response of the system gain. Once "triggered" the avalanche amplification stayed on for the remainder of the plasma light emission.

Because of the presence of reflected laser light and continuum plasma radiation, it was necessary to attenuate the initial intensity reaching the avalanche diode using neutral density filters (the maximum intensity of light that could be incident on the diode before saturation, and possible damage, was only 6μW). It should be noted that for fully time-resolved detection an external gating device would be required, like e.g. an optical modulator based on total internal reflection (FTIR) described elsewhere [1].

The signal output from the detector amplifier was sampled and averaged by a boxcar integrator (Stanford Research, *SR250*); its gating was adjusted to mimic the delay / gate acquisition characteristics, on a microsecond scale, in standard LIBS measurement systems.

Overall, the instrumentation described here represents a very low-cost, compact realization to directly measure the intensity of a single spectral line in LIBS analysis. The overall system set-up is sketched in Fig. 1.

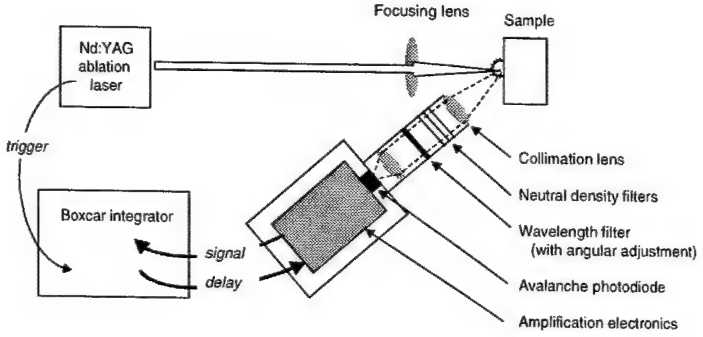

Fig. 1. Layout of a minimalist LIBS system with interference filter and avalanche diode detector.

3. Results

In the nuclear industry radioactive waste is often vitrified for long-term storage. This process involves the mixing of high-level radioactive waste with a glass-like substance in its molten form, and encasing it in steel containers. During the process there is a need to monitor the possible spillage of this glass to the outside of the drums. The glasses which are normally used for this purpose exhibit a high concentration of sodium. Hence, by "scanning" the relevant sections of the drum's surface, which is prone to spillage, using a LIBS probe for the presence of excess sodium would provide a convenient method of detection. Particularly suitable are the sodium D-lines at 589.0nm / 589.6nm since only extremely weak lines of elements of the drum material are present in the spectral interval at around 590nm. Hence, even a 10nm band pass interference filter suffices to realize the required LIBS analysis for the presence of Na. It is this particular example of single element analysis which is discussed in detail in this presentation, as a proof-of-principle.

A sodium discharge lamp was used for wavelength calibration of the interference filter in the light detection pass. The filter was angle-adjusted to its maximum transmission ("element detection") but also tuned to far off-resonance positions ("background check"). The angular dependence of the filter transmission is displayed in Fig. 2.

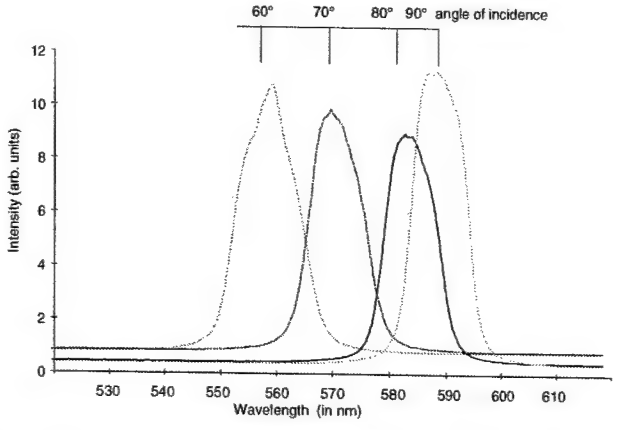

Fig. 2. Shift of transmission maximum of a 590nm interference filter, as a function of angle of incidence.

In order to proof that sodium within a sample could be detected, two specific targets were ablated, namely a *NaCl* crystalline slab and a vitrification glass blank (provided by BNFL Sellafield). The concentration of *Na* in both samples was substantial; however, the detection at trace level concentration was not an issue here, and no major efforts were undertaken at this stage to push the system for enhanced sensitivity. However, quantification seems feasible, since the different amounts of *Na* in the two samples yielded substantially different signal strengths. For control purposed, samples of typical steels used in storage drum making were also ablated, with the IF set to the same wavelengths as for the *Na* measurements.

For all measurements, the delay of switching on the light detection gain, with respect to the laser pulse, was varied in the range 50ns to 5μs; the signal integration period of the boxcar integrator was set to 0.5-1.0μs, as is typical in many LIBS experiments. The signals were averaged over 100 laser pulses for each time delay. Some typical data are summarized in Fig. 3 for a vitrification sample and a steel sample.

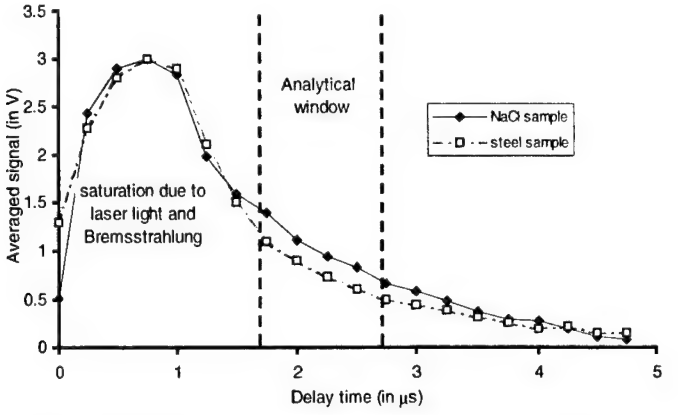

Fig. 3. LIBS signal response at interference filter setting 590nm. for *NaCl* and steel samples, as a function of delay time.

In both cases initial saturation of the detector due to excessive light was evident in our measurement, but the overall signal amplitude followed the typical time behavior encountered in the early stages of the plasma evolution, which is dominated by Bremsstrahlung up to about 1μs. The largest difference between a *Na*-carrying sample and a blank was found in the region 2-3μs, and this delay range was used as the analytical window. Again, this time scale is typical for standard LIBS plasmas. The signal response from the *NaCl* sample matched that from the steel blank when the interference filter was tuned to a transmission maximum of about 565nm. Further test measurements carried out for dried *NaCl* solution spots on a steel surface will be discussed.

These simple experiments demonstrated that this minimalistic LIBS implementation could measure the difference between a sodium-rich sample and a sodium-depleted sample, and as such could be used as the basis for a dedicated on-line detector. Finally, in principle the methodology could be used in other applications as well, in which only single element detection is required and the LIBS spectra are sparse, and where costs of a sophisticated spectrometer would probably be prohibitive. Such a case is encountered e.g. in dentistry where it could be used as a cheap monitor for carries detection during laser drilling, where only qualitative spectral line information is required for identification [2].

4. References

1. D.C.S. Beddows, O. Samek and H.H. Telle: "The application of frustrated total internal reflection devices to analytical laser spectroscopy". To be presented at LIBS2002.

2. O. Samek, H.H. Telle and D.C.S. Beddows: "Laser-induced breakdown spectroscopy: a tool for real-time, *in vitro* and *in vivo* identification of carious teeth". *BMC Oral Health* 2001, **1**:1. (http://www.biomedcentral.com/1472-6831/1/1).

The application of frustrated total internal reflection devices to analytical laser spectroscopy

D.C.S. Beddows, O. Samek[†] and H.H. Telle[*]

Department of Physics, University of Wales Swansea, Singleton Park, SwanseaSA2 8PP, United Kingdom

[†] Permanent address: Institute of Physical Engineering, Technical University of Brno, Technická 2, 616 69 Brno, Czech Republic

[*] Telephone: +44-1792-295847, fax: +44-1792-29532, e-mail: h.h.telle@swansea.ac.uk

Abstract: Novel implementations of single-fiber set-ups for laser-induced breakdown spectroscopy (LIBS) and laser-induced fluorescence spectroscopy (LIFS) systems in remote analysis applications are described, based on gated light switches exploiting Frustrated Total Internal Reflection (FTIR).

1. Introduction

Increasingly laser-induced breakdown spectroscopy (LIBS) is being exploited in qualitative and quantitative analysis of samples, without much need for any sample preparation. While the technique has been around for a number of years the recent, rapid development in laser and detector technology have made it possible to also implement the technique for use in real-time and remote analysis. The technique is at a stage where new on-line applications can be realised using dedicated wavelength specific detection systems, which can either monitor the concentration of trace elements or simply identify bulk materials.

Gateable spectrometers play an important role in LIBS. However their cost can make up a significant fraction of the overall capital expenditure for the apparatus. Spectrometers without gating capabilities, using e.g. standard, or intensified photodiode (PDAs) or charge-coupled device (CCDs) array detectors are significantly cheaper. However, by and large they cannot be used for most LIBS applications.

Here we describe a possible solution to this shortcoming of many low-cost, non-gated detectors. Specifically, we incorporated electro-mechanic modulators into the experimental set-up for time gating of the collected plasma emission, prior to entering the spectrometer. In principle, the use of such devices could significantly reduce the cost of gating the recording of LIBS spectra when only un-gated detectors are available.

2. The principle of FTIR modulators

The modulator, or switch used in this study is based on the principle of Frustrated Total Internal Reflection (FTIR). The device was used to demonstrate the potential of FTIR devices in analytical laser spectroscopy. It consisted of two quartz prisms whose hypotenuse planes were "bonded" to each other. The centers of the hypotenuse plane of each prism were highly polished oval surfaces, which - when matched together - formed the active surface of the modulator. The spacing between the two prisms was controlled using high-precision piezo-electric disk transducers, mounted on flat surfaces parallel to the active face of the FTIR. When the planes make contact with each other, light passes through the FTIR switch. When the contact is broken and the hypotenuse separation is larger than about 1.5μm (which is larger than all wavelengths typically encountered in LIBS), the entire light incident on the hypotenuse plane undergoes total internal reflection (see Fig. 1).

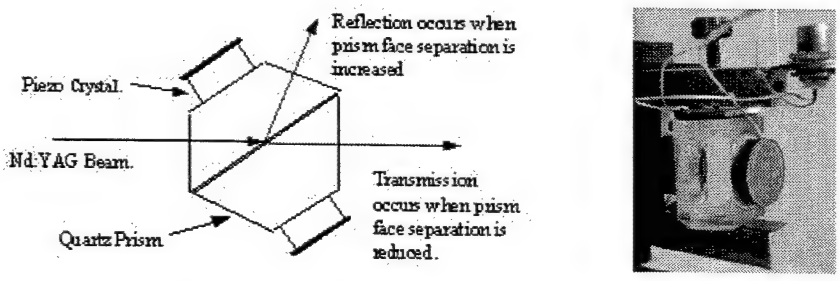

Fig. 1. Principle of FTIR modulator device (left) and set-up of the actual device (right).

The use of Frustrated Total Internal Reflection (FTIR) modulators for optical switching has been well documented in the field of Q-switching of solid-state lasers (e.g. in Nd:YAG and Er:Cr:YSGG lasers), where the high optical durability and fast, variable switching times are the important features. Transferring this technology to analytical laser spectroscopy, the optical switching properties of the FTIR modulator can be exploited for the gating of laser-detection systems. Furthermore, if made from quartz, then FTIR modulators offer a (nearly) non-wavelength dependent alternative to dichroic mirrors for beam combination and beam separation. This makes the FTIR modulator an ideal tool for Laser-induced Breakdown Spectroscopy (LIBS) and Laser-induced Fluorescence Spectroscopy (LIFS) of laser-induced plasma [1]. For example, in LIBS it becomes possible to separate the laser pulses, used to generate the plasma, and the returning luminous emission of the plasma; consequently, the latter can be re-directed into the analyzing spectrometer. Selected practical examples for quantitative and qualitative analytical spectral analysis are discussed.

3. Application of FTIR modulators to laser-induced breakdown spectroscopy

Here we report on test experiments of using FTIR modulators for "gating" LIBS plasma emission. Spectra from steel samples have been collected using the ARC500 spectrometer (Acton Research) coupled with an IPDA detector (Princeton Instruments), which operated in free-running mode, with the FTIR modulators in the light pass between the plasma and the entrance slit of the spectrometer. Spectra recorded in this way were compared with others recorded under the same experimental condition, but without the FTIR modulator and using the gating capability of the IPDA detector.

The modulator was synchronized with the laser pulses so that these were reflected out of the first prism and focused down onto the sample surface to form a plasma. The optical emission of the plasma was then imaged through the active surface of the FTIR onto the end of the spectrometer fiber. The principle of this arrangement is shown in Fig. 2).

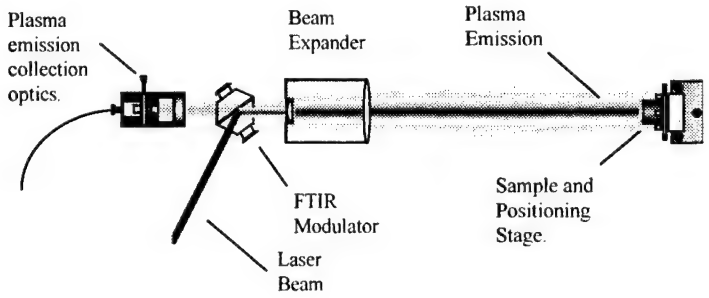

Fig. 2. Experimental realization of LIBS using a FTIR modulator.

The period of imaging / light collection was governed by the duration of the control HV pulse to the piezo-elements of the FTIR switch. The delay between the laser pulse generating the plasma and the transmission of light into the spectrometer can be adjusted more or less at will, from no delay up to the typical maximum delay times of ~20μs. The rise time of the modulator opening is of the order 100-200ns. The duration of the transmission status, and hence the data accumulation time per LIBS plasma event, is adjustable as well but due to the mechanical and electrical relaxation times of the modulator has a minimum width of about 2.5-3.0μs.

If larger distances are to be achieved, like in remote analysis, the Nd:YAG laser radiation has to be transferred via fiber as well. Traditionally, two-fiber assemblies have been used for this, one for the delivery of laser energy and the other for the collection of spectral emissions from the micro-plasma (see e.g. [2]). The alignment difficulties associated with the traditional approach may be overcome by using a single-fiber arrangement through which both the laser pulse is transmitted and the plasma emission light is collected. Furthermore, the cost associated with expensive quartz fibers is reduced if only one single fiber is used. This is of particular importance if the fiber has to be regularly replaced, for instance when used in a hazardous (radioactive) environment.

If such a coaxial, single fiber arrangement is selected for analysis, then a method has to be adopted which is capable of separating the returning plasma emissions from the laser pulses coupled to the end of the fiber. Current single-fiber delivery and collection systems utilize dichroic mirrors to separate the returning signal exiting the fiber from that entering the fiber. However, this method may severely affect spectroscopic analysis for which a very broad range of wavelengths is usually required. Dichroic mirrors exhibit strong wavelength dependence, and specifically

problems arise in the UV - often the most important range in the analysis process. We demonstrated that using a FTIR modulator, which is nearly independent of wavelength, this problem could largely be overcome when using an arrangement based on the principle shown in Fig. 2, by inserting a suitable fiber assembly between the FTIR modulator and the target.

An example for the recording of LIBS spectra is shown in Fig. 3; a wider discussion of this novel approach in LIBS analysis will be given. The discussion will include issues like gating precision, mechanical oscillations (which cause repetitive opening of the modulator), achromatic behavior, and other effects, which might affect reproducibility and sensitivity.

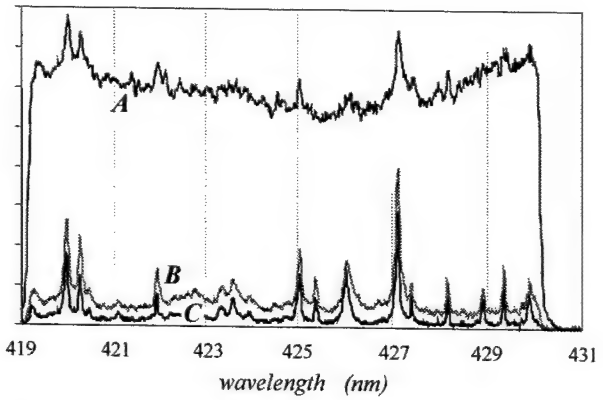

Fig. 3. LIBS spectra of stainless steel sample, recorded with FTIR modulator (open for 3μs). Trace A - 0.1μs delay; trace B – 0.5μs delay; trace C – 1.0μs delay. The time evolution in Bremsstrahlung background and elemental emission lines, typical for LIBS on this time scale, is evident.

4. Application of FTIR modulators to laser-induced fluorescence spectroscopy of laser-generated plasmas

As well as for beam separation, the optical gating capability of the FTIR modulators can be exploited for beam combination. For lower limits of detection and increased sensitivity, the laser produced plume formed on the surface of the ablated material can be probed with a second tunable laser by using the secondary technique of laser-induced fluorescence spectroscopy (LIFS) [1]. If this is to be implemented remotely, then both the ablation laser and tunable laser have to be combined into one beam before being coupled with the radiation delivery optics. A set of two FTIR modulator has been successfully used in our experiments to perform this operation, without the problem of the wavelength dependence encountered with dichroic mirrors. Some representative examples will be discussed.

5. References

1. H.H. Telle, D.C.S. Beddows, G.W. Morris and O.Samek "Sensitive and selective spectrochemical analysis of metallic samples: the combination of laser-induced breakdown spectroscopy and laser-induced fluorescence spectroscopy", Spectrochim. Acta Part B **56**, 947-960 (2000).

2. O. Samek, D.C.S. Beddows, J. Kaiser, S. Kukhlevsky, M. Liška, H.H. Telle and J. Young, "The application of laser induced breakdown spectroscopy to in situ analysis of liquid samples". Opt. Eng. **39**, 2248-2262 (2000).

Comparison between intensified CCD and non-intensified gated CCD detectors for LIPS analysis of solid samples

M. Sabsabi, R. Heon, V. Detalle, L. St-Onge, A. Hamel
National Research Council Canada, Industrial Materials Institute
75 de Mortagne Blvd., Boucherville, Quebec, J4B 6Y4 Canada
Email: mohamad.sabsabi@nrc.ca

1.0 Introduction

Laser-induced plasma spectroscopy (LIPS), also known as laser-induced breakdown spectroscopy (LIBS), is a form of atomic emission spectroscopy (AES). LIPS is being used as an analytical method by a growing number of research groups [1,2]. The growing interest in LIPS, particularly in the last decade, has led to an increasing number of publications on its applications, both in the laboratory and in industry. Despite all these activities, the LIPS technique is still not widely accepted in analytical chemistry. Nevertheless, the LIP spectrochemical analysis has become an important tool for answering chemical questions and diagnosing industrial problems.

LIPS is concerned with the radiation emitted by the microplasma induced by focusing a powerful laser on the sample. LIP emission is space and time dependent. In the initial moments, the plasma emission consists of an intense radiation continuum superimposed with very broadened lines. Thus, temporally gating off the earlier part of the plasma is essential for spectrochemical analysis. This dictates an important difference based on time-gated detection of the atomic emission between the detector requirements for LIPS and other techniques based on AES. Most modern LIPS investigations use a Czerny-Turner spectrometer coupled with an intensified charge coupled device (ICCD) to yield an accurate control of the detector exposure time after the laser pulse. The disadvantage of LIPS instrumentation compared to conventional techniques includes the high cost of the ICCD and its relative complexity compared to alternative technologies. However the advent of new low cost gated CCD will be useful for the LIPS technique and its application.

For analytical spectrochemistry by LIPS, the appropriate choice for the experimentalist is based on the combination of spectrometer and detector which requires a compromise between wavelength coverage, spectral resolution, read time, dynamic range and detection limit. To our knowledge no work has been reported in the literature to evaluate the new gated CCD for LIPS applications. In this presentation we report a comparison between the performance of a spectrometer/ICCD (system A) and spectrometer/non intensified gated CCD (system B) in terms of the spectrochemical analysis of metallic alloy samples by LIPS.

2.0 Results and discussion

In order to evaluate the performance of the two detectors, we examined them in the same experimental conditions, and we then studied each detector separately in its best conditions with the same laser induced plasma on aluminum alloy. System A is composed of a TRIAX spectrometer (blazed at 300 nm, 600 g/mm, 55 cm focal, reciprocal linear dispersion of 3.2 nm/mm or 0.08 nm/pixel of 25μm) coupled to an Andor ICCD detector (Nickel coated intensifier GEN I UV enhanced, active diameter of 25 mm, wavelength response range from 160 to 800 nm,

quantum efficiency of 20% in the window of measurement around 300 nm, CCD from Marconi EEV 3011 chip 258x1000 pixels (26x26 μm) with an active area of 6.7x26.6 mm, 16 bits A/D). System B is composed of an Ocean Optics spectrometer HR2000 (10 cm focal, 2400 g/mm, blazed around 300 nm) coupled to a gated CCD detector (chip Sony ILX511, 2048x 1 pixels, 14 x 200 μm pixels, quantum efficiency around 40% at 300 nm, 12-bits A/D). A pulsed Nd:YAG laser (Surelite from Continuum) was used to perform classical LIPS measurements. The laser emits at 1064 nm and delivers laser pulses of 60 mJ with duration of 6 ns at a low repetition rate of 2 Hz. The laser pulses were focused by a lens of 75 cm focal length to generate the plasma on an aluminum alloy sample (spot diameter was 1 mm). Optical emission from the plasma plume was collected with a lens of 15 cm focal length (image ~1:5) coupled to fiber optics of 500 μm and delivered to the 5 μm entrance slit of system B. In the case of system A, the light is coupled to the entrance of a circular bundle composed of 25 fibers of 100 μm, which at the exit are arranged in linear manner and form the entrance slit of the TRIAX 55 spectrometer. In both configurations the laser beam and the light collection are colinear. The spectral coverage is 85 and 80 nm for systems A and B respectively.

The CCD of system B was operated in external trigger mode to synchronize data acquisition with the laser pulse. In our case the delayed acquisition was 1 μs after the laser pulse to improve signal-to-noise ratio for individual emission lines of the spectrum. Unfortunately system B has a jitter of 250 ns between the trigger from the laser pulse and the beginning of acquisition, and the readout was 1 ms.

The acquisition of the ICCD of system A was delayed by 1 μs after the laser pulse with a jitter of ~2 ns. However to avoid saturation of the detector, the integration time was limited to 0.5 μs and the electron gain was set to a minimum.

A set of standard aluminum samples was studied to establish calibration curves for 4 elements (Cu, Mn, Mg, Be) by the two systems. Our results indicate that the limit of detection of these elements obtained by system A are better than those obtained by system B by more than 1 order of magnitude (see Table 1). Furthermore, when optimization was made for each system separately in terms of light collection, signal-to-noise ratio, etc., we obtained an improvement to the limit of detection for both systems but the limit of detection for system A was still better by at least one order of magnitude than for system B. Also, the dynamic range of system A (16 bits) was better than that of system B (12 bits).

Table 1: Comparison of limits of detection between the spectrometer/ICCD and spectrometer/gated CCD systems

Element	Wavelength (nm)	Limit of detection (ppm) System A Spectrometer/ICCD	Limit of detection (ppm) System B Spectrometer/gated CCD
Mg	285.21	0.9	176.2
Be	313.0	0.4	5.2
Cu	324.75	1.5	484.6
Mn(II)	294.9	32.4	682.8

3.0 Conclusion

In summary we have carried out a performance comparison between spectrometer/ICCD and spectrometer/ non intensified gated CCD systems in terms of spectrochemical analysis of four elements in aluminum alloy samples. The results show that the ICCD detector affords significant advantages in terms of spectral resolution, intensity, dynamic range and sensitivity. However for applications which do not require high resolution or high sensitivity (in the range of 100 ppm) the non intensified gated CCD/spectrometer seems to be an appropriate choice for low cost LIPS instrumentation.

[1] D.A. Rusak, B.C. Castle, B.W. Smith, J.D. Winefordner, Fundamentals and applications of laser-induced breakdown spectroscopy, Crit. Rev. Anal. Chem. **27**, 257-290 (1997).

[2] J. Sneddon, Y.-I. Lee, Novel and recent applications of elemental determination by laser-induced breakdown spectrometry, Anal. Lett. **32**, 2143-2162 (1999).

A specific case of correction for laser-target coupling effect

Louis Barrette, Daniel Michaud and Jean-Guy Chartrand
COREM. 1180, rue de la Mineralogie, Quebec, Qc, Canada G1N 1X7,
louis.barrette@corem.qc.ca
Marc L Dufour
CNRC, 75 de Mortagne, Boucherville, Qc, Canada, J4B 6Y4
François Lippens
EPSIMAGE, 66 Dubois, suite 215, St-Eustache, Qc, Canada, J7P 4W9

Summary:

1. Introduction

COREM is a mineral research center dedicated to transferring the available and pertinent technology to the mineral industry in order, for the latter, to improve its performance. We look for simple effective solutions to perform on-line and as close as possible to real-time measurements on industrial processes. Using LIBS technology, we noticed that the quantity of ablated and excited material is highly affected by the target surface material. This problem was brought up and solutions have been proposed for specific situations [1,2,3]. A specific case of NaCl estimation in the range of 80 to 100% concentration is discussed here.

2. Experimental conditions

The laser used is a "Q-switched Nd : YAG ", model CFR-200, produced by BigSky Laser Technologies inc. It can produce 1064 nm pulses of about 10 ns and 200 mJ at 5 Hz frequency. The beam is focused to a 0.5 mm^2 surface on the target.

The spectrometer used is of the "Czerny-Turner " type. The Jobin Yvon-Spex product, model TRIAX 550, has a 550 mm focal length and f/6.4 numerical aperture. It is equipped with a remotely controlled entrance slit and three interchangeable diffraction gratings. The 1200 l/mm, blazed at 650 nm, was used for the present work.

Emission spectra are detected by an ICCD camera, product of Andor Technology. The intensifier, composed of 690 x 128 elements of 26 x 26 µm, extends the spectral range from 180 nm to 850 nm.

An automated X-Y table is used in synchronization with the laser to make controlled ablation pattern matrices.

3. Na detection on raw material

Blocks of salt of about 5 cm of different NaCl concentrations were used as test samples. NaCl concentration evaluation was made using the Na doublet net emission line 4p 2Po - 3s 2S (330,2 nm) measured at 660 nm in second order. We noted that the Na signal was not correlated to NaCl concentration but rather to the Ca and Mg signals. Mapping of Ca, Mg, Na and background, presented in Fig. 1, clearly shows this correlation.

4. Background correction

The ratio of the net Na peak over the related background can be used to somehow correct the matrix effect. But the poor statistic for the background measurement limits the precision of the results to about 10% based on one standard deviation.

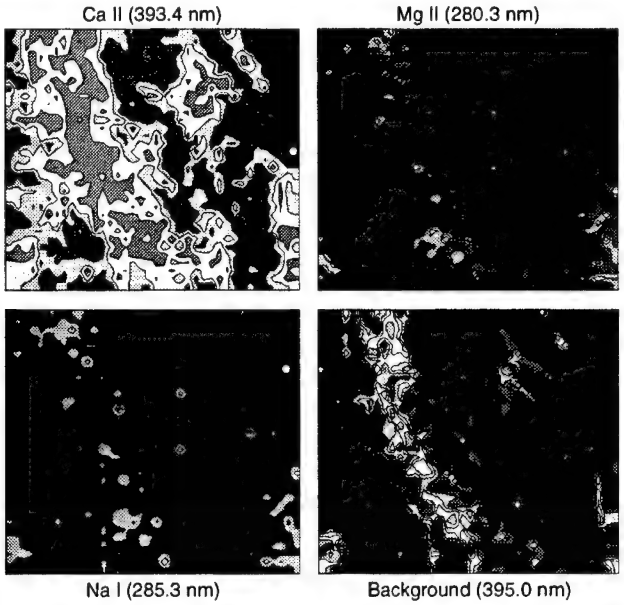

Fig. 1. The four intensity contour maps correspond to the same 4 x 4 cm surface. They represent the net detected signal for Ca, Mg, Na and a background.

5. Laser-matter coupling standardization

Synthetic samples were prepared to study the laser-target coupling effect. These are 25 mm diameter pellets made of finely ground salt samples mixed with a binding agent and additives opaque to the 1064 nm radiation. Twelve samples described in Table 1 were prepared to get a basic understanding of the coupling effect.

Table 1. Pellet chemical composition

Pellet	Salt (g) a: 84% NaCl b: 97% NaCl	Cellulose (g)	Fe_2O_3 (g)	C (g)
$1_{a,b}$	4			
$2_{a,b}$	3.5	0.5		
$3_{a,b}$	3.5	0.4	0.1	
$4_{a,b}$		0.5	3.5	
$5_{a,b}$	3.5	0.4		0.1
$6_{a,b}$		0.5		3.5

The results of the measurements made on those samples are interesting. They show that the addition of a small quantity of the appropriate material can generate a dominant laser-matter coupling effect resulting in a standardization of the matrix effect. A qualitative analysis of the ablated craters is presented in Table 2.

Table 2. Qualitative observations on the ablated craters

Pellet	Observation
$1_{a,b}$	The inversion for Na signal, observed on raw samples, is confirmed. Craters are deep and have a semi-spherical shape.
$2_{a,b}$	The inversion is attenuated. Craters are similar to 1.
$3_{a,b}$	The measured Na net signal is proportional to the real concentration. The craters are shallow and have a cylindrical shape.
$4_{a,b}$	The craters are very shallow (0.1 time the depth observed in 3)
$5_{a,b}$	Idem as 3.
$6_{a,b}$	Idem as 4.

6. Internal referencing

Furthermore, the optical coupling agent can be used as an internal standard to improve the precision of the measurements. In this regard, hematite is a very useful agent because of the dense Fe spectrum which facilitates internal referencing.

7. Correction by ablated volume measurement

To avoid the steps of sample preparation, one can also use 3D imaging techniques to measure the volume of the ablated material. A profilometer based on low coherence interferometry was used to generate surface profiles of the target areas after the laser shots. The volume of material vaporized by the laser was then calculated from the surface profiles. Although the measurements for this experiment were done off-line, this technique has been demonstrated by Dufour et al. [4,5] to be feasible in real-time within a LIBS spectrometer. As shown in Fig. 2, on-line measurement may be done by mixing the LIBS laser beam with the low coherence measurement beam by using a dichroic mirror. This emerging technique was tested and is compared with previously described procedures.

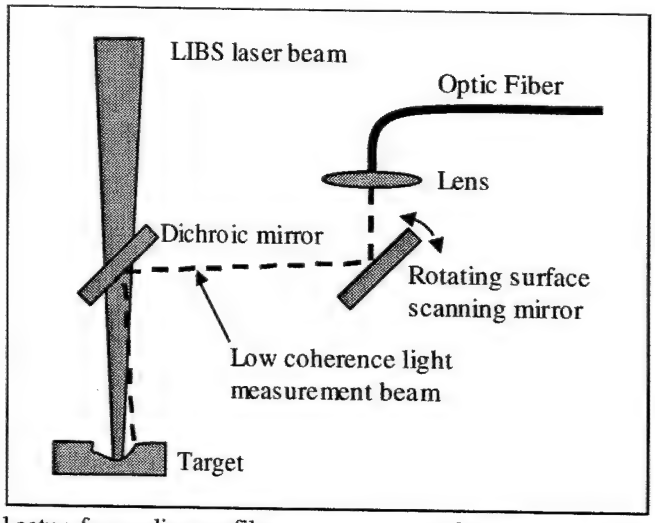

Fig. 2. Experimental setup for on-line profile measurements of the craters produced by laser beam on solid target.

8. Conclusion

LIBS is an interesting measurement technology for process control. The possibility of on-line and real-time analysis – with no preparation – is appealing, but it has limits in specific situations. Considering the sometimes relatively slow dynamics of industrial processes, solutions implying simple and fast sample preparation can constitute interesting alternatives to cope with laser-target coupling effects.

9. References

1. Kay Niemax, "Laser ablation – reflexions on a very complex technique for solid sampling," Fresenius J. Anal. Chem. **370**, 332-340 (2001).
2. C. Chaleard, P. Mauchien, N. Andre, J. Uebbing, J. L. Lacour and C. Geertsen, "Correction of Matrix Effects in Quantitative Elemental Analysis With Laser Ablation Optical Emission Spectrometry," J. Anal. At. Spectrom., **12**, 183-188 (1997)
3. Aaron S. Eppler, David A. Cremers, Donald D. Hickmott, Monty J. Ferris and Aaron C. Koskelo, "Matrix Effects in the detection of Pb and Ba in soils using laser-induced breakdown spectroscopy," Appl. Spectrosc., **50**, 1175-1181 (1996)
4. Marc L. Dufour, Bruno Gauthier, "Applications industrielles de l'interferometrie en lumière faiblement coherente," CMOI Methodes et techniques optiques pour l'industrie, 197-202 (Nov. 2001)
5. V. Detalle, M. Sabsabi, R. Heon, L. St-Onge, "Improvement of depth profile analysis by laser induced plasma spectroscopy," 6th Int. Conf. On Laser Ablation, PT-25, (2001)

Use of LIBS to determine carbon in soil for terrestrial carbon sequestration programs

David A. Cremers[1], Mike Ebinger[2], Monty J. Ferris[1], David Breshears[2], Pat J. Unkefer[3]
[1]*Advanced Diagnostics and Instrumentation, MS J565*
[2]*Environmental Dynamics and Spatial Analysis, MS J495*
[3]*Environmental Dynamics and Spatial Analysis, MS J495*
Los Alamos National Laboratory, Los Alamos, NM 87545
Tel: 505-665-4180; Fax: 505-665-6095;e-mail: cremers_david@lanl.gov

1. Introduction

International treaties are being discussed to reduce the effect of global warming believed to be the result of releasing carbon into the atmosphere. The flux of carbon in the air can be reduced by either (1) reducing the processes that produce the emissions or by (2) removing carbon from the air through some remediation process. One process that is being considered is terrestrial carbon sequestration. Here plants would be grown on lands that otherwise have low growth. Plant growth will remove carbon from the atmosphere and sequester it in the first meter of soil. Estimates have indicated that the amount of carbon that can be sequestered in this way is substantial.

If terrestrial carbon sequestration is to be a viable process, measurement methods that are fast and economical must be developed to measure carbon in soil to verify the efficiency of a sequestration program [1-3]. Currently, there is no "off-the-shelf" method of measuring carbon in this way.

There is interest in LIBS for this application because of its many unique analysis capabilities most important being the speed with which an analysis can be made and the field-deployability of the technique. We have been investigating LIBS for measuring carbon in soil [4] and have developed instrumentation for field-tests.

2. Experimental apparatus

Initial experiments were carried out using a laboratory instrument to assess the capabilities of LIBS carbon detection. This system consisted of a Nd:YAG laser, spectrograph (0.5 m), and a gated intensified CCD array detector. The second system was a field-deployable instrument developed for field tests of the technology. This instrument is described below.

3. Detection of carbon

Carbon is easily detected in soil using LIBS via the strong emission lines at 193.0 nm and 247.8 nm in the ultraviolet spectral region. Spectra of these lines are shown in Figure 1. Each was taken using the laboratory apparatus with the soil sample in air. Spectral interferences were observed for both lines but using a resolution of 0.1-0.2 nm, it was possible to monitor the carbon line unambiguously. In terms of observed line intensity, the 247.8 nm line was greater. Reduced fiber optic transmission was mainly responsible for reducing the intensity of the 193.0 nm C-line.

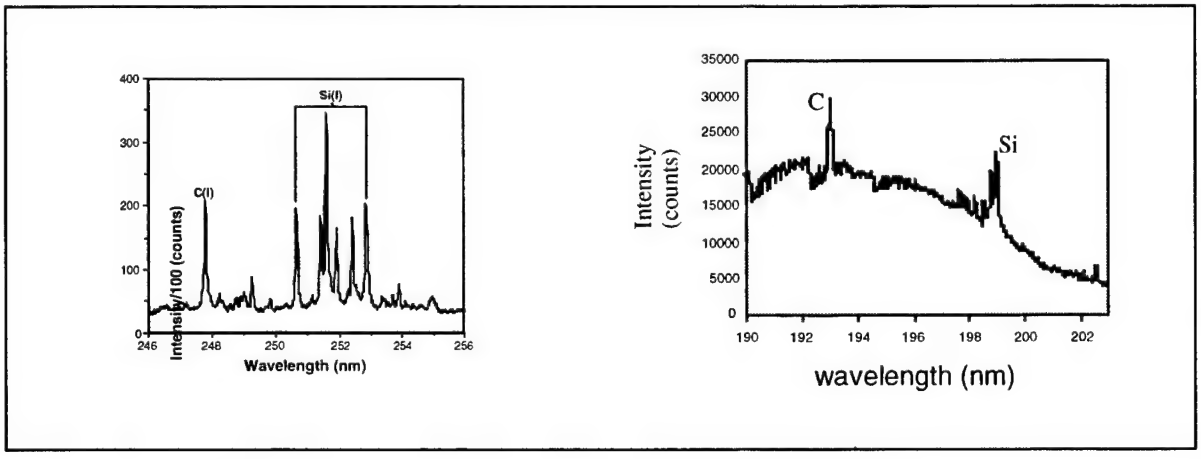

Fig. 1. Strong emission lines of carbon (from a soil sample) obtained using LIBS.

A calibration curve for carbon in soil obtained using LIBS and the 247.8 nm C-line is shown in Figure 2. The

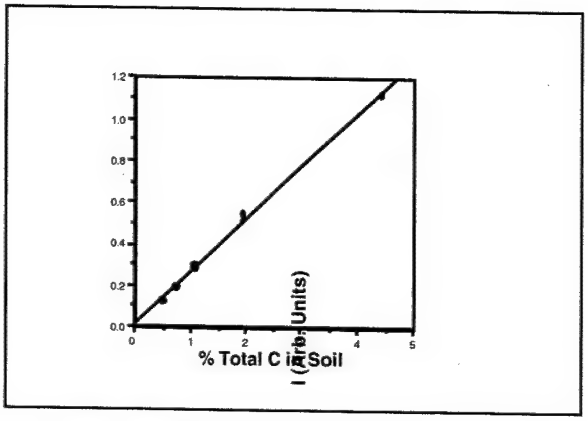

Fig. 2. Calibration curve for the detection of carbon in soil.

samples used to prepare this curve were previously analyzed for total carbon content using conventional analytical methods (e.g. dry combustion). It should be noted that the time required to obtain each data point on the curve was less than 30 seconds.

Our results indicate that LIBS rapidly and efficiently measures soil carbon with detection limits ~300 mg/kg, a precision of 4-5%, and an accuracy of 3-14%. These values are comparable to those obtained using dry combustion. Initial testing shows that LIBS measurements and dry combustion analyses are highly correlated with $r^2 = 0.96$ for soils of distinct morphology.

4. Field deployable carbon analyzer

The field analyzer is shown in Figure 3. It consists of a 10Hz Nd:YAG laser (100 mJ/pulse), a compact echelle spectrograph monitoring the range (192-783 nm), and a gated-intensified CCD array detector. The unit can analyze discrete soil samples or core samples up to 1 meter in length. A laptop computer controls the instrument and provides data analysis. A 90-cm long core can be analyzed by the instrument in about 15 minutes. Each analysis consists of about 120 individual averaged spectra corresponding to adjacent positions along the core. Analysis of each spectrum is provided by software that locates the emission peak(s) of interest and computes the carbon concentration.

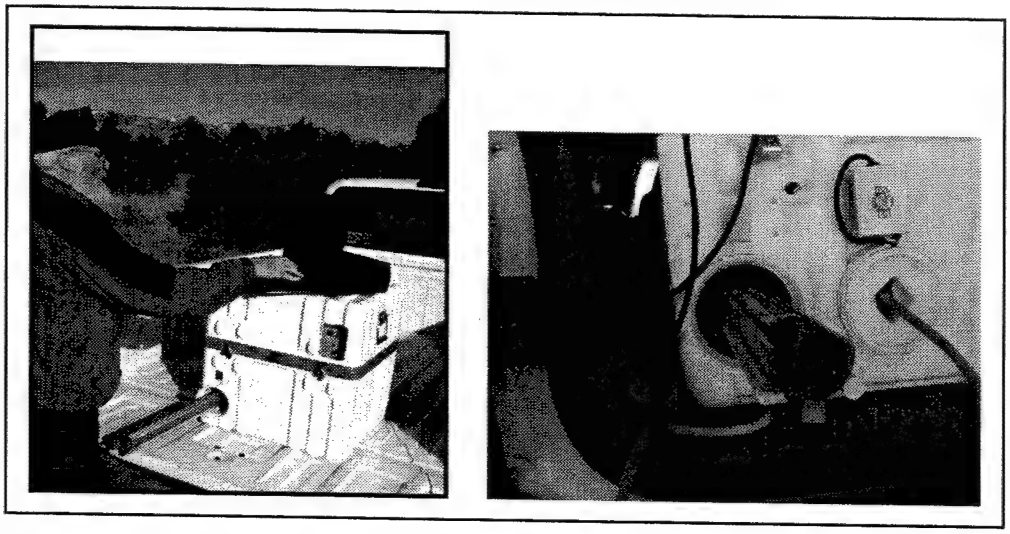

Fig. 3. Field-deployable soil carbon analyzer (left). A core sample (right) inserted into the device is analyzed in 15 minutes.

5. References

1. G.W. McCarty and J.B. Reeves III, "Development of rapid instrumental methods for measuring soil organic carbon," p. 371-380. In R. Lal, J. M. Kimble, R. F. Follett, and B. A. Stewart (ed.) Assessment methods for soil carbon, (Lewis, Boca Raton, LA, 2001).

2. Department of Energy (DOE). 1999. Carbon sequestration research and development. DOE Report DOE/SC/FE-1, Washington, D. C. (Available on-line at http://www.ornl.gov/carbon_sequestration).

3. Greenland, D.J., "Carbon sequestration in soil: knowledge gaps indicated by the symposium presentations," p. 591-594. In R. Lal, J. M. Kimble, R. F. Follett, and B. A. Stewart (ed.) Soil processes and the carbon cycle. (CRC Press, Boca Raton, FL, 1998).

4. D.A. Cremers, M.H. Ebinger, D.D. Breshears, P.J. Unkefer, S.A. Kammerdiener, M.J. Ferris, K.M. Catlett & J.R. Brown, "Measuring total soil carbon with laser-induced breakdown spectroscopy (LIBS)," Journal of Environmental Quality **30***: 2002-2206* (2001).

2-D and 3-D chemical mapping of heterogeneous samples using microline-imaging laser-induced plasma spectrometry

M.P. Mateo, L.M. Cabalín and J.J. Laserna
Department of Analytical Chemistry, Faculty of Science, University of Málaga.
Campus de Teatinos, E-29071 Málaga, Spain.
Phone: +(34) 952131881, Fax: +(34) 952132000, E-mail: laserna@uma.es

Abstract: The performance and application of plasma spectrometry induced with a line-focused laser beam in generating fast 2 and 3-Dimensional compositional maps of different manufactured materials as well as of inclusionary material in stainless steel will be discussed.

OCIS codes: (160.0160) Materials

Summary

Surface characterization is playing an ever more important part in all aspects of our modern technological society. The information on the physical topography, interfacial morphology, chemical composition, structure and properties at the surface is obtained from a wide variety of instrumental techniques. The selection of a suitable method for each particular task of surface analysis is in principle quite difficult. The main reasons for this is the magnitude of methods available and the fact that most of the methods are still inaccessible to most researchers. Another typical feature of the situation is the sudden expansion of surface technology to almost all fields of manufactured materials with greatly varying characterization needs.

The spatial resolution as well as the surface sensitivity achieved by some of classical surface analysis techniques, particularly those using electrons and ions, is in the nanometer range allowing the study of phenomena such as adsorption or corrosion processes. However, due to this feature, some applications involving large sampling areas or depth analysis of thick layers, would require very long analysis times and could even be impossible to solve due to an incompatibility of the sample characteristics with restrictions in space and vacuum conditions of the commercial instruments. These difficulties are more critical when 3-D compositional maps must be performed.

Laser-induced plasma spectrometry (LIPS) has been successfully applied to surface characterization. Chemical images can be readily obtained by translating (raster) the sample position under the laser beam, so that the analyzed region is moved across the static laser beam. The multichannel LIPS spectrum is stored for each position of the sample, followed by computer-based reconstruction of two-dimensional selective images (maps) from intensity profiles at several wavelengths. The information derived from these sequentially collected spectra is called point-to-point mapping.

A new LIPS mapping approach consists of generating a microline plasma by focusing the laser beam to a line with a cylindrical lens. This LIPS arrangement produces long and narrow craters on the sample surface instead of the common circular craters formed with the laser beam focused using spherical lenses (Fig. 1). The emitted light from the microline plasma can be imaged into a spectrometer that projects the wavelength axis along one CCD axis and the position along the line along the other axis. Thus, the spatial and wavelength axes are analyzed by the CCD detector, while the X axis of the sample is scanned by rastering the line-focused laser beam. If several laser shots are applied in the same sample position additional depth information is achieved. The end result is a multi-dimensional data set of LIPS signal intensity versus wavelength and versus X, Y and Z positions on the sample.

In the application of LIPS to compositional mapping it is crucial to obtain a good lateral resolution, which is defined in the microline approach by the microline crater width. To optimize the latter, several experimental parameters including lens focal length, beam diameter and laser pulse energy have been studied. The results demonstrated that the narrowest microline crater was obtained by decreasing laser pulse energy, by using a cylindrical lens with short focal length, and by increasing the laser beam diameter. On the other hand, a homogenous distribution of energy across the beam is required to produce uniform ablation along the sampled area. For this purpose, after evaluating two Nd:YAG lasers, a Gaussian laser and a flat top laser, the latter was chosen due to its uniform energy distribution along the beam cross section. Finally, as a trade off between lateral resolution and spectral signal, the experimental conditions were 50-mm lens focal length, beam expander 3x and pulse energy of 40 mJ.

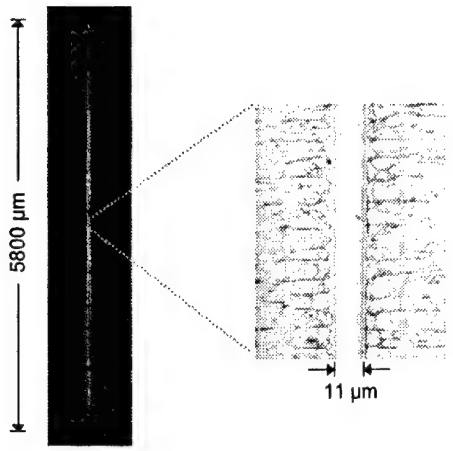

Fig. 1. Photograph of a microline crater in stainless steel. The inset shows the crater area in detail.

The potential of a microline imaging LIPS system for surface and depth analysis of heterogeneous solid samples in air at atmospheric pressure will be presented. 2 and 3-Dimensional chemical maps of different manufactured materials including printed circuit boards and photovoltaic cells, as well as inclusionary material (Al, Ca, Mg, Mn, and Ti) in different steel grades, will be presented. The results illustrate the capability of microline imaging for fast mapping of large area samples and for depth profiling purposes. Simplicity of operation and rapid data acquisition are the main characteristics of this LIPS approach.

Characterization and Identification of Ammunition by Laser Induced Breakdown Spectroscopy

Scott R. Goode, Andrea Thomas, Alexander A. Nieuwland, and Stephen L. Morgan
Department of Chemistry and Biochemistry, The University of South Carolina, Columbia, SC 29208
Phone: 803-777-2601 FAX: 803-777-9521 Email: goode@sc.edu, slmorgan@sc.edu

Abstract: Laser induced breakdown spectroscopy was used to characterize bullets, jackets, and cartridge cases from a small number of different manufacturers. LIBS spectra of these samples showed significant differences and could be accurately classified by source.

OCIS codes: (300.6210) Spectroscopy, atomic (070.5010) Pattern recognition and feature extraction

1. Introduction

Identifying bullets, fragments of bullets, and cartridge cases is a common task for the forensic analyst. Often, only ammunition fragments are recovered, which precludes identification by matching striation patterns. A much-discussed alternative is to use elemental analysis for characterization of ammunition fragments (1-5).

Laser induced breakdown spectroscopy (LIBS) can provide an emission spectrum from a small sample of a solid, without sample preparation or dissolution. This direct spectroscopic method produces spectra that can be easily interpreted to identify specific elements present in the sample. Further, if spectra from diverse samples are sufficiently different and reproducible, then an unknown spectrum can be identified by comparison to a library. We have employed computer-assisted pattern recognition methods to classify LIBS spectra from various ammunition fragments.

2. Experimental

Samples of bullets and cartridges were obtained from 6-12 manufacturers. Since most bullets were jacketed, the bullet lead was exposed by removing the jacket on a lathe. The bullet with exposed lead surface was placed in a simple mount that allowed x-y positioning under computer control. The computer also controlled the z-axis by moving the focusing lens as needed. Emission was collected by an Echelle spectrometer with an intensified charge couple device (ICCD) camera (6). Six bullets were chosen from each manufacturer, and five replicate spectra were obtained from each bullet. Similar experiments were performed with the copper jackets and brass cartridge cases.

The echellograms were converted to spectra and then to ASCII data files. The spectra were simplified by rounding wavelengths to the nearest 1 nm increment and summing all peaks within the same one nm interval to produce a spectral file having emission intensities at 640 wavelengths (200-840 nm). These files were input to a series of statistical analysis programs for principal component analysis and multiple linear discriminant analysis.

3. Results and Discussion

Figure 1 shows representative LIBS spectra of ammunition from two manufacturers each of bullet lead, copper jacket material, and brass cartridge cases. The LIBS spectra are quite intense and have high signal-to-noise ratios. The spectra of bullets, jackets, and cases from these different sources show noticeable differences that are distinguishable by eye. This ability to discriminate the groups of ammunition from different sources was validated by the use of principal component analysis and multiple linear discriminant analysis. As an example, a projection of the lead bullet spectra from five different manufacturers is shown in Figure 2. Each separate cluster in this plot consists of projections of 5 replicate spectra on six different bullets. The clusters are small, indicating small intra-group variation, and well separated, indicating large inter-group variation.

Similar results were obtained for the jackets and cartridge cases.

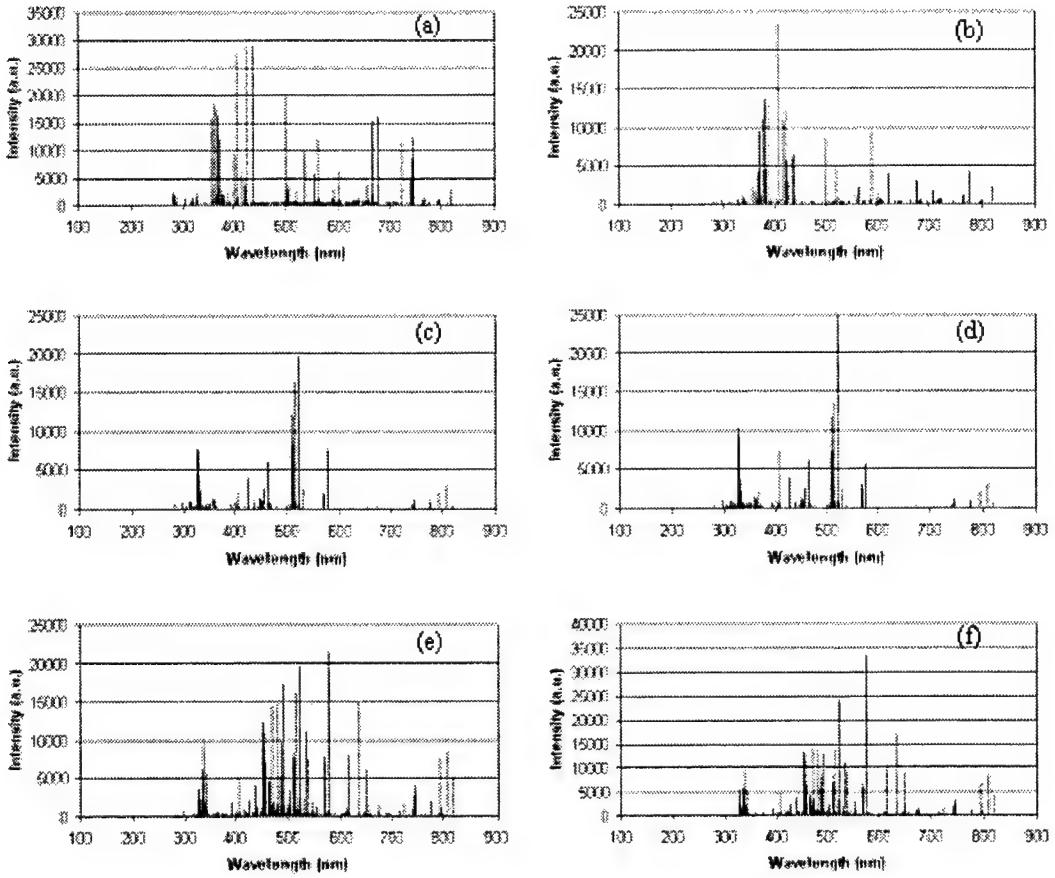

Figure 1. Representative LIBS spectra from samples of: (a) Speer's GoldDot bullet; (b) Speer's Lawman bullet; (c) Speer's GoldDot jacket; (d) Speer's Lawman jacket; (e) Fiocchi case; and (f) Winchester case.

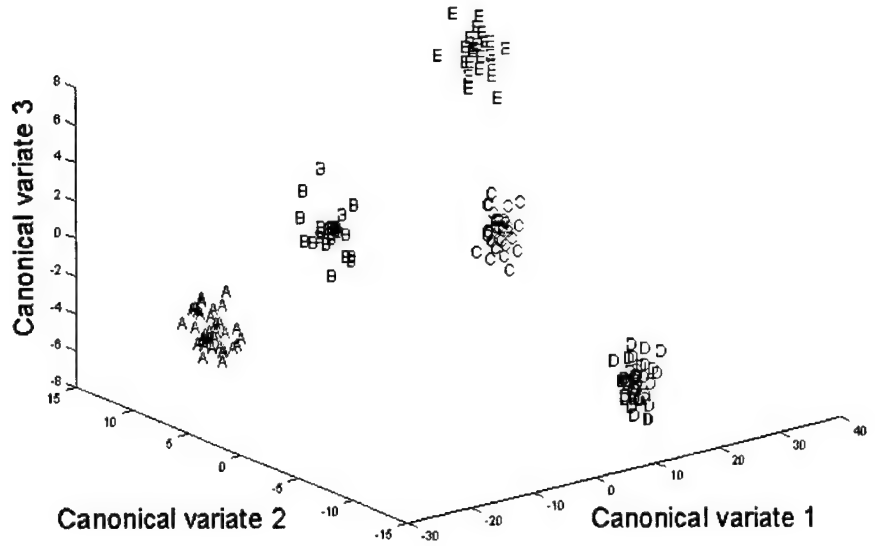

Figure 2. Projection of the LIBS spectra from 5 different types of bullet lead into the space of the first three canonical variates. A: Speer's GoldDot; B: CCI Blazer Clean Fire; C: Federal Cartridge Company's American Eagle; D: Remington's Union Metallic Cartridge Company; E: Winchester

4. Conclusion

LIBS combined with computer-assisted pattern recognition methods is a powerful tool for the discrimination and identification of ammunition fragments. In this study we have shown the ability to differentiate bullets, jackets, and cases from a limited number of manufacturing sources. The LIBS technique is rapid: 100s of spectra can be recorded in a single day. In each data set studied, spectra of replicate analyses and/or replicate analyses clustered together, indicating good precision.

5. References

(1) Guinn, V. P. "JFK Assassination: bullet analyses," *Anal. Chem.* 1979 , *51* , 484A-493A.
(2) Kaplan, J., Klose, R., Fossum, R., Di Maio, V.J.M. "Centerfire frangible ammunition: wounding potential and other forensic concerns," *Am. J. Forensic Med. Path.* 1998 , *19* , 299-302.
(3) Gillespie, K. A., Krishnan, S.S. "Analysis of Lead Shot - a comparison of analyses using atomic absorption spectrometry and neutron activation analysis," *Canad. Soc. Forensic Sci. J.* 1969 , *2* , 95-103.
(4) Peters, C. A., Havekost, D.G., Koons, R.D. "Multielement analysis of bullet lead by inductively coupled plasma-atomic emission spectrometry," *Crime Lab. Digest* 1988 , *1*, 33-38.
(5) Peele, E. R., Havekost, D.G., Peters, C.A., Riley, J.P., Halberstam, R.C. *Comparison of bullets using the elemental composition of the lead content.* ; in: Proceedings of the international symposium of the forensic aspects of trace evidence; Je 24-28; Quantico (VA). Washington DC: USDOJ, (ISBN 0-932115-12-8) 1991, 1991, pp 57-68.
(6) Goode, S. R., Morgan, S.L., Hoskins, R., Oxsher, A. "Identifying alloys by laser-induced breakdown spectroscopy with a time-resolved high resolution echelle spectrometer," *J. Anal. At. Spectrom.* **2000**, *15*, 1133-1138.

Spectral analysis of the acoustic emission of laser-produced plasmas

S. Palanco and J.J. Laserna
Department of Analytical Chemistry, Faculty of Science, University of Malaga.
Campus de Teatinos, E-29071 Malaga, Spain.
Phone: +(34) 952131881, Fax: +(34) 952132000. E-mail: laserna@uma.es

Abstract: The acoustic analysis of shock wave emission from laser produced plasmas is presented. Characteristic frequency domain spectra from a number of elements and alloys are discussed.

OCIS codes: (300.6360) Spectroscopy, Laser; (160.2120) Materials, Elements

Summary

Laser produced plasmas have been widely studied by a number of researchers who have devoted their investigations to fundamental issues and applications. Concerning the latter, laser produced plasmas are used as atom reservoirs for mass spectrometry and atomic emission. To a minor extent, the utility of the shock wave accompanying the plasma formation has been demonstrated as a complementary tool for signal normalization in an attempt to improve the precision of LIPS.

Main plasma characteristics such as temperature, pressure and expansion velocity depend on the propagation mechanism. At an early stage, a high-pressure absorption wave is formed which, depending on the irradiance level, can develop through three different paths: laser supported combustion wave (LSC) for irradiances approximately less than 107 W cm^{-2}, laser supported detonation wave (LSD) for irradiances between 107 and 109 W cm^{-2}, and laser supported radiation wave (LSR) for irradiances over 109 W cm^{-2}. Well defined frontiers do not exist between the three types of plasma and transitions from one to other are not perfectly understood. To date, the acoustic spectra of the shock waves have not yet been explored to a significant degree.

In the present work a simple and low-cost technique with capabilities for plasma diagnosis and qualitative analysis of materials is presented. The technique makes use of a home computer and a standard sound card to digitize the shock waves. Further processing of the signals involves calculations of the energy transported by the shock wave and obtaining the frequency-domain spectra through fast Fourier transform. For the present study, irradiance levels ranged between 1.7×10^{8} W cm^{-2} and 1.6×10^{10} W cm^{-2} what made possible to identify LSD wave and LSR wave regimes.

Development and testing of a prototype LIBS instrument for a NASA Mars rover

David A. Cremers[1], Roger C. Wiens[2], Monty J. Ferris[1], and James D. Blacic[3]
[1]*Advanced Diagnostics and Instrumentation, MS J565*
[2]*Atmospheric and Space Sciences, MS D466*
[3]*Geophysics, MS D443*
Los Alamos National Laboratory, Los Alamos, NM 87545
Tel: 505-665-4180; Fax: 505-665-6095:e-mail: cremers_david@lanl.gov

1. Introduction

Through funding from NASA's Mars Instrument Development Program (MIDP), we have been evaluating LIBS for future use on landers and rovers to Mars [1]. Part of this work was the design and fabrication of a compact LIBS instrument for stand-off analysis of geological samples. The instrument was constructed of mainly "off-the-shelf" commercially available components. The instrument was tested in the laboratory and on a NASA rover operated by NASA AMES Research Center at a field site in the Nevada desert [2]. The purpose of the LIBS instrument was (1) to develop an optical system for focusing the laser pulse on and collection of the light from the remotely formed laser plasma, (2) to demonstrate significant down-sizing of a LIBS instrument, and (3) to demonstrate that LIBS can provide useful data in field tests. The results of this preliminary work show the promise of LIBS as a new instrument for use on future missions to Mars.

2. Description of the prototype instrument

The instrument consists of two main sections: (1) the sensor head mounted atop a mast fixed to the rover body and (2) an analysis unit located in the body of the rover. The compact sensor head (Figure 1) is about 35 cm long by 7.5 cm in diameter (without the range finder) and houses the laser, optical system with adjustable focus, light collection components, and fiber optic cable. The mass of the sensor head is 900 grams (including range finder). A simple two-lens beam expander is used to focus the pulses on a remotely located target. One lens of the expander is translatable by a motorized stage (computer-controlled) to adjust the focus from 2-20 meters. The laser is a flashlamp-pumped Nd:YAG (Kigre) specially constructed for this project to generate 80 mJ/pulse. Because the laser is only conductively cooled, the repetition rate was kept to 0.1 Hz. Light from the remote target was collected by the beam expander, split off by a Glan-Focault prism, and then focused onto a fiber optic cable. The fiber transmited the plasma light to the spectrograph and array detector contained in the main body of the rover. The spectrograph (focal length = 110 mm) provided detection over a narrow spectral range (e.g. 250-320 nm) but the grating could be moved to monitor different spectral regions sequentially. The detector was a gated-intensified CCD array. The LIBS instrument installed on the NASA AMES K-9 rover at the field site is shown in Figure 2. The top of the mast is about 2 meters from the ground.

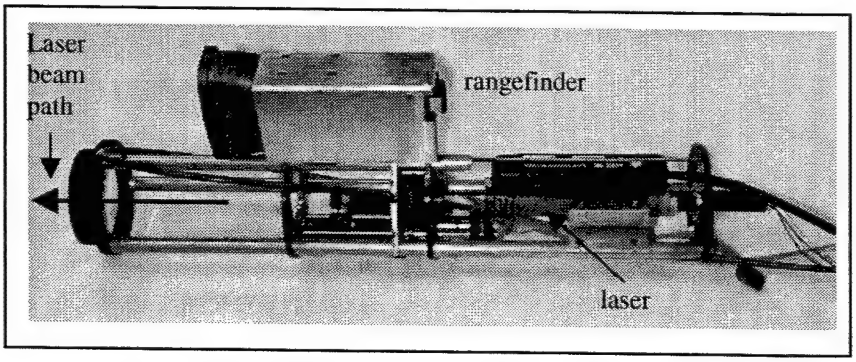

Fig. 1. LIBS sensor head built for NASA MIDP.

On the rover mast, the sensor head was affixed to a pan and tilt system adjacent to a set of cameras. This permitted aiming the camera at selected objects. Although designed and tested in the laboratory for measurements at distances of up to 20 meters, in the field test, the maximum distance was restricted to 8 meters.

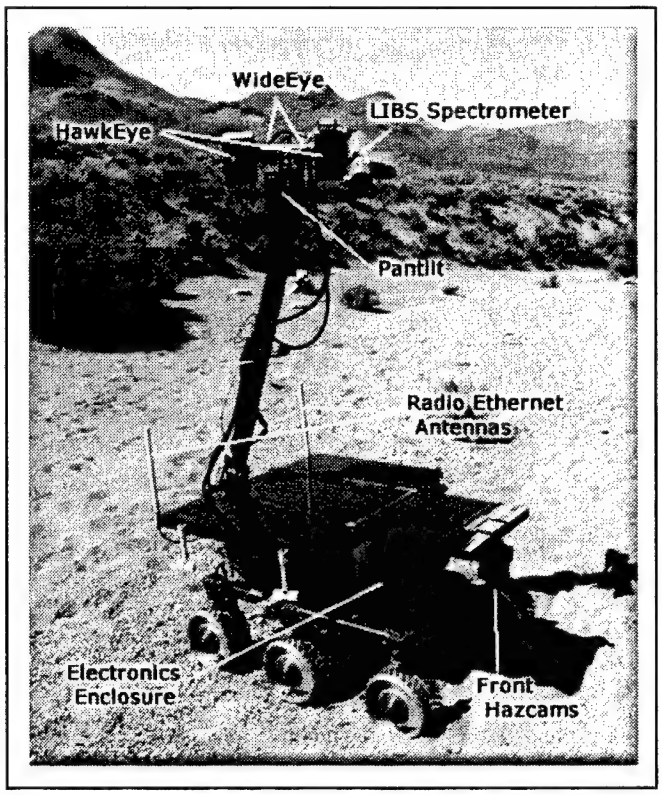

Fig. 2. LIBS instrument on board NASA AMES K-9 Rover during field test at Black Rock Summit, Nevada.

3. Tests results

The first field test of the LIBS instrument was part of a joint FIDO/K-9 rover test at Black Rock Summit, Nevada in early May 2000. Prior to the field test, the LIBS instrument was mechanically integrated into the K-9 rover at AMES. The spectrograph, detector, laser power supply, and optics controller were built into a single chassis that dropped into the rover body. During the field test, the LIBS instrument was controlled by a computer connected to the rover by a long cable. After arriving at the field test site, a wildfire broke out in the national forest next to Los Alamos that threatened the city and required complete evacuation for several days (eventually over 400 homes were destroyed in Los Alamos by the fire). The fire and subsequent evacuation required that the Los Alamos personnel return to New Mexico immediately. Before leaving, AMES personnel were shown how to operate the LIBS instrument and they were able to acquire a small amount of data. These data consisted of single shot spectra on "uncleaned" areas of 14 rock samples in two spectral regions. The samples interrogated in the field were removed from the test site and returned to the laboratory for further interrogation. Dual measurements using LIBS and visible and near-IR reflectance (VISIR) spectroscopy (by Washington University personnel) provided complimentary data sets. VISIR provided surface mineral abundances, while LIBS provided chemical abundances and used its depth profiling capability to determine whether minerals reported by VISIR were surface contaminants or comprised the bulk rock. In addition, LIBS was able to identify rock types. This is demonstrated by the spectra shown in Figure 3. On the left is a LIBS spectrum from field specimen A01 and on the right is a spectrum of the same region taken with a basalt standard (JB-2) as the sample. Each spectrum was the result of a 20 shot average. Even with the low resolution of the 110 mm spectrograph, the spectra are basically identical. Similar results were obtained for the other field samples which included dolostone, altered rhyolite, basalt, and iron oxides. Of particular note in this work was the comparison between VISIR and LIBS for samples with weathering coatings. Here LIBS definitively showed which VISIR features were caused by the weathering layer and which were intrinsic to the rock itself. A clear feature of the weathering layers was the H emission line, indicative of the water bound in the clay-weathering layer [2].

Based on results of the first field test, additional laboratory testing, and the availability of a new compact echelle spectrograph, the LIBS prototype was modified for a second field test in May 2001 at the same location used for the FIDO '01 exercise (the desert outside of Baker, CA). For this test, the echelle spectrograph with a resolution

$\lambda/\Delta\lambda$= 2500 was integrated into the system hardware and connected to a gated-intensified camera with a high pixel density.

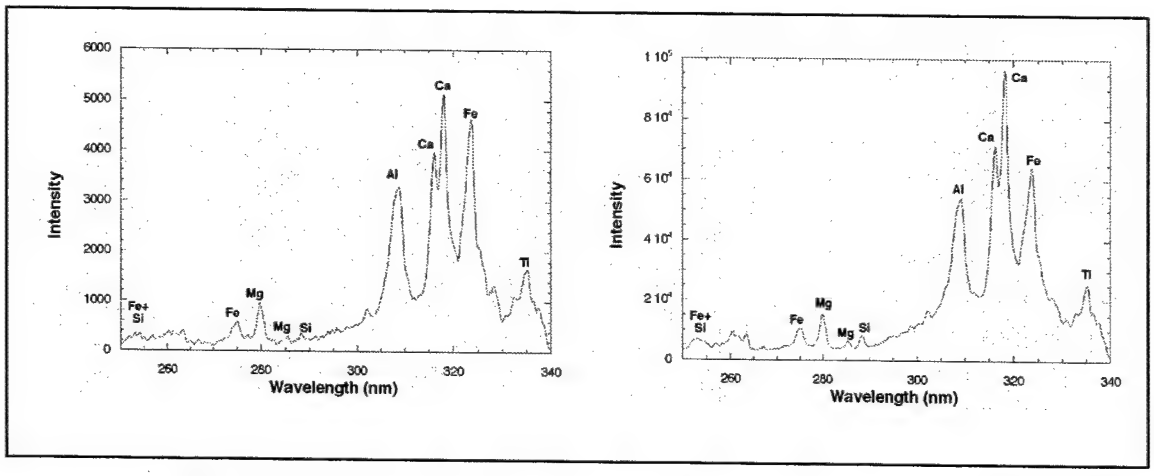

Fig. 3. Comparison of LIBS spectra from a field sample (left) and a basalt standard (right).

The echelle allowed us to (1) significantly increase our spectral resolution over that achievable using the small spectrograph used in the first prototype and (2) permitted us to monitor most of the spectral region (200-1000 nm) useful for LIBS on each laser shot. This greatly increased the data acquisition rate over that achievable with the first system. For the 2001 field test the instrument was mounted on a tripod, as the K9 rover was not at this test and the FIDO rover was fully instrumented. However, just by quick-look comparisons in the field we were able to make a number of qualitative conclusions regarding the range of compositions at the site, the weathering surfaces, etc. It was immediately clear from the shape of the spectra that nearly all the rocks had the composition of diorites and metagabbros. In addition, we were able to immediately answer questions (from the rover team) about the presence of calcite/dolomite in the weathering products, observe high Mn, Sr in desert varnish coatings, and observe very high Ba concentrations (confirmed by 2 high Ba peaks in the same spectrum) in an isolated sample.

4. References

1. A.K. Knight, N.L. Scherbarth, D.A. Cremers, and M.J. Ferris, "Characterization of Laser-Induced Breakdown Spectroscopy (LIBS) for Application to Space Exploration," Appl. Spectrosc. 54, 331 (2000).

2. R.C. Wiens, R.E. Arvidson, D.A. Cremers, M.J. Ferris, J.D. Blacic, and F.P. Seelos,IV, "Combined remote mineralogical and elemental measurements from rovers: Field and laboratory tests using reflectance and laser induced breakdown spectroscopy," J. Geophys. Res., Planets, accepted for publication (2002).

LIBS for Real-Time Equivalence Ratio Measurements in a Spark-Ignited Engine

[1]Francesco Ferioli, [2]Paulius V. Puzinauskas, [1]Steven G. Buckley*

[1]Department of Mechanical Engineering, University of Maryland, College Park, MD
* = Corresponding Author; 301-405-8441, buckley@eng.umd.edu

[2]Department of Mechanical Engineering, U.S. Naval Academy, Annapolis, MD

Abstract:

The instantaneous air-to-fuel ratio (A/F) has a large effect on spark-ignited engine performance. Specifically, fluctuations in A/F influence performance, efficiency, and engine-out emissions. Benefits of improved control of A/F include enhancement of the aforementioned metrics, as well as potential for extension of the lean limit. Current direct research measurement methods providing data for individual charge A/F are limited to in-cylinder Raman scattering measurements of nitrogen and fuel. Indirect methods that have been applied to transient engine control include mapping using neural network algorithms, applied to engine airflow, and feed-forward control based on engine models. Emission sensing has been primarily limited to flow sensors such as the UEGO (Universal Exhaust Gas Oxygen) sensors, which are too slow to resolve individual cylinder / charge A/F.

This paper examines the ability of LIBS to measure individual charge A/F using atomic emission signals of C, H, O, and N in distinct combinations, particularly using lines in the 700-800 nm range. The distinct advantage of this technique over Raman scattering is that it can be done post-combustion, in the exhaust header, and still provide nearly instantaneous information for feedback and control. Measurements were made at up to 20 Hz in a GM Quad 4 engine. The benefits and accuracy associated with various spectral regions are evaluated and the optimum measurement strategy is assessed for its usefulness as a real-time engine A/F diagnostic for engine monitoring and control.

ENHANCEMENT IN THE SENSITIVITY OF LIBS USING MAGNETIC FIELD AND SEQUENSIAL DOUBLE LASER PULSE

V. N. Rai*, A. Kumar, F. Y. Yueh and J. P. Singh
Diagnostic Instrumentation and Analysis Laboratory
Mississippi State University
205 Research Boulevard, Starkville, MS 39759-7704 (USA)
e-mail:singh@dial.msstate.edu, * on leave from CAT, Indore-452013, India

ABSTRACT

The study of emission from laser-produced plasma from liquid jet is reported. Laser –induced plasma expanding in the magnetic field provides a 1.5-2 times enhancement in the plasma emission where as sequential double laser pulse excitation enhances the emission by more than four times.

1. INTRODUCTION

Laser-induced breakdown spectroscopy (LIBS) is a laser-based diagnostics being used as an analytical tool for determining the elemental composition in solid, liquid and gaseous samples [1-2]. It provides information much faster than other laser or chemical analysis techniques. An important feature of this technique is that it requires either a little or no sample preparation and can be used in harsh as well as difficult environmental conditions. It typically samples a very small amount of material (0.1 μg to 1 mg) for analysis purpose, which makes LIBS as a non-destructive technique. A high intensity pulsed laser operating at a fixed frequency is utilized to generate luminous micro-plasma from different types of targets. The elemental analysis of the sample using this technique is accomplished by recording the emission from the elemental atoms or ions present in the plasma plume. Although, comparatively less attention has been paid to the study of liquid samples, the requirement of online monitoring of some long half-life radioactive material in nuclear waste such as technetium (Tc) has made this subject more interesting. LIBS has been found as a suitable technique for online monitoring of trace elements at high and moderate concentrations, but still a serious effort is needed to make this system versatile for very low concentration measurements. Various techniques such as application of high intensity pulsed magnetic field [3], the use of purge gas, oblique incidence of lasers and double pulse excitation [4] were used to improve its sensitivity.

The main aim of the present study is to evaluate the effect of steady magnetic field and double pulse excitation on the sensitivity of LIBS in the study of liquid samples in order to improve its sensitivity.

2. EXPERIMENTAL SET-UP

The experimental set-up used for recording the LIBS spectrum from the laminar jet of liquid uses a Q-switched, frequency-doubled Nd:YAG laser (Continuum Surelite III) that delivers energy of ~ 400 mJ at 532 nm in 5-ns time duration. The laser was operated at 10 Hz during this experiment and was focused on the target (in the center of the liquid jet) using an ultraviolet (UV) grade quartz lens of 20-cm focal length. The same focusing lens was used to collect the optical emission from the laser-induced plasma. Two UV grade quartz lenses of focal length 100 mm and 50 mm were used to couple the LIBS signal to an optical fiber bundle. The fiber bundle consists of a collection of 80 single fibers of 0.01-mm core diameter. The rectangular exit end of the optical fiber was coupled to an optical spectrograph (Model HR 460, Instrument SA, Inc., Edison, NJ.) and used as an entrance slit. The spectrograph was equipped with 1800 and 3600-l/mm diffraction grating of dimension 75 mm × 75 mm. A 1024 × 256 element intensified charge-coupled device (ICCD) (Princeton Instrument Corporation, Princeton, NJ), with a pixel width of 0.022 mm, was attached to the exit focal plane of the spectrograph and used to detect the dispersed light from the laser-produced plasma. The detector was operated in gated mode with the control of a high voltage pulse generator (PG-10, Princeton Instruments Corporation, Princeton, NJ) and was synchronized to the laser output. Data acquisition and analysis were performed using a personal computer. The gate delay time and gate width were adjusted to maximize the signal-to-background (S/B) and signal-to-noise (S/N) ratio, which is dependent on the emission characteristics of the elements as well as the target matrix. Around 100 pulse spectra were accumulated to obtain one spectrum in order to increase the sensitivity of the system and reduce the standard deviation. To study the effect of magnetic field, liquid jet was passed in between the poles of two magnets providing ~5 kG magnetic field. Another Nd:YAG laser having nearly similar parameters as the previous laser was used for the double pulse experiments. The laser beams from

both the lasers were made collinear using a thin film polarizer. Both the lasers were focused nearly at the same place. However, a programmable pulse generator decides the time delay in the arrival of both the lasers at target.

3. RESULTS AND DISCUSION

3.1 Effect of Steady Magnetic Field

Manganese (Mn) and magnesium (Mg) were chosen as the surrogate element of technetium for laboratory experiments. The optical emission from the laser-induced plasma from a liquid jet target having manganese in low concentration (10 ppm) was recorded in the absence and presence of magnetic field (~5 kG). All the spectra in the case of manganese were recorded after a 10-μs time delay from the laser pulse so as to avoid the high background emission from the hot plasma. Fig. 1 shows the spectra of Mn solution recorded in the absence and presence of the magnetic field, when the laser was operated at a laser energy of ~ 140 mJ. Three strong peaks were observed at the wavelengths of 403.08, 403.31 and 403.45 nm. These lines were assigned as neutral line emissions from the Mn atom. Similar spectrum was observed in the presence of the magnetic field, but with an enhancement of ~ 1.5 times in the intensity of line emission. Enhancement was nearly the same for all the emission lines at three wavelengths. The Mn spectra recorded at the laser energy of ~ 280 mJ, in the absence of magnetic field, showed that both the line as well as the background intensity increased with an increase in laser energy. This increase in emission with an increase in laser intensity is due to an increase in ablation from the target, which is directly proportional to laser intensity.[1] However, it was found that both the background as well as the line emission intensity decreased in the presence of the magnetic field (laser energy 280 mJ).

Emission spectra of various other elements, such as magnesium (Mg), chromium (Cr) and titanium (Ti) in the liquid solution, were recorded in the presence of a magnetic field. Similar enhancement was noted in the emission intensity in the presence of magnetic field for all these elements. Magnesium, chromium and titanium all have three strong emission lines in the wavelength range near 279, 425 and 363 nm, respectively. The spectrum of chromium in aqueous solution in the presence of a magnetic field showed an enhancement in intensity of nearly ~1.8 times at a laser energy of 280 mJ. The enhancement factors were different for different elements, which ranged from 1.3-1.8 for similar experimental conditions in lower to higher laser energy range. This indicates that the enhancement factors may be dependent on the transition probabilities of the emission lines and the dynamics of the atoms in the plasma.

The limit of detection (LOD) of manganese in the absence of magnetic field (1.74 ppm) improved (0.72 ppm) in the presence of magnetic field

3.2 Effect of Double Pulse Excitation

In the double pulse excitation experiment, study was performed on a Mg solution, which has triplet line emission in UV spectral range. The spectrum of this element was helpful in simultaneous study of the behavior of line emission from ions and neutral atoms under the effect of double pulse excitation. The spectrum of magnesium was recorded in the single and double pulse excitation mode. The double pulse excitation spectrum was recorded at 4 μs gate delays for 2 μs inter-pulse separations between the lasers, when emission was nearly maximum. The single pulse excitation spectrum was recorded at 1 μs gate delay where the emission is maximum. The spectrum showed mainly two dominant line emission due to ion at 279.55 and 280.27 nm. The spectrum under double pulse excitation shows more than 4 times (peak to peak) enhancement in the line emission intensity. Background emission also had a higher level in double pulse than the single pulse excitation. Either no or very small neutral line emission was seen here at 285.20 nm, because the spectrum was recorded at lower gate delay, when the plasma remained hot, and the observation of neutral atomic line was negligibly small.

Figure 2 shows the spectra recorded in double pulse mode when the inter-pulse interval between both the lasers was zero and 3 μs. A very small enhancement was noted in the emission intensity when the delay between both the lasers was zero in comparison to single pulse experiment. In fact, this is the case of addition of intensity. However, emission intensity was enhanced by nearly > 4 times (peak to peak) when the delay between both the lasers were increased to 3 μs. This indicated that the first laser pulse induced the plasma, which expanded normal to the target surface, and the second laser interacted with preformed plasma. The interaction of the second pulse with expanding plasma increased the probability of absorption of the laser, which heated the plasma and finally excited more numbers of plasma particles to its excited

state. Even the second laser added up in the vaporization (ablation) of the material. This could be the reason behind the enhancement in the emission intensity of magnesium in the presence of a delayed second laser, clearly indicating that the enhancement in the signal was not due to the simple addition of intensity of lasers.

A strong emission from magnesium neutral line (285.20 nm) was also observed in this experiment at 10 μs gate delay, because the plasma was comparatively cool at that time. The neutral line emission also showed similar enhancement in the emission when the inter-pulse delay was increased from zero to 3 μs. At the same time, background emission decreased with an increase in inter-pulse separation. The LOD of magnesium improved from 0.23 ppm in single pulse excitation to 61 ppb in double pulse excitation mode.

4. CONCLUSION

It was found that presence of steady magnetic field and double pulse excitation enhanced the sensitivity of LIBS, which may be helpful in making a technetium monitor based on LIBS technique.

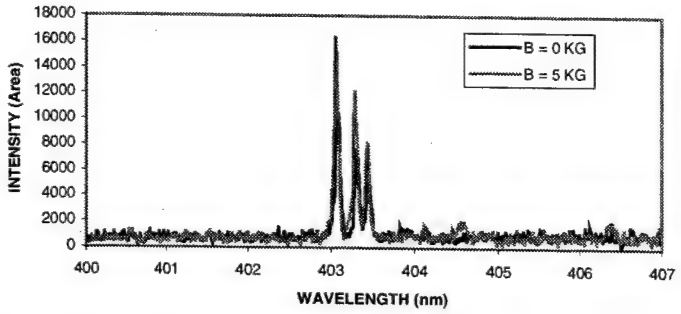

Fig. 1 LIBS spectra of manganese in the absense (B = 0 kG) and presence (B = 5 kG) of magnetic field

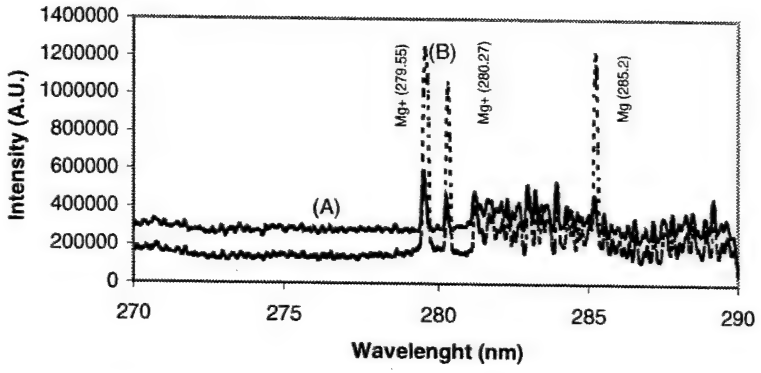

Fig. 2 LIBS spectra of magnesium (A) Single pulse and (B) Double pulse Excitation

ACKNOWLEDGMENT

This work is supported by U.S. Department of Energy cooperative agreement no. DE-FC26-98 FT 40395

REFERENCES

1. L.A.Radziemski, D.A.Cremers (Ed.)."Spectrochemical analysis using plasma excitation,"in Laser-Induced Plasma and Applications, Marcel Dekker, New York, NY, Ch 7, pp.295-325 (1989).
2. F.Y.Yueh, J.P.Singh and H. Zhang, "Laser induced breakdown spectroscopy: Elemental analysis," Encyclopedia of Analytical Chemistry, John Willey & Sons, Ltd. Vol. **3** 2065-2087 (2000).
3. K.J.Mason and J.M.Goldberg, "Production and initial characterization of a laser induced plasma in a pulsed magnetic field for atomic spectroscopy," Anal. Chem. **59** 1250-1255 (1987).
4. S. Nakamura, Y.Ito, K. Sone, H. Hiraga and K.I. Kaneko, " Determination of iron suspension in water by laser induced breakdown spectroscopy," Anal. Chem. **68** 2961-2966 (1996).

Assessment of Metal and Chlorine Emissions from Molten Salt Oxidation using Laser-Induced Breakdown Spectroscopy

[1]Jaya Kumar P. Patil, [2]Jerry S. Salan, [1]Steven G. Buckley*

[1]Department of Mechanical Engineering, University of Maryland, College Park, MD
* = Corresponding Author; 301-405-8441, buckley@eng.umd.edu

[2]Indian Head Naval Surface Warfare Center, Indian Head Division, Indian Head, MD

Abstract:

Molten salt oxidation is used by the U.S. military and other organizations as a treatment process for waste and demilitarized propellants, mixed wastes, and hazardous wastes. In this process, a salt such as sodium carbonate is heated above its melting point, and the waste is introduced into the molten salt bath, where it oxidizes. Benefits to this technology include the high thermal mass of the salt, which enhances the stability of the oxidation process in comparison with traditional combustion processes, the controllable residence time in the salt bath, and the chemical and physical characteristics of the salt. Salts such as sodium carbonate tend to bind chlorine ($Na_2CO_3 + 2Cl \Rightarrow 2NaCl + CO_2 + 0.5O_2$), significantly reducing acid gas emissions and potentially preventing dioxin and furan formation downstream. In addition, the high surface area of the bubbles formed during the oxidation process may trap particulate matter, reducing particulate and toxic metal emissions.

This investigation focuses on the retention of metals and chlorine from chlorinated and metal-containing waste injected into a laboratory-scale molten salt reactor (Fig 1). Trichloroethane and chlorobenzene are injected into the reactor, and Cl emissions are measured. Particular metals, such as Mg and Al (common in propellants) are injected into the reactor to assess their retention in the salt using LIBS. In addition, using LIBS we assess the impact of salt vaporization / mobilization as a loss mechanism for salt in these reactors. Surprisingly, we were also able to monitor the deterioration of the reactor itself (Fig. 2 is shown as an example). The results outlined in this work provide an understanding of the effectiveness of molten salt oxidation in retention of halides and metals across a range of operating conditions, and highlight some of the advantages and disadvantages associated with the molten salt oxidation process.

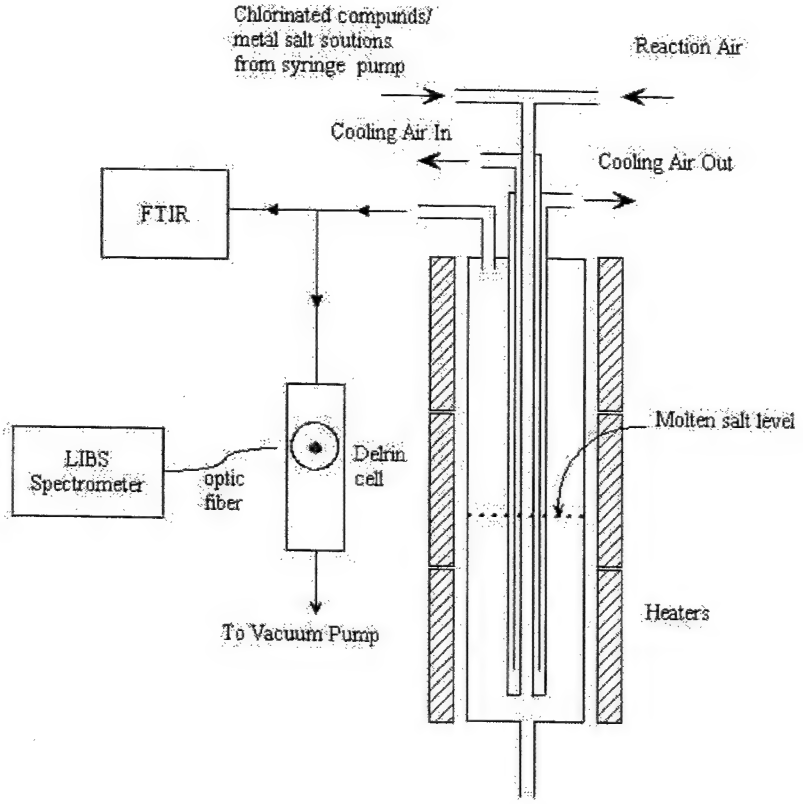

Figure 1: The UMCP molten salt oxidation reactor.

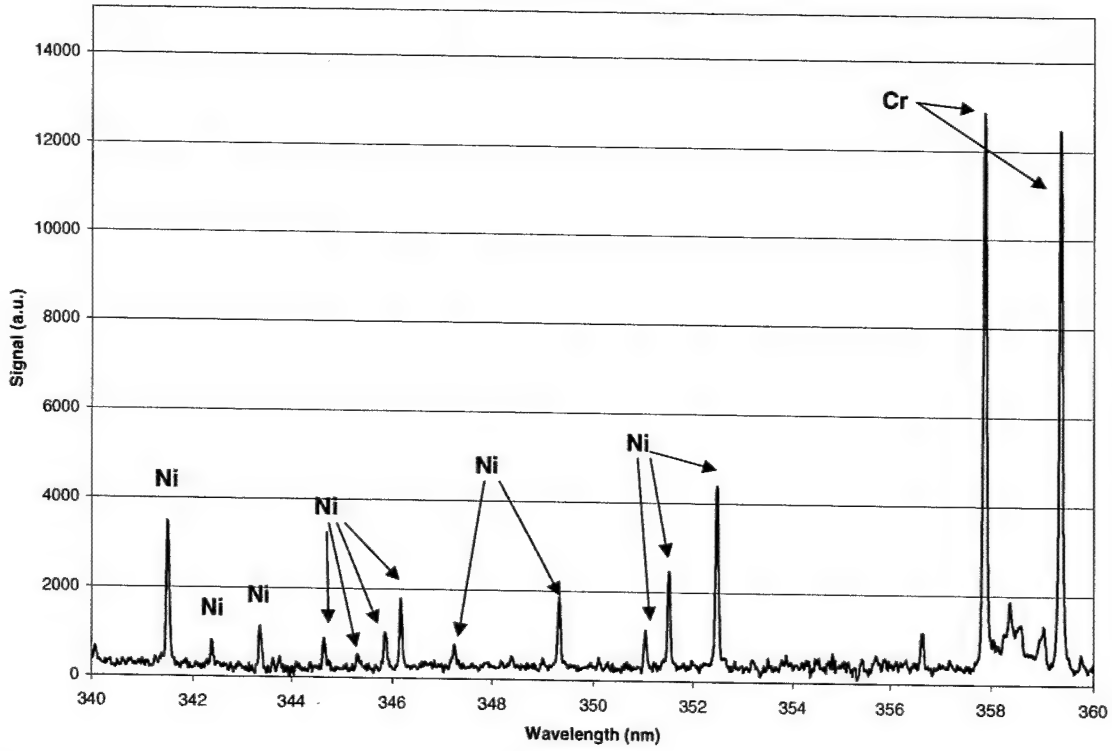

Figure 2: Corrosion from the Inconel MSO reactor revealed in exhaust.

Influence of Spark Size and Temperature on LIBS Gating for Optimal Detection Limits for Toxic Metals

Steven G. Buckley*, Gregg Lithgow, Francesco Ferioli, Elizabeth Smallwood

[1]Department of Mechanical Engineering, University of Maryland, College Park, MD
* = Corresponding Author; 301-405-8441, buckley@eng.umd.edu

Abstract:

Recent work[1] has experimentally measured temporal gating parameters that optimize the signal-to-noise ratio for six of the Resource Conservation and Recovery Act (RCRA) metals, arsenic, beryllium, cadmium, chromium, lead, and mercury. This work was accomplished at relatively large laser pulse energies (175 and 330 mJ / pulse), and over a wide range of temporal delay (2 – 50 μs) and gating (2 – 150 μs) in various combinations. This work concluded that each element had a distinct optimum in the delay and gate yielding the best signal-to-noise ratio.

This work builds upon this previous study, experimentally investigating additional parameters, ignored in the previous study, that affect the optimal temporal gating and the signal strength for the selected RCRA metals. Specifically, the initial size and temperature of the plasma relate to the rate of heat loss that will be experienced in the plasma volume; this temperature history has an impact upon the optimal delay and gate for a particular metal. In addition, the size of the plasma and the optical density of the plasma at a particular wavelength relate to the signal that will be collected for a particular elemental mass concentration in the plasma volume. Experiments are performed relating the initial size and temperature of the plasma to the optimum detection delay, gate, and the observed SNR for submicron aerosol of the RCRA metals. The results are compared with simple theoretical analysis predicting emission intensity, based on transition probabilities and line strengths, for the measured conditions. This analysis, thus facilitates optimization of LIBS parameters for detection of these RCRA metals, and may be extended to additional elements.

[1] B.T. Fisher, H.A. Johnsen, Steven G. Buckley, and David W. Hahn, "Temporal Gating for the Optimization of Laser-Induced Breakdown Spectroscopy Detection and Analysis of Toxic Metals." *Applied Spectroscopy*, 55:10, pp. 1312-1319 (2001).

Reduction of spatial effects on emission line intensity observed from single aerosol particles via diffuse reflectance from an integrating sphere

Emily Gibb, Erica Corbett, Igor Gornushkin, Ben Smith, David Hahn, Jim Winefordner, Univ. of Florida, USA.

Collection of emission via diffuse reflectance from an integrating sphere reduces the influence of spatial effects observed when viewing LIBS plasma emission from the backscatter collection mode.

Summary

The precision in laser-induced breakdown of single particles in air is limited by geometric factors relating to the position of the particle in the breakdown plasma and the variability in the location of breakdown along the laser beam waist. Fluctuations in laser power, choice of analytical line, and timing parameters such as gate delay and gate width also play a role and have been widely investigated.[1] Poor precision in single particle measurements can limit the ability to extract particle size distributions from spectral intensities.[2]

The typical collection geometry for single particle LIBS in air uses a pierced or dichroic mirror to view the plasma emission in the backscatter configuration. In this viewing geometry, the intensity of the observed emission for a single particle interaction with the laser beam is highly dependent upon the location of the particle when it interacts with the laser pulse. Generally, the location of the breakdown event is dictated by the presence of a particle[3] and therefore depends upon the trajectory of particles through the laser volume. We have evaluated an integrating sphere as a means of homogenizing the light collection process and reducing the influence of spatial effects within the laser-particle interaction. This integrated sphere was constructed from aluminum and is coated with barium sulfate, which diffusely reflects a large amount of the plasma emission. This emission is collected via a fiberoptic bundle that mounted at the surface of the sphere wall. The schematic for both of these collection geometries is illustrated in Figure 1.

The precision and signal magnitudes were compared for both the backscatter and integrated sphere collection geometries. Various sample systems were employed including pure gases, and mixed gases with and without aerosols formed in pneumatic and ultrasonic nebulizers. Particle size distributions obtained from the two collection geometries and were compared to size distributions obtained from a traditional laser light scattering instrument.

---

[1] Castle, B.K.; Talabardon, K.; Smith, B.W.; Winefordner, J.D. *Applied Spectroscopy* **1998**, 52, 649-657.

[2] Hahn, DW *Spectrochimica Acta PartB: Atomic Spectroscopy* **2002**, *in press.*

[3] Hsieh, W.F.; Eickmans, J.H.; Chang, R.K. *Journal of the Optical Society of America B* **1987**, 4, 1816-1820.

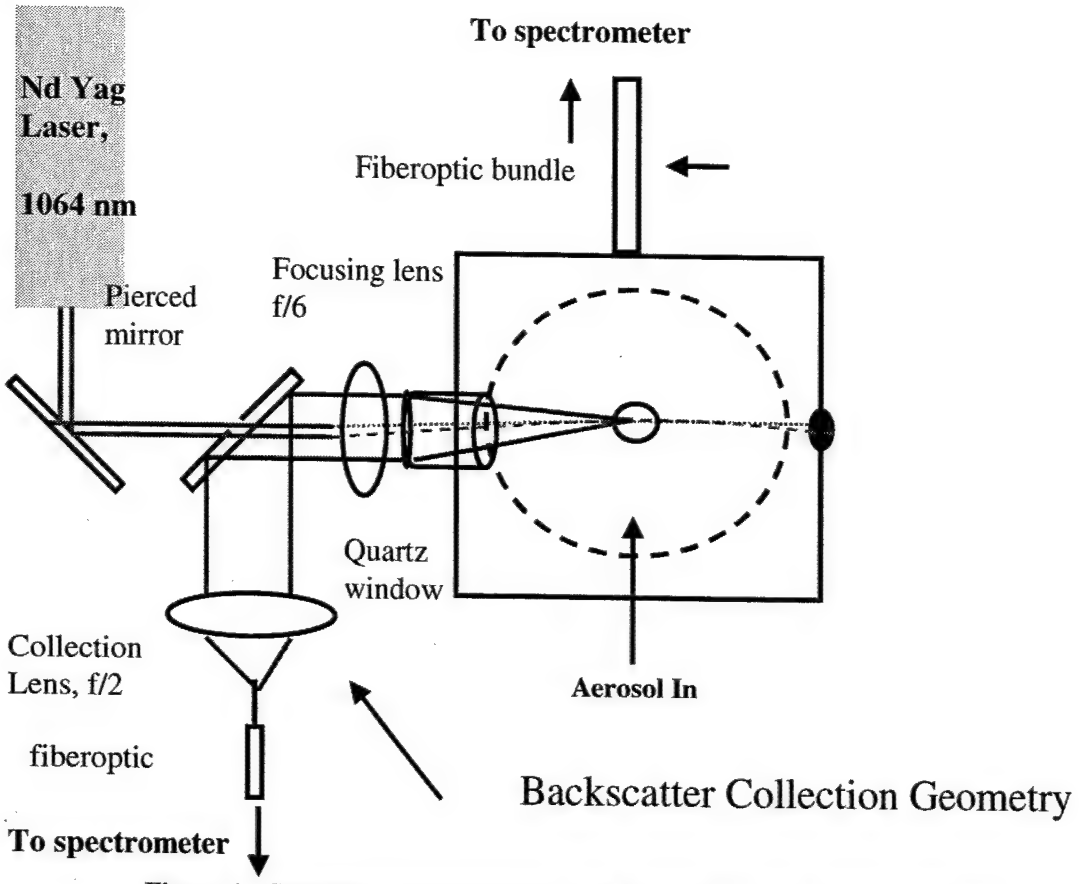

Figure 1: Schematic of backscatter and integrated sphere light collection.

Two-photon excited fluorescence of donor-acceptor conjugated organic materials in crystalline form

Ekaterina V. Sevostiyanova, David. M. Sammeth, Mikhial Yu. Antipin
Department of Chemistry, New Mexico Highlands University, Las Vegas, New Mexico 87701
katerina@kremlin.nmhu.edu

Abstract: Several organic materials were found to possess high efficiency two-photon excited fluorescence in crystalline form. They do not display considerable molecular two-photon absorption (TPA) resonance that is due to intramolecular charge transfer. The crystal structures of the compound were investigated. It was determined that tight stacking packing of molecules in all crystals with short distances between stacking planes results in high degree of pi-orbital overlap between molecules. These pi-systems interactions lead to new electronic states and, we believe, responsible for the fluorescent properties in the crystals.

OCIS codes: (160.0160) Materials

1. Introduction

Two-photon absorption is the simultaneous absorption of two photons that combine their energies to produce an electronic excitation that is conventionally caused by a single photon. Materials with high TPA cross section are used widely in optical applications such as optical data storage, up-converted lasing, lithographic microfabrication [1-2]. Although different classes of two-photon TPA active molecules have been discovered [3-5], only a small number of organic molecules were reported to have remarkable two-photon pumped (TPP) up-conversion lasing properties. Among them, just few have lasing efficiencies specified for practical devices. Most of neutral molecules pack in the lattices with van der Waals interactions or with weak chemical interactions as hydrogen bonds. As in that kind of structure probability of the intermolecular charge transfer is negligible, electronic properties of most molecular crystals can be described by characteristics of corresponding molecules. During the past decade a number of organic crystals with so high TPA efficiency that could not be deduced from molecular features were reported [6-8].

2. One- and two- photon excited fluorescence

We found several materials ([(9-ethyl-9*H*-carbazol-3-yl)methylene]malononitrile **(I)**, {(2*E*)-3-[4-(dimethylamino)phenyl]prop-2-enylidene}malononitrile **(II)**, and [4-(dimethylamino)benzylidene]malononitrile **(III)**) that display high efficiency TPA properties only in crystalline form and investigated the crystal structure features responsible for the properties. The powdered crystals were excited using 1064 nm Q-switched Nd:YAG laser (7ns, 10 Hz, 10 mJ per puls). The fluorescence greenish-yellow (545 nm maximum), red (740nm maximum),

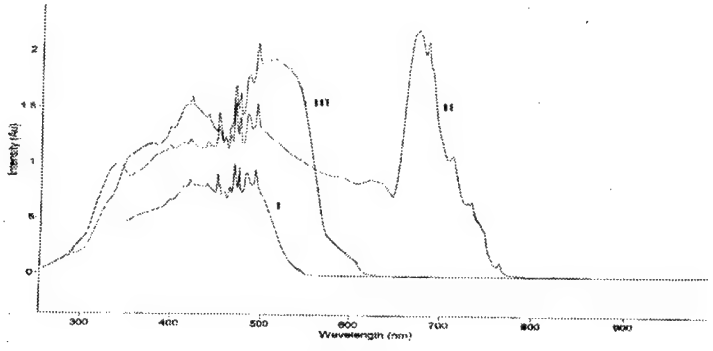

Fig. 1. One-photon excitation spectra for compounds **I**, **II**, and **III** in crystalline form

and orange (570 nm maximum) light of compounds **I**, **II**, and **III** respectively was detected using Hamamatsu HC-120 photomultiplier assembly. The centrosymmetric crystal structure of **I** and **II** materials prevents any second

harmonic generation. Although compound **III** crystallizes in noncentrosymmetric P21 space group it does not show any considerable second order response at 1064 nm [9]. Fluorescence intensity versus laser intensity square dependence was obtained to confirm two-photon process. One-photon excited fluorescence properties were investigated as well. Both excitation and emission spectra were measured using double-grating JY HORIBA spectrofluorometer FL3-22. The excitation spectra of all compounds in crystalline form display broad bands in UV-visible region. No bands were found in infrared region at 1064 nm for one-photon excitation process. Fig. 1.

3. X-ray analysis

The investigation of X-ray data was carried out for each compound. The space groups and lattice constants are P21/c (a=12.731(0) Å, b=4.216(0) Å, c=26.640(0) Å), P21/c (a=10.060(2) Å, b=15.957(3) Å, c=7.938(2) Å) [9], P21 (a=3.951(4) Å, b=14.078(11) Å, c=9.499(9) Å) [10] for **I, II, III**, respectively. All structures reveal close stacking packing with short distances between the stacking planes. In **I** planar molecules pack in columns along (010) direction in the crystal. The molecules in the column are related by translation along *b* axis. The distance between staking planes was calculated 3.56 Å. The crystal packing for the compound **I** is shown in the Fig. 2. In **II** planar molecules are packed in layers parallel to the unit cell diagonal (10-1). Angle between this crystallographic plane and the mean molecular plane is 4.2°. The distance between stacking planes is equal to 3.59 Å. In **III** planar molecules pack in columns along (100) direction. The molecules in the columns are related by translation along *a* axis. The distance between stacking planes was found to be 3.54 Å. All calculations were performed using SHELXL97 program package [11].

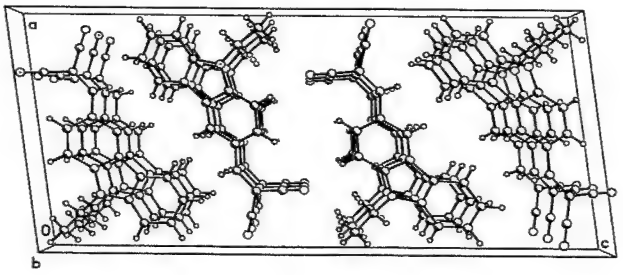

Fig. 2. Crystal packing diagram for the compound **I** down the *b* axis

4. Discussion

This tight molecular packing results in a π-systems interaction between adjacent molecules along the stack. To prove it one-photon excited fluorescence spectra were measured in solutions (DMF, EtOH) and in crystalline form for each compound. The large red shift of the solid-state emission to the emission in solution that results from high degree intermolecular π-π interaction was observed in the spectrum of each compound. The correlation of the bathochromic shift of the crystalline fluorescence band with the degree of intermolecular π-π interaction has already been done for some alkenes and polycyclic aromatic molecules [12]. This large shift (about 150 nm) for the compound **II** is shown in Fig. 3.

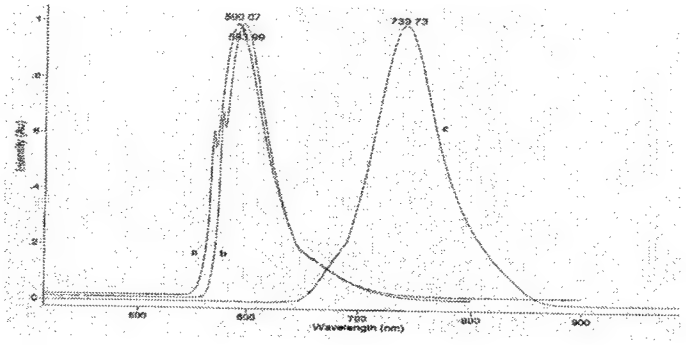

Fig. 3. One-photon excited fluorescence spectrum of compound **II**: a) EtOH solution; b) DMF solution; c) crystalline form

The high degree of π-orbital overlap between molecules leads to new electronic states in the crystal that causes high efficiency two-photon fluorescence that could not be deduced from molecular responses.

5. References

1. S. Maruo, O. Nakamura, and S. Kawata, "Three-dimensional microfabrication with two-photon-absorbed photopolymerization", Opt. Lett. **22** (**2**), 132-134 (1997).

2. J. H. Stricker and W. W. Webb, Opt. Lett. **16**, 1780 (1991)

3. M. Albota , D. Beljonne, J.-L.Bredas, J. E. Ehrlich, J.-Y. Fu, A. A. Heikal, S. E. Hess, T. Kogej, M. D. Levin, S. R. Marder, D. McCord-Maughon, J. W. Perry, H. Rockel, M. Rumi , G. Subramaniam, W. W. Webb, X.-L. Wu, C. Xu, "Design of organic molecules with large two-photon absorption cross sections", Science **281**, 1653 (1998).

4. Sung-Jae Chung, Kyoung-Soo Kim, Tzu-Chau Lin, S. He. Guang, J. Swiatkiewicz, and P. N. Prasad, "Cooperative enhancement of two-photon absorption in multi-branched structures", J. Phys. Chem. B **103**, 10741-10745 (1999).

5. B. A. Reinhardt, L. L. Brott, S. J. Clarson, A. G. Dillard, J. C. Bhatt, R. Kannan, L. Yuan, G. S. He, P. N. Prasad, "Highly active two-photon dyes: design, synthesis, and characterization toward application", Chem. Mater. **10**, 1863 (1998).

6. V. S. Gorelin, E. A. Kozulin, "Two-photon excitation of luminescence in organic crystals", Kratk. Soobshch. Fiz. **7**, 66-70 (1992).

7. P. Feneyrou and P.L. Baldeck, "Intermolecular effects on the two-photon absorption spectrum of DEANST crystal", J. Phys. Chem. A **104** (**20**), 4764-4766 (2000).

8. G. Puccetti, S. G. Bott, R. M. Leblanc, "Efficient two-photon-induced fluorescence in a new organic crystal", J. Opt. Soc. Am. B **15**(**2**), 789-801 (1998)

9. T. V. Timofeeva, V. N. Nesterov, F. M. Dolgushin, Y. V. Zubavichus, J. T. Goldshtein, D. M. Sammeth, R. D. Clark, B. Penn, M. Yu. Antipin, "One-pot polymorphism of nonlinear optical materials. First example of organic polytypes", Crys. Ing. **3**, 263-288 (2000)

10. M. Yu. Antipin, T. V. Timofeeva, R. D. Clark, V. N. Nesteron, M. Sanghadasa, T. A. Barr, B. Penn, L. Romero, and M. Romero, "Molecular crystal structures and nonlinear optical properties in the series of dicyanovinylbenzene and its derivatives", Phys. Chem. A **102** (**37**), 7222-7232 (1998)

11. G. M. Sheldrick, "SHELXL97. Program for the solution of crystal structures", University of Goettengen, Germany (1997).

12. I. Ortmann, S. Werner, C. Kruger, S. Mohr, K. Schaffner, J. Am. Chem. Soc. **114**, 5048 (1992)

LIBS analyses of Martian soils under controlled atmosphere

F. Colao, R. Fantoni, V. Lazic, A.Paolini[1]

ENEA, FIS-LAS, C.R. Frascati, V. E. Fermi 45, Frascati (RM), Italy
Tel. 06 94001, Fax 06 94005400

Abstract: LIBS measurements were performed under controlled atmosphere on the samples with the composition similar to the Martian crust. The experiment demonstrated that quantitative LIBS analyses are feasible in Mars-similar conditions.

Keywords: LIBS, soil, Mars

OCIS codes: (120.280) General

1. Introduction

Forthcoming international projects for extraterrestrial explorations include the development of compact instrumentation for in-situ analysis of Martian soil. LIBS technique, not requiring any sample preparation and suitable to multi-elemental analysis in different atmospheres, is very promising for such an application.

LIBS spectroscopy is well suitable as virtually non destructive technique for the remote sensing of geological material in situ as part of a lander scientific instrument package. The final instrument for extraterrestrial exploration must undergo very rigid constraints because of the hostile environmental conditions in terms of large temperature ranges, UV radiation sampling problem due to chemically active Martian dust. To this end the assessment of LIBS technique is now performed in several laboratories.

In order to ascertain the feasibility of in-situ operation of a LIBS probe on a Martian ROVER, in our laboratory LIBS measurements were performed on soil and rock samples with a composition very similar to the presumed composition of Martian crust [1-2]. Although the examined sample are of terrestrial origin, the results obtained are of significance because they represent how a direct LIBS analysis can be applied in a Martian environment.

Qualitative measurements were performed both in air at standard Earth atmospheric condition and in a synthetic Mars atmosphere in order to identify the most important spectral parts for the elemental analysis and to check the detectability of various trace elements in different operating conditions [3]. Quantitative analyses, for which we apply the plasma modeling and apply calibration coefficients [4], were preceded by the plasma characterization under air at atmospheric pressure and under the rarefied carbon dioxide rich Martian atmosphere. The latter measurements were aimed to determine the experimental parameters for which the plasma could be considered in Local Thermal Equilibrium in the case of use of the technique on board of a planetary exploration vehicle. The evolution of the excitation temperature for different atomic and ionic species was studied, together with the temporal behavior of the plasma emission and electron density. Once the optimal experimental conditions were found, LIBS analyses were performed on the samples with the known matrix composition in order to obtain calibration coefficients for all the detectable elements.

2. Experimental

The LIBS instrumentation is based on a Nd:YAG laser (Quanta System SYL-20, 1064 nm; 800 mJ; 8 ns; 10Hz) whose beam is focused by a quartz lens (f=20 cm) upon a solid sample to a spot of approximately 150μm diameter, generating an irradiance up to 5GW/cm^2. The samples are inserted in a three window cell which can be operate in vacuum down to 10^{-3} torr, or in controlled atmosphere. Six different samples can be introduced into the measuring chamber and measurements can be done in sequence for each sample. Every sample is selected when needed and

[1] ENEA student

contained in a rotating holder and thus exposing a fresh surface to each laser pulse. The chosen collection geometry is coaxial so minimising the effects related to sample miss-positioning, surface roughness, crater formation or attenuation from the aerosol cloud. The plasma emission is collected by means of a lens condenser matching a fiber optic bundle with the entrance slit of a Jobin-Yvon half meter spectrometer (TRIAX 550) equipped with a 2400 grooves/mm grating, allowing for a spectral resolution of 0.15 Å. The emission spectra are recorded by a gated optical ICCD (ANDOR Instaspec IV). Spectra are stored in a table top Personal Computer (Intel Pentium) which is also used for controlling experimental parameters and performing data elaboration.

The samples are rocks coming from different terrestrial sites. The samples E1, E2, E3, E4 and E5 are basalts form Etna (Sicily – Italy), while samples A1, A2, A3, A7, A8, A18, M5 and M6 are rock samples form Chilean Andes. A great care was taken to be certain that samples are not altered or contaminated by terrestrial pollution.
Conditions chosen for synthetic Mars atmosphere were the following: total pressure 10 mbar of pure CO_2 flowing at room temperature in a vacuum chamber formerly evacuated down to 10^{-2} mbar (with a residual O_2 pressure around 10^{-3} mbar).

3. Preliminary results

Data have been taken on samples in both conditions of normal laboratory air and rarefied CO_2 atmosphere. Preliminary data were taken examining several Chilean Andes samples in exactly the same experimental conditions (i.e. focussing and collection geometry, laser power, delay and width of the acquisition gate). At a first glance, the plume appears different in the two cases: at low CO_2 pressure the plume is diffuse with an approximately spherical shape with a well reproducible signal intensity, whereas in air it is brighter and characterized by great variations of both shape and signal intensity.

The general appearance of the collected spectra is the same, but they do differ in several respects. The intensity of spectrum in air is larger, as averaged on the full spectral range from the UV to the far red. This higher intensity can be explained taking into account the better coupling of the plume shape with the optical imaging characteristics of the collecting optics. However, in the UV region below 300nm features detected under rarefied CO_2 atmosphere are more prominent, due to the absence of atmospheric nitrogen absorption.

Another remarkable general feature is the observed narrowing of the emission linewidth under rarefied CO_2 atmosphere. The phenomenon is observed in all the examined spectral range, a significant example is shown in **Figure 1** in the UV. An even stronger effect has been detected on the Na emission near 588nm (not shown here), where the doublet appears completely resolved. A straightforward explanation is related to the reduced collisional broadening in the rarefied CO_2 atmosphere.

After collection LIBS spectra have been spectrally calibrated and emission assignment to major and minor constituents was performed. Qualitative analyses of different samples were bases on identification of atomic and ionic emission lines in the spectral region between 240 and 750 nm. The major elements detected in all the examined samples were: Al, Ba, Ca, Fe, Mg, Mn, Na, Si, Ti. Other elements detected in traces were: Cr, Cu, Mo, Ni, Sr, V, Zn.

Since our procedure of plasma modeling to obtain quantitative information on sample composition is based on the assumption of the LTE during the selected plasma observation window and on spectroscopic evaluation of the temperature, the latter parameter has been obtained for all the examined samples under different atmosphere. For each sample Boltzmann plot was applied on atomic iron emission in the spectral rang 300-500nm, temperature values were confirmed on spectral lines of atomic titanium in approximately the same spectral range. In the present experimental conditions the temperature value for samples in air resulted to be the same for the examined samples: T=7000+/- 1000 K, a value which is appreciably lower than T=11000+/-1000K obtained under rarefied CO_2 atmosphere. The latter result may be related to the less effective collisional cooling of the plasma produced under diluted CO_2 and might lead to a longer lasting spectrum. This observation would suggest to optimize conditions in Martian atmosphere by increasing both the observation window and the delay to lead to a further improvement in spectral resolution.

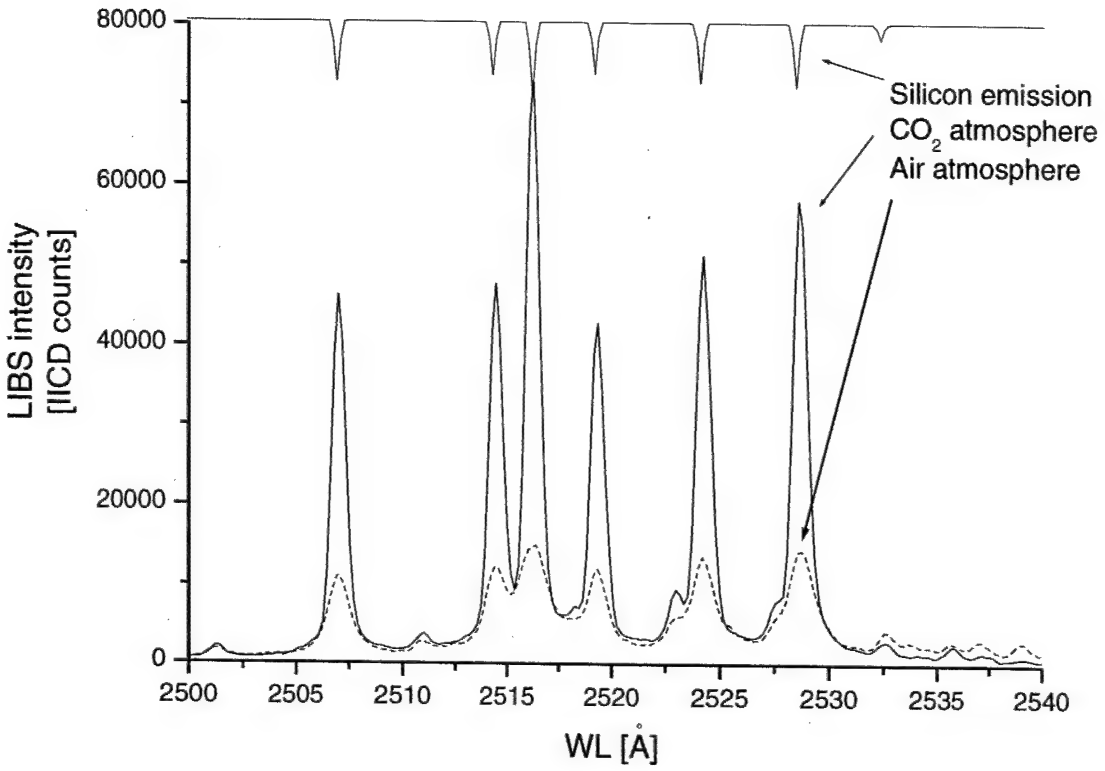

Figure 1 – An UV significant portion of LIBS spectra of the A18B sample taken under Earth and Martian atmosphere. The Silicon emission spectrum is shown for comparison.

4. Conclusions

In this work we demonstrate that LIBS technique can be successfully applied on Martian atmosphere to characterize rocks and dust at least as far as major constituents are concerned.

Optimization of the experimental parameters like laser energy, collection optics (FOV, image magnification), gate delay and width of the detector might lead to a sensitivity comparable or even better than for trace heavy elements in Earth atmosphere (better than 1ppm).

5. References

[1] R.Rieder, T.Economou, H.Wänke, A.Turkevich, J.Crisp, J.Brückner, G.Dreibus, H.Y.McSween Jr., "The Chemical Composition of Martian Soil and Rocks", Science, **278**, 1771-1774, (1997).

[2] H.G.M. Edwards, D.W. Farwell, M.M. Grady, D.D. Wynn-Williams, I.P. Wright, "Comparative Raman microscopy of a Martian meteorite and Antarctic lithic analogues", Planetary and space science, **47**, 353-362, (1999).

[3] F. Capitelli, F. Colao, M.R. Provenzano, R.Fantoni, G. Brunetti, N. Senesi "Determination of heavy metals in soils by laser induced breakdown spectroscopy", Goederma, **106**, 46 – 62 (2002).

[4] V. Lazic, R. Barbini, F. Colao, R. Fantoni, A. Palucci "Self-absorption model in quantitative laser induced breakdown spectroscopy measurements on soils and sediments" Spectrochimica Acta B, **56**, 807-820 (2001).

6. Acknowledgment

This work was undertaken under the ASI/ENEA contract n. 1/R/065/01.

NOTES

Femtosecond LIBS

Friday, September 27, 2002

Yoshihiro Deguchi, Mitsubushi Heavy Ind. Ltd., Japan,
Presider

FA
8:30am–9:50am
Room: Royal Palm III

Exotic LIBS-Femtosecond Domain

Dr. Dennis R. Alexander
University of Nebraska-Lincoln, 248 WSEC, Lincoln, NE 68588, USA
402-472-3091, FAX 402-472-5083, Email: alex@femto.unl.edu

Abstract: Femtosecond lasers with pulse lengths down to 5 fs are available for performing femtosecond laser induced breakdown spectroscopy (FLIBS). The linear and nonlinear effects of these short pulses interacting with materials produce complicated ionization processes and plasmas. Experimental FLIBS has been carried out and the results will be presented on several materials.

OCIS codes: (280.0280) Remote Sensing, (300.0300) Spectroscopy

1. Introduction

Lasers generating ultrashort light pulses from about 5 to 100's of femtoseconds are now available to researchers for carrying out femtosecond laser induced breakdown spectroscopy. Recent technological advances in ultrafast technologies have resulted in the generation of light packets consisting of only a few cycles of the electric and magnetic fields. The spatial extension of these wave packets along the direction of propagation is limited to a few times the wavelength of the radiation (~ 0.5-1 μm in the visible and near-infrared spectral range). On the other hand a 100 fs pulse has a packet length of 30 μm. When using diffraction limited parabolic mirror for focusing and moderate pulse energies of one microjoule, peak intensities at the focal spot of over 10^{15} W/cm^2 can be achieved. The corresponding amplitude of the electric field at these intensities approaches 10^9 V/cm^2. These field strengths are high enough to trigger optical field ionization. Hence, detachment of the first electron is completed at substantially higher field strength and the optical-field ionization rate becomes comparable to the laser field oscillation frequency. The released electrons gain unprecedented kinetic energies (up to and beyond the keV level) during the first field oscillation cycle following their detachment, and a substantial fraction of the ionization occurs during one cycle of light. In comparison, long pulsed laser systems containing many field oscillation cycles depletes the atomic ground state. The above linear and nonlinear processes result in very precise thresholds for plasma formation since femtosecond interactions produce their own source of free electrons to initiate the plasma formation process. Longer nanosecond pulses produce breakdown at less defined thresholds. This paper discusses some preliminary results into the use of femtosecond lasers for performing FLIBS.

2. Experimental Facilities

The Center for Electro-Optics at the University of Nebraska-Lincoln has three femtosecond laser systems that can be used for FLIBS. The first system is a Spectra Physics Millennium pumped Tsunami oscillator that is then amplified with an Applied Photonics Industries Nd:YLF laser. This system typically produces 100's of fs pulses at a center wavelength of 795 nm. The system is capable of producing 900 mJ pulses at a frequency that can be selected from 1 to 1000 Hz. The second laser system is a FemtoSource Compact manufactured by FemtoLasers, Viena, Austria. This system is capable of producing < 10 fs pulses. The laser operates at a wavelength centered at 795 nm and at a frequency of 75 MHz. The third femtosecond laser system is a Spectra Physics Millennium Pumped Spitfire system that is pumped with a Kapteyn-Murnane oscillator. This system produces < 35 fs pulses at a frequency of 1000 Hz with 900 mJ of pulse energy. Plasmas are produced by focusing the laser pulses on the material of interest using both lens and parabolic mirrors. Femtosecond produced plasmas are collected on an Instruments SA Optical Multi-channel Analyzer (OMA). The detection device is a Princeton Instruments gated CCD array, Model ICCD-1-24MG-E, with a 6-phase array.

3. Results

In many LIBS applications there is a need to limit the degree of damage to the surrounding material. Because of the unique breakdown thresholds offered by the femtosecond laser, it is possible to produce very small damage sites. Shown in Fig. 1 is a one micron hole drilled in a silicon wafer. In this application, FLIBS was used to investigate the penetration of a beam to various layers in the silicon chip. By monitoring the spectral components of the emission, it is possible to determine which layer in the chip one has reached. This has important applications in chip failure analysis.

One of the problems with using longer pulsed lasers is that they produce plasmas containing large continuum components. The usual mode of performing LIBS is to wait for these components to die out before the collection of the longer lived atomic emission lines. Fig. 2 compares the difference between femtosecond produced plasmas on an aluminum target and the nanosecond case. The advantage of the femtosecond spectrum is that the peaks emerge from the base line while in the nanosecond case the peaks appear on top of a broad continuum. Fig. 3 demonstrates the difference in the size of the damage region for nanosecond laser ablation as compared to that achieved for femtosecond ablation. Further information will be presented that relate the plasma formation and the damage to the unique way that plasmas are produced during femtosecond interactions. Advantages and disadvantages of using femtosecond LIBS will be presented in greater details.

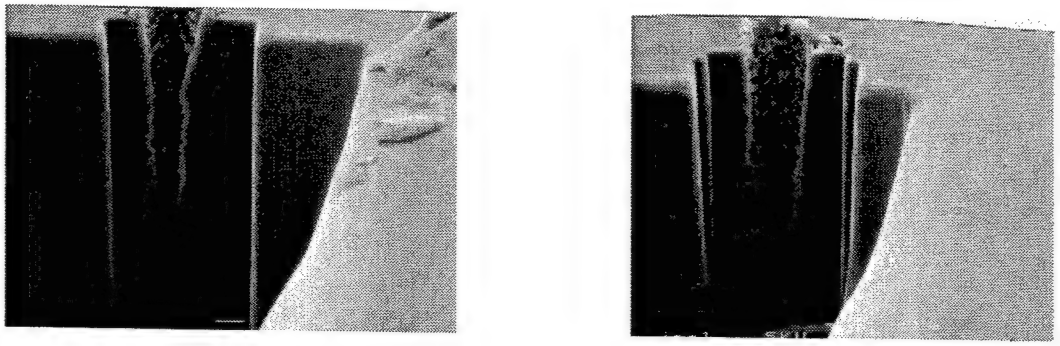

Fig. 1 Femtosecond lasers allow less the than the diffraction limit holes to be placed in materials. Another advantage is that high aspect ratio holes can be drilled in materials. The material in these images is an AMD silicon chip.

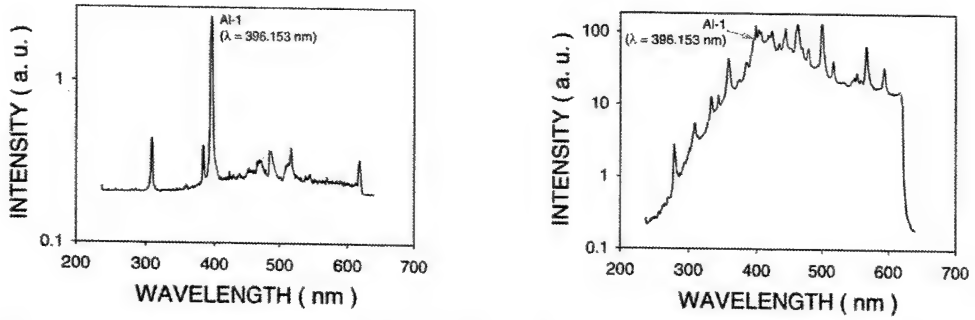

Fig. 2 Comparison of femtosecond produced plasma emission lines (left) or aluminum film and those obtained from a nanosecond formed plasma (right). The broad background emission is not present in the femtosecond case.

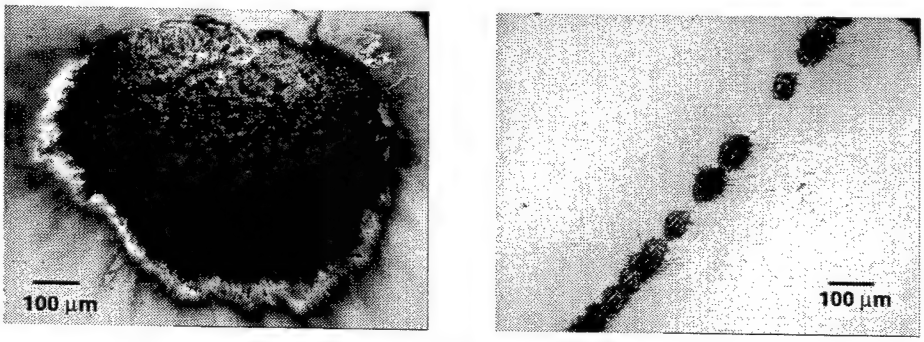

Fig. 3. These images show the difference between the size of the ablation damage spot size for the nanosecond (left) and femtosecond (right) ablation of aluminum films

Investigation of femtosecond laser produced plasma expansion by laser-induced fluorescence imaging

V. Margetic, F. Leis, K. Niemax, R. Hergenröder
Institute of Spectrochemistry and Applied Spectroscopy (ISAS), Bunsen-Kirchhoffstraße 11, D-44139 Dortmund, Germany
hergenroeder@isas-dortmund.de

T. Ban
Institute of Physics, Bijenicka 46, 10000 Zagreb, Croatia

O. Samek and V. Malina
Institute of Physical Engineering, Brno University of Technology, Technicka 2, 616 69, Brno, Czech Republic
ota@fyzika.fme.vutbr.cz

Abstract: In order to investigate temporally and spatially resolved expansion dynamics of the femtosecond laser-induced plasma we measured fluorescence light emission. To obtain the radial distribution of emitting atoms the Abel inversion was employed.

Summary

Though, available since only few years fs-lasers have found wide spread and numerous applications in different fields are described in literature. The ultra-short pulses are suitable to initiate processes in atoms, molecules, liquids or solid samples and to study the temporal behavior of these processes. However, plasma generation by focused radiation of fs-lasers for chemical analysis, so far, is rather limited and only few papers dealing with the use of fs-lasers for the laser-induced-breakdown spectroscopy (LIBS) analysis of solids have been published, for example [1-4].

The extremely short pulse length of fs-lasers accounts for some remarkable features being important for LIBS and other analytical methods using lasers as atomizers. In contrast to ns-lasers, the impact of the fs-laser energy on the sample has ceased before the plasma is formed. No plasma shielding occurs and no laser energy is directly dissipated in the plasma. The ablation threshold is lower than for ns-lasers and the energy is more localized in the sample and allows a better spatial resolution [1]. Due to the decoupling of laser-sample interaction and development of the plasma, the ablation process with fs- lasers is easier to understand than with long laser pulses which interact with the solid, liquid and gaseous phase.

Laser induced fluorescence (LIF) is an established technique for spectroscopic measurements demanding high spatial, temporal and spectral resolution. Thus, LIF technique was used in our study for the investigation of femtosecond laser-induced micro-plasmas. Investigations of this type are very useful for a better understanding of the basic processes in the plasma and can serve as a starting point for optimization and improvement of analytical measurements, pulsed-laser deposition and similar techniques based on laser ablation. LIF-measurements on plasmas produced by ns-lasers have been reported by several authors, for example [5,6]. To our knowledge combination of fs-LIBS with LIFS measurements for fs-plasma expansion measurements is here reported for the first time. The lack of investigations of this type and the intention to do subsequent time-of-flight measurements under non-vacuum conditions were the motivation for our LIF-measurements.

Experimental details on the femtosecond laser system used in our investigation can be found in our previous publications [1-3]. Copper and pure silicon samples were used as the targets. Samples were placed in a vacuum chamber that was connected to an argon line and a rotary pump. The gas pressure was varied between 0.02 and 1000

mbar. The chamber could be moved in three perpendicular directions. To probe the plasma at different heights, the whole chamber was moved vertically.

In order to obtain temporally and spatially resolved expansion dynamics of the femtosecond laser-induced plasma we used the two following fluorescence techniques:

a) the dye laser (probe) beam was directed to the fs-plasma using a telescope. The beam diameter intersecting the fs-plasma was about 0.2 mm. The fluorescence light was imaged by a lens and via the fibre to the Echelle spectrometer.

b) the dye laser beam was shaped into a thin sheet and consequently used for excitation of atoms within the fs-plasma plume. The fluorescent light was imaged by a lens - through the interference filter - directly onto the gateable, intensified diode array detector. This technique is known as planar laser-induced fluorescence (PLIF) [7]. In order to obtain the radial distribution of emitting atoms the Abel inversion was employed.

The expansion of a laser pulse created plasma into an ambient atmosphere is understood in the frame of a simplified explosion model which is based on the laws of mass, momentum, and energy conservation [8]. This model yields satisfactory results in the case of ns-laser ablation. It is obvious that the results obtained with fs-laser pulses should be still in good agreement with this model. Our LIFS measurements which have been performed in this work on the temporally and spatially resolved expansion dynamics of the fs-plume support the model.

References

1. V. Margetic, A. Pakulev, A. Stockhaus, M. Bolshov, K. Niemax, R. Hergenröder, "A comparison of nanosecond and femtosecond laser-induced plasma spectroscopy of brass samples," Spectrochim. Acta, Part B **55,** 1771-1785 (2000).
2. V. Margetic, K. Niemax, R. Hergenröder, "A study of non-linear calibration graphs for brass with femtosecond laser-induced breakdown spectroscopy," Spectrochim. Acta, Part B **56,** 1003-1010 (2001).
3. V. Margetic, M. Bolshov, A. Stockhaus, K. Niemax, R. Hergenröder, :"Depth profiling of multi-layer samples using femtosecond laser ablation," J. Anal. At. Spectrom. **16,** 616-621 (2001).
4. B. Le Drogoff, J. Margot, M. Chaker, M. Sabsabi, O. Barhelemy, T.W. Johnston, S. Laville, F. Vidal, Y. von Kaenel, "Temporal characterization of femtosecond laser pulses induced plasma for spectrochemical analysis of aluminium alloys," Spectrochim. Acta, Part B **56** , 987-1002 (2001).
5. H.H. Telle, D.C.S. Beddows, G. W. Morris, O. Samek, "Sensitive and selective spectrochemical analysis of metallic samples: the combination of laser-induced breakdown spectroscopy and laser-induced fluorescence spectroscopy," Spectrochim. Acta, Part B **56,** 947-960 (2001).
6. F. Hilbk-Kortenbruck, R. Noll, P. Wintjens, H. Falk, Ch. Becker, "Analysis of heavy metals in soils using laser-induced breakdown spectroscopy combined with laser-induced fluorescence," Spectrochim. Acta, Part B **56,** 933-945 (2001).
7. J.B. Kirby, R.K. Hanson, "Planar laser-induced fluorescence imaging of carbon monoxide using vibrational (infrared) transitions," Appl. Phys. B **69,** 505-507 (1999).
8. N. Arnold, J. Gruber, J. Heitz, "Spherical expansion of the vapor plume into ambient gas: an analytical model," Appl. Phys. A **69,** 87-93 (1999).

In-depth Profiling of Multi-layer Samples with Femtosecond Laser

Vanja Margetić, Kay Niemax, and Roland Hergenröder
Institute of Spectrochemistry and Applied Spectroscopy, Bunsen-Kirchhoff-Str. 11, 44139 Dortmund, Germany
e-mail: margetic@isas-dortmund.de

Abstract: Femtosecond laser induced plasma spectroscopy (LIBS) and femtosecond laser ablation time of flight mass spectrometry (LA-TOF-MS) were used for analysis of multi-layered samples with sub-micrometer thickness. Feasibility of the fs-LA in-depth profiling is discussed.

OCIS codes: (000.0000) General

Summary

Multi-layered structures of different materials are in wide use in contemporary material science and industry. The layers are becoming thinner and new methods for their analysis are to be developed. Laser ablation (LA) has a potential advantage over the other, already established surface analysis techniques (GD, XPS, SIMS..) in so far that it could be applied under atmospheric conditions, for remote, *in situ* and fast on-line analysis. Our aim is to explore the feasibility of the femtosecond laser ablation in this analytical field.

When a laser pulse of sub-picosecond duration is used for the ablation, the deposition of the laser energy into the sample is so fast that the thermal diffusion length is determined by the diffusion of hot electrons before the energy-transfer to the lattice takes place. In this case the diffusion length is on the order of or less than 100 nm, compared to approximately 1 μm in the case of longer, e.g. nanosecond pulses. Less pronounced thermal diffusion provides better lateral and depth resolution and is the base for the successful applications of femtosecond pulses in material processing and microstructuring.

Ablation of less than 10 nm per shot has been demonstrated [1-3], and that is close to depth resolutions of the best established surface analysis techniques (typically 5-10 nm). At the same time those techniques have different lateral resolutions, in the range from 100 nm to few mm. The laser spot size is in the middle of that range (normally 10 to 100 μm, but in principle limited only by the delivering optics and the wavelength). Although the best results should be expected at the ultra-high vacuum (UHV) conditions that are necessary for most of the established techniques, the laser ablation in-depth profiling could be performed also at atmospheric conditions or in the presence of a noble gas. That is significant for many possible applications where a fast, on-line analysis is needed and UHV should be avoided. Simultaneously is the depth range of laser ablation much longer than of the other sputtering techniques (tens of micrometers, depending on the lateral resolution, compared to ~1 μm).

On its own, the precise material removal is not sufficient for LA in-depth profiling. One needs a detection technique suitable for single shot multielement analysis. LIBS with an echelle spectrometer satisfies this condition, but there is a limitation imposed on the ablation rates: laser fluences should be so high that the plasma emission can be detected (the removed material should be atomized/ionized and excited). Much lower fluences can be applied for analysis in the TOF-MS, since ionic signals are finite even for fluences that are below the threshold determined from the visible surface damage inspection.

Elemental signals are taken as a function of the number of applied laser pulses. The real depth information has to come from an independent depth measurement. Alternatively, for materials for which the ablation rate dependence on fluence is known, the depth could be calculated from experimental parameters.

170 fs Ti-sapphire laser was used for in-depth profiling of sub-micrometer multi-layer structures. LIBS and direct LA-TOF-MS were used for elemental analysis. Sandwiches of two and three Cu-Ag layers of about 600 nm thickness per layer were measured by laser induced breakdown spectroscopy in argon. The laser craters geometry, directly connected to the beam intensity distribution, has a decisive influence on the profiling results. A TiN/TiAlN system with five double-layers was investigated by LA-TOF-MS. The thickness of each individual layer was 280 nm. Despite the Gaussian laser beam profile which results in bell-shaped craters, the position of all ten layers could be resolved [4]. Hard Ti-containing coatings [5], as well as some other transition-metal nitrides and carbides can be microstructured with high precision with ultrashort lasers, so that a better depth resolution can be expected.

Several beam shaping methods were used in attempts to obtain a flat-top beam profile and craters with flat bottom. Many of the standard beam shaping methods cannot be applied to the ultrashort pulses and alternative approaches were necessary. Some other multi-layered systems of different thickness were studied. The results were correlated with the white light interferometer measurements of the craters.

The measurements clearly demonstrate that the femtosecond laser ablation is a suitable sampling method for a demanding microanalytical task as it is the in-depth profiling. With depth resolutions of the order of 100 nm or better and latteral resolutions of 10 μm, it could be a good alternative to the established methods such as a glow discharge or ion sputtering. From these first experiments, the strategic guidelines for further development of the femtosecond laser ablation in-depth profiling method can be derived.

References

1. S. Nolte, C. Momma, H. Jacobs, A. Tünnermann, B. N. Chichkov, B. Wellegehausen, and H. Welling, "Ablation of metals by ultrashort laser pulses," J. Opt. Soc. Am. B **14**, 2716-2722 (1997).

2. M. K. Kim, T. Takao, Y. Oki, and M. Maeda, "Thin-Layer Ablation of Metals and Silicon by Femtosecond Laser Pulses for Application to Surface Analysis," Jpn. J. Appl. Phys. **39**, 6277-6280 (2000).

3. M. Lenzner, J. Krüger, W. Kautek, and F. Krausz, "Precision laser ablation of dielectrics in the 10-fs regime," Appl. Phys. A **68**, 369-371 (1999).

4. V. Margetic, M. Bolshov, A. Stockhaus, K. Niemax, and R. Hergenröder, "Depth profiling of multi-layer samples using femtosecond laser ablation," J. Anal. At. Spectrom. **16**, 616-621 (2001).

5. J. Bonse, P. Rudolph, J. Krüger, S. Baudach, and W. Kautek, "Femtosecond pulse laser processing of TiN on silicon," Appl. Surf. Sci. **154-155**, 659-663 (2000).

NOTES

LIBS for Materials Analysis

Friday, September 27, 2002

Dennis Alexander, Univ. of Nebraska, USA,
Presider

FB
10:20am–12:20pm
Room: Royal Palm III

In situ LIBS analysis of steel pipes at high temperature

G. Cristoforetti, M. Corsi, M. Hidalgo, D. Iriarte, S. Legnaioli, V. Palleschi, A. Salvetti, E. Tognoni
Istituto per i Processi Chimico-Fisici del Consiglio Nazionale delle Ricerche, Via Moruzzi 1, 56124 Pisa , Italy
e-mail: stefanol@ifam.pi.cnr.it

S. Green
Progressive Energy Technology Ltd. (UK)

D. Bates
DRB Materials Technology (UK)

A. Steiger, J. Fonseca, J. Martins
UNINOVA (Portugal)

J. McKay
ENICHEM (UK)

B. Tozer, D. Wells, R. Wells
LASERMET (UK)

Abstract: The results of a measurement campaign for analysis of steel pipes in a styrene plant are reported. The measurements were performed during the normal operation of the plant.

OCIS codes: (140.3440) Laser-induced breakdown, (120.4290) Non destructive testing

1. Introduction

One of the most interesting features of the LIBS technique is its ability to perform elemental analysis without preparation of the samples, in standard atmosphere. This characteristics make LIBS the election technique for in-situ remote analysis, since optical access to the sample is the only requirement for performing the measurements. In particular, the LIBS technique is particularly suited for diagnostics of industrial processes and structures because of its operating capabilities even in very hostile environments.

Surprisingly enough, very few examples are reported in the scientific literature of in-situ applications of the LIBS technique. In fact, the use of the LIBS technique out of the laboratory is still very limited by the difficulties associated with transportation of the experimental equipment and, in case of quantitative analysis, by the difficulty of constructing appropriate calibration curves in the specific experimental conditions typical of in-situ analysis.

The results here reported refer to the first time application of LIBS technique to remote and quantitative elemental analysis of hot steel pipes in a styrene plant, performed during the normal operation cycle of the plant.

The experimental activity, performed in the framework of the EC project LIBSGRAIN, was made possible on one side by the use of compact experimental equipment and on the other by the application of the CF-LIBS technique, which allowed the quantitative measurement of hot steel pipe composition without use of any reference sample or calibration curve.

2. Experimental

The LIBS experimental apparatus was composed by a compact Nd-YAG laser, operating in the fundamental wavelength and delivering about 50 mJ in 7 ns pulses, with a repetition rate of 10 Hz, and a wide band Echelle spectrometer with spectral range between 200 and 800 nm.

The laser beam was focused on the hot steel pipe (typically operating at temperatures around 700 ^{0}C) using an optical head realized by LASERMET. The optical head was equipped with three stepping motors which allowed for 2D scanning of the surface and focusing of the laser beam on the surface.

The optical head movements were guided by a dedicated software, designed by UNINOVA, which also controlled the automatic focusing of the laser beam on the surface and the scanning spatial step during the LIBS measurements.

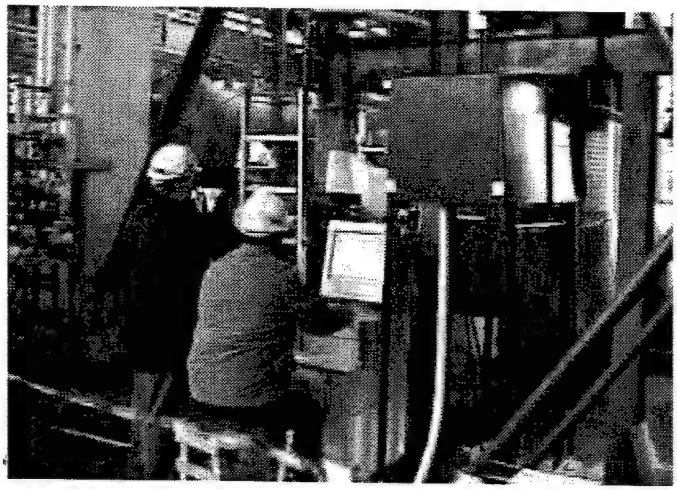

Fig. 1. The LIBS system operating at the styrene plant. Note the safety cover (at the right) for avoiding stray reflections.

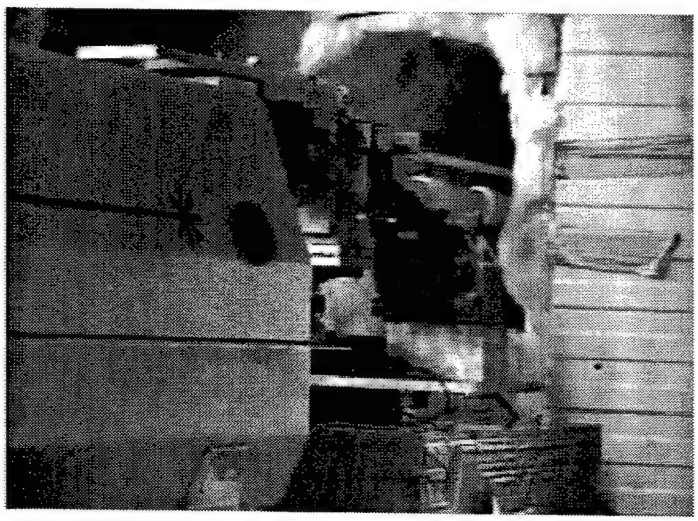

Fig. 2. A detail of the laser and the optical head focusing the laser beam on the pipe.

The LIBS signal was acquired on-axis using an optical fiber fitted in the back of the optical head which delivered the breakdown light to the Echelle spectrometer. The LIBS spectra obtained by the spectrometer were then analyzed with the LIBS++ software developed by the Applied Laser Spectroscopy Laboratory in Pisa and the resulting elemental compositions were converted in false-colors 2D compositional maps.

3. Results

The results obtained on the plant, in two different sites (Site A, far from a welding and Site B, across a welding) have shown different spatial distributions of the main components of the steel alloy (Fe, Ni, Mn, Cu, Al, Ti and Ni) which are currently under study by PET and DRB for correlating these information with the metallographic conditions of the pipes, thus obtaining an estimate of the probability of failure of the plant and operating in advance for repairing the sections involved before the failure would occur.

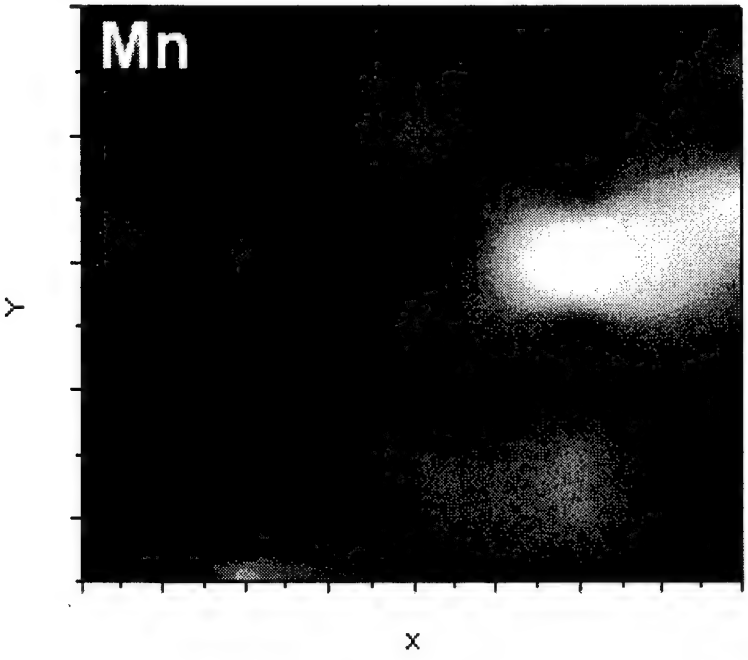

Fig. 3. 2D mapping of the Mn distribution over a 75µm x 250 µm grid. The bright spot at the right corresponds to a higher concentration of Mn with respect to the background.

Detecting gunshot residue by laser induced breakdown spectroscopy

Scott R. Goode, Christopher R. Dockery, Michael F. Bachmeyer, Alexander A. Nieuwland, and Stephen L. Morgan
Department of Chemistry and Biochemistry, The University of South Carolina, Columbia SC 29208
Phone: 803-777-2601 FAX: 803-777-9521 Email: goode@sc.edu, slmorgan@sc.edu

Abstract: Laser induced breakdown spectroscopy was used to detect gunshot residue (GSR) on a shooter's hand. Double sided tape pressed to the skin of the shooter was directly analyzed. Characteristic emission lines identified GSR presence.

OCIS codes: (300.6210) Spectroscopy, atomic (120.6200) Spectrometers and spectroscopic instrumentation

1. Introduction

Whenever a gun is fired, gunshot residues (GSR) are expelled from the gun. The origins of GSR can be the primer, propellant, lubricant, bullet, bullet jacket, cartridge case, and gun barrel. The presence of GSR have been used to show that a person had recently fired a gun and patterns of residues have been used to predict firing distances.

The gunshot is initiated when the hammer or striker crushes the primer cup, causing the primer compound lining the inside of the primer cup to ignite. The flame emitted from the primer cup ignites the propellant, which decomposes and drives the bullet down the barrel. Heat generated by the ignition of the primer causes the inorganic compounds in the primer to vaporize, but these vapors condense into droplets. With expansion and cooling on leaving the barrel, many of these droplets freeze in their existing form. GSR from primer contains distinct particles with the characteristic elements of the primer compounds. In addition to the "primer particles," lead particles can arise from lead bullets. GSR also may contain intact, or partially burned, propellant with particle sizes ranging from large visible particles to a fine dust (1-7).

2. Experimental

Samples were obtained by going to a firing range and firing rounds from personal weapons. Samples were obtained by pressing a small (0.5-inch diameter) piece of double sided tape to the hand of the shooter. The tape was mounted in a time-resolved echelle LIBS spectrometer (8) and a single laser pulse was used to vaporize and excite the analyte.

3. Results and discussion

The laser sampled an area approximately 0.3 mm in diameter. Figure 1 shows representative spectra of a blank spectrum, a LIBS spectrum from a sample taken from the shooter's hand after firing weapon, and a spectrum taken from the shooter's hand after washing with soap and water. The blank sample was taken from the same person, but from an area under the sleeve on the opposite arm before firing. Spectral differences between the spectra taken after firing and the blank have been identified. The lines in the blank are due to sodium, calcium, and atmospheric emission. The majority of the lines in the samples after shooting are due to the presence of barium; some lead lines are also present. The time required for the analysis was approximately 2 min.

A single laser shot ablates 0.06% of the surface, leaving the remaining 99.94% of the sample preserved for SEM/EDX analysis. Additional sensitivity may be attained by averaging additional laser pulses at new locations, thus improving the signal-to-noise ratio. The sensitivity appears to be excellent; the shooters were asked to wash their hands carefully using soap and water. The firing hand was re-sampled with a new piece of tape. The results show that gunshot residue can be detected, although the intensity after washing (Figure 1C) drops noticeably (compared to Figure 1B). Samples were also taken after 1, 3, and 10 shots were fired. All spectra are qualitatively identical.

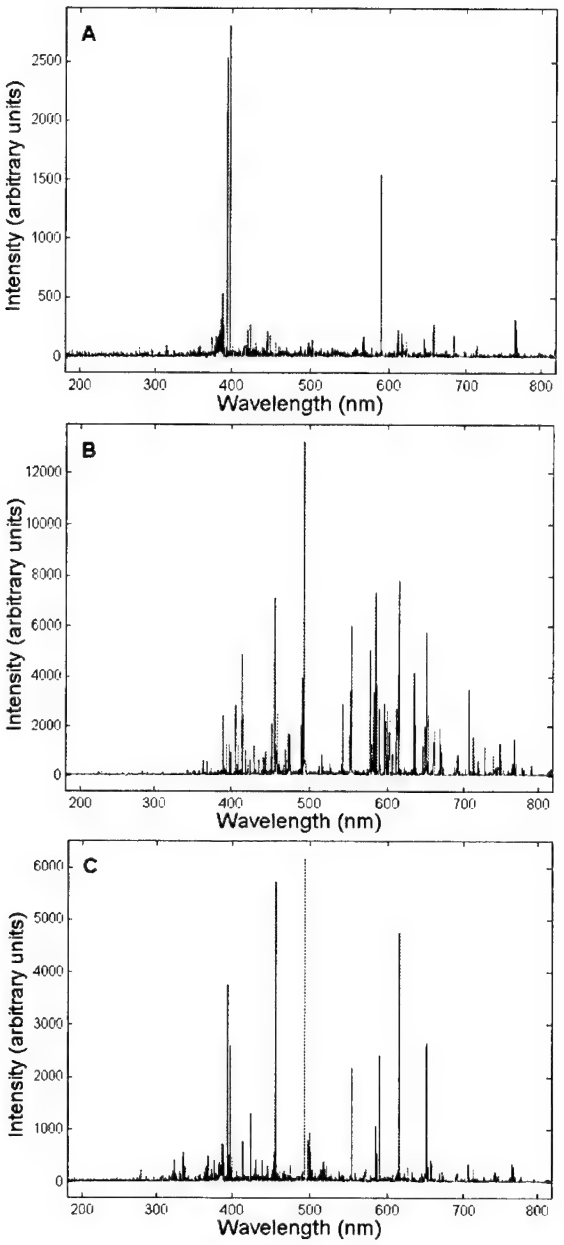

Figure 1. LIBS spectra: (A) blank taken from underneath the shooter's shirt before firing; (B) GSR sampled from shooter's hand after firing weapon; (C) GSR spectra taken from shooter's hand after washing with soap and water.

3. Conclusion

There are two approaches to the interpretation of inorganic GSR results. The first approach is based on finding particles with a "unique composition" that could only have originated from the explosion of a primer. The second approach is based on finding particles that are consistent with the gun and ammunition used. The first approach is limited by a low number of positives in actual casework, and the fact that the use of lead-, antimony- and barium-free primers is on the rise. The second approach is only possible if the gun or ammunition is recovered along with the particles (3).

The results presented here support use of LIBS for detection of gunshot residue. We have successfully used LIBS to detect residue on the hands of a shooter who has fired a weapon. Characteristic emission lines are observed from elements known to be present in GSR, principally barium and lead. The spectra of GSR samples are quite different

from those of the blank. We have also found that, even after washing, detectable amounts of GSR remain. The results reported here are preliminary and further work is in progress to confirm and validate the applicability of these results.

4. References

1. Meng, H. H., Caddy, B. "Gunshot residue analysis-a review," *J. Forensic Sci.* **1997**, *42*, 553-570.
2. Miyauchi, H., Kumihashi, M., Shibayama, T. "The contribution of trace elements from smokeless powder to post firing residues," *J. Forensic Sci.* **1998**, *43*, 90-96.
3. Romolo, F. S., Margot, P. "Identification of gunshot residue: a critical review," *J. Forensic Sci. Int.* **2001**, *119*, 196-211.
4. Wessel, J. E., Jones, P. F., Kwan, Q. Y., Nesbitt, R. S., Rattin, E. J. "Equipment systems improvement program gunshot residue detection," The Aerospace Corporation, USA, 1974.
5. Wolten, G. M., Nesbitt, R.S., Calloway, A.R., Loper, G.L., Jones, P.F. "Particle analysis for the detection of gunshot residue. I: Scanning electron microscopy/energy dispersive X-ray characterization of hand deposits from firing," *J. Forensic Sci.* **1979**, *24*, 409-422.
6. Ward, D. C., "Gunshot residue collection for scanning electron microscopy," *Scanning Electron Microscopy* **1982**, *111*, 1031-1036.
7. Krishman, S. S. "Detection of gunshot residue: present status," in Saferstein, R., Ed., *Forensic Science Handbook*, Prentice-Hall, Inc., NJ, 1982.
8. Goode, S. R., Morgan, S.L., Hoskins, R., Oxsher, A. "Identifying alloys by laser-induced breakdown spectroscopy with a time-resolved high resolution echelle spectrometer," *J. Anal. At. Spectrom.* **2000**, *15*, 1133-1138.

LIBS analysis of pharmaceutical solid dosage forms

Yves Mouget, Patrick Gosselin, Martine Tourigny, and Simon Bechard
Pharma Laser Inc., 75 rue de Mortagne, Boucherville, QC, Canada J4B 6Y4
Tel: 450-641-5356 Fax: 450-641-5117 Email: yves.mouget@pharmalaser.com

Abstract: Speed of analysis and minimal sample preparation make LIBS ideal for the analysis of pharmaceutical solid dosage forms for blend, content, and coating thickness uniformities. Inter-tablet %RSD values of less than 4% are easily achieved.

ACIS codes: (140.3440) Laser-induced breakdown; (300.6360) Spectroscopy, laser.

Introduction

Approximately 70% of the pharmaceutical drug products on the market are in solid dosage form. The uniform distribution of the active ingredients and the excipients within tablets are critical parameters towards the performance of a drug. However the proper blending of powders, essential towards achieving a uniform distribution, has always contributed to the difficulties involved in the manufacture of pharmaceutical tablets. Coatings are sometimes applied to tablets for cosmetic and functional purposes. In the latter case, the uniformity of the coating thickness can significantly affect the performance of a drug as well.

Current methodology to determine the content and coating uniformity frequently involves lengthy sample preparation steps where the sample must be brought into solution. Laser induced breakdown spectroscopy is revealing itself to be a fast and versatile technique for the qualitative and quantitative analysis of pharmaceutical samples. An inherent feature of LIBS technology is the very small target size being sampled. The spot size ablated by the laser is approximately 200 μm in diameter. The ability to target specific areas of the sample can be used to assess the distribution of components. As well, by focusing successive laser pulses onto the same spot, it becomes possible to probe into the sample core, and therefore determine the homogeneity of an ingredient throughout the tablet and the uniformity of coatings.

Method

The laser induced breakdown spectrometry instrument used for these experiments was a PharmaLIBS™ 200. The instrument features an Nd:YAG laser operating at 1064 nm and up to 200 mJ at 10 Hz. The spot size on the target is 200 microns. The plasma emissions are focused by an ellipsoid mirror onto a fibre optic bundle, and subsequently transmitted to a spectrograph of Czerny-Turner configuration. The spectrum created by one of the three gratings (1200 g/mm blaze 750 nm, 1200 g/mm blaze visible, and 600 nm blaze 1000 nm) is detected by an interline readout CCD. The samples are mounted in dies, which are then guided to the laser targeting point by an XY rotational stage.

In order to determine the applicability of LIBS to the study of powder blends, a mixture of 50:50 lactose (Pharmatose DCL21, DMV) and microcrystalline cellulose (Avicel PH101, FMC Corp.) was blended at 38 rpm in an 8L low shear blender filled to 40% of its volume capacity. Magnesium stearate - 0.5% by weight, (Mallinckrodt, passed through a 60 mesh sieve), croscarmelose - 3% by weight, (Ac-Di-Sol, FMC Corp.), and chlorpheniramine maleate - 10% by weight (Sigma Aldrich) were subsequently added to the blender as a lubricant, disintegrant and active compound, respectively. At predetermined number of rotations, samples of the blends were taken at ten locations on top of the blend.

A 300 mg aliquot from each sampling site were then compacted into 12 mm round flat tablets using a hydraulic press (Globe Pharma, NJ) set to two metric tons. The wavelengths chosen were 517 nm for Mg, 589 nm for Na, and 837 nm for Cl; laser energy 150 mJ; camera delay 0.7 μsec, exposure 4 μsec; 7 sites, 10 pulses per site.

Coating uniformity studies were performed using commercially available enterically coated omeprazole tablets. The emissions lines of titanium, present in the coating, and sulfur, present in the core, were monitored at 522 nm and 921 nm, respectively. The laser energy was set to 150 mJ; camera delay 1 μsec, exposure 5 μsec; 7 sites in a linear pattern, 21 pulses (The results from the 1st pulse were ignored).

Results and Discussion

During the tablet manufacturing process, determining the end point of a blending process has implications not only with regards to the performance of the drug, but also with regards to the financial investment and potential earnings. Therefore, the time required to obtain accurate results on the homogeneity of a blend is a critical factor. Current techniques, such as HPLC or NIR, are either time consuming or not readily applicable to certain components. The ability of LIBS to analyze solid materials, thus reducing or even eliminating extensive sample preparation, places the technology in a unique analytical position with respect to pharmaceutical processes and materials.

Three ingredients commonly found in pharmaceutical formulations - an active, a disintegrant, and a lubricant – were blended and sampled during the blending process at several locations within the blender. Figure 1 shows the inter-tablet %RSD values for magnesium stearate, croscarmellose sodium, and chlorpheniramine after 20, 40, 80, 200, and 400 rotations. The tendency of chlorpheniramine maleate to agglomerate, hence requiring a longer blending time, is clearly shown since the blend becomes uniform after 400 rotations. On the other hand, croscarmellose sodium, a free flowing powder, is uniformly distributed in the blend after only 40 rotations with inter-tablet %RSD values of about 2%.

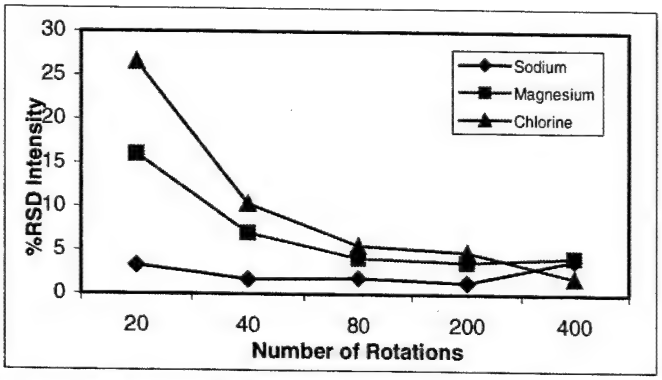

Figure 1: % RSD of croscarmellose sodium, magnesium stearate, and chlorpheniramine maleate as a function of the number of blender rotations.

While the previous results were obtained by sampling several sites across the blend and compacting the powder into tablets, inhomogeneity can also be determined within a single tablet. The fact that the laser ablates a certain amount of material with each pulse allows the core of a tablet to be sampled without cutting the tablet. A surface plot of the chlorine distribution in a tablet that was compacted from a non-uniform blend is shown in Figure 2.

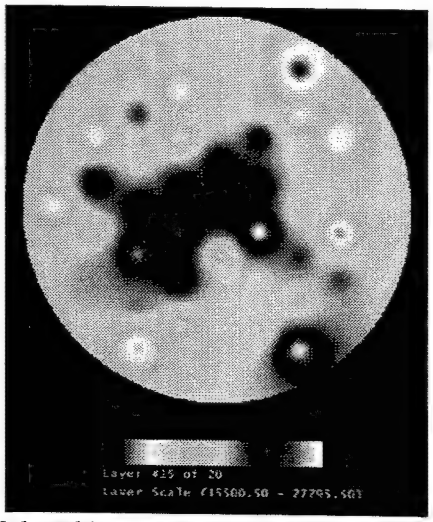

Fig. 2. Surface plot in the XY plane of the chlorine intensity after 15 pulses in a non-uniformly blended tablet.

By selecting the signal intensity after the 15th pulse for each site, the plot can be likened to a horizontal slice through the tablet. When examining the distribution of the drug in terms of signal intensity in a single tablet, significant non-uniformity in drug distribution is observed.

The fact that this technique ablates a small amount of material provides the ability to probe the core of a tablet without removing the film coating. This allows the uniformity of the film coating and of the active drug product to be determined. Several tablets were examined for coating thickness uniformity. Two examples are plotted in Figure 3, which shows the average titanium and sulfur signals with respect to the laser pulse number. The plots clearly show differences between the tablets, not only in terms of the number of shots required to penetrate the coating, but also in the amount of sulfur in the core. The coating of the 10 mg tablet seems thinner than the coating of the 20 mg tablet, since the crossover point of the titanium and sulfur signals occurs earlier for the 10 mg tablet. The inter-tablet %RSD values for the both dose strengths are approximately 8% when calculated from the sulfur signal at pulses 14 to 19. These results improve when the number of sites per tablet is increased. Typically, the penetration rate is approximately 50-100 μm per pulse in the core of a tablet, while on film coatings it is about 10-15 μm per pulse.

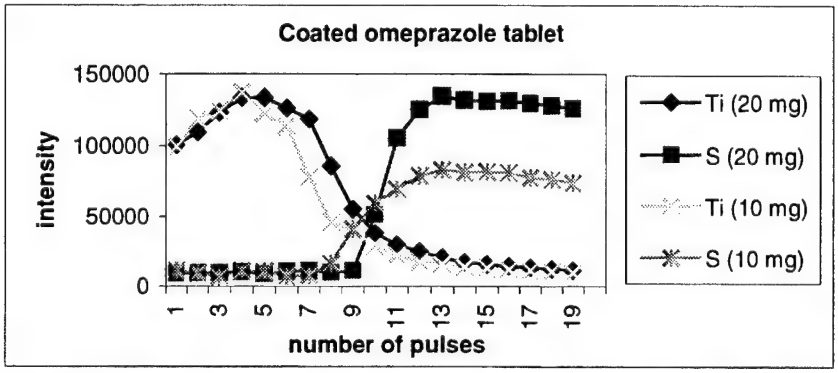

Fig. 3. Profile showing the titanium and sulfur signals with respect to laser pulses on an enterically coated omeprazole tablet.

Conclusion

LIBS is an effective tool to rapidly probe the surface and the core of pharmaceutical solid dosage forms for various compounds and determine their distributions throughout the sample. Lack of uniformity in distribution can be clearly demonstrated in the surface plots obtained from a single tablet, both by means of surface distribution and depth profile. As well, distribution and coating uniformity also can be determined.

Analysis by LIBS of complex solids, liquids and powders with an echelle spectrometer

Pascal FICHET, Denis MENUT, Rene BRENNETOT, Annie RIVOALLAN
CEA Saclay, Fuel Cycle Division, LALES DEN/DPC/SCPA Bâtiment 391, 91191 Gif Sur Yvette France
Tel.: (33) 1 69 08 77 52 FAX.: (33) 1 69 08 77 38
e-mail: FICHET@carnac.cea.fr

1. Introduction.

Laser Induced Breakdown Spectroscopy (LIBS) due to its principle where only laser photons are sent to the target and photons emitted by the plasma are detected can allow direct and in situ measurements of numerous elements in complex materials. LIBS has been applied for experiments on liquids [1] and different materials [2] but the use of an echelle spectrometer in the different experimental set-up is rather sparse [3, 4, 5]. The subject of this paper is to show the high potentiality of a commercial echelle spectrometer for multielemental analysis by LIBS and to compare detection limits obtained with such system and with a standard Czerny Turner spectrometer.

2. Experimental set-up

Different applications have been investigated. For liquid applications (see Figure 1) the plasma is ignited by a Nd:YAG laser operating at 532 nm (Quantel Brilliant B, France). Three reflective mirrors up to a focussing lens guide the laser. The last mirror is a reflective quartz one at 45° in order to allow plasma recording in the same direction. For quantitative determination in bulk liquids the laser direction is tilted at an angle of 15° to the liquid surface. Therefore it avoids splashing on the optics, an actual drawback that can affect the reliability of the LIBS technique.

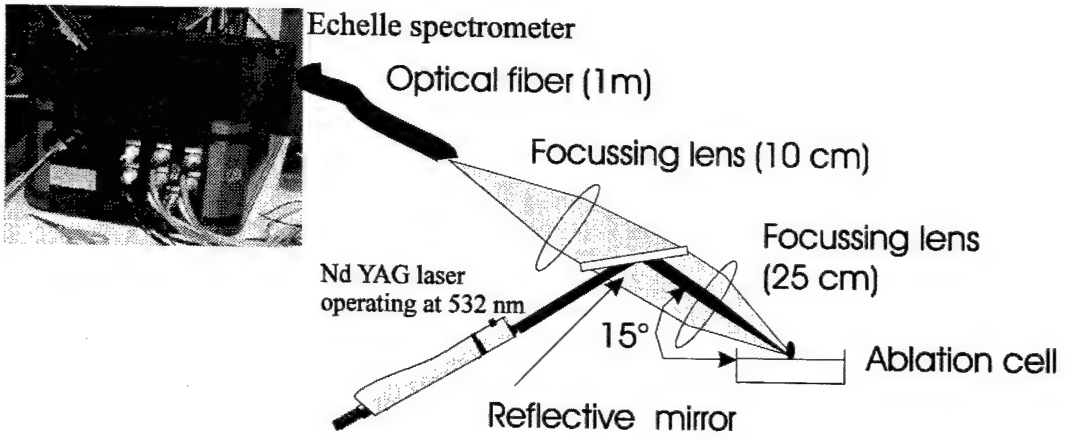

Figure 1: Experimental set up for LIBS technique on liquids.

For solids and powders investigations exactly the same experimental set up has been used except the tilt choice. For both materials the laser beam direction is perpendicular to the sample surface.

At the beginning of the development of our researches on LIBS technique, a Czerny-Turner spectrometer (THR 1000, Jobin-Yvon, France) was systematically used with an ICCD detector (Princeton Instruments, USA). But because of the requirement for very fast multielemental analysis, one of the most promising approach for LIBS experiments involves the use of an echelle spectrometer. Therefore, a commercial echelle spectrometer was chosen (ESA 3000, LLA, Germany) because it allows the simultaneous recording of the complete spectral range from 200 to 780 nm with a high resolution of $\lambda/\Delta\lambda = 10\,000$.

3. Main results

Even if LIBS results on liquids are less studied than those on solids, the preparation of standard samples are obviously much easier. Solutions were purchased in SPEX Certiprep company. With different solutions at concentrations of 10 000 $\mu g\ ml^{-1}$ or less, the corresponding spectra were obtained with the echelle spectrometer detector. A home made software was written in order to extract automatically the different emission lines of interest and to build a spectral database obtained by LIBS. Up to now LIBS spectra for 46 elements are gathered in our spectral database. Moreover, the software is able now to give very quickly the qualitative determination of an unknown sample.

The capability of an echelle spectrometer (see Figure 2 for an example of a calibration curve of Cd in water, detection limit found = 14 $\mu g\ ml^{-1}$) to give reliable results was assessed also by the comparison for some elements of the detection limits obtained in the same conditions but with a classical Czerny Turner spectrometer. The possibility to use systematically an internal standard is also an essential feature of the echelle spectrometer. Moreover, if the time resolution remains constant and if different gain of the ICCD must be used to improve the dynamic of the system, the calibration curve do not change.

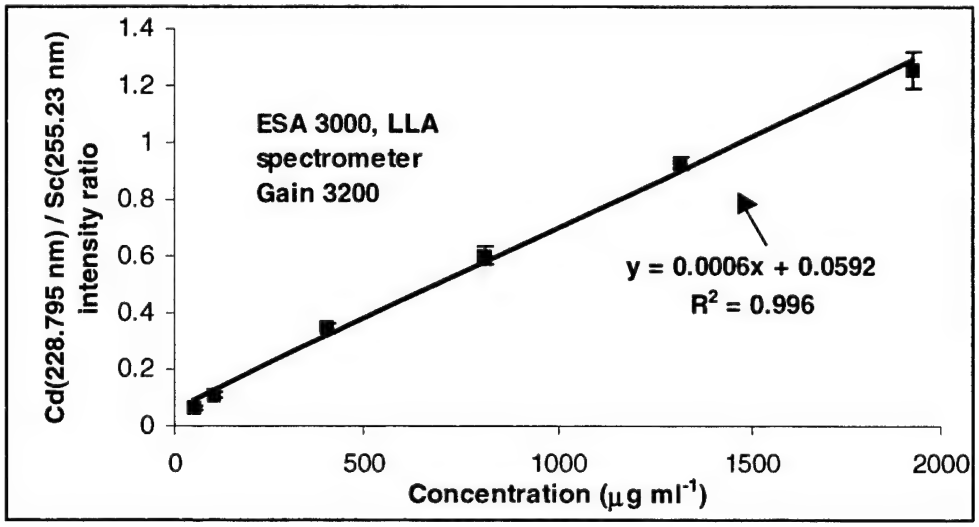

Figure 2 : Calibration curve for Cd (internal standard Sc) in pure water with the use of an echelle spectrometer.

The echelle spectrometer has been also evaluated on aluminium alloys. This apparatus has been an interesting choice to record and choose the most sensitive lines for different trace elements to be analysed. With different aluminium alloys 12 calibration curves have been obtained by LIBS. The detection limits are

very close from those that can be found in the literature (for example a detection limit of 0.13 µg/g was found for Mg), but obviously all different trace elements can be investigated at the same time and thus very quickly.

Because of the spectral database obtained experimentally by LIBS on liquids, completely unknown samples can be studied. Examples on coins, powders and on rocks have already highlighted the high capability of the LIBS experiment connected with an echelle spectrometer to investigate unknown samples.

4. Conclusions

For different applications of LIBS analysis on liquids, solids, ... , the use of an echelle spectrometer is a very attractive choice. The quantitative results are very close compared to a standard Czerny-Turner apparatus. Because a large domain of the spectrum is investigated simultaneously, many elements can be studied at the same time.

4. References

[1] P. Fichet, P. Mauchien, J.F. Wagner and C. Moulin, *Quantitative elemental determination in water and oil by laser induced breakdown spectroscopy*, Anal. Chim. Acta, 269-278, (2001)

[2] D.A. Rusak, B.C. Castle, B.W. Smith and J.D. Winefordner, *Fundamentals and applications of Laser-Induced Breakdown Spectroscopy*, Crit. Rev. Anal. Chem., 27(4), 257-290, (1997).

[3] V. Detalle, R. Heon, M. Sabsabi, L. St-Onge, *An evaluation of a commercial echelle spectrometer with intensified charge-coupled device detector for materials analysis by laser-induced plasma spectroscopy*, Spectrochim Acta, B56, 1011-1025, (2001)

[4] C. Haisch, U. Panne, R. Niessner, *Combination of an intensified charge coupled device with an echelle spectrograph for analysis of colloidal material by laser-induced plasma spectroscopy*, Spectrochim Acta, B53, 1657-1667, (1998).

[5] A. Uhl, K. Loebe, L. Kreuchwig, *Fast analysis of wood preservers using laser induced breakdown spectroscopy*, Spectrochim Acta, 56B, 795-806, 2001.

Progress in LIBS Analysis for Military Applications: Explosives Detection

Russell S. Harmon
Army Research Office, US Army Research Laboratory, Research Triangle Park, NC, 27709

Andrzej W. Miziolek and Kevin L. McNesby
US Army Research Laboratory, Aberdeen Proving Ground, MD 21005

Thomas F. Jenkins and Marianne Walsh
Cold Regions Research and Engineering Laboratory, US Army Engineer Research and Development Center, Hanover, NH, 03755

LIBS has a variety of intrinsic characteristics that make it a very attractive sensor technology for military applications. These attributes include: an ability to detect all elements at high sensitivity; a capability for field-portable, real-time, and in-situ analysis; and the ability to undertake both point and standoff detection. The Army Research Laboratory has been engaged in LIBS analysis for over a decade and recently has been investigating the potential to apply broadband LIBS analysis to specific military problems.

The instrument utilized in this study is a prototype 7-spectrometer array developed by Ocean Optics Inc. which has the following salient features: (i) spectral coverage over the region 200-940 nm, (ii) spectral resolution of 0.1 nm, and (iii) instantaneous response time. Common explosives consist of a variety of different chemicals (e.g. Ammonium Nitrate; Black Powder [potassium nitrate or sodium nitrate, charcoal, and sulfur], RDX: [1,3,5-trinitro-1,3,5-triazacyclohexane], Comp A3 [RDX and wax], Comp B [RDX, TNT, and wax], Comp C4 [RDX, di(2-ethylhexyl)sebacate, polyisobutylene, and motor oil]) and therefore should have unique LIBS spectra. This supposition is borne out by a broadband LIBS survey of common explosive materials reveals a very reproducible analysis and a characteristic spectrum for different types of explosive (Figures 1 and 2).

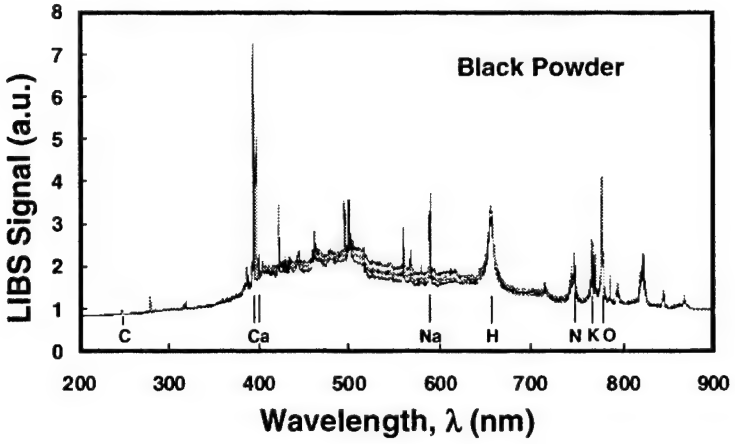

Figure 1. Five (5) single-shot broadband LIBS intensity spectra for Black Powder from 200 to 950nm.

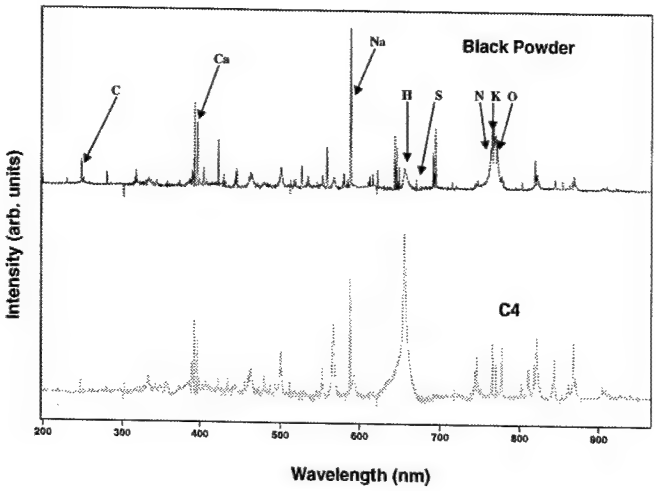

Figure 2. Comparison of broadband LIBS intensity spectra from 200 to 950nm for two explosive materials - Black Powder and Comp C4.

These characteristic spectra for explosive materials could be readily identified in explosive residues on snow and in soils from Army firing ranges at Ft Drum, NY and the Ethan Allen Firing Range, VT that were collected as part of an environmental study to determine the magnitude and variability of explosives in surface soils resulting from activities at US Army training facilities. This work suggests that there is potential to develop a field-portable LIBS instrument for explosive detection applications including the location and assessment of environmental contamination and the standoff discrimination of buried landmines and unexploded ordnance.

Spark-Induced Breakdown Spectroscopy (SIBS) Field Screening Monitor for Toxic Metal Detection in Soil

A. J. Ray Hunter, R. T. Wainner, L. G. Piper, S. J. Davis
Physical Sciences Inc.
20 New England Business Center
Andover, MA 01810

SIBS is a recently developed analytical method based upon atomic fluorescence emitted following the formation of an electrically generated pulsed plasma on the surface of a non-conductive sample. This plasma ablates and ionizes a portion of the sample. As in the more familiar laser-induced breakdown spectroscopy (LIBS), this plasma is allowed to cool and recombine prior to observing the atomic fluorescence from the sample. The wavelength and the intensity of these atomic features are used to identify the element of interest and quantify the amount present, respectively.

SIBS was originally developed at PSI for the real-time determination of lead and chromium in airborne particulate material. SIBS in this application can generate a data point every 1-30 seconds, and can access levels as low as 5-10 micrograms/cubic meter of air. In view of this success, SIBS has more recently been applied to the analysis of toxic metals in soil. By creating sparks on the surface of soil, sensitive and rapid analysis of metallic pollutants can be performed. Quantification is aided by the application of standard addition procedures and normalization to persistent matrix lines.

This presentation will focus on the use of SIBS to probe metals contents in a variety of soil types. We have focused much of our work on the analysis of soil for Pb and Cr, but have also used SIBS to perform near real-time analysis of Hg, Ba and Cd in polluted soils. As shown in figure 1, small additions of a pollutant to an ordinary soil sample can readily be seen against the background of matrix lines. With the use of the standard addition scheme, detection limits of 20-30 mg/kg (ppm) have been observed for all of these elemental species.

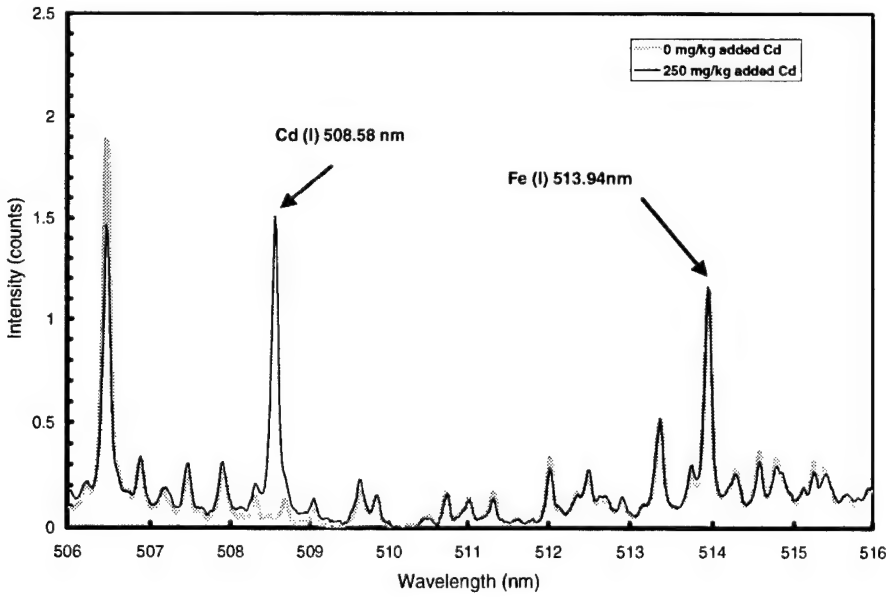

Figure 1. SIBS Spectrum of loose Andover soil between 506 and 516 nm, with and without the addition of 250 mg/kg Cd.

We will present data that demonstrates good agreement between National Institute of Standards and Technology (NIST) standard reference material certified values, and also data that shows insensitivity to chemical form. We will also demonstrate that there is not an adverse influence on the analysis by other common co-contaminants such as oil and other metals. Recently, we have begun miniaturization efforts in earnest and continue to improve the associated analytical methodology.

NOTES

LIBS Analysis of Particulate Matter

Friday, September 27, 2002

Simon Bechard, PharmaLaser Inc., USA,
Presider

FC
2:00pm–3:00pm
Room: Royal Palm III

Single Particle LIBS

David W. Hahn and Jorge E. Carranza
Department of Mechanical Engineering, University of Florida
Box 116300, Gainesville, FL 32611-6300
Phone: 352-392-0807, Fax: 352-392-1071, E-mail: dwhahn@ufl.edu

Abstract: Laser-induced breakdown spectroscopy (LIBS) is ideally suited to function as a real-time, *in situ* monitor characterized by speed and experimental simplicity, and is sensitive enough for measuring aerosol elemental composition as well as overall mass concentrations. Ensemble averaging has historically been used to overcome the extensive laser shot-to-shot spectral fluctuations, thereby improving sensitivity of the LIBS technique. Ensemble averaging, however, reaches a natural limit when low to very low aerosol concentrations comprise the analyte species of interest. For the unique problem of aerosol analysis, the point-sampling nature of the LIBS technique plays an important role in LIBS data processing, and conditional spectral analysis may be used as defined by the presence or absence of discrete particles in a corresponding plasma volume. Conditional data analysis algorithms applied to individual spectra can improve signal-to noise ratios as well as enable the study of single-shot LIBS spectra corresponding to individual aerosol particles. Single-shot LIBS analyses of aerosols raises new questions regarding shot-to-shot fluctuations and data precision, as well as issues involving the fundamental interaction between the laser-induced plasma and aerosol particles. These issues are explored in the context of quantitative LIBS-based analysis of single aerosol particles.

OCIS codes: 300.0300, 300.6210

1. Introduction

The analysis of aerosol particles encompasses a wide range of applications and technical disciplines, including for example, advanced process monitoring, effluent waste stream monitoring, and the analysis of ambient fine particulate matter. The characterization needs for these aerosol populations may include particle size distributions, particle number densities, total species concentrations, and particle species composition. Laser-induced breakdown spectroscopy (LIBS) is well suited to identify constituent atomic species resulting from individual aerosol particles in a laser-induced microplasma, enabling a direct, simultaneous measurement of particle mass and composition. Relevant to LIBS-based single-aerosol analysis, several recent review papers have focused specifically on the use of LIBS for aerosol measurements and environmental monitoring [1-3]. This paper will focus on the recent developments of individual aerosol particle analysis using laser-induced breakdown spectroscopy.

The specific application of LIBS for the detection and analysis of aerosols may be considered in terms of the discrete nature of individual aerosol particles suspended in a gas matrix. In an earlier publication, particle-sampling rates (defined as the percentage of laser pulses for which a particle is present in the plasma volume) were calculated for typical LIBS parameters as a function of aerosol size and mass concentration [4]. The results demonstrated that particle sampling rates are on the order of 0.1% for many aerosol loading conditions, including those expected for the effluent streams of modern incineration facilities and for many aerosol species in ambient air. Traditional ensemble averaging of LIBS spectra under such low aerosol sampling rates will produce poor signal-to-noise ratios and consequently poor species detection limits. It is advantageous, therefore, to consider LIBS aerosol sampling under dilute conditions as a binary problem, in which particles are either present or absent from the sample volume corresponding to *each* laser pulse. The subset of LIBS spectra corresponding to aerosol particles present in the microplasma can contain very significant atomic emission corresponding to the particle's constituent species [4]. It follows that if all null data is rejected using a suitable conditional data analysis scheme, significant increases in signal-to-noise ratios and species detection limits may be realized. A similar approach for the analysis of LIBS data was reported by Schechter [5]. Utilization of such a scheme makes the LIBS technique well suited for the detection and analysis of single aerosol particles.

The basis of LIBS as an analysis technique for discrete aerosol particles, including conditional data analysis and quantitative size measurements, was developed in earlier publications [6-7]. The goals of this paper are to examine the use of LIBS for the direct analysis of individual aerosol particles, including the interaction between the laser-induced plasma and aerosol particles, shot-to-shot fluctuations, and data precision.

2. Experimental Methods

The LIBS system has been described in an earlier publication, hence only a brief overview of the system will be presented [8]. The laser-induced plasma was generated using a Q-switched Nd:YAG laser at the fundamental frequency, with a 10-ns pulse width, 320-mJ pulse energy, and a 5 Hz pulse repetition rate. The expanded laser beam (12-mm diameter) was focused in the aerosol sample chamber using a 75-mm UV grade lens (50-mm diameter). The plasma emission was collected along the direction of the incident beam and separated using a pierced mirror. The plasma emission was fiber-coupled to a 0.275-m spectrometer, dispersed with a 2400-groove/mm grating, and recorded with an intensified, charge-coupled device (iCCD) detector array. Signal integration was performed using delay times ranging from 20 to 40-μs with respect to the incident laser pulse, and integration times ranging from 30 to 150 μs. Plasma temperatures were on the order of 10,000 K during these temporal windows, as measured using a Boltzmann plot based on either neutral chromium or iron atomic emission lines.

Aerosol source streams were generated using a pneumatic-type medical nebulizer. Standard aqueous solutions (ICP grade in 5% nitric acid solution) were nebulized and introduced into a bulk nitrogen or air flow stream, where the droplets subsequently dried to produce a dispersion of fine, solid particulates. Precise calibration flows were generated with known total mass concentrations ranging from 500 to 10,000 micrograms per cubic meter ($\mu g/m^3$) of sample gas. In addition to the aqueous solutions, particle suspensions of monodisperse silicon oxide particles were nebulized and introduced into the bulk carrier gas flow stream. Additional measurements were made in a gas flow of purified air, using the 247.86-nm carbon I atomic emission line, which originated from the presence of carbon dioxide in the ambient air. The use of carbon dioxide in the purified air stream provided a homogeneous carbon source (~100 ppm of atomic carbon) at the molecular level. Such uniform dispersion of the analyte species is not readily achieved by the introduction of aerosol species via nebulization and subsequent drying.

3. Results and Discussion

Laser-induced breakdown spectroscopy was evaluated as a means for quantitative analysis of the size, mass, and composition of individual micron to submicron-sized aerosol particles over a range of well-characterized experimental conditions as well as for the analysis of ambient air particulate matter. Conditional data analysis was used to identify LIBS spectra that correspond to discrete aerosol particles under low aerosol particle loadings. The size distributions of monodisperse particle source flows were measured using the LIBS technique for calcium-based and magnesium-based aerosols. The resulting size distributions were in very good agreement with independently measured size distribution data based on laser light scattering. A lower size detection limit of about 200 nm was determined for a number of analyte species, including calcium, magnesium, chromium, and sodium based particles, which corresponds to a detectable absolute mass on the order of several femtograms. In addition, the accuracy of the LIBS technique for the interference-free analysis of different particle types was verified using a binary aerosol system of chromium and calcium particles.

A statistical analysis of single-shot spectral data was performed for LIBS analysis of carbon emission stemming from carbon dioxide in purified air. Fluctuations in both atomic emission and plasma continuum emission were investigated in concert for a homogenous gaseous flow, and fluctuations in plasma temperature were calculated based on iron atomic emission in an aerosol-seeded flow. The degree of laser pulse energy absorption by the laser-induced plasma was investigated as a function of pulse energy, revealing a saturation regime above which the percentage of absorbed laser energy was constant. The ratio of the analyte atomic emission intensity (247.86-nm carbon line) to the continuum emission intensity (peak/base) provided a robust signal for single-shot LIBS analysis. Moreover, at optimal temporal delay, the precision of the LIBS signal was maximized for pulse energies within the saturation regime with respect to plasma absorption of incident energy. Finally, single-shot temperature measurements were analyzed, leading to the conclusion that spatial variations in the plasma volume formation and

subsequent plasma emission collection play important roles in the overall shot-to-shot precision of the LIBS technique for gaseous and aerosol analysis [9].

Finally, the laser-induced plasma vaporization of individual silica microspheres in an aerosolized air stream was investigated. The upper size limit for complete particle vaporization corresponds to a silica particle diameter of about 2 microns for a laser pulse energy of 320 mJ, as determined by the deviation from a linear mass response of the silicon atomic emission signal. Comparison of the measured silica particle sampling rates and those predicted based on Poisson sampling statistics and the overall laser-induced plasma volume suggests that the primary mechanism of particle vaporization is related to direct plasma-particle interactions as opposed to a laser beam-particle interaction. Finally, temporal and spatial plasma evolution is discussed in concert with factors that may influence the vaporization dynamics of individual aerosol particles, such as thermophoretic forces and vapor expulsion.

4. References

1. M.Z. Martin, M.D. Cheng, and R.C. Martin, "Aerosol measurement by laser-induced plasma technique: A review," Aerosol Science & Technology 31, 409-421 (1999).
2. J. Sneddon and Y-I Lee, "Novel and recent applications of elemental determination by laser-induced breakdown spectrometry," Analytical Letters, 32, 2143-2162 (1999).
3. B.W. Smith, D.W. Hahn, E. Gibb, I. Gornushkin, and J.D. Winefordner, "Laser induced breakdown spectroscopy for the characterization of aerosols and particulates," Kona No.19, 25-33 (2001).
4. D.W. Hahn, W.L. Flower, and K.R. Hencken, "Discrete particle detection and metal emissions monitoring using laser-induced breakdown spectroscopy," Applied Spectroscopy, 51, 1836-1844 (1997).
5. I. Schechter, "Direct aerosol analysis by time resolved laser plasma spectroscopy. Improvement by single shot measurements," Analytical Science & Technology, 8, 779-786 (1995).
6. D.W. Hahn, "Laser-induced breakdown spectroscopy for sizing and elemental analysis of discrete aerosol particles," Applied Physics Letters, 72, 2960-2962 (1998).
7. D.W. Hahn and M.M. Lunden, "Detection and analysis of aerosol particles by laser-induced breakdown spectroscopy," Aerosol Science and Technology, 33, 30-48 (2000).
8. D.W. Hahn, J.E. Carranza, G.R. Arsenault, H.A. Johnsen, and K.R. Hencken, "Aerosol generation system for development and calibration of laser-induced breakdown spectroscopy instrumentation," Review of Scientific Instruments, 72, 3706-3713 (2001).
9. J.E. Carranza and D.W. Hahn, "Sampling Statistics and Considerations for Single-Shot Analysis Using Laser Induced Breakdown Spectroscopy," Spectrochimica Acta Part B, 57, 779-790 (2002).

Monitoring of heavy metals in particulates suspended in flue gas by LIBS

R. Yoshiie and M. Nishimura
Human and information systems, Faculty of Engineering, Gifu University, 1-1, Yanagido, Gifu, Japan, 5011193
Phone & Fax +81-58-293-2588, e-mail ryoshiie@cc.gifu-u.ac.jp

H. Moritomi
Environmental and renewable energy systems, Gifu University, 1-1, Yanagido, Gifu, Japan, 5011193

Abstract: Objective in the present study is to quantify a concentration ratio of heavy metal to major element in particulates, such as fly ash suspended in flue gas. The concentration ratio is important information to estimate the enrichment factor, which shows the partitioning behavior of heavy metals in combustion process. Aluminum is not only a normalizing element for an enrichment factor but also an internal reference element for the spectroscopic analysis in this study. Calibration lines for relative line intensities of iron against its concentration ratio in particle samples, simulating fly ash, are presented in this paper. To generalize the calibration lines, plasma temperature decreasing after breakdown was also investigated via Boltzmann plots of iron lines.

OCIS codes: (140.3440) Laser-induced breakdown

1. Introduction

The emission of toxic heavy metals from coal combustion and waste incineration processes into the atmosphere is becoming a worldwide problem recently. Then the online monitoring method for heavy metals in the flue gas needs to be developed. Laser induced-breakdown spectroscopy (LIBS) is known as one of the techniques to quantify many kinds of trace elements in gas. The application of LIBS to the analysis of gas component has been developed for various fields. [1-3] The technique of LIBS has the merit of offering a fast, simple and real-time method of elemental analysis. However, it has been reported that LIBS spectra are much affected by the gas condition and other matrix elements. [4] Then, to quantify the concerned elements in gas using LIBS with a simple calibration curve, the calibration data needs to be obtained under the completely same condition as the practical measuring point. This fact makes LIBS technique much inconvenient to utilize for analysis of the hot flue gas at actual plants.

According to the latest investigation into the partitioning of volatile heavy metals during combustion process [5-7], heavy metals are hardly remained in bottom ash due to their high volatility. They are more enriched on the fly ash or finer particulates suspended in flue gas. To estimate the partitioning behavior of heavy metals in the combustion process, enrichment factors, that is defined as

$$\text{E.F.} = \left(\frac{(C_{HM})_{output}}{(C_{NE})_{output}} \right) \Bigg/ \left(\frac{(C_{HM})_{fuel}}{(C_{NE})_{fuel}} \right) \qquad (1),$$

are widely used, where C_{HM} is the concentration of a heavy metal and C_{NE} is that of a normalizing element, that is non-volatile major element like aluminum. [8] Subscript *fuel* means the quantity in fuel stream, so that the denominator in Eq.(1) can be calculated from the result of elemental analysis for the fuel. Subscript *output* means the quantity in output stream like fly ash, then the numerator in Eq.(1) expresses the concentration ratio of heavy metal to normalizing element in particulates suspended in flue gas. Then our objective in this study is to estimate this concentration ratio using LIBS technique as direct monitoring of heavy metal. It makes calibration procedures much easier, because the normalizing element to estimate an enrichment factor can be used as an internal reference for the spectroscopic analysis and the absolute concentration of heavy metals in gas is not required to measure.

In this study, the calibration lines are obtained between relative line intensities and the concentration ratio of heavy metal to a normalizing element in particle samples simulating fly ash. Moreover, the plasma temperature is estimated as a representative parameter to generalize the calibration data. It offsets the variation of plasma conditions and makes the calibration lines more reasonable.

2. Sample Preparation and Experimental Apparatus

Particle samples simulating fly ash containing heavy metals were prepared via the dry impregnation method. Alfa-alumina particles (particle size ~ 15 μm) were impregnated with either iron chloride or lead nitrate solutions. Four

iron samples and three lead samples were made up for the experiment, in which concentration ratios of iron to aluminum are 0.42%, 1.43%, 3.60% and 9.70%, and concentration ratios of lead to aluminum are 0.50%, 0.81% and 2.55% respectively.

Specifications for our particle feeding system and LIBS setup are summarized in table 1. Sample particles are entrained by nitrogen gas and injected into quartz cell, where the laser beam is concentrated by a convex lens to generate the laser-induced breakdown plasma. In the detection system, gate delay time after breakdown was varied from 3 to 30 μsec as an experimental parameter.

Table 1. Specifications for the particle feeding system and LIBS system

Particle feeding system		LIBS system	
Particle driver	Piezoelectric oscillator	Pulse width	6 ~ 9 ns
Particle feeding rate	~ 1.8 g/min	Wavelength	532 nm
Gas flow rate (Nitrogen)	2.0 L/min	Energy used	400 mJ per pulse
Gas velocity in the test cell	2.83 m/sec	Repetition rate	10Hz
Temperature in the test cell	298K	Gate delay	2 ~ 30 μsec
		Gate width	5 μsec

3. Results and Discussion

Relative intensities of iron line at the wavelength of 381.58nm are plotted against concentration ratios of iron in particle samples in Fig.1. When estimating the relative line intensities of iron lines, aluminum line at 394.40nm was selected as intensity of an internal reference. Gate delay times of 3, 5, 10, 15, 20 and 30μsec were examined here. It is found that the relative line intensities I_{Fe}/I_{Al} are increased with the concentration ratio of Fe/Al, but the shape of solid line connecting data points for each gate delay time are non-linear and much irregular. It was caused by the fact that plasma temperature varied with both iron concentration in particles and delay time after the breakdown. Figure 2 shows plasma temperatures estimated via Boltzmann plot of iron lines with various gate delay time for each iron concentration sample. It is well known that plasma temperature diminish with time after breakdown. In addition, it was confirmed that higher concentration of iron in particles made plasma temperature lower. In order to generalize experimental data in Fig.1, relative intensities of iron line at plasma temperature of 4500, 4600, 4700, 4800 and 4900K were calculated by interpolating (partially extrapolating) plots in Fig.2 for each iron concentration sample and the result are re-plotted against concentration ratios of iron in Fig.3. They are no longer irregular and can be considered as calibration lines of relative line intensities of iron to aluminum for each plasma temperature. It means that concentration ratio of iron to aluminum can be obtained from line intensity ratio of iron to aluminum and plasma temperature, where all values required to measure in the actual analysis are not absolute but relative. It makes the application of LIBS to the field analysis much easier.

Increasing rate of relative intensities with iron concentration becomes flatter at higher plasma temperature, as shown in Fig.3. It implies that self-absorption becomes considerable with higher plasma temperature, but further study will be required to confirm that. Calibration lines of relative line intensities of lead to aluminum were obtained in the same way as iron, although the problem of low spectral sensitivity has remained because of weak line intensities and low concentration of lead in actual fly-ash.

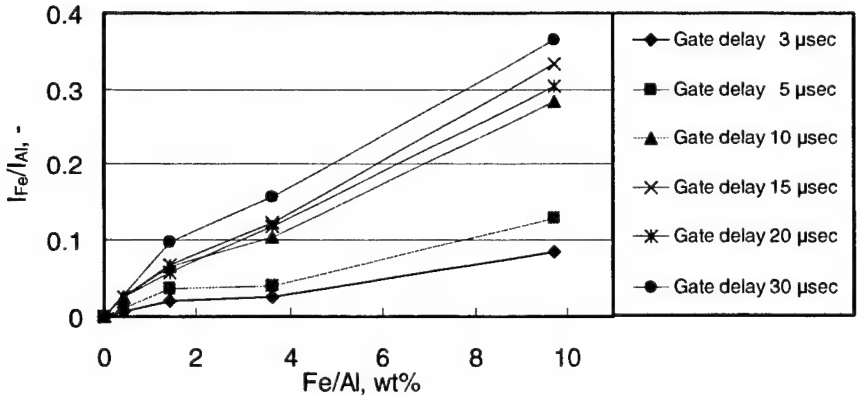

Fig. 1. Relative line intensities of iron at 381.58nm vs. concentration ratios of iron to aluminum in particle samples for different gate delay times

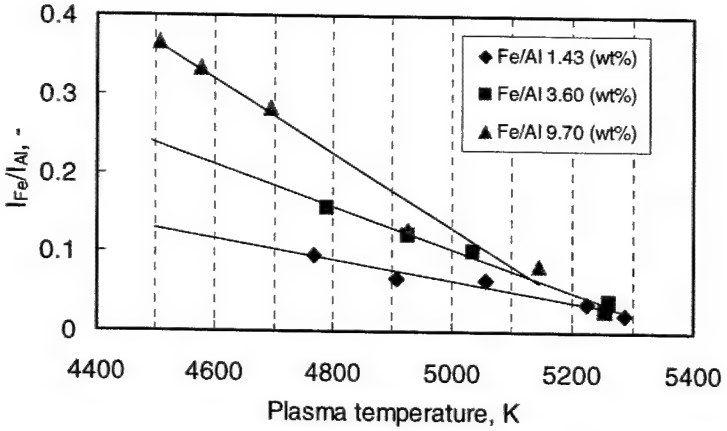

Fig. 2. Relationship between relative line intensities of iron and plasma temperatures estimated via Boltzmann plot of iron lines with various gate delay time for each iron concentration sample

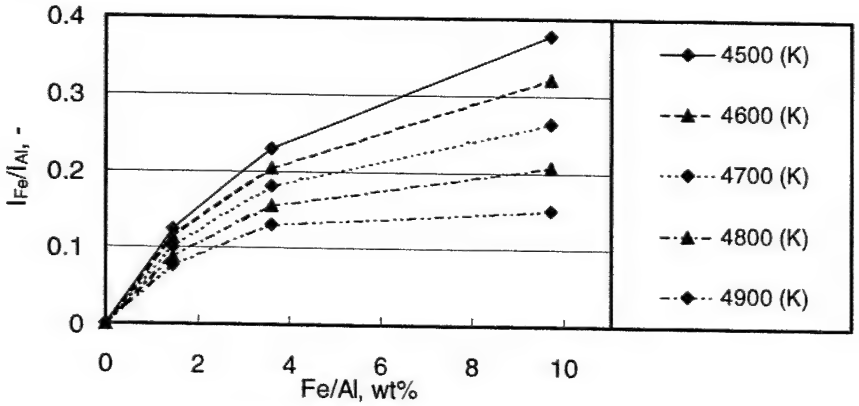

Fig. 3. Relative line intensities of iron against concentration ratios of iron at several plasma temperatures, calculated by interpolating experimental results

4. Conclusions

The LIBS technique was introduced to the measurement of heavy metals in particulates entrained in flue gas. The calibration lines of relative line intensities for iron and lead were obtained against their concentration ratios in the particle samples. Aluminum, which was typical matrix element contained in fly ash, was used as the internal reference element for spectroscopic analysis. Plasma temperature derived from the Boltzmann plots of iron line intensities was also estimated to generalize calibration lines. In the present analysis, all values required to measure are relative and it makes the application of LIBS much easier. If the calibration data are extended to wide range of plasma temperature and various elements, it will be useful for estimating the enrichment factor that shows the distribution behavior of heavy metals in combustion process.

[1] D. K. Ottesen, J. C. F. Wang, L. J. Radziemski, "Real-time laser spark spectroscopy of particulates in combustion environments," APPLIED SPECTROSCOPY, **43**(6), 967-976 (1989)
[2] J. P. Singh, F. Yueh, H. Zhang, R. L. Cook, "Study of laser induced breakdown spectroscopy as a process monitor and control tool for hazardous waste remediation," Process Control and Quality, **10**, 247-258 (1997)
[3] H. Zhang, F. Yueh, J. P. Singh, "Laser-induced breakdown spectrometry as a multimetal continuous-emission monitor," APPLID OPTICS **38**(9), 1459-1466 (1999)
[4] G. M. Weyl, "Physics of laser-induced breakdown: An update" *in Laser-induced plasmas and applications*, L. J. Radziemski, D. A. Cremers, ed. (Marcel Dekker, New York, 1989).
[5] E. Hatanpaa, H. Hoffren, M. Hahkala, I. V. Oy, T. Laitinen, K. Larjava, M. Tolvanen, "Distribution of the Trace elements in coal-fired power plant streams," in Proc. of EPRI/DOE Int. Conf. on Managing Hazardous and Particulate Air Pollutants, (Toronto, Canada, 1995), Book2
[6] H. Moritomi, R. Yoshiie, K. Sonoda, T. Mori, "Behavior of heavy metals in incineration process of sludge waste," in Proc. of 5th Int. Conf. on Technologies and Combustion for a Clean Environment, (Lisbon, Portugal, 1999), pp.39-42
[7] L. L. Sloss, I. M. Smith, *Trace element emissions* (IEA Coal Research, England, 2000)
[8] I. M. Smith, L. L. Sloss, *PM10/PM2.5 – emissions and effects* (IEA Coal Research, England, 1998)

NOTES

Laser Ablation and Desorption

Friday, September 27, 2002

Ulrich Panne, Tech. Univ. of Munich, Germany,
Presider

FD
3:00pm–4:00pm
Room: Royal Palm III

Influence of Crater Dimensions on Laser-Induced Plasma Properties

Richard E. Russo, Xianzhong Zeng, Samuel S. Mao, Chunyi Liu, Xianglei Mao
Lawrence Berkeley National Laboratory, Berkeley, CA 94720

Introduction

When a pulsed, high-powered laser beam is focused onto the surface of a target (solid or liquid sample), a portion of the illuminated mass is ablated into vapor-phase constituents. In many cases, the energy and irradiance of the laser beam is significant to convert this vapor into a luminous plasma above the sample surface. Spectroscopic interrogation of the plasma is a powerful technology for direct multi-elemental chemical analysis; a technology termed laser-induced breakdown spectroscopy (LIBS). LIBS is attractive for the chemical analysis because any material can be ablated without sample preparation, data are measured in real time, and the plasma provides a complete chemical signature of the sample constituents.

The ability to utilize LIBS as an analytical tool depends on understanding the plasma properties. The plasma temperature and electron number density influence the spectral line, as well as background, emission intensities. Plasma formation and expansion in time will also significantly influence these intensities. In many applications, time-resolved measurements are required to achieve good signal to background and signal to noise ratios for accurate and precise measurements. In addition, the crater dimensions will influence such measurements. Depth analysis variations in solid samples are important for a variety of micro analytical applications; e.g., inclusion analysis, diffusion studies. Previous studies showed that the crater depth-to-diameter (aspect) ratio was an important parameter determining the degree of elemental fractionation using ns-laser ablation. Elemental fractionation becomes significant when the crater aspect ratio is greater than six [1,2]. Laser energy coupling to a solid increases as a crater is formed in the target [3,4]. For an aspect ratio varying from 0 to 5, the amount of energy absorbed varied from 1 to 10 times the energy absorbed by a flat surface.

Because laser energy coupling increases, and the plasma is restricted at early times, it is reasonable to assume that a laser-induced plasma in the crater will have a larger electron number density and higher plasma temperature, compared with a LIBS plasma induced on a flat surface. To determine the plasma properties, we chose fused silica as the sample and measured the Si emission lines inside and outside of several craters. The spatial distribution of plasma temperature and electron number density were determined by measuring Stark broadening of the emission lines and the relative line-continuum ratio at times from 60 ns to 300 ns after the laser pulse.

Experimental system

The experimental system includes a quadrupled Nd:YAG laser (266 nm wavelength, 3-ns pulse width) used as the ablation laser, and a lens to image the laser-induced plasma into the entrance slit of a Czerny-Turner spectrometer. The spectra were detected by an intensified charge-coupled device (ICCD), which consists of a thermoelectrically cooled CCD and a Microchannel Plate image intensifier. This detection system provides a spectral window of ~13 nm and resolution of typically 0.125 nm. Gating the ICCD and changing the delay time enables the spectra to be temporally resolved. The gate width was set at 30 ns. This study emphasizes the

early phase (<300 ns) of the plasma characteristics. A diagram of the experimental system can be found in Liu et al. [5].

Fused silica samples were cut into pieces of 2 mm width and 2 mm height, and placed on an *xyz* translation stage. Craters with different diameters and depths were fabricated by ablating the silica under repetitively pulsed conditions with known laser beam energies and spot sizes. A white-light interferometric microscope was used to measure crater dimensions. The silicon emission line Si(I) at 288.16 nm was measured.

Results and Discussion

Effects of aspect ratio

Plasma temperatures and electron number densities were measured in three craters and compared to the data from flat surface LIBS. The crater diameters were 80, 160 and 490 microns; all had the same depth of about 480 micron. The data are shown in Fig. 1a (plasma temperature) and Fig. 1b (electron number density). The inset in figure 1a shows the crater profiles. The plasma temperature is higher in the crater; e.g., for the crater aspect ratio of six, the plasma temperature decreases from 77000 K (in the crater) to 40000 K (1.0 mm from the crater bottom), and electron number density falls from 2×10^{19} to 5×10^{18} cm^{-3}. On a flat surface, the plasma temperature and electron number density are much lower, 20000 K and 2×10^{18} cm^{-3}, respectively, and do not change significantly with distance from the surface.

The plasma temperature and electron number density in the small crater (aspect ratio=6) are much greater than in the larger craters (aspect ratio=3 and 1). As the diameter increases, the plasma temperature and electron number density in the crater approach the flat surface result.

Effects of time

To evaluate the temporal evolution of the plasma properties, spectra were measured at two locations for the crater and one for the flat surface (points A-C in inset of figure 2a). For the crater with depth = 0.5 mm, one point is in the crater (distance from the bottom surface is 0.2 mm) and the second point is outside of the crater (distance from the bottom surface is 0.7 mm). For the flat surface, the distance was 0.2 mm.

Initially, the plasma temperature and electron number density in the crater are much higher than the plasma from the flat surface. At a time of about 90 ns, the plasma temperature and electron number density in the crater are 97000 K and 6.0×10^{18} cm^{-3}, respectively; while the temperature and electron number density of the plasma from the flat surface are much lower, 40000 K and 3.0×10^{18} cm^{-3}, respectively.

As time increases, the plasma temperature and electron number density in the crater, $T_e=A_1 t^{-1.75}$ and $n_e=A_2 t^{-1.51}$, respectively, decrease faster than outside of the crater, $T_e=A_3 t^{-0.90}$ and $n_e=A_4 t^{-0.98}$, respectively. The plasma inside the crater expands out of the crater and this results in a dramatic decrease of the plasma temperature and electron number density inside the crater. For the flat surface, $T_e=A_5 t^{-0.90}$ and $n_e=A_6 t^{-0.95}$. These data will be used to describe the expansion dynamics of the plasmas, which will be presented in future work.

References

[1] A.J.G. Mank, P.D. Mason, J. Anal.At.Spectrom. 14 (1999) 1143
[2] O.V. Borisov, X. Mao, R. E., Russo, Spectrochim. Acta Part B 55 (2000) 1693
[3] S. H. Jeong, J. Appl. Phys. Vol. 80, No. 4, (1996) 1996
[4] M. A. Shannon, Applied Surface Science, Vol 127-129 (1998) 218
[5] H.C. Liu, X.L. Mao, J.H. Yoo, R.E. Russo, Spectrochim. Acta Part B 54 (1999) 1607

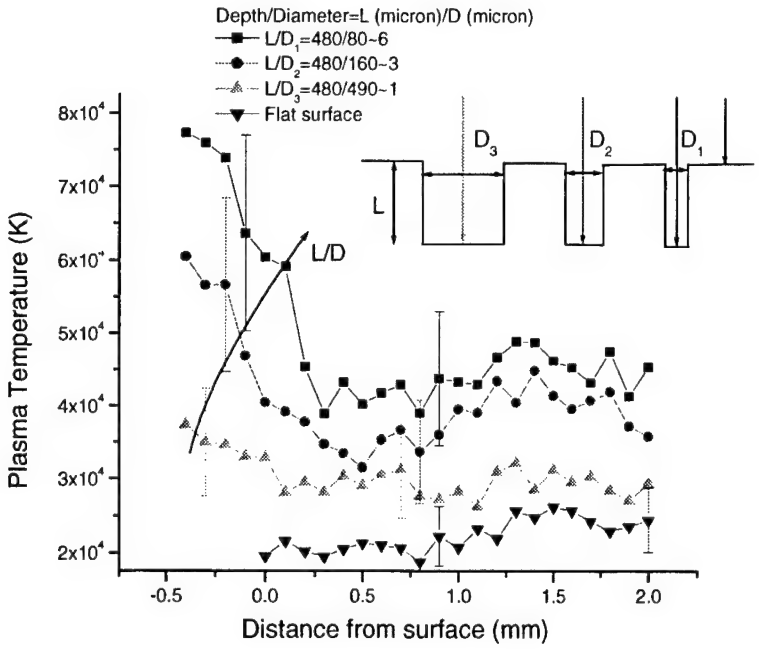

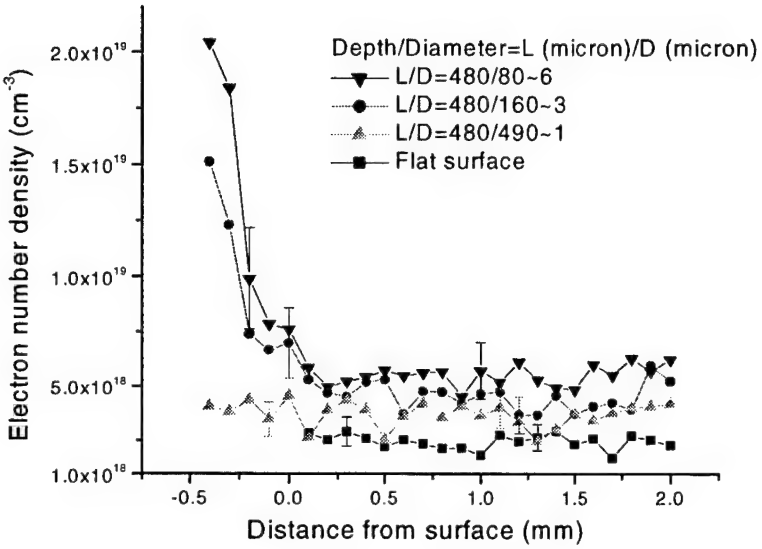

Fig. 1) Temperature and electron number density and vs. distance from surface. Time = 100 ns and irradiance = 6.9 GW/cm^2

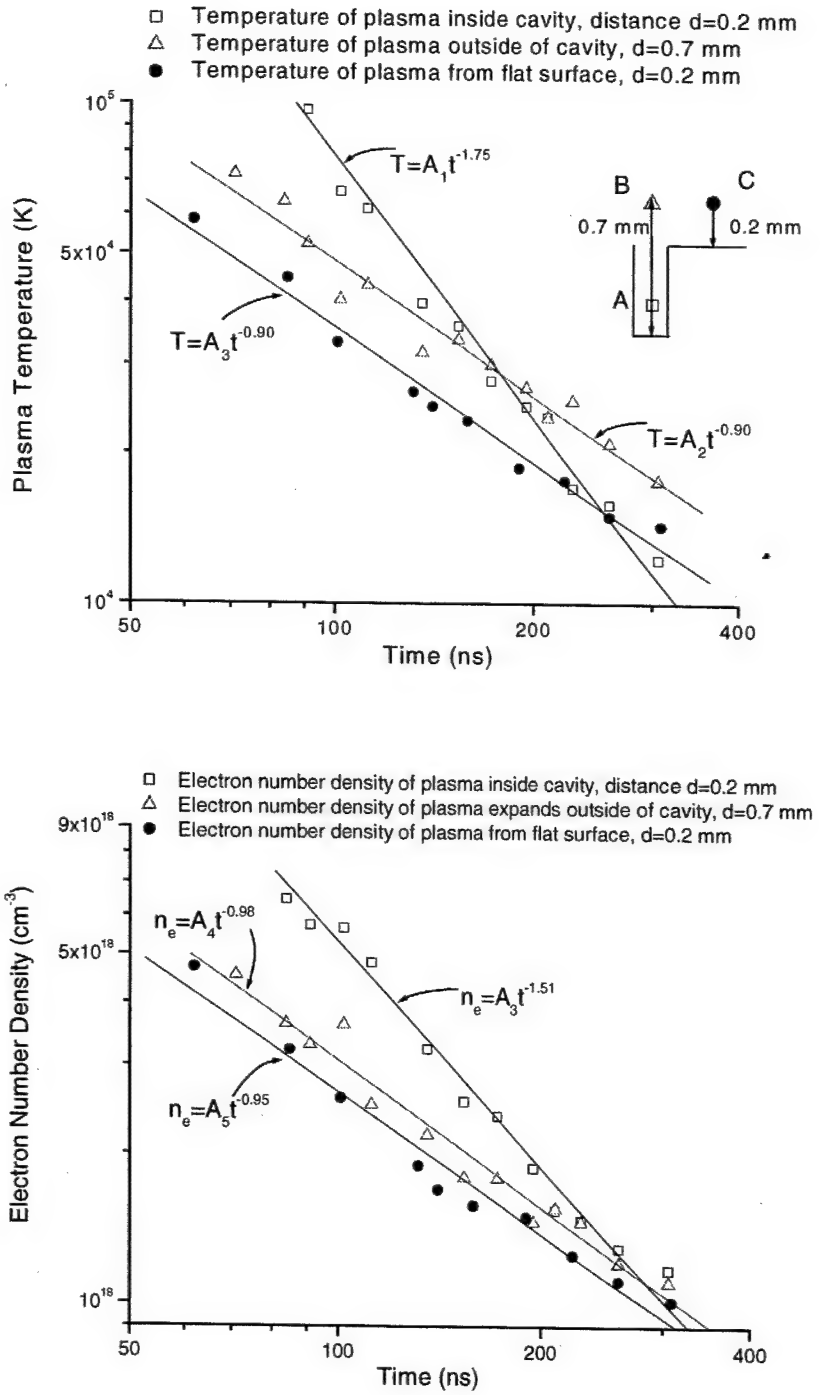

Fig. 2) Time evolution of plasma temperature and electron number density inside and outside of the crater. Crater diameter is 80 micron and depth 480 micron. Irradiance is 7.67 GW/cm^2.

The effect of laser-induced crater depth in LIBS analysis and shock wave dynamics

M. Corsi, G. Cristoforetti, M. Hidalgo, D. Iriarte, S. Legnaioli, V. Palleschi, A. Salvetti and E. Tognoni

Istituto per i Procesi Chimico-Fisici del Consiglio Nazionale delle Ricerche, Via Alfieri 1, 54124 Pisa (Italy)

Abstract: The influence of the crater depth on the laser-produced plasmas properties has been studied. The dynamics of the shock waves resulting from the laser-sample interaction inside and outside the craters and the results of in-depth LIBS analysis of metallic samples are discussed.

OCIS codes: (300.0300) Spectroscopy

1. Introduction

Laser- Induced Breakdown Spectroscopy (LIBS) technique is being used in the recent years as a viable tool for fast and accurate analysis of metals [1,2]. One of the most appealing characteristics of LIBS is the possibility of sampling the composition of the materials well under the surface, using the laser itself as a micro-drill. It has been shown in the literature that laser- induced crater depth can be controlled by varying the number of the laser shots on the surface, and that the ablation rate decreases with the increasing depth of the crater. Moreover, the material ablated from the bottom of the crater appears at the surface of the metal with a measurable delay, which increases with the crater depth and, therefore, is a function of the number of laser shots addressed on the surface. It has been also proposed that the shock wave resulting from the laser-matter interaction, could further ionize the surrounding atmosphere, thus enhancing the spectroscopic signal and increasing the sensitivity of the LIBS analysis.

This work is focused to the study of the influence of the laser-induced crater depth on the nature of the resulting plasmas and LIBS signal, which is particularly useful for depth profiling analysis of solid samples. The spectroscopic analysis was accompanied with a study of the formation and evolution of the laser-induced shock wave inside and outside the different craters

2. Determination of the laser ablation rate

The relation between crater depth and number of laser shots on the surface of a copper alloy sample was measured using the method introduced by Russo [3]. A copper disk was cut in two parts, which were superimposed and held firmly together in order to present at their junction a smooth edge over which the laser was shot. With this particular geometry was possible, after separating the two pieces of metal, to obtain the sections of the laser-produced craters whose depths could be easily evaluated.

From this measurement was easily calculated the relation between crater depth and number of laser shots. as shown in Figure 1.

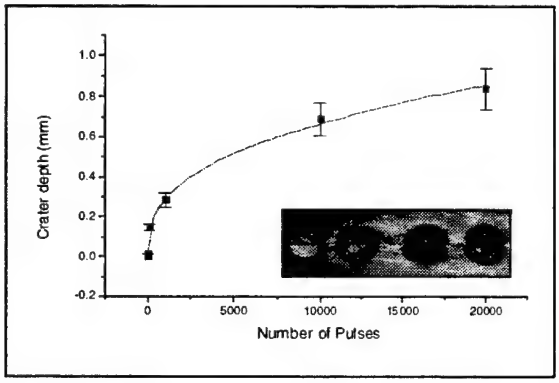

Fig. 1. Crater depth vs. number of laser shots

3. Study of shock wave dynamics

The interaction of an intense laser beam with a metallic surface produces a strong shock wave that propagates in the surrounding atmosphere according to the laws of strong explosion. The mechanical expansion of the shock wave is one of the most effective ways in which the laser-induced plasma lose its energy; it is therefore interesting to experimentally determine the propagation laws of the shockwave inside and outside the laser-produced crater.

In order to derive these laws was necessary to measure the position of the shock wave front as a function of time in the first few microseconds after the laser pulse. This was accomplished using the high-speed Schlieren shadowgraphy method, and acquiring successive shadowgrams at intervals of 1 μs with a DTA CCD camera coupled with a.frame camera. From the shadowgrams was possible to measure the position of the shock wave front at the different times, and thus to obtain the propagation law R(t) of the shock wave front. The same measurements, repeated after multiple laser shots, i.e. at different crater depths, resulted in the plot shown in Figure 2a.

According to the strong explosion theory of the laser-produced shock waves, the propagation of a (semi-) spherical shock front can be represented (for $t > t_0$) as:

$$R(t) \propto (t - t_0)^{2/5} \tag{1}$$

where t_0, representing the time needed to the shock wave for exiting the crater, is zero at the sample surface. From the best fitting of the experimental data with eq. (1) was possible to derive the relation between t_0 and the number of laser shots and then, using the results shown in Figure 1, between t_0 and crater depth. This relation is shown in Figure 2b. The dependence shown in this figure can be represented in a form similar to eq. (1), except for the exponent (1/5 instead of 2/5).

$$R(t) \propto t^{1/5} \tag{2}$$

The 1/5 exponent in this equation is consistent with an almost-planar propagation of the shock wave inside the crater. This behaviour was confirmed by the results of a numerical simulation carried out using a variation of the hydrodynamic code GASDYN, a 2D Eulerian hydrodynamic code based on the conservation equation for an ideal fluid along with the equation of state of a perfect gas [4].

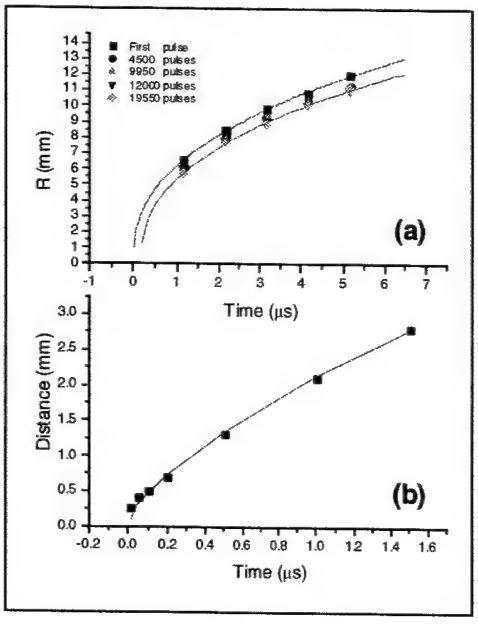

Fig.2. Propagation law of the shock wave front after different number of laser shots al the sample surface (a), and travel time inside the laser produced crates as a function of crater depth (b)

4. The effect of crater depth in the LIBS measurements

The influence of the laser parameters and sample nature on the laser-induced crater has been studied by many authors. Mitchell *et al* [5] found that the higher the laser repetition rate, the higher the atomic emission signal and subsequently, the greatest the mass ablated and laser induced crater depth. Allemand and Ishizuka [6] have shown that the reflectivity of the sample surface, the density, the specific heat and the boiling point temperature of the solid target have an important influence on the shape and size of craters. For depth profiling analysis, however, could be very interesting to know how laser-induced crater depth influences the observed LIBS signal, and consequently, the in-depth analysis of the material.

To study this influence, laser plasmas were produced at the bottom of craters having different depths in a copper alloy disk. Plasmas produced inside the craters were spatially and temporally resolved and then compared with those produced at the surface of the metallic sample.

Crater walls interact with the spark modifying the spatial and temporal distribution of the plasma plume temperature an electronic density, and consequently affecting the observed LIBS signal A clear example of this phenomenon is shown in Figure 3. Here is represented the spatial distribution of the 216.51 nm Cu(I) atomic line (a) and 214.89 nm Cu(II) ionic line observed from plasmas produced at the sample surface and at the bottom of two craters of 1.0 mm and 1.5 mm depth respectively. As can be seen, both lines present different emission profiles depending upon the crater depth. Emission from plasmas generated inside the 1.0 mm crater depth is intensified due to its interaction with the crater walls, which in this case produce a sort of plasma confinement effect. Deeper craters, however, actuate as a plasma cooling, absorbing the plasma radiation which results in a decrease in the observed LIBS signal as shown in Figure 3.

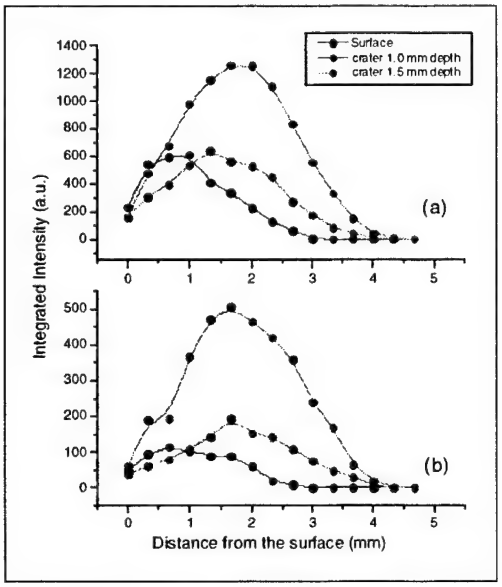

Fig. 3. Spatial distribution of Cu (II) line at 214.89 nm (a), and Cu(I) line at 216.51 nm (b) of plasmas produced at different crater depths

5. References

[1] L. Radziemski and D.A. Cremers, Laser Induced Plasmas and Applications. Marcel Dekker, New York (1989)
[2] D.A. Cremers, Appl. Spectroc., **41**, 572 (1987)
[3] W.J. Chan and R.E. Russo, Spectrochim. Acta B, **46**, 1471 (1991)
[4] P.A. Vojnovich, A.I. Zhmakin and A.A. Fursenko, Program for computation of multidimensional non steady inviscid shoked flows (in Russian). Preprint No 1268. A.F. Ioffe Physicotech Inst.. Academy of Science. Leningrad (USSR), 1988.
[5] P.G. Mitchell, J.Sneddon and L.J. Radziemski. Appl. Spectrosc., **41**, 141 (1987).
[6] C.D. Allemand. Spectrochim. Acta B, **27**, 185 (1973)

Imaging, Surface Mapping and Stratigraphy by LIBS

Friday, September 27, 2002

Demetrios Anglos, Inst. of Electronic Structure and Laser, Greece,
Presider

FE
4:30pm–5:30pm
Room: Royal Palm III

Laser Microanalysis of Glass and Tool Steel

K. Loebe, H. Lucht, A. Uhl*
** Corresponding Author*
LLA Instruments GmbH, Schwarzschildstr. 10,
12489 Berlin, Germany, www.LLA.de, mail@LLA.de,

A fast technique for micro analytical characterization of glass and tool steel is now available.

The local resolved analysis of the chemical composition of glass is one of the main application fields for microanalysis using LIBS. Competing conventional techniques require high efforts for sample preparation. The electron spectroscopy as method of choice often leads to wrong interpretation of results, due to the insulator properties of glass and corresponding charge effects [1].

A glass defect in a tumbler (Fig. 1) has been characterized by a micro-LIBS line-scan, using a 266 nm diode-pumped Nd:YAG-laser for excitation. Three characteristic elements have been selected, showing significant changes in absolute intensity at the transient matrix-defect (Fig. 2). The results prove the possibility of at-line microanalysis of glass defects. Semi-quantitative measurements of glass defects by comparison of plasma spectra of the defect and of the surrounding area satisfy the industrial requirements. Impurities of raw material can be identified and characterized. A particular monitoring of element impurities in the ppm-range is possible. By measurement of calibration samples with known concentration of the corresponding element a correlation between the intensity of spectral lines and the element concentration was achieved, too.

Tool steel has been characterized by laser microanalysis, too. The change of elemental composition at the transient stellite-solder has been determined. An area scan (Fig. 3) gave a complete two-dimensional picture of the selected elements, showing abrupt changes along the solder edge. On the basis of the results it is shown, that laser microanalysis is a suitable technique for quality control in steel production as well as for fundamental research of dynamic changes (e.g. diffusion) in steel.

A new laser microscope system has been developed and used for micro-analytical characterization of complex material by multi-element-analysis within a few seconds. A local resolution below 10 pm is possible. The universal measuring principle of LIBS in combination with an Echelle optics permits real simultaneous multi-element-analysis over a range of 200 nm - 780 nm with a spectral resolution of a few pm.

Variations in main elemental composition as well as impurities by trace elements are detected at the same time. The element specific detection limits are in the range of 10 - 100 ppm. The developed microscope system features a completely UV-transparent optics, resisting high laser power, and an optical laser-microscope-coupling, adjustable to the excitation wavelength of the laser. The integrated step-motor driven x-y-table allows a scanning range on the sample of 75 mm x 25 mm, with a repetition accuracy of better than 1 µm.

The use of laser microanalysis is not limited to glass and tool steel only, it is a prospective method for other material as well, e.g. wood [2].

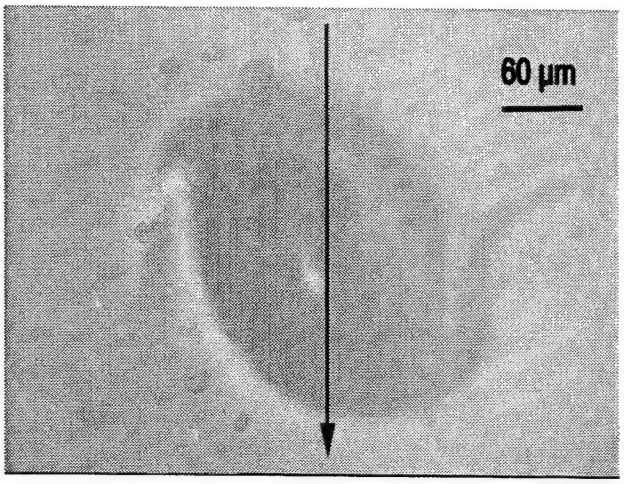

Figure 1: Microscope picture of glass defect (point defect) in a tumbler

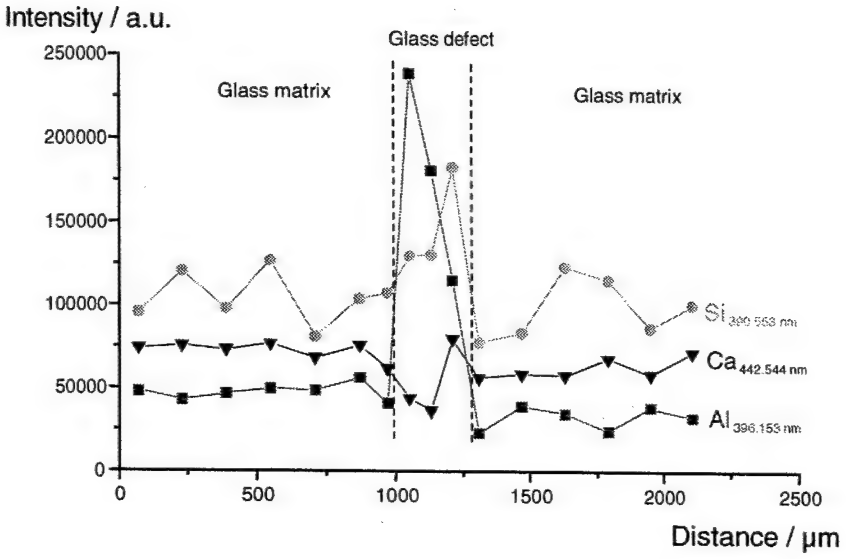

Figure 2: Changing elemental composition of a glass defect (point defect) in a tumbler - Line scan

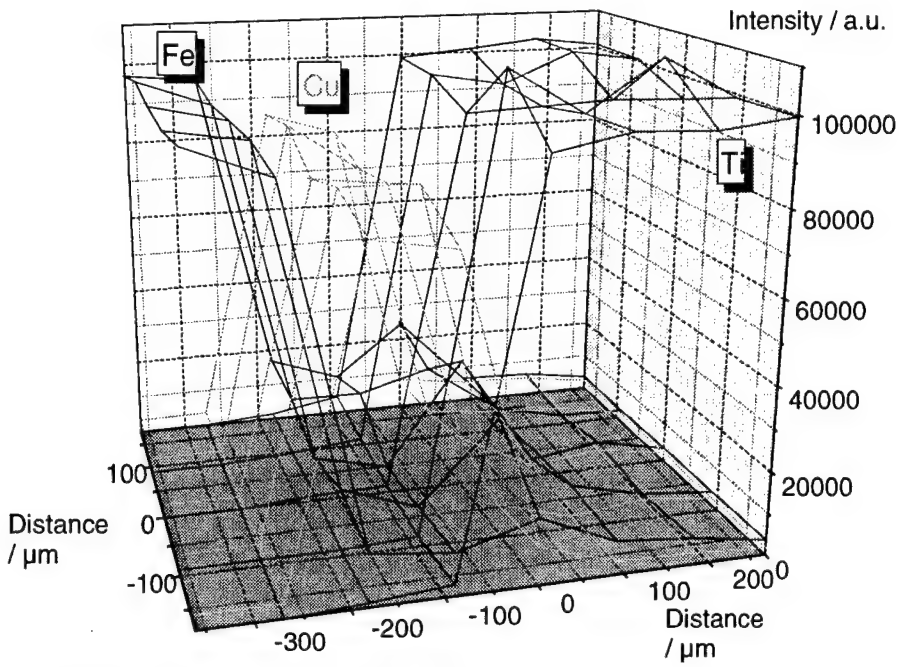

Fig. 3: Elemental distribution along the solder edge of a tool steel - Area scan

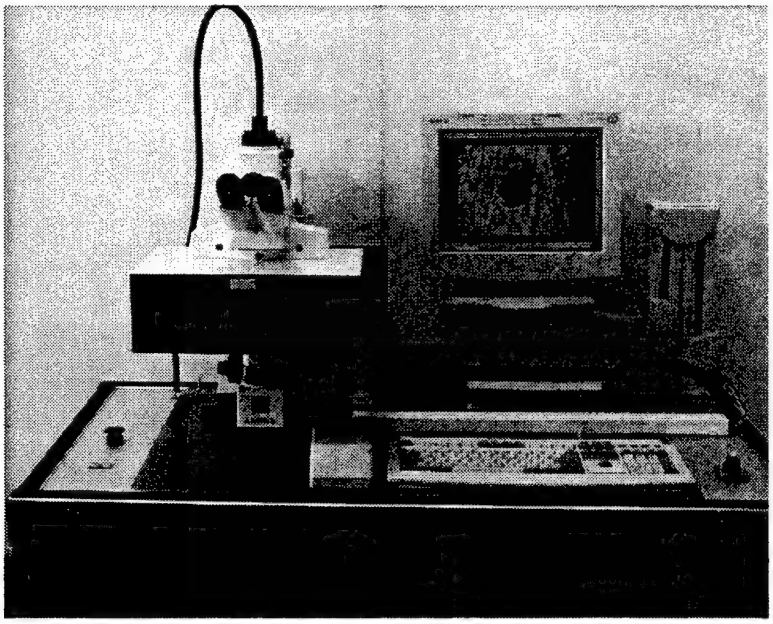

Fig. 4: New developed Laser micro analyzer

[1] Bange, K., Müller, H. and Strubel, C.: Characterization of defects in glasses and coatings on glasses by micro analytical technique, Mikrochimica Acta, **0/589**, 1999, p. 1

[2] Uhl, A., Loebe, K., Kreuchwig, L.: Fast Analysis of Wood Preservers using Laser Breakdown Spectroscopy, Spectrochimica Acta B **56/6**, 2001, pp 795-806

Micro-LIBS and micro-Raman spectroscopic analysis of ancient pottery

G. Cristoforetti, M. Corsi, M. Giuffrida, M. Hidalgo, D. Iriarte, S. Legnaioli, V. Palleschi, A. Salvetti, E. Tognoni
Istituto per i Processi Chimico-Fisici del Consiglio Nazionale delle Ricerche, Via Moruzzi 1, 56124 Pisa , Italy
e-mail: vince@ifam.pi.cnr.it

G. Boschian and S. Mazzoni
Dipartimento di Scienze Archeologiche dell'Università di Pisa, Via Santa Maria 53, 56126 Pisa, Italy
e-mail:boschian@archeo.unipi.it

Abstract: Several samples of oriental colored pottery have been analyzed with micro-LIBS and micro-Raman technique in order to get information about the elemental composition and molecular structure of the pigments used.

OCIS codes: (140.3440) Laser-induced breakdown, (300.6450) Spectroscopy, Raman

1. Introduction

The idea of using Laser Induced Breakdown Spectroscopy for analysis and characterization of materials used in Cultural Heritage was proposed several years ago by FORTH Institute in Crete (Greece) and former IFAM (now Institute for Chemical-Physical Processes) in Pisa (Italy).

More recently, the same laboratories have developed multi-technique instruments for micro-LIBS and micro-Raman analysis with the aim of obtaining quantitative elemental characterization of the materials by LIBS, and qualitative discrimination of the molecular structure of the same using micro-Raman spectroscopy. The joint use of the two techniques, in fact, allows for a complete characterization of the material used. In many cases, the information obtained by Raman spectroscopy could clarify the findings of LIBS analysis (a typical case is the analysis of pigments with similar composition but different molecular structure) and, vice-versa, the LIBS analysis could be useful for the identification of materials characterized by weak Raman response.

The Applied Laser Spectroscopy Laboratory in Pisa has already successfully exploited the benefits of joint LIBS/Raman measurements in the analysis of fragments of Roman frescoes coming from "Villa di Giulia" in Ventotene and Cividade Camuno, in northern Italy. Moreover, a detailed analysis by LIBS and Raman on a small fragment of a painting from Domenico di Pace, called "Il Beccafumi" has been recently completed, allowing the complete characterization of the red pigment used as foreground color and the blue pigment used as a base.

2. Description

In this paper, we report the results obtained by LIBS and Raman analysis of fragments of "*Red-Black Burnish*" pottery, coming from surface findings in Tell el-Bek, near Harim in the Oronte valley in the northern part of Syria. The pottery is dated to the cupper age and is characterized by the presence of red and black colors.

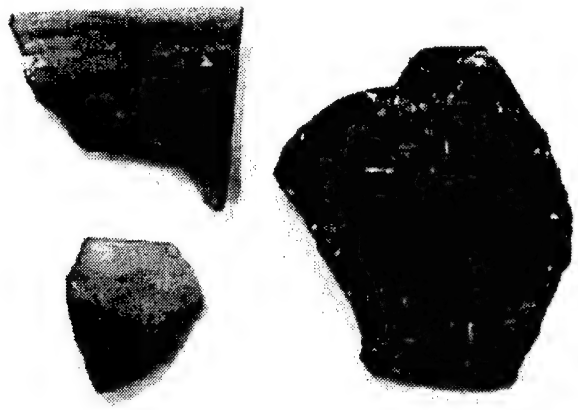

Fig. 1. Some of the ceramic fragments analyzed by LIBS and Raman

Both the black and red parts have been analyzed. The Raman spectrum of the black part of the fragment is shown in figure 2, together with the Raman spectra of the so-called Ivory Black (carbon-based black ($[Ca_3(PO_4)^2]$ + $CaCO_3$ +C),) and magnetite (Fe_3O_4), a iron-based black pigment that could have been produced by the thermal treatment of the substrate in reducing environment.

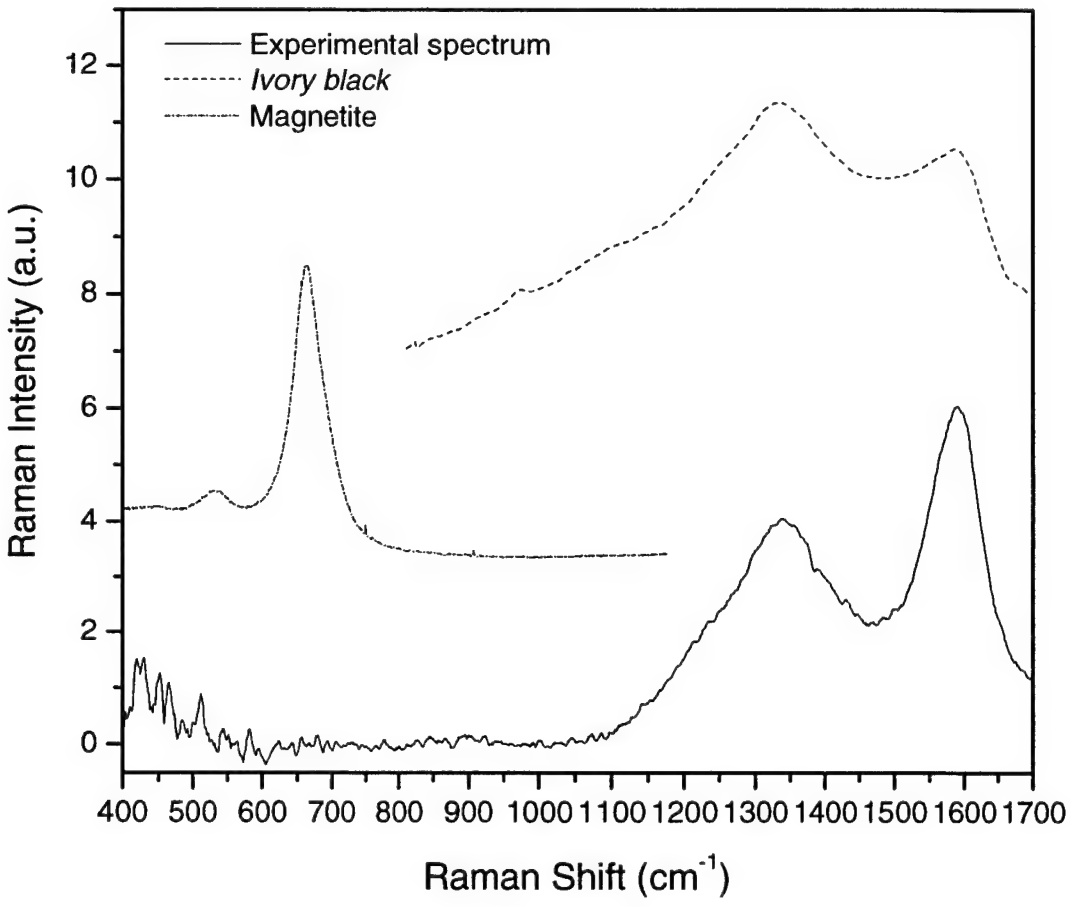

Fig. 2. Experimental micro-Raman spectrum of the black pigment, compared with reference spectra of Iron Black and Magnetite

3. Discussion

The identification of the black pigment as Iron black seems to be quite straightforward, supporting the hypothesis that the black color was generated during firing of the argillaceous clay material in the presence of organic material (wood, leafs, etc..).

Moreover, the LIBS spectrum of the same black pigment allows excluding the use of Manganese Oxide (another material that could have been added to the substrate for obtaining the black color).

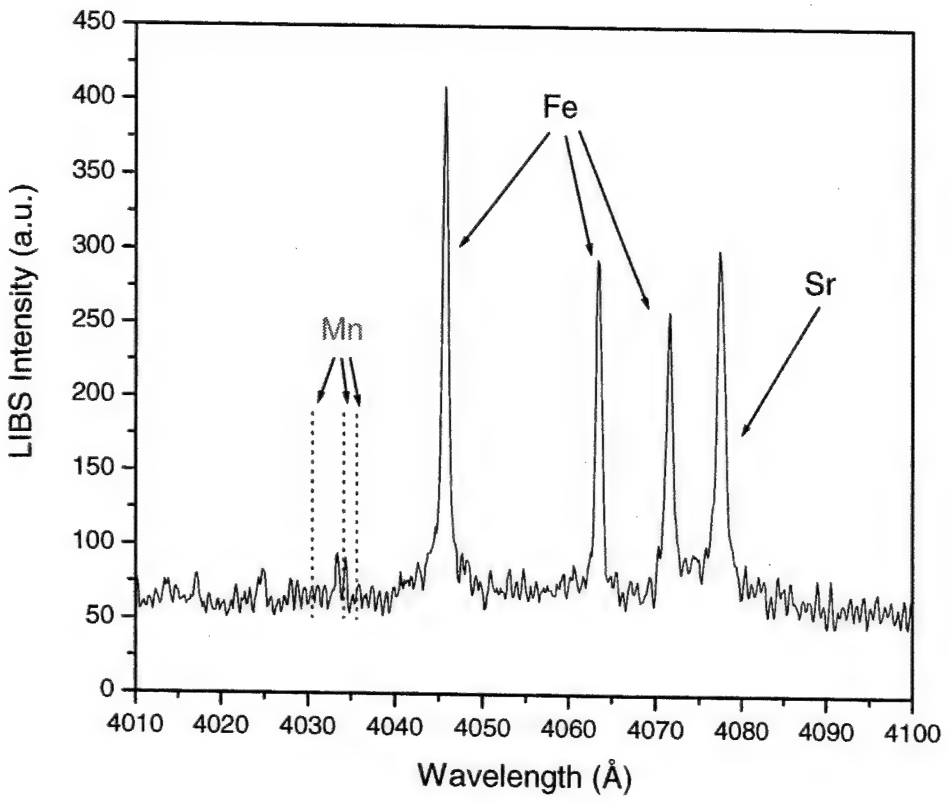

Fig. 3. A portion of the LIBS spectrum of the black pigment, showing the absence of Mn lines. Lines from Iron and Strontium (elements present in the substrate) are also shown.

Similarly, the Raman and LIBS spectra of the red pigment show the evidence of use of Hematite (Fe_2O_3).

The present findings are qualitatively confirmed by microscopic analysis performed on thin sections of the same pottery. The microscopic analysis shows, in correspondence of the reddish parts of the pottery, a thin colored layer spread over a deep black substrate which is almost surely resulting from the firing treatment of the clay argillaceous material of the substrate.

Laser Emission Spectroscopy (LIBS) for Plated Layer Thickness Identification

George Asimellis, Bruce Bromley, and Stu Rosenwasser

Advanced Power Technologies, Inc. 1250 24th Street NW, Suite 850
Washington, DC 2003
(202) 223-8808 stuartr@apti.com

Abstract: A commercial Laser-Induced Breakdown Spectroscopy instrument is being used to identify plated layer thickness on steel core coins plated alternating layers of Nickel, Copper, and Nickel. Tracer 2100™ can determine layer thickness by identifying the layer boundaries using successive shots and proprietary analytical methods, with a precision of less than 0.5 microns in less than 10 minutes total analysis and preparation time.

OCIS codes: (300.0300 -300.6210) Spectroscopy-Atomic Spectroscopy
(100.0100-100.2960) Image Processing-Image analysis

1. Introduction

The plating facility in Winnipeg for the Canadian Royal Mint has identified a problem with QC of the plated layer thickness of their coins. Typically, the coins are of Iron core, plated with approximately 40-to-80 micron-thick alternating layers of Nickel, Copper, and Nickel. Current mechanical methods are slower and labor intensive.

This work is focusing on the applicability of LIBS: We believe that this is a unique LIBS application where no other current spectroscopic method (ICP or XRF) can be applied. The method is going to be discussed and results with pre-calibrated coins are going to be presented.

2. Method development

2.1 Methodology

First, one has to identify a single spectral window, in which, by one LIBS shot one can determine simultaneously all three elements of interest, Cu, Ni and Fe. Consideration must be given that maximum resolution has to be maintained. We identified the following lines of interest that can be obtained with a single LIBS shot, as shown in Figure 1 below:

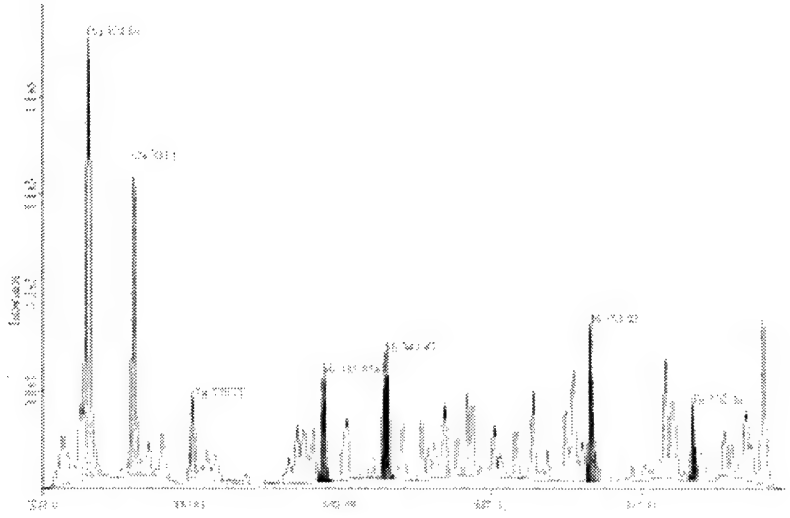

Fig. 1. Spectral lines of the three elements of interest, Cu, Ni and Fe, that can be obtained with a single LIBS measurement.

Depending on the dispersion formula used in the spectroscopic analysis, the line identifiers may slightly change. The absolute wavelength numbers for the lines in use are summarized in the table 1 below:

Table 1. Spectral lines of interest in identifying layer thickness

Element	Cu	Ni	Fe
Lines (nm)	324.753	338.057	358.119
	327.395	342.476	
	330.795	352.90	

As the layer penetration depth increases, not all of these lines are present, nor their relative strength is as shown in Fig. 1. As penetration occurs, for example from the Ni to the Cu layer, the Cu line strength compared to the Ni lines increases substantially, and this can be an indicator of layer boundary. Similarly, early shots have no Fe peak presence, and we employ the first presence of the Fe peak as an indicator of the layer appearance. By simply counting the number of shots required for these changes to appear, one may calibrate the layer thickness.

2.2 Method Example

The following example in Fig. 2 shows the evolution of the 358 Fe peak strength (counts) as shot numbers increase (horizontal axis). A determination can be made that the Fe layer occurs after shot # 240.

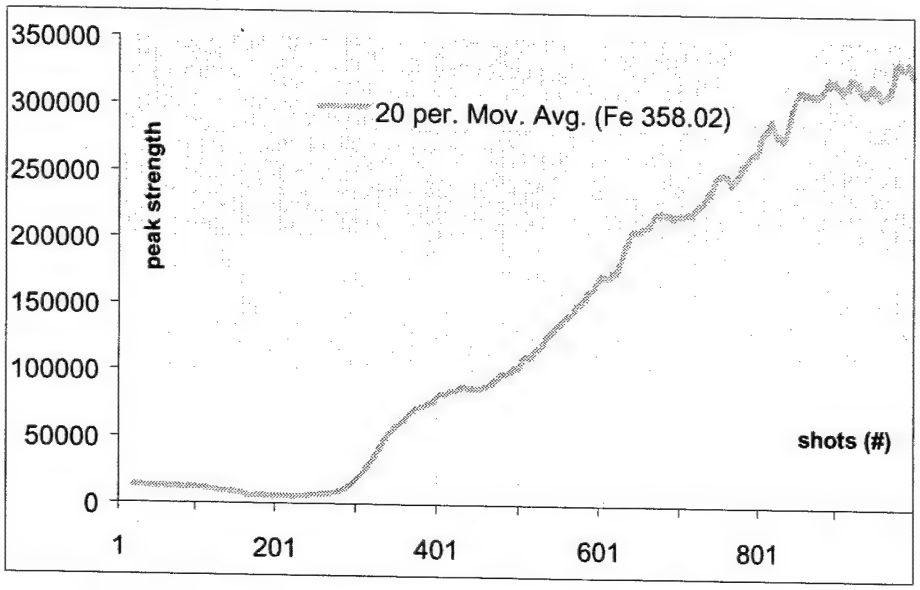

Fig. 2: Fe 358nm line strength (counts) evolution as shot numbers increase

Similarly, other transitions that involve newly-encountered element, eg. from Ni to the Cu layer can be made with quite ease. However, when a subsequent layer consists of an element already encountered in previous layer, (eg. a new Ni layer) the transition is not obvious. Many factors can be accounted for this: material ablated through LIBS interaction is partially re-deposited in the pit; material is not only ablated from the lower end of the pit but also from the 'walls' of the pit, which, as penetration depth increases to more than 40 microns has increasing material contribution in the ablation which contains all the previous constituents.

By observing these variations, and applying proprietary analysis techniques, we determined that thickness measurements is possible with a relative standard deviation of around 10% on layer thickness of about 25 microns. Table 2 presents data obtained from a quality control sample of pre-determined layer thickness. Sixteen different spots of around $2mm^2$ sample size were used as a test to our method.

Table 2. 16-point Statistics on Layer thickness determination using LIBS

Sample 3-layer QC #5	Layer 3 (top)	Layer 2	Layer 1 (Bottom)
	Shot #s	Shot #s	Shot #s
Spot 1	62	78	69
Spot 2	61	80	40
Spot 3	53	104	31
Spot 4	50	83	53
Spot 5	54	100	34
Spot 6	66	84	34
Spot 7	54	94	36
Spot 8	47	72	69
Spot 9	48	69	70
Spot 10	54	101	50
Spot 11	48	100	61
Spot 12	76	73	88
Spot 13	61	112	82
Spot 14	74	105	64
Spot 15	70	94	73
Spot 16	65	93	77
Average	60.27	90.64	64
RSD (%)	18	13	13

3. Summary

Tracer 2100™ can determine layer thickness by identifying the layer boundaries using successive shots and proprietary analytical methods, with a precision of less than 0.5 microns in less than 10 minutes total analysis and preparation time with precision less than 20%.

Key to Authors and Presiders

Laser Induced Plasma Spectroscopy and Applications
Technical Program Committee

Committee Chairs

Andrzej Miziolek, *ARL, USA, Program Chair*
Vincenzo Palleschi, *IFAM, Italy, General Chair*

Committee Members

Dennis Alexander, *Univ. of Nebraska-Lincoln, USA*
S. Michael Angel, *Univ. of South Carolina, USA*
Demetrios Anglos, *FORTH, Greece*
Simon Bechard, *PharmaLaser, Canada*
Bruce L. Chadwick, *CRC, Australia*
David Cremers, *Los Alamos Natl. Labs., USA*
Yoshihiro Deguchi, *Mitsubishi Heavy Industries, Japan*
Mohamed Abdel Harith, *NILES Inst., Egypt*
Russell S. Harmon, *ARO/ARL, USA*
Amy Hunter, *P.S. Inc., USA*
Javier Laserna, *Univ. of Malaga, Spain*
Patrick Mauchien, *CEA, France*
Kevin McNesby, *ARL, USA*
Nicolò Omenetto, *Univ. of Florida, USA*
Ulrich Panne, *TUM, Germany*
Leon Radziemski, *Washington State Univ., USA*
Mohamed Sabsabi, *NRC, Canada*
Israel Schechter, *Technion, Israel*
Andrew Whitehouse, *Applied Photonics Ltd., UK*
Ben Smith, *Univ. of Florida, USA*